UNIVERSIDADE ESTADUAL DE CAMPINAS
Faculdade de Engenharia Mecânica

Marcela Rodrigues Machado

A spectral approach for damage quatification and parameter estimation in stochastic dynamic systems

Uma abordagem espectral para a detecção de danos e estimação de parâmetros em sistemas dinâmicos estocásticos

CAMPINAS
2016

Marcela Rodrigues Machado

A spectral approach for damage quantification and parameter estimation in stochastic dynamic systems

Uma abordagem espectral para a detecção de danos e estimação de parâmetros em sistemas dinâmicos estocásticos

Tese de Doutorado apresentada à Faculdade de Engenharia Mecânica da Universidade Estadual de Campinas como parte dos requisitos exigidos para obtenção do título de Doutora em Engenharia Mecânica, na Área de Mecânica dos Sólidos e Projeto Mecânico.

Orientador: Prof. Dr. José Maria Campos dos Santos
Coorientador: Prof. Dr. Sondipon Adhikari

ESTE EXEMPLAR CORRESPONDE À VERSÃO FINAL DA DISSERTAÇÃO DEFENDIDA PELA ALUNA MARCELA RODRIGUES MACHADO, E ORIENTADO PELO PROF. DR. JOSÉ MARIA CAMPOS DOS SANTOS.

....
ASSINATURA DO(A) ORIENTADOR(A)

CAMPINAS
2016

Agência(s) de fomento e nº(s) de processo(s): CNPq, 141190/2012-4

Ficha catalográfica
Universidade Estadual de Campinas
Biblioteca da Área de Engenharia e Arquitetura
Elizangela Aparecida dos Santos Souza - CRB 8/8098

Machado, Marcela Rodrigues, 1983-
M18s A spectral approach for damage quantification and parameter estimation in stochastic dynamic systems / Marcela Rodrigues Machado. – Campinas, SP : [s.n.], 2016.

Orientador: José Maria Campos dos Santos.
Coorientador: Sondipon Adhikari.
Tese (doutorado) – Universidade Estadual de Campinas, Faculdade de Engenharia Mecânica.

1. Análise espectral - Método. 2. Danos. 3. Estimativa de parâmetro. 4. Análise estocástica. I. Santos, José Maria Campos dos,1953-. II. Adhikari, Sondipon. III. Universidade Estadual de Campinas. Faculdade de Engenharia Mecânica. IV. Título.

Informações para Biblioteca Digital

Título em outro idioma: Uma abordagem espectral para a detecção de danos e estimação de parâmetros em sistemas dinâmicos estocáticos
Palavras-chave em inglês:
Spectral analysis - Method
Damage
Parameter estimation
Stochastic analysis
Área de concentração: Mecânica dos Sólidos e Projeto Mecânico
Titulação: Doutora em Engenharia Mecânica
Banca examinadora:
José Maria Campos dos Santos [Orientador]
José Roberto de França Arruda
Helio Fiori de Castro
Rubens Sampaio
Michael John Brennan
Data de defesa: 29-02-2016
Programa de Pós-Graduação: Engenharia Mecânica

UNIVERSIDADE ESTADUAL DE CAMPINAS

FACULDADE DE ENGENHARIA MECÂNICA

COMISSÃO DE PÓS-GRADUAÇÃO EM ENGENHARIA MECÂNICA

DEPARTAMENTO DE PROJETO MECÂNICO

TESE DE DOUTORADO

A spectral approach for damage quantification and parameter estimation in stochastic dynamic systems

Uma abordagem espectral para a detecção de danos e estimação de parâmetros em sistemas dinâmicos estocásticos

Autor: Marcela Rodrigues Machado
Orientador: José Maria Campos dos Santos
Coorientador: Sondipon Adhikari

A Banca Examinadora composta pelos membros abaixo aprovou esta Tese:

Prof. Dr. José Maria Campos dos Santos, Presidente
DMC - Faculdade de Engenharia Mecânica - UNICAMP

Prof. Dr. José Roberto de França Arruda
DMC - Faculdade de Engenharia Mecânica - UNICAMP

Prof. Dr. Helio Fiori de Castro
LAMAR - Faculdade de Engenharia Mecânica - UNICAMP

Prof. Dr. Rubens Sampaio
DEM - Departamento de Engenharia Mecânica- PUC-RIO

Prof. Dr. Michael John Brennan
Departamento de Engenharia Mecânica - UNESP-Câmpus de Ilha Solteira

Campinas, 29 de Fevereiro de 2016.

Dedication

To my daughter Sofia ♡

Acknowledgements

I would like to thank all who in one way or another contributed to the completion of this thesis.

I wish to express my sincere thanks to my supervisor Prof. Dr. José Maria Campos dos Santos for his continuous support, pleasant discussions, and his patience during this research. His continuous motivation with science have inspired me and motivates my future career. I also wish to express my gratitude to my co-supervisor Prof. Dr. Sondipon Adhikari who has provided a great support for this thesis. I would like to thank him for his interest, for the continuous discussions, insightful comments and encouragement. I am also so grateful for his efforts to provide me a pleasant stay in Wales-UK.

I would also like to thank Prof Dr. José R. F. Arruda for his interest into my research, guidance and incentive through course work and through valuable advice regarding on it.

I am also grateful the Department of Computational Mechanics of the Faculty of Mechanical Engineering at UNICAMP, in special, in special Elizabeth Vianna by providing me the facilities necessary to the development of this thesis.

I wish to express my sincere gratitude to my friends and fellow labmates, Thais Pegoretti, Daniela Damasceno, Pricila Brandao, Guilherme Paiva, Elson, Edílson Dantas, Claudia, Flávio Bannwart, Josh Labaki, Nilson Inocente, Elizabeth Viana, Heloi Genari, and all friends of DMC departmentt. Our pleasant discussions, long ours of hard work, and all the fun we have had in the last six years have certainly contributed to make the difficult moments less hard.

I would like also to thank the College of Engineering Swansea University and my fellow labmates Sudip Dey, Jianjun chen(Jeff), Abshikey Kundu, and Amerita Kundu for the support during the stay in Swansea.

My sincere thanks to all the friends I made in Swansea, in special to Karina and Mary Lupatelli, Rosemaria Fuhrmann, Alua and Alba Nascimento, Nawalax Thongjub, Molly and all from English Corner, they made me feel like home even far away from Brazil.

I am thankful to CAPES - Ciencias sem Fronteiras through process numbers BEX 19018/12-6 for providing me the financial support necessary and the opportunity of doing a research internships abroad during this thesis and to CNPq -Conselho Nacional de Desenvolvimento Científico e Tecnológico, for the financial support

My special thanks to my daughter Sofia, my parents Jose Carlos and Terezinha, my brother Carlos Renan, and my friend Matthias Gretemeier for their unconditional support throughout this thesis. I am really thankful for their encouragement and effort to help whenever I need. I am also so thankful to my cousin Helena and all my family and friends for encouragement throughout this thesis.

Resumo

MACHADO, Marcela Rodrigues. Uma abordagem espectral para a detecção de danos e estimação de parâmetros em sistemas dinâmicos estocásticos. 2016. 158p. Tese (Doutorado). Faculdade de Engenharia Mecânica, Universidade Estadual de Campinas, Campinas.

Esta tese relata um estudo sobre identificação de propriedades estruturais e detecção de danos em sistemas dinâmicos estocásticos baseados em um tratamento espectral. Intrínseca em todas as estruturas reais, a incerteza nos parâmetros pode ser encontrada nas propriedades de materiais e geometrias. Muitos parâmetros estruturais, tais como, módulo de elasticidade, coeficiente de Poisson, espessura, densidade, etc., são distribuídos espacialmente por natureza. Assim, hà o interesse no desenvolvimento de eficientes métodos que incluam essas incertezas com uma certa acurácia.

A estimação de parâmetros estruturais pode ser afetada por essas incertezas. No presente trabalho, parâmetros com suas características distribuídas e não homogêneas são considerados. Os parâmetros são tomados como campos aleatórios espacialmente correlacionados e são expandidos em uma decomposição espectral Karhunen-Loève (KL). Usando a expansão KL, a matriz de rigidez dinâmica espectral da estrutura é expandida em uma série com termos de parâmetros discretizados, que podem ser estimados utilizando técnicas baseadas em sensibilidade. Testes numéricos e experimentais envolvendo uma viga com rigidez de flexão distribuída bem como densidade de massa distribuída ao longo do comprimento são usados para verificar o método proposto. Também, são apresentados testes numéricos de uma barra com rigidez longitudinal distribuída e densidade de massa destribuida ao longo do comprimento. Esta extensão do método de ajuste de modelo pode ser usada para melhorar a descrição dinâmica de modelos dinâmicos estruturais.

Da mesma forma, duas técnicas para a detecção de danos estruturais na presença de incertezas nos parâmetros são presentadas. A primeira técnica propõe uma detecção de dano explícita usando uma mudança relativa da FRF. A mudança relativa da FRF e os momentos estatísticos são calculados usando modelos estruturais estocásticos. Um elemento espectral danificado estocástico é desenvolvido considerando os parâmetros distribuídos como um campo aleatório espacialmente correlacionado. O campo aleatório é expandido usando a expansão Karhunen-Loève. Uma vez que alguns parâmetros não podem ser assumidos com uma distribuição marginal Gaussiana, eles são trasfomados para uma base não-Gaussiana utilizando a técnica da transformação memoryless. Os modelos da estrutura com dano são utilizados para calcular a FRF do sistema e, consequentemente, a mudança relativa da FRF. Testes numéricos e experimentais de uma viga carregada axialmente são analisados. A segunda técnica apresenta um estudo sobre os fluxos de energia incluindo incertezas em parâmetros geométricos. A dissipação de energia estrutural é modificada pela presença de descontinuidades, como uma trinca por exemplo. A nucleação e propagação da trinca reduz a rigidez estrutural, o que constitui o indicador de dano. Neste estudo o fluxo de energia é usado para localizar danos em uma barra, a qual inclui incerteza em um parâmetro geométrico. O problema é resolvido em dois passos. Primeiro, a estrutura é modelada pelo Método do Elemento Espectral. A média e a variância das respostas do deslocamento são obtidas usando a expansão em Polinomio do Caos (PC). No PC as soluções estocásticas são expandidas em uma base de polinômios ortogonais em função dos parâmetros aleatórios de entrada. Usando os deslocamentos obtidos, a média e variância das energias são calculadas através da aplicação do momentos estatísticos nas equações de densidade de energia e do fluxo de energia. No entanto, esta abordagem produz equações incomuns para os valores esperados e covariâncias. Como exemplo, o valor esperado de um produto de três variáveis aleatórias correlacionadas, cuja solução compreende a covariância entre uma variável e um produto de duas outras variáveis. Uma formulação é desenvolvida para resolver este problema. Simulação de Monte Carlo é usada para validar os resultados obtidos para essas soluções.

Palavras-chave:Método do Elemento Espectral, Modelo Estocático, Quantificação de Incertezas, Estimação de Parâmetro, Detecção de Danos.

Abstract

MACHADO, Marcela Rodrigues. A spectral approach for damage detection and parameter estimation in stochastic dynamic systems. 2016. 158p. Tese (Doutorado). Faculdade de Engenharia Mecânica, Universidade Estadual de Campinas, Campinas.

This thesis reports a study about structural properties identification and damage detection in stochastic dynamic systems based on a spectral treatment. Intrinsic to all real structures, parameter uncertainty can be found in material properties and geometries. Stochastic methods have been used to include these uncertainties in the structural model. Many structural parameters, such as, elastic modulus, Poisson's rate, thickness, density, etc., are spatially distributed by nature. Hence, there has been much interest in developing efficient uncertainty-based methods with a good degree of accuracy.

Structural parameter estimation may be affected by the uncertainties present in the system. In the present work, the distributed and non-homogeneous characteristics of these parameters are considered in the model updating. The parameters are taken as spatially correlated random fields and are expanded in a spectral Karhunen-Loèeve (KL) decomposition. Using the KL expansion, the spectral dynamic stiffness matrix of the beam structure is expanded as a series in terms of discretized parameters, which can be estimated using sensitivity-based model updating techniques. Numerical and experimental tests involving a beam structure with distributed bending rigidity and mass density are used to verify the proposed method.

Likewise, two techniques for structural damage detection under the presence of parameter uncertainties are addressed. The first technique proposes an explicit damage detection using FRF relative change. Stochastic structural models are used to calculate the FRF relative change, thus statistical moments can be included in the estimation. A stochastic damaged spectral element is developed with distributed parameters as a spatially correlated random field. The random field is expanded using the Karhunen-Loève expansion. Since some parameters cannot be assumed with a marginal Gaussian distribution, a non-Gaussian translation random field is used based on memoryless non-linear transformations. These models are used to calculated the system's FRF and consequently the FRF relative change. Numerical and experimental tests in an axially vibrating rod with distributed parameters are presented. The second study uses the energy flow patterns theory including uncertainties in a geometric parameter to localize the damage. The structural energy dissipation pattern is modified by the presence of discontinuities like a crack. Crack nucleation and growth reduces the structural stiffness which makes this effect useful as a damage indicator. The problem is solved in two steps. First, the structure is modelled by the Spectral Element Method. The mean and variance of displacement responses are obtained by using the Polynomial Chaos expansion (PC). In PC, the stochastic solutions are expanded as orthogonal polynomials of the input random parameters. Second, by using the displacements obtained in the previous step, the mean and variance of energies are calculated and used into the equations of energy density and energy flow. However, this approach produces unusual equations for expected values and covariances, where as the expected value of a product of three random correlated variables, whose solution includes the covariance between one variable and a product of two other variables. A formulation is developed to solve this problem. Monte Carlo Simulation is used to validate the results obtained by these solutions.

Keywords: Spectral Element Method, Stochastic model, Uncertainty Quantification, Parameter estimation, Damage detection.

List of figures

List of Tables

List of Abbreviations and Acronyms

Matrices and Vectors

$\mathbf{C}$	-	Damping matrix
$\Delta\mathrm{C}$	-	Random part of damping matrix
$\mathbf{D}$	-	Dynamic stiffness matrix
$\Delta\mathrm{D}$	-	Random part of dynamic stiffness matrix
$\mathbf{f}$	-	Force vector
$\mathbf{g}$	-	Shape function
$\mathbf{u}$	-	nodal displacement
$\mathbf{H}$	-	Transfer function matrix
$\mathbf{K}$	-	Stiffness matrix
$\Delta\mathrm{K}$	-	Random part of Stiffness matrix
$\mathbf{M}$	-	Mass matrix
$\Delta\mathrm{M}$	-	Random part of mass matrix
$\mathbf{S}$	-	Sensitivity matrix
$\mathbf{W}_e$	-	Positive definite weighting matrix
$\mathbf{W}_p$	-	Parameter weighting matrix
$\mathbf{\Lambda}$	-	FRF relative change

Latin Letters

A	-	Cross-section area
b	-	Cross-section base
$\mathtt{b}$	-	Correlation length
C	-	Covariance
e_p	-	Potential energy density
e_k	-	Kinetic energy density
E	-	Young's modulus
EA	-	Longitudinal rigidity
EI	-	Flexural rigidity
f	-	Force
$\mathrm{F}(X)$	-	Cumulative Density Functions
h	-	Cross-section high
$\mathtt{h}_n(x)$	-	One-dimensional Hermite polynomials
i	-	Unit imaginary number, $i = \sqrt{-1}$
I	-	Moment of inertia
k	-	wavenumber
L	-	Structure length
L	-	Deterministic part of the stochastic operator
L_1	-	Crack position
N	-	Number of modes in KL expansion
q	-	Energy flow
t	-	Time domain
$p(x)$	-	Probability Density Functions
$\mathrm{V}(X)$	-	Variance

Greek Letters

α	-	Crack depth
γ	-	Correlation coefficients
ε	-	Error
ζ	-	Regularization parameter
η	-	Damping factor
θ	-	Characteristic random constant
λ	-	Eigenvalues of the KL expansion
μ	-	Mean value
ξ	-	Random variable
ϖ	-	Random process
ρ	-	Mass density
ρA	-	Mass per unit of length
σ	-	Standard variation
φ	-	Eigenfunctions of the KL expansion
ω	-	Frequency domain
Θ	-	Crack flexibility
Θ_b	-	Bending crack flexibility
$\bar{\Lambda}$	-	Mean of the FRF relative change
$\mathbf{\Pi}$	-	Random part of the stochastic operator
Ψ_n	-	Polynomial Chaos of order n
Ω	-	Maxima frequency
$\mathit{\Omega}$	-	Sample space

Acronyms

ARMA	-	Auto Regressive Moving Average
BEM	-	Boundary Element Method
CDF	-	Cumulative Density Functions
COV	-	Coefficient of variation
DOF	-	Degrees of freedom
DFT	-	Discrete Fourier transform
DSM	-	Dynamic Stiffness Method
EFA	-	Energy flow analysis
FEM	-	Finite Element Method
FFT	-	Fast Fourier transform
FRF	-	Frequency Response Function
IFFT	-	Inverse fast Fourier transform
KL	-	Karhunen-Loèeve expansion
LS	-	Last Squares Method
LRS	-	Left-hand side
MC	-	Monte Carlo Simulation
NDE	-	Non-Destructive Evaluation
ODE	-	Ordinary Differential Equation
PC	-	Polynomial Chaos expansion
PDE	-	Partial Differential Equation
PDF	-	Probability Density Functions
RF	-	Random Field
RV	-	Random Variable
RHS	-	Right-hand side
SAM	-	Spectral Analysis Method
SDE	-	Stochastic Differential Equation
SEM	-	Spectral Element Method
SFEM	-	Spectral Finite Element Method
SHM	-	Structural Healthy Monitoring
SPDE	-	Stochastic Partial Differential Equation
WFEM	-	Wave Finite Element method

Others

$\mathbb{E}[\bullet]$	-	Expectation or mean value
$\mathbb{C}$	-	Space of complex numbers
$\mathbb{R}$	-	Space of real numbers
$\Re(\bullet)$	-	Real part of $(\bullet)$
$\Im(\bullet)$	-	Imaginary part of $(\bullet)$
$\in$	-	Belongs to
$\forall$	-	For all
$(\bullet)^T$	-	Matrix transpose of $(\bullet)$
$(\bullet)^{-1}$	-	Matrix inverse of $(\bullet)$
$(\bullet)^*$	-	Complex conjugate of $(\bullet)$
$(\bullet)'$	-	First derivative of $(\bullet)$
$(\bullet)''$	-	Second derivative of $(\bullet)$
$(\bullet)_0$	-	Deterministic value of $(\bullet)$
$(\bullet)_{an}$	-	Analytical model
$(\bullet)_m$	-	Measure test specimen
$(\bullet)_u$	-	Undamaged
$(\bullet)_d$	-	Damaged
$(\bullet)_L$	-	Left
$(\bullet)_R$	-	Right
$\vert \bullet \vert$	-	Absolute value of $(\bullet)$
$\Vert\bullet\Vert$	-	Norm of $(\bullet)$

Contents

1 Introduction

1.1 Research motivation

An analysis of a dynamic system depends of numerous factors that can affect the response, for example environmental conditions, loads, system analyses, manufacturing processes, etc. Considering that the questions are: '*How does system uncertainty impact the dynamic response*? *What is the physical meaning*? *How can we model uncertainty in dynamic systems*? *Do we 'know' the uncertainty sources*? *How can we efficiently quantify uncertainty in the dynamic response*? 'In the last few decades, an important effort research has been made in order to answer these questions.

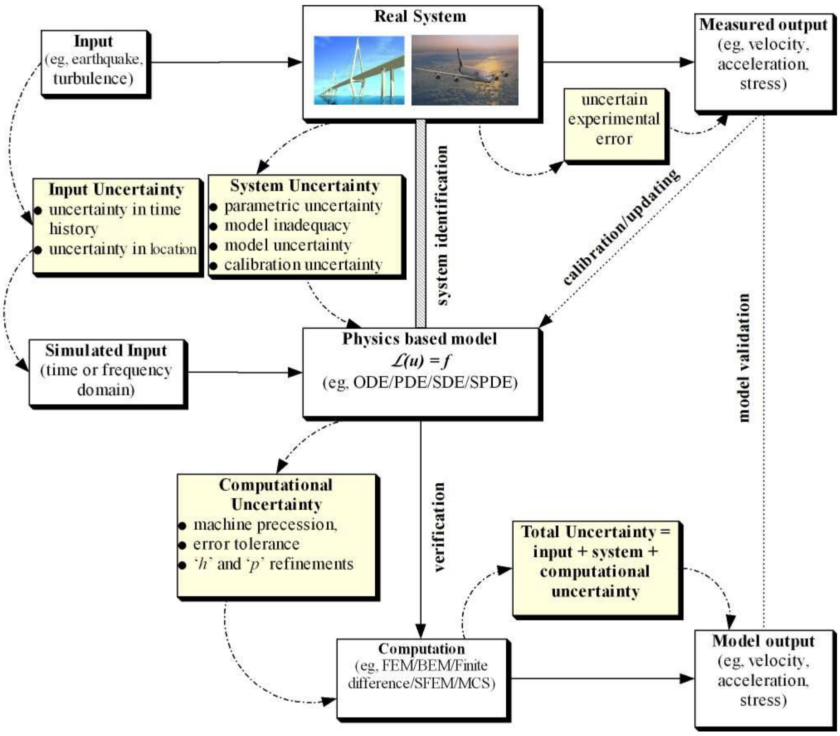

Figure. 1.1: The scheme of uncertainty in computational science (ODE: Ordinary Differential Equation; PDE: Partial Differential Equation; SDE: Stochastic Differential Equation; SPDE: Stochastic Partial Differential Equation; FEM: Finite Element Method; BEM: Boundary Element Method; SFEM: Stochastic Finite Element Method; MC: Monte Carlo Simulation).

The idea of uncertainty modelling in the structural system models can be seem in figure 1.1[1]. Starting with a simple linear problem representing an experimental process, when there is a measured output derived from an input force acting in the real system. Additionally, we can have this procedure in a numerical version so that the model output originated from a simulated input acting in a numerical/computational model. Sources of uncertainties can arise from many origins, as shown in a flowchart in the transition between the real system and the

[1]Flowchart reprinted from http://engweb.swan.ac.uk/ adhikaris.

physical model. The randomness presented in the real system/input force can be introduced in the numerical model by using uncertainty quantification techniques or stochastic methods. Some of the related methods will be treated throughout this thesis. Repeated measurements of a physical phenomenon can generate multiple results, in order to demonstrate the influence of uncertainties in the systems response, three examples complain different problem are showed.

Durand et al. (2008) presented a study of the randomness in measurements due to the presence of uncertainty in systems. The authors performed an experimental vibroacoustic measurements for 20 cars of the same type with optional extra. Variabilities are due to the manufacturing process and are due to small differences in the configurations (optional extra). Measurements of the FRF for the internal noise in the 20 cars induced by engine solid excitations applied to the structure are showed in figure 1.2[2]. They used this database to perform the experimental identification of the probability model parameters and to validate the stochastic computational model.

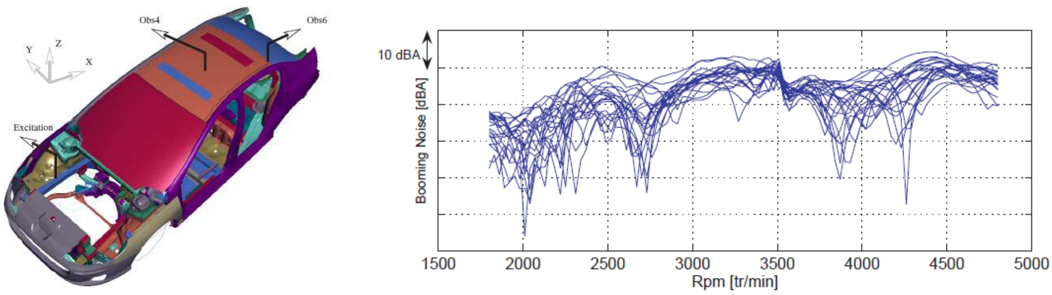

Figure. 1.2: Experimental illustration of variability in a real system, model and measurements.

An experimental test performed in a free-free uniform rod in axial vibration shows the effect of variability in a dynamic structure. It can exhibit how uncertainty acts throughout dynamical models. This experiment simulates random errors in the mass matrix, and how they affect dynamic system behaviour. The experiment used a free-free uniform rod in axial vibration with 8 masses placed at random locations. The total random mass is about 2.3% of the total rod mass. Hundred "nominally identical" dynamical systems are created and individually tested in the VibroAcoustics Laboratory of the University of Campinas (LVA). In each of the 100 measurements, the masses are positioned at different places along the rod as show in A uniform distribution of the 100 samples is used to generate the mass locations it is exemplify with the firsts fifty position at figure 1.4. Figure 1.3 shows the real structure, amplitude of the rod's FRF measured at beam point 2 with 8 randomly placed masses, 100 FRFs samples, ensemble mean, 5 and 95 confidence interval. Important to realise that the ensemble mean follows the result of the baseline system only in the low-frequency range. The relative variance of the amplitude of the FRF remains more or less constant in the mid and high-frequency ranges. Such behaviour

[2]Reprint results of paper published by Durand et al. (2008).

is directly associated with the structural damping. The influence of structural dynamic under uncertainty behaviour is a topic in the Adhikari (2013).

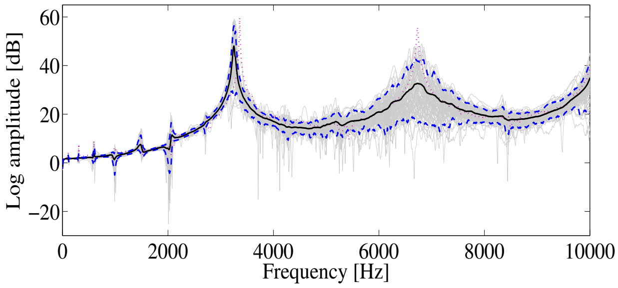

Figure. 1.3: Free-free uniform rod in axial vibration with 8 randomly placed masses (LRS). Mean FRF amplitude of the rod at node 2, 100 samples, 5 and 95 confidence intervals are shown (RHS).

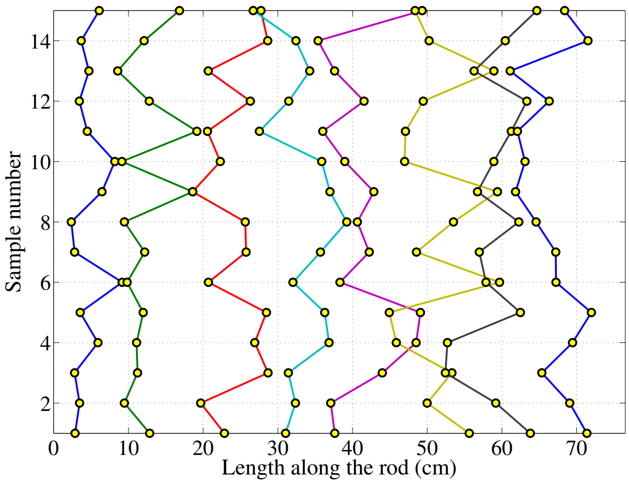

Figure. 1.4: Distribution of 15 samples used to generate the mass locations.

By supposing a damaged detection procedure when a beam structure presents a damage and randomness in the flexural rigidity. In regard to the damage, it is a crack positioned at L_1 and a depth equal to 10% of the beam cross section as shown in figure 1.5 at left-hand side. A damaged beam spectral element connected with a throw-off beam spectral element was used as numerical model the structure. It is assumed a free-free boundary condition where the structure is excited at node 2 by a tone-burst impulsive force. Considering the specified values for the means and covariances of the structural random parameters, 100 samples of acceleration responses were calculated and compared with the deterministic response. For the simulated test the excitation force is applied at node 2 of the beam element, and the acceleration response is obtained at the same node. Figure 1.5 at right-hand side shows the time acceleration response for the damaged structure. It presents four pulses, one at the excitation moment (first pulse) and the other at the reflection moment (third pulse). The pulse wave travels through the structure until reaches node 1 where it is reflected back to node 2 and continues through the throw-off element to the infinity. Throw-off element works as an anechoic termination dissipating the remaining energy into the signal. Due to structural damping the amplitude of vertical acceleration decreases through the structure length. The acceleration response also shows two small additional pulses, one between the excitation and reflection moments and the other after the reflection moment. These additional pulses characterizes the waves partially reflected and transmitted due any structural discontinuity, which could be a crack. These results show that the SEM model is able to reproduce the wave propagation behaviour in the damaged beam structure and to localize the crack.

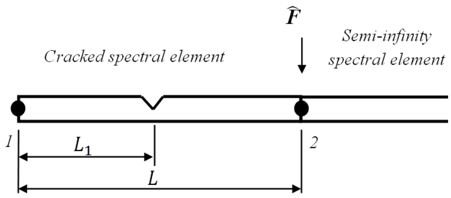

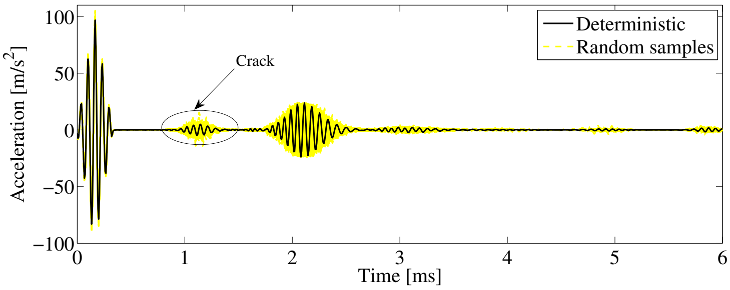

Figure. 1.5: Damaged structural models (LRS) and comparison between deterministic and random system temporal response with 100 samples (RHS).

Indeed, uncertainties have a great impact in dynamic systems. Based on this, the present research is particularly aimed at structural parameter identification and damage detection taking into account uncertainties in the dynamic system. In this Chapter, we begin our discussion about uncertainty quantification in dynamic system and methods for parameter identification and damage detection in the presence of uncertainty. A brief introduction about methods used in this research is made. Based on the literature review, some open problems have been identified which are also discussed in this Chapter.

1.2 Uncertainty quantification and stochastic methods

Engineering structures are manufactured with a certain level of uncertainty. Uncertainty source can originate from manufacturing variability and/or properties of an individual system. There is also change in properties due to environmental conditions, load, application, etc. The effects of uncertainties in the structure may imply change in its dynamic response. As a result, issues are raised concerning safety, reliability, quality of performance, structural behaviour and so on. Regarding this system variability, in the last decades a growing number of research works able to consider uncertainties in numerical models. Numerical model of physical systems are generally used to idealize approximations, such as in parameter values and boundary conditions, which cannot be certainly determined. Stochastic models incorporate variability by adding a probabilistic description of the uncertain quantities. The main goals of uncertainty propagation and quantification in a model are in the framework of simulation test validation, analysis of the system response variation around its mean value, reliability or risk assessment analyses, and uncertainty management.

Uncertainty can be classified as *epistemic uncertainty*, mainly caused by the lack of knowledge and insufficient information which can be associated with either the choice of a numerical method or the accuracy of modelling, and the *aleatory uncertainty* which includes randomness in parameters and variability. Uncertainty propagation techniques for the stochastic systems, can be classified in statistical sampling based simulations for probabilistic methods, non-statistical analytical methods, and non-probabilistic methods. In this research, we focus on probabilistic methods.

A variety of methodologies have been developed to introduce the effects of uncertainty in models. One of the most popular methods used is the Monte Carlo simulation (MC). The idea behind this technique is to generate a sample realization of random inputs and obtain statistical information (e.g mean and variance) from the sample set. However, the computational cost of MC is often high, because for an accurate response system approximation it is required to repeat the analysis many thousands of times. In view of such factors as slow convergence rate, cost MC can be impracticable for large structures, it because often there are many uncertain parameters. Since MC presents these limitations, some improved sampling techniques are used to accelerate the convergence of MC, for example, importance sampling, Latin hypercube sampling, and quasi-Monte Carlo. The limitations of these techniques are directly linked with the dimension of the stochastic space. The options to sampling techniques are methods that provide an explicit functional relationship between the input random variables, which allow easy evaluation of the statistics analysis. Examples are Perturbation Method, Neumann Expansion Method, Moment Equations, and Polynomial Chaos expansion. Also, methods like Stochastic Galerkin Method, Stochastic Partial Differential Equations (PDEs), and Stochastic Finite Element Method are commonly used to solve engineering problems.

1.3 Spectral element method

How to model structural characteristics and static/dynamic behaviour is a wide topic in the literature. A powerful and popular technique used in many engineering areas is the Finite Element Method (FEM). However, a disadvantage in using FEM in a dynamic system in high frequencies is that a large number of finite elements are required for an accurate analysis. Thus, the FEM solution in certain cases can become expensive or impracticable from a computational point of view. An alternative method is the dynamic stiffness method (DSM) (Banerjee, 1997). In this approach, the exact dynamic stiffness matrix is formulated in the frequency domain by using exact dynamic shape functions that are derived from exact wave solutions to the governing differential equations. The advantage in using the exact dynamic shape functions solution is that it treats the mass distribution in a structure member exactly. Therefore, a single element is sufficient to model the homogeneous structure. This important feature reduces significantly the number of elements needed in the structure model and improve the accuracy of the dynamic system solution.

Beskos and Narayanan (1978) presented the first concept of the spectral element method (SEM) by combining DSM with the Spectral Analysis Method (SAM). Methods governing by differential equations in the time-domain are used in the vibration analysis, such as numerical integration and model analysis methods. Besides these, there are methods based on frequency-domain formulation, where SAM is one of the most used. In SAM, the solutions of the governing differential equations are expressed by the superposition of an infinite number of wave modes of different frequencies (or periods). This approach implies in determining an infinite set of spectral components (or Fourier coefficients) in the frequency domain and perform the inverse Fourier transformation to reconstruct the time histories of the solutions. Based on the idea of Beskos and Narayanan by linking the features of FEM (meshing and the assembly of finite elements), DSM (exactness, the minimum number of DOFs.) and SAM (superposition of wave modes via DFT/FFT) the Spectral Element Method was built.

The SEM uses the exact dynamic stiffness matrices obtained by DSM to build the structure element. The dynamic responses are assumed to be the superposition of a finite number of wave modes of different discrete frequencies based on the DFT theory. The SEM is an element method similar to FEM, therefore the mesh refining is applied in the SEM when any geometric or material discontinuities in the spatial domain, as well as any external forces. The spectral elements are assembled to form a global system matrix equation or the whole problem domain by using exactly the same assembly techniques used in the FEM. The linear problem solution is solved by using global system matrix equation related with global spectral nodal DOFs. In the necessity of the time-domain solutions the procedure uses the inverse-FT (IFT).

SEM assumes the exact frequency-domain solution which implies a high accuracy of the system approximation. Smallness of the problem size and DOFs, low computation cost, effectiveness in dealing with frequency-domain problems, effective to deal with the non-reflecting boundary conditions of the infinite or semi-infinite-domain problems are advantages of this method (Lee, 2004). At the same time, the exact wave solutions are not available for certain types of structure. In this case, the application of the other techniques such as the Wave Finite Element method (WFEM) or FEM is necessary.

Over decades, methods based on the exact dynamic stiffness matrices have been used and improved. Doyle (1997) approaches in his book the wave propagation method in structures and dedicated a chapter to formulate the SEM for different types of structures. Lee (2004) presented an extensive study about the Spectral Element Method in structural dynamics and a variety of applications of the method. In one of the applications, Lee proposed an identification of damage in the structure by using SEM. Other authors like Krawczuk (2002)and Ostachowicz (2008) also proposed methods to detect damage using SEM. A more substantially literature review will be presented in Section 3.

1.4 Model updating method in structural dynamics

Model updating is basically about to correct the inaccurate in the model improving the agreement between the experimental results and numerical models. The first step to identify a parameter is to determine the appropriate mathematical structural model. This way, the problem of system identification turns into a parameter estimation. The most popular class of parameter estimation techniques has its base on the Least Squares Method (LS) developed by Carl Friedrich Gauss. Since that, LS suffered many improvements, as problems with non-linearities, varying uncertainty, instrumental variability, cross-section between responses (minimum variance), and model parametrisation. Also, LS was applied in the parameter estimation with a stochastic process purpose. Methods like maximum likelihood and Auto Regressive Moving Average (ARMA) are examples of the stochastic approaches.

The validation of the numerical model consists of comparing numerical with acquired experimental data, although discrepancies occur due to irregularities present in measurement(e.g, noises) and inaccurate estimation of parameter. Therefore, model updating has the possibility to adjust the parameters of the model, so that the fitting between predictions and test results is improved. Methods available for model updating can be classified as direct methods as iterative methods using modal/FRF data. Direct methods is the identification of the system without updating the reference model. The major disadvantage of these methods is the lack of knowledge about the modelling errors. In the iterative methods using modal or FRF data, an iterative procedure based on sensitivity analysis is required in order to minimise an objective function.

It is known that in the practical application of model updating, errors can be associated not only with the numerical model (approximations of the structure and parameters), but also with experimentally measured data, which can be incomplete and variable. The experimental variability arises from different sources, e.g. measurement noise, the use of sensors which affect the measurement or signal processing that may introduce bias. Other known problem is related with temperature, environment, etc. Moreover, the experimental variability might be due to structure variability such as manufacturing and material variability which are not reducible and should be treated as part of the model. Dynamic analysis should seek of better accuracy of measured data and a better estimation by the updating method. Recent research has incorporated the variability in the model, considering the stochastic model and statistical techniques.

Model parameterization is an important task in model updating. In practical problems, the amount of information that may be achieved from vibration test data is limited and, in this case, taking more measurements can be useless. Likewise, additional measurements do not mean more parameters can be estimated. The model updating problem should be an over-determined but this is not always possible. Usually, the resulting equations are ill-conditioned and it is necessary to use regularisation techniques. The selection of parameters should been physical meaning. Thus, the chosen parameters should have a physical understanding, or at least based on the physical problem. It is not always possible in practice to select a 'physical' parameter. Therefore, when choosing parameters, it is always advisable to try to understand the behaviour of the structure globally and locally in order to minimise the discrepancies in predictions.

Mottershead and Friswell (1993) provide a survey until the middle of the 1990s about model updating by using a dynamic response from test structure. In their paper they give an accurate review and introduce the main model updating techniques. Friswell and Mottershead (1995) addressed the principles of model updating and cover aspects of model preparation and data acquisition that are necessary for updating. Also, various methods for parameter selection, error localisation, sensitivity and parameter estimation are described in detail. Natke (1988b) presented a survey about updating computational models in the frequency domain based on measured data. Grafe (1998) investigates the fundamental concepts of model updating methods using FRF and identifies the underlying principles of these limitations, also proposed two new FRF correlation functions.Mares et al. (2006); Khodaparast and Mottershead (2008) described a stochastic model updating problem when the variability in measured vibration data and parameters are taken into account. Mottershead et al. (2006); Khodaparast (2010) also used stochastic model updating problem and presented experimental test by applying the theory. A tutorial about sensitivity method in the Finite Element Model Updating, which is widely used in the problem of model updating is given by Mottershead et al. (2011).

1.5 Damage detection in structures

Damage detection and structure monitoring are extensively treated in the literature. The reason for the research in this area bears relation to the interest in monitoring a structure and to detect damage at the earliest possible stage. Non-destructive techniques are amply used and directly affect topical issues regarding the design of new buildings and the repair and monitoring of existing ones. Health monitoring has large acceptance in the engineering communities, especially because, from the measured structural responses, they provide orientation on the validation of structural descriptions or on the mathematical models of material behaviour. Regarding this feature, with repeated tests over time, it can indicate the appearance of discontinuities(damage) occurring during the structure's lifetime.

Methods for damage detection under non-destructive treatment are either visual or localized techniques such as acoustic, ultrasonic methods, magnet field methods, radiography, and thermal field methods. Among these techniques, the dynamic methods that work with structure response have shown to be potential by effective in damage diagnostic . Based on these circumstances, dynamic methods can be employed in a global scale and do not require a priori information on the damaged area. Damage can induce changes in local and global properties of a structure, where this change under inspection can be associated with damage parameters. These changes include dynamic response signals captured from the structure. Modern techniques have been developed to detect damage. Some of these dynamic methods can be grouped as modal-data-based, electro-mechanical-impedance-based, static-parameter-based, acoustic emission, and elastic-wave-based (Su and Ye, 2009).

Modal-data-based methods are based on the fact that in presence of structural damage reduces structural stiffness, shifts eigenfrequencies, changes frequency response function and mode shapes. Advantages and applications of this method are simple, low cost, and particularly effective for detecting larger damages in larger infrastructure or rotating machinery. Disadvantages and limitations are insensitivities to smaller damage or damage growth, difficulties to excite high frequencies, large number of measurement points needed, and hypersensitive to the boundary and environmental changes.

Electro-mechanical-impedance-based methods are related in the fact that the composition of a system contributes for a certain amount to its total electrical-mechanical impedance, and the presence of damage modifies the impedance in a high-frequency range, normally higher tan 30 kHz. Advantages and applications of this method are low cost and simple for implementation, particularly effective for detecting defects in planar structures. Disadvantages and limitations are that this method is unable to detect damage distant from sensors, and it is not highly accurate. It performs better for larger damages only.

Static-parameter-based methods are related to the observation that in presence of damage causes changes in displacement and strain distribution in comparison with the benchmark. Advantages and applications of this method are locally sensitive to defects, it is simple to apply and cost-effective. Disadvantage and limitations are that it is relatively insensitive to undersized damage or the evolution of deterioration.

Acoustic emission is based on the fact that rapid release of strain energy generates transient waves, whereby presence or growth of damage can be evaluated by capturing damage-emitted acoustic waves. Advantages and applications of this method are able to triangulate damage in different modalities including matrix cracks, fibre fractures, delaminations, microscopic deformations, welding flaws and corrosion. Furthermore, it is able to predict damage growth, surface mountable and good coverage. Disadvantages and limitations are its prone to contamination by environmental noise, complex signals, its high damping ratio of the wave and therefore, it is only suitable for locating damage in small structures.

Elastic-wave-based methods are based on the fact that structural damage causes unique wave scattering phenomena and mode conversion, whereby the quantitative evolution of damage can be achieved by scrutinizing the wave signals scattered by the damage. Advantages and applications of this method are cost-effective, fast and repeatable, able to inspect a large structure in a short time, sensitive to small damage, low energy consumption and it is able to detect both surface and internal damage. Disadvantages and limitations are: it needs sophisticated signal processing due to a complex appearance of wave signals, multiple wave modes available simultaneously, difficult to simulate wave propagation in complex structures, high dependence on prior models or benchmark signal.

This research is concentrated on methods using elastic wave propagation in structures at medium and high frequencies. These methods use the evidence that material discontinuities, such as a crack, generate changes in elastic waves propagating in the structure. Elastic wave-based damage detection presents some particular advantages like the capability of propagation over significant distances and high sensitivity to discontinuities near the wave propagation path. Recent works regarding wave propagation for health monitoring and damage detection starts to include uncertainties in parameters as well as modelling and measurement errors which can inherently influence the damage detection procedure.

An extensive literature review to detect, locate, and characterize damage in structural and mechanical systems by examining changes in measured vibration response,vibration-based, is given by Doebling et al. (1996, 1998). Dynamic methods for damage detection in structures was the approach in (Morassi and Vestroni, 2008), where the authors presented an overview of theoretical and experimental aspects of dynamic non-destructive methods. Su and Ye (2009) provide in their book a comprehensive description of damage identification using Lamb waves from fundamental theory through case studies to engineering applications. Ostachowicz (2008) presented a review of the theory and applications of damage modelling and elastic waves propagation by using the Spectral Element Method. A more extensively literature review of damage detection in structures using the SEM can be seen in Section 5.

1.6 Objective

In relation to the existing literature in a context of the Spectral Element Method, a small amount of research which treated the SEM with a stochastic approach. Moreover, we missed in the literature some developed spectral element formulation for damaged structure based on the approach presented by Krawczuk et al. (2006b) with a stochastic basis. Damaged and undamaged spectral elements are in the scope of this research. More precisely, it is about the Spectral Element Method with a stochastic treatment. Therefore, the first objective of this research is *to* *formulate a stochastic spectral element for damaged structure*.

Damage detection has an extensive literature. There are many methods for damage detection and to estimate damage severity (crack depth). Our focus in this research is on methods based on spectral element method using frequency band. Methods based on wave propagation and SEM to detect damage including the treatment of uncertainty in parameters are not very well explored. On this purpose, the second objective is *to develop a damage detection method using wave propagation including uncertain parameters*. The benefit of this proposal is a more accurate damage estimation, where the uncertainties of the system have been taken into account.

In the parameter estimation subject, the main goal is to use sensitivity-based model updating methods with measured FRFs to *estimate spatially distributed parameters*. The distributed parameters are assumed stochastic, which is more realistic due to the given variability caused by the manufacturing processes. Such distributed variability are unknown a priori, and therefore can be considered to sample from a random field, which is discretized into random variables using the KL expansion.

1.7 Outline of the thesis

Motivated by the existing lack and open subject pointed out in the last section, this thesis will be organised as follows. In this Chapter the motivation of this research is given, an introductory idea about the theories approached in this study, the main references for each subject addressed in this work, and objectives based on the gaps in the actual literature are given. The thesis is divided into 6 chapters and one Appendix.

Chapter 2 presents statistical techniques used in this thesis and A literature review of these techniques. Section2.2 treats Monte Carlo simulation theory and Section2.3 is about the Moment Equation method. In Section2.4, formulation and simulation methods for Gaussian random field and non-Gaussian random field are described. The Gaussian random process is simulated using KL expansion and the translation for a target distribution is done based on memoryless transformation. This technique is detailed in an analytical and numerical version. The Polynomial Chaos (PC) expansion and the Stochastic Finite Element Method (SFEM) are introduced.

In Chapter 3, the central theme is the formulation of the Spectral Element Method for deterministic and stochastic dynamic systems. A general derivation of the spectral element matrices is presented. The spectral element for an undamaged rod in a deterministic and stochastic case are formulated in Section 3.3. Deterministic spectral element for a damaged rod and the new stochastic spectral element for a damaged rod are developed in Section 3.4. Similar to rod spectral element, we also described the deterministic and stochastic spectral element for an undamaged beam in Section 3.5, deterministic spectral element for a damaged beam, and the new stochastic spectral element for a damaged beam in Section 3.6.

Chapter 4 presents a general literature review of the model updating techniques for a deterministic case and the presence of uncertain measured data with reducible and irreducible uncertainty. The main goal is to use sensitivity-based model updating with measured FRFs to estimate spatially distributed parameters of the structure, then a description of the techniques in model updating and sensitivity-based updating method are given. Section 4.2 illustrates the model updating using frequency response function, which includes the Least Squares Method and choice of weighting matrices. Section 4.3 shows discussions about frequency response function sensitivities and the types of sensitivities formulation. Also in this section, a parametric sensitivity for a stochastic system is developed. Finally, numerical and experimental tests in two different types of structure demonstrate the performance of the proposed technique which is presented in Section 4.4.

In Chapter 5, the basic issue is to detect damage in dynamic systems containing uncertain properties. The technique proposed for damage detection is shown in Section 5.2, followed by theory, numerical simulations, and an experimental test. The method developed detects damage based on the energy method with uncertain parameters. Theory and numerical test are presented in Section 5.3.

Finally, Chapter 6 presents the conclusions emerging from this research and a few suggestions for further works. Appendix A shows the terms of the matrices that have been developed for spectral elements presented in Chapter 2. Thus, the deterministic undamaged and damaged element, as well as the stochastic undamaged and damaged element are described.

2 Uncertainty quantification and stochastic methods

2.1 Introduction

Quantifying uncertainty using numerically simulated results is not new. However, during the last decades, this research area has undergone remarkable development, in special for dynamic systems. The method commonly used is Monte Carlo (MC) simulation (Sobol', 1994). Otherwise, non-sampling approaches may be used, such as the Perturbation method (Kleiber and Hien, 1992), Neumann expansion method (Yamazaki et al., 1988; Zhu et al., 1992), Moment Equations (Xiu, 2010), Polynomial Chaos (PC) expansion and Generalized Polynomial Chaos (Ghanem and Spanos, 1991; Xiu, 2010), Stochastic Galerkin method (Maître and Knio, 2010), Stochastic Partial Differential Equations (SPDEs), and Stochastic Finite Element method (Ghanem and Spanos, 1991).

The stochastic approach to understand the magnitude of uncertainty with simulated results is addressed in this Chapter. It can be treated in the scope of the random variable, which is understood as a function defined on a sample space whose outputs are random numerical values, and the random field, which is a generalization of a stochastic process such that the underlying parameter is no longer a single value, but a multidimensional vectors, whose values are spatially distributed (Papoulis and Pillai, 2002). The most used method is the Monte Carlo (MC) simulation. It is a sampling method which can generate independent samples of random variables, based on their probability distributions, and solving the deterministic problem for each realization. By collecting an ensemble of solutions, the statistical moments can be calculated (Sobol', 1994). Although easy to apply, a large number of samples is needed to obtain convergence, which means high computational costs. The Moment Equations or Direct method consists in directly applying the statistical moment equations to obtain the random solutions. The unknowns are the moments and their equations are derived by taking averages over the original stochastic governing equations. The problem is that a statistical moment almost always requires information about higher moments. A non-sampling approach, known as Perturbation method, consists of expanding the random fields in a truncated Taylor series around their mean. Its main drawback is the limitation of the magnitude of uncertainties which cannot be too large, typically less than 10% (Xiu, 2010). Another method widely used as considering random field is the Karhunen-Loève (KL) expansion (Ghanem and Spanos, 1991; Papoulis and Pillai, 2002; Xiu, 2010). The KL expansion may be used to discretize the random field by representing it by orthogonal random variables and continuous deterministic functions. By truncating the expansion, the number of random variables becomes finite and numerically treatable. The KL expansion has Gaussian distribution basis, and then it is used to model Gaussian random fields. However it is possible to extend the KL expansion to non-Gaussian processes. Poirion and Soize (1999); Sakamoto and Ghanem (2002); Phoon et al. (2005) show how to handle a non-

Gaussian random field with Karhunen-Loève (KL) expansion. The technique presented in this work consists of generating a non-Gaussian random process from a Gaussian random process by a memoryless transformation. This technique is explained in the works of Grigoriu (1998); Vio et al. (2001); Puig and Soize (2002); Schevenels et al. (2004); Weinberg and L.Gunn (2011).

The stochastic Finite Element Method (SFEM) is a robust method used to solve computational stochastic mechanics (Ghanem and Spanos, 1991). It is an extension of the deterministic Finite Element Method (FEM) to solve static and dynamic problems with stochastic material properties, geometries, or loading (Stefanou, 2009). Adhikari (2011) presented a double Spectral Stochastic Finite Element Method, where the Spectral Element Method (SEM) is given a stochastic treatment. Both techniques, SFEM and doubly Spectral SFEM, are formulated in a context of random fields. In this section some statistical techniques and fundamentals of spectral expansions of random parameters and processes are presented. Additionally, the theory and application of memoryless transformations are showed. PC method and a brief introduction of SFEM are also illustrated.

2.2 Monte Carlo simulation

The Monte Carlo simulation has been used for decades, it is a method based on random samples used in approximations. The name itself is taken from the famous casino located in Monte Carlo (Sampaio and Lima, 2012). Simulation methods are also named exact methods, because the simulation result leads to exact outcomes when the sample number goes to infinity. To avoid certain approximations which occur in analytical methods and to be a non-intrusive method are another advantages of this type of techniques. Thus, the general idea of the method is solving mathematical problems by the simulation of random variables (Sobol', 1994). An Monte Carlo method example of application is the multidimensional integral approximation. Supposing the integral of a given real multidimensional function g in a certain region $B \subset \mathbb{R}$,

$$I = \int_B g(\mathbf{x})d(\mathbf{x}) \tag{2.1}$$

If g is a simple function, its integral (I) can be calculated easily. However, if g is a difficult function or is defined in a region with complicated contour can does not exist a closed form for (I). In such cases, numerical integration methods must be applied for if approximations for (I), such as the trapeze method, Simpson method and Monte Carlo simulation. Assuming that (I) is a one-dimensional integral, p and function density probability of a random variable $\mathbf{X}$, rewriting equation (2.1) it is

$$I = \int_B h(\mathbf{x})p(\mathbf{x})d(\mathbf{x}) \tag{2.2}$$

where $h(\mathbf{x}) = g(\mathbf{x})/p(\mathbf{x}) \forall \mathbf{x} \in B$. The integral I can be interpreted as the expected value of

$h(\mathbf{x})$, it is:

$$I = \mathbb{E}[h(\mathbf{x})] = \int_B h(\mathbf{x})p(\mathbf{x})d(\mathbf{x}) \tag{2.3}$$

Thus, and approximation $(\hat{I})$ for the integral can be expressed as

$$\hat{I} = \sum_{i=1}^{n} h(\mathbf{x}^i) \tag{2.4}$$

where $x(1), x(2), ..., x(n)$ are samples of the random vector $\mathbf{X}$ with probability density function p.

The mean and the standard deviation of the result are calculated through the samples generated. Let $X(\xi, \omega)$ be the frequency response of the stochastic system calculated for a realization ξ, generated by the Monte Carlo method (Rubinstein, 2008). The mean-square convergence analysis with respect to independent realizations of the random variable X, denoted by $X_j(\xi, \omega)$, is carried out studying the function $n_S \mapsto conv(n_S)$ defined by:

$$conv(n_S) = \frac{1}{n_S} \sum_{j=1}^{n_S} \int_B \|X_j(\xi, \omega)\|^2 \, d\omega \tag{2.5}$$

The generation of random distribution according to certain variables is the basis for Monte Carlo simulation. However, computers do not have the ability to generate truly random numbers, as they make use of an algorithm to generate a sequence of numbers. Thus, computers have the ability to produce sequences of numbers that exhibit statistical properties according to a given distribution. Such sequences may be pseudo-random or quasi-random type Calfisch, 1998; Dutang, 2008. A feature of the Monte Carlo simulation is the generation of a series of values of one or more random variables with a specific probability distribution. Method of inverse processing is a usual method of variables generation. Assuming that $\mathrm{F}_x(x_i)$ is the cumulative distribution function of the random variable x_i. By definition, $\mathrm{F}_x(x_i)$ has value into a interval of $[0,1]$. Considering that ν_i is the random number generated uniformly distributed, the method of inverse transformation is used to match ν_i to $\mathrm{F}_x(x_i)$ as follows:

$$\mathrm{F}_x(x_i) = \nu_i \quad ou \quad x_i = \mathrm{F}_x^{-1}(\nu_i) \tag{2.6}$$

From the generated uniform random number, the amount of CDF uniform distribution and the target distribution can be easily obtained. Thus, it is possible to obtain the random number of PDF target using equation (2.6).

Stochastic solution convergence

Monte Carlo method is used as stochastic solver. It consists in solving the problem repeated times, each one of them with a new random input. The mean and the standard deviation of the result are calculated through the samples generated. Let $X(\xi, \omega)$ be the response of the stochastic system calculated for a realization ξ, generated by the Monte Carlo method (Rubinstein, 2008). The mean-square convergence analysis with respect to independent realizations of the random variable X, denoted by $X_j(\xi, \omega)$, is carried out studying the function $n_S \mapsto conv(n_S)$ defined by:

$$conv(n_S) = \frac{1}{n_S} \sum_{j=1}^{n_S} \int_B \|X_j(\xi, \omega)\|^2 \, d\omega \tag{2.7}$$

where n_S is sample number used in MC simulation.

2.3 Moment Equations approach

In statistics, the method of moments has the objective to calculate statistical moments, e.g, expected value or variance directly. The explicit calculations of the moments are based on random variable properties. Some usual formulas from the statistical literature used in this thesis, as the mean and variance of the product of two independent random variables, are described here. The expectation or mean value of a random variable X, Y and Z with probability density p_{X} is

$$\mu_{\mathsf{X}} = \mathbb{E}[\mathsf{X}] = \int_{\infty}^{-\infty} x p_{\mathsf{X}}(x) dx \tag{2.8}$$

and the variance of X is given by

$$\sigma_{\mathsf{X}}^2 = V(\mathsf{X}) = \int_{\infty}^{-\infty} (x - \mu_x)^2 p_{\mathsf{X}}(x) dx \tag{2.9}$$

From the properties of the expected value and variance of a product with two correlated random variables (Goodman, 1960),

$$\mathbb{E}[\mathsf{XY}] = \mathrm{C}(\mathsf{X},\mathsf{Y}) + \mathbb{E}[\mathsf{X}]\mathbb{E}[\mathsf{Y}] \tag{2.10}$$

where C is the covariance. Under multivariate normality Bohrnstedt and Goldberger (1969) show that

$$\mathrm{C}(\mathsf{X},\mathsf{YZ}) = \mathbb{E}[\mathsf{Y}]\mathrm{C}(\mathsf{X},\mathsf{Z}) + \mathbb{E}[\mathsf{Z}]\mathrm{C}(\mathsf{X},\mathsf{Y}), \tag{2.11}$$

and Miller and Childers (2012) show the variance of a complex random variable as

$$\mathrm{V}(\mathsf{Z}) = \mathrm{C}(\mathsf{Z},\mathsf{Z}^*) = \mathbb{E}[\mathsf{Z}\mathsf{Z}^*] - \mathbb{E}[\mathsf{Z}]\mathbb{E}[\mathsf{Z}^*] \tag{2.12}$$

The covariance between two variables is defined as

$$\mathrm{C}(\mathsf{X},\mathsf{Y}) = \gamma_{\mathsf{X},\mathsf{Y}}[\mathrm{V}(\mathsf{X})\mathrm{V}(\mathsf{Y})]^{1/2} \tag{2.13}$$

where $\gamma_{\mathsf{X},Y}$ is the linear correlation coefficient. Expected value of a product of two squared correlated random variables (Bohrnstedt and Goldberger, 1969) is given by

$$\mathbb{E}[\mathsf{X}^2\mathsf{Y}^2] = \mathrm{V}(\mathsf{XY}) + \mathbb{E}^2[\mathsf{XY}] \tag{2.14}$$

Considering that the variance and squared expected value of a product of two correlated random variables

$$\mathrm{V}(\mathsf{XY}) = \mathbb{E}^2[\mathsf{X}]\mathrm{V}(\mathsf{Y}) + \mathbb{E}^2[\mathsf{Y}]\mathrm{V}(\mathsf{X}) + 2\mathbb{E}^2[\mathsf{X}]\mathbb{E}^2[\mathsf{Y}]\mathrm{C}(\mathsf{X},\mathsf{Y}) + \mathrm{V}(\mathsf{X})\mathrm{V}(\mathsf{Y}) + \mathrm{C}^2(\mathsf{X},\mathsf{Y}) \tag{2.15}$$

and

$$\mathbb{E}^2[\mathsf{XY}] = (\mathrm{C}(\mathsf{X},\mathsf{Y}) + \mathbb{E}[\mathsf{X}]\mathbb{E}[\mathsf{Y}])^2 \tag{2.16}$$

and substituting equations (2.15) and (2.16) in equation (2.14), we obtain

$$\mathbb{E}[\mathsf{X}^2\mathsf{Y}^2] = \mathbb{E}^2[\mathsf{X}]\mathrm{V}(\mathsf{Y}) + \mathbb{E}^2[\mathsf{Y}]\mathrm{V}(\mathsf{X}) + 4\mathbb{E}[\mathsf{X}]\mathbb{E}[\mathsf{Y}]\mathrm{C}(\mathsf{X},\mathsf{Y}) + \mathrm{V}(\mathsf{X})\mathrm{V}(\mathsf{Y}) + 2\mathrm{C}^2(\mathsf{X},\mathsf{Y}) + \mathbb{E}^2[\mathsf{X}]\mathbb{E}^2[\mathsf{Y}]. \tag{2.17}$$

These moment properties are presented in view of the application in Section 5. More properties can be found in the statistics literature.

2.4 Karhunen-Loève expansion

In probability theory, a stochastic process or random process is indexed by a subset of the real random variables representing the evolution of some system of random values over time. It can also consider more general parameter spaces so that the stochastic process becomes a random function of more than one variable. This type of stochastic processes is usually called a random field (Papoulis and Pillai, 2002). The random field is discretized in terms of random variables. By doing this, many mathematical procedures can be used to solve the resulting discrete stochastic differential equations. The procedure applied here is a random field spectral decomposition using the Karhunen-Loève (KL) expansion. The random field is described by various points expressed by random variables, therefore, a large number of points is required for a good approximation. The non-zero mean random process ($\varpi(\mathbf{x},\theta)$) is decomposed as follows:

$$\varpi(\mathbf{x},\theta) = \varpi_0(\mathbf{x}) + Y(\mathbf{x},\theta) \tag{2.18}$$

where $\varpi_0(\mathbf{x})$ is the mean value of the random process. By assuming that the covariance function is finite $C(\mathbf{x}_1,\mathbf{x}_2)$ defined in a space $\mathcal{D}$, symmetric and positive definite, it can be represented by a spectral decomposition. Thus, a random field $Y(\mathbf{x},\theta)$ can be expressed like a generalized Fourier series projected of the process on the Hilbert space[1] $\xi_j(\theta)$ as,

$$Y(\mathbf{x},\theta) = \sum_{j=1}^{\infty} \xi_j(\theta)\sqrt{\lambda_j}\varphi_j(\mathbf{x}) \tag{2.19}$$

Here θ denotes an element of the sample space Ω, so that $\theta \in \Omega$; $\xi_j(\theta)$ are uncorrelated random variables. The subscript 0 implies the corresponding expected value. By definition of the covariance function, it is bounded, symmetric and positive definite with spectral decomposition ,

$$C(\mathbf{x}_1,\mathbf{x}_2) = \sum_{j=1}^{\infty} \lambda_j\varphi_j(\mathbf{x}_1)\varphi_j(\mathbf{x}_2) \tag{2.20}$$

where constants λ_j and functions $\varphi_j(\mathbf{x})$ are, respectively, eigenvalues and eigenfunctions satisfying the Fredholm integral equation

$$\int_{\mathcal{D}} C(\mathbf{x}_1,\mathbf{x}_2)\varphi_j(\mathbf{x}_1)d\mathbf{x}_1 = \lambda_j\varphi_j(\mathbf{x}_2) \quad \forall j = 1,2,\ldots. \tag{2.21}$$

The discretization of the process $\varpi(\mathbf{x},\theta)$ is achieved by a truncation of the infinite series at N terms. Rewriting equation (2.18) it has

$$\varpi(\mathbf{x},\theta) = \varpi_0(\mathbf{x}) + \sum_{j=1}^{N} \xi_j(\theta)\sqrt{\lambda_j}\varphi_j(\mathbf{x}) \tag{2.22}$$

By multiplying equation (2.19) by $\varphi_j(\mathbf{x})$ and integrating over the domain $\mathcal{D}$ an explicit expression for $\xi_j(\theta)$ is given,

$$\xi_j(\theta) = \frac{1}{\sqrt{\lambda_j}} \int_{\mathcal{D}} Y(\mathbf{x},\theta)\varphi_j(\mathbf{x})d\mathbf{x} \tag{2.23}$$

with mean and covariance function given by

$$\begin{aligned} \mathbb{E}[\xi_i(\theta)] &= 0 \\ \mathbb{E}[\xi_i(\theta)\xi_j(\theta)] &= \delta_{ij} \end{aligned} \tag{2.24}$$

[1] An inner product space which is complete with respect to the norm induced by the product is called a Hilbert space. A complete theory with applications can be found in https://www.math.washington.edu/greenbau/Math555/CourseNotes/555notes5.pspages.pdf and in (Cursi and Sampaio, 2012)(in portuguese).

where δ_{ij} is the Kronecker-delta function.

The integral in equation (2.23) can be interpreted as an infinite series of zero mean Gaussian variables. If the process $\varpi(\mathbf{x},\theta)$ has a Gaussian marginal PDF, then $Y(\mathbf{x},\theta)$ reduces to a zero mean Gaussian variable for a fixed position x (Schevenels et al., 2004). The KL coefficients are independent uncorrelated standard Gaussian variables.

Here, one dimensional space is considered. Since a Gaussian random field is representative of many physical systems and closed form expressions for the KL expansion may be obtained, then a Gaussian autocorrelation function with exponential decaying will be used. It can be expressed as,

$$C(x_1,x_2) = e^{-|x_1-x_2|/\mathtt{b}} \tag{2.25}$$

where $\mathtt{b}$ is the correlation length, which is an important parameter to describe the random field. A random field becomes a random variable if the correlation length is very larger as compared with the domain under consideration. An analytical solution in the interval $-\mathtt{a} < x < \mathtt{a}$ where it is assumed that the mean is zero, produces a random field of equation (2.22). Defining that $\mathtt{c} = 1/\mathtt{b}$, the corresponding eigenvalues and eigenfunctions for odd j are given by,

$$\lambda_j = \frac{2\mathtt{c}}{w_j^2 + \mathtt{c}^2}; \quad \varphi_j(r)\frac{\cos(w_j\frac{L}{2})}{\sqrt{\mathtt{a} + \frac{\sin(2w_j\mathtt{a})}{2w_j}}} \qquad \text{where} \quad \tan(w_j\mathtt{a}) = \frac{\mathtt{c}}{w_j} \tag{2.26}$$

and for even j are expressed as,

$$\lambda_j = \frac{2\mathtt{c}}{w_j^2 + \mathtt{c}^2}; \quad \varphi_j(r)\frac{\sin(w_j\frac{L}{2})}{\sqrt{\mathtt{a} - \frac{\sin(2w_j\mathtt{a})}{2w_j}}} \qquad \text{where} \quad \tan(w_j\mathtt{a}) = \frac{w_j}{-\mathtt{c}} \tag{2.27}$$

In random processes where the analytical solution of the integral equation (2.21) for KL expansion is not trivial, then a numerical approximation is used. The problem of eigenvalue/eigenvector can be solved by a Galerkin procedure as presented by Ghanem and Spanos (1991) and Huang et al. (2001). The eigenfunction is approximated for a linear combination of N base functions $(\varphi_1(\mathbf{x}),\varphi_2(\mathbf{x}),\ldots,\varphi_N(\mathbf{x}))$ as:

$$\varpi_i(\mathbf{x}) \approx \sum_{p=1}^{N} \varpi_{ip}\phi_p(\mathbf{x}) \tag{2.28}$$

where ϖ_{ik} are constant coefficients for the ith eigenfunction. Substitute equation (2.28) and (2.25) into equation (2.21) it becomes

$$\sum_{p=1}^{N} \varpi_{ip}\left[\int_{\mathcal{D}}\int_{\mathcal{D}} C(\mathbf{x}_1,\mathbf{x}_2)\phi_p(\mathbf{x}_1)\phi_j(\mathbf{x}_2)d\mathbf{x}_1 d\mathbf{x}_2\right] - \lambda_j \int_{\mathcal{D}} \varphi_p(\mathbf{x}_2)\varphi_j(\mathbf{x}_2)(\mathbf{x}_2) = 0 \tag{2.29}$$

or

$$\mathsf{AD} = \Lambda\mathsf{BD} \tag{2.30}$$

where

$$\mathsf{A}_{ij} = \int_{\mathcal{D}}\int_{\mathcal{D}} C(\mathbf{x}_1,\mathbf{x}_2)\varphi_k(\mathbf{x}_1)\phi_j(\mathbf{x}_2)d\mathbf{x}_1 d\mathbf{x}_2 \tag{2.31}$$

$$\mathsf{D}_{ij} = \varpi_{ik} \tag{2.32}$$

$$\Lambda_{ij} = \delta_{ij}\lambda_j \tag{2.33}$$

$$\mathsf{B}_{ij} = \int_{\mathcal{D}} \varphi_k(\mathbf{x}_2)\varphi_j(\mathbf{x}_2)(\mathbf{x}_2) \tag{2.34}$$

Thus, a generalized algebraic eigenvalue problem of equation (2.30) may be solved to obtain λ_j and ϖ_{ik}. These eigenvalues and eigenfunctions will be used to obtain the stochastic dynamic stiffness matrices for undamaged and damaged spectral elements.

For practical applications, the equation (2.19) is truncated with N numbers of terms, which could be selected based on the amount of information to be kept. Its value is also related with the correlation length and the number of eigenvalues kept, provided that they are arranged in decreasing order (Ghanem and Spanos, 1991; Adhikari and Friswell, 2010; Xiu, 2010). Figure 2.1 shows the number of terms required to capture 90% of the infinite series for different correlation lengths. It can be seen that more terms are needed as smaller is the correlation length, than more orthogonal variables are required for random fields with smaller correlation lengths and vice-versa.

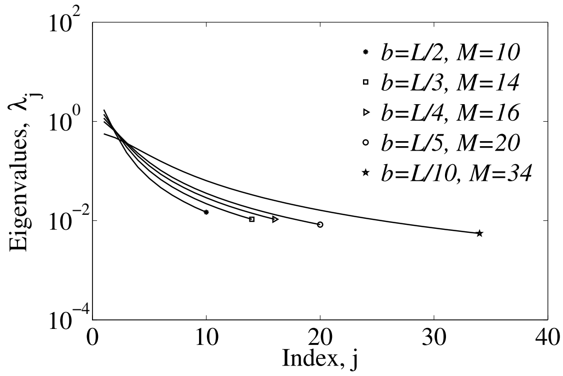

Figure. 2.1: The eigenvalues of the Karhunen-Loève expansion for different correlation lengths, b, and number of terms, N, required to capture 90% of the infinite series.

In the present example, the covariance function of the random process in Fig. 2.3 is assumed to be exponential as equation (2.25) with correlation length $\mathsf{b} = L/3$. In order to demonstrate the influence of the order N of the KL decomposition, the discretization is performed with $N = 4$ and $N = 10$. Figure 2.2 shows the eigenfunction as defined by equations (2.26) and (2.27) for different terms in KL expansion, and for $\mathsf{a} = 2$.

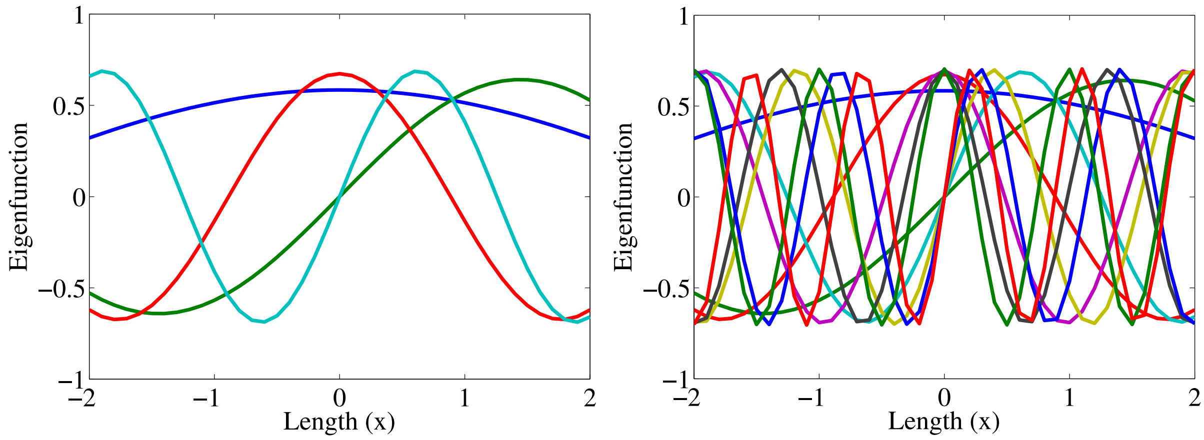

Figure. 2.2: Eigenfunctions of the KL expansion $\varpi_j(\mathbf{x},\theta)$ for $-2 \leq x \leq 2$ with number of terms equal to 4 (LHS) and 10 (RHS); Exponential Covariance, and Correlation length=1/3.

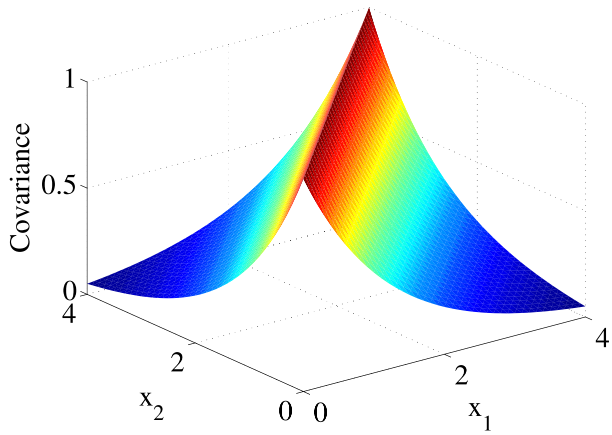

Figure. 2.3: Covariance surface versus x_1 and x_2;Correlation length=1/3.

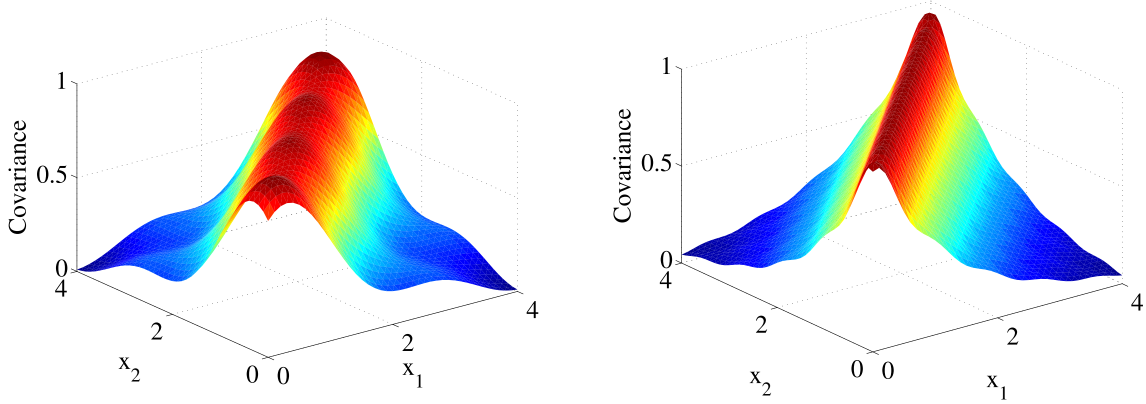

Figure. 2.4: KL approximation of the covariance surface with number of terms equal to 4 (LHS) and 10 (RHS).

The truncated spectral representation of the covariance function related with the restriction to the highest N eigenvalues and eigenfunctions implies in the KL approximation converges to the exact covariance function. Figure 2.4 illustrates the influence of the number of terms in

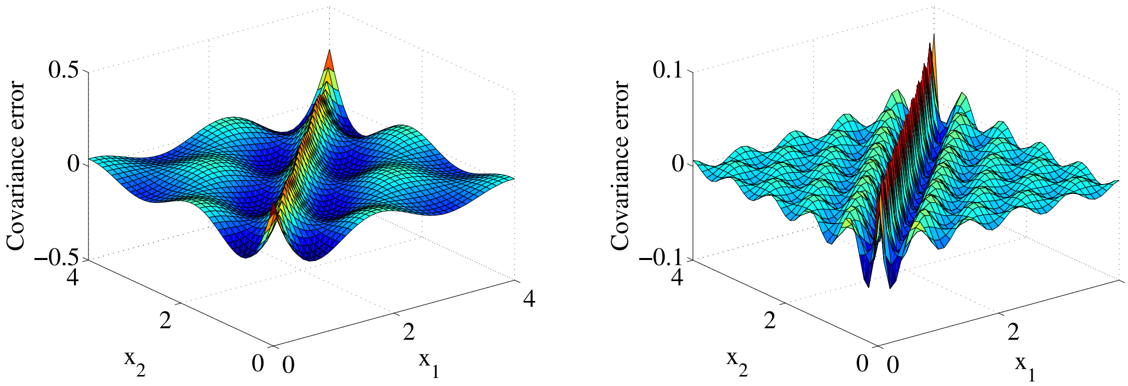

Figure. 2.5: Covariance surface error approximation with number of terms equal to 4 (LHS) and 10 (RHS).

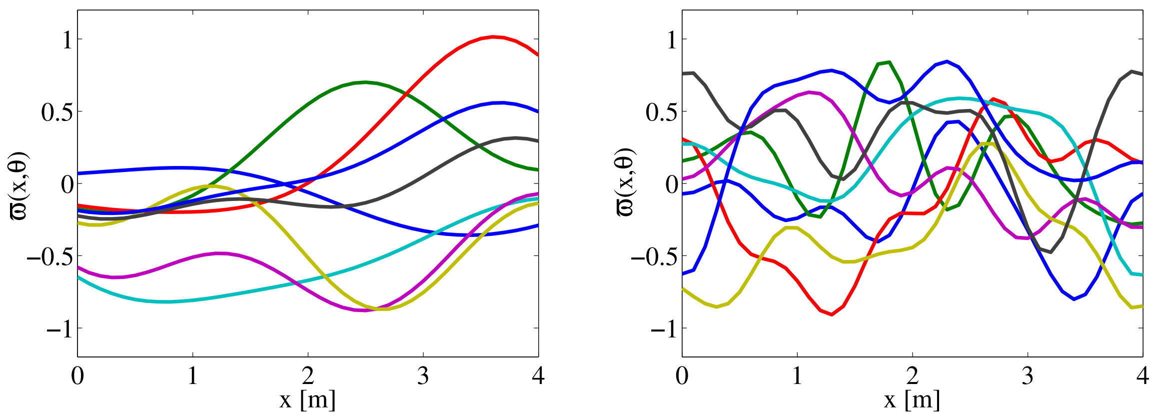

Figure. 2.6: $N-th$ order realizations of the Gaussian process $\varpi_j(\mathbf{x},\theta)$ with $N=4$ (LHS) and $N=10$ (RHS).

KL expansion and Fig. 2.5 shows the error estimated by the difference between the exact covariance function with approximated covariance function. As the number of terms increased from 4 to 10 an approximation of the covariance function improve and the error reduce.

Figure 2.6 shows some random realizations of the process described in equation (2.22). In the following, the process $\varpi_j(\mathbf{x},\theta)$ is assumed to be Gaussian and the highest N eigenvalues and eigenfunctions of the covariance function are performed as previous simulations. Huang et al. (2001) presented a closer analysis by using KL to modelled a random field, among them he showed the effect of using analytical and numerical eigen-solutions to simulate processes, as well the influence in ratio of the length of the process over the correlation parameter, the form of the covariance function, and the number of terms used in the KL expansion.

2.4.1 Memoryless transformation

In the KL expansion the approximation of the random field involve a finite number of uncorrelated random variables, which will be uncorrelated and independent if the PDF of the process is Gaussian. Hence the random field approximated using KL expansion provides a way to parametrize a Gaussian process by a finite number of independent Gaussian random variables (Xiu, 2010). However, Gaussian distribution is not applicable for most of the physical systems which, on the contrary, are expected to be characterized by non-Gaussian behaviour (Vio et al., 2001). This section will consider the problem of the analytical and numerical simulation of non-Gaussian processes. There are three categories of methods used to simulate non-Gaussian random processes. Memoryless transformation, method of the linear filters and method of the non-linear filters. Here, a non-Gaussian process is expressed as a memoryless transformation of an underlying Gaussian process. The memoryless transformation is a nonlinear mapping from a specified probability distribution to a target or request distribution. This method allows to start with any distribution and convert it into a target one. The application regards a correlated Gaussian stochastic process and produces a correlated process having the distributional characteristics of interest. In more detail and with application of the memoryless transformation method can be found in the works of Grigoriu (1998); Vio et al. (2001); Schevenels et al. (2004); Weinberg and L.Gunn (2011).

The main idea of most techniques for simulating a non-Gaussian scalar or random field $R(t)$, with a prescribed correlation function, $C_R(\tau)$, and a prescribed one-dimensional marginal $\mathrm{F}_R(x)$, is to generate a zero-mean and unit-variance, scalar or Gaussian random field $Z(t)$ with a prefixed correlation structure $C_Z(\tau)$ and a mapping (transformation) $Z(t) \longrightarrow R(t)$. This mapping is called memoryless transformation,

$$R(t) = F_R^{-1} Z(t) \tag{2.35}$$

Numerical technique

In cases where the analytical solution is not practicable, it is necessary to resort to numerical methods. The covariance function $C(x_1,x_2)$ of the underlying Gaussian process is chosen so that the transformation leads to a non-Gaussian process with the proposed covariance function $C_R(x_1,x_2)$. A non-Gaussian process $Y(x,\theta)$ is expressed as a memoryless transformation of an underlying standard Gaussian process $Z(\mathbf{x},\theta)$ by means of the Cumulative Density Functions (CDF) of both processes:

$$Y(\mathbf{x},\theta) = \mathrm{F}_{Yx}^{-1}(\mathrm{F}_Z(Z(\mathbf{x},\theta))) \tag{2.36}$$

where $\mathrm{F}_{Yx}(y)$is the marginal CDF of the non-Gaussian process and $\mathrm{F}_Z(z)$ is the standard Gaussian CDF. An approximation of the transformation can be obtained in terms of the one-dimensional Hermite polynomials of order P:

$$Y(\mathbf{x},\theta) \approx \sum_{n=0}^{P} a_n(\mathbf{x})\mathtt{h}_n(Z(\mathbf{x},\theta))) \tag{2.37}$$

where the one-dimensional Hermite polynomials is defined by Rodirguez's formula (Hazewinkel, 1989; Xiu and Karniadakis, 2003), so that the orthonormal one-dimensional Hermite polynomials are expresses by

$$\mathtt{h}_n(z) = \frac{1}{\sqrt{n!}}\mathtt{H}_n(z) \tag{2.38}$$

and the polynomial $\mathtt{H}_n(z)$ follows from the recurrence relation:

$$\mathtt{H}_0(z) = 1 \qquad \mathtt{H}_1(z) = z \qquad \mathtt{H}_{n+1}(z) = z\mathtt{H}_n(z) - n\mathtt{H}_{n-1}(z) \tag{2.39}$$

The coefficients $a_n(x)_n$ are obtained based on the orthogonality of the Hermite polynomials $\mathtt{h}_n(z)_n$ and $Y(\mathbf{x},\theta)$ is a stationary process. It can be expressed as:

$$a_n(\mathbf{x}) = \int_{\infty}^{\infty} \mathrm{F}_{Yx}^{-1}(\mathrm{F}_Z(z))\mathtt{h}_n(z)p_Z(z)dz \tag{2.40}$$

Equating the covariance of equation (2.37) leads to:

$$C_R(\mathbf{x}_1,\mathbf{x}_2) \approx \sum_{n=0}^{P} a_n(\mathbf{x}_1)a_n(\mathbf{x}_2)[C(\mathbf{x}_1,\mathbf{x}_2)]^n \tag{2.41}$$

If $Y(\mathbf{x},\theta)$ is a stationary process, then the covariance can be reduced to:

$$C_R(\Delta\mathbf{x}) \approx \sum_{n=0}^{P} a_n^2[C(\Delta\mathbf{x})]^n \tag{2.42}$$

Applications

Certainly, an efficient way to apply the memoryless transformation for generating $R(t)$ is in analytical handling. However, this is a difficult approach and it has been possible to find out the analytical relationship between $C_Z(\tau)$ and $C_R(\tau)$ only in a limited number of cases. Here an example using a Lognormal distribution is approached, more analytical applications can be found in Vio et al. (2001). Supposing a homogeneous, zero-mean, unit-variance Gaussian field $Z(t)$, with correlation function $C_Z(\tau)$, an analytical non-Gaussian, in this case, Lognormal distribution based, is expressed as

$$\mathtt{L}(t) = e^{\mu+\sigma Z(t)} \tag{2.43}$$

The one-dimensional marginal Lognormal PDF with mean and variance are given by,

$$p_{\mathrm{L}}(l) = \frac{1}{l\sigma\sqrt{2\pi}} e^{-(\ln l-\mu)^2/(2\sigma^2)} \tag{2.44}$$

$$\mu_{\mathrm{L}} = e^{\mu+\sigma^2/2} \tag{2.45}$$

$$\sigma_{\mathrm{L}}^2 = e^{2\mu+\sigma^2}(e^{\sigma^2}-1) \tag{2.46}$$

The relation between $C_L(\tau)$ and $C_Z(\tau)$ proposed by Grigoriu (1995) can be expressed of the form

$$C_{\mathrm{L}}(\tau) = \frac{e^{\sigma^2 C_Z(\tau)}-1}{e^{\sigma^2}-1} \tag{2.47}$$

In the above formulations, the analytical and numerical approaches of the memoryless transformation are presented. In a first analysis, the closed-form relationship between the input and output autocorrelations of the memoryless transformation (equations 2.43- 2.47) with numerical treatment (equations 2.36- 2.42) are compared, both used to simulate the Lognormal distribution. In the second one, we investigate the influence of the Hermite polynomial degree related with covariance convergence, and approximation of the target PDF obtained from a Gaussian based distribution.

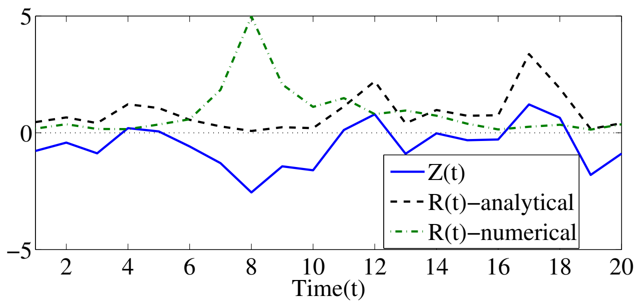

Figure. 2.7: Gaussian translation process with target distribution (Lognormal) calculated by using analytical and numerical approaches.

Figure 2.7 provides a comparison between of a homogeneous Gaussian field (with zero mean, unit variance, and exponential covariance function) and the result of the memoryless transformation with a series truncation by using numerical and analytical methods. Figure 2.9 shows the covariance function compared with numerical and analytical methods. These two techniques showed good conditions satisfied a translation process to match a target covariance. Grigoriu (1998) proposed a different method of this presented, although closer results presented with his paper are found. Both results present by Grigoriu is illustrated in figures 2.8 and 2.9.

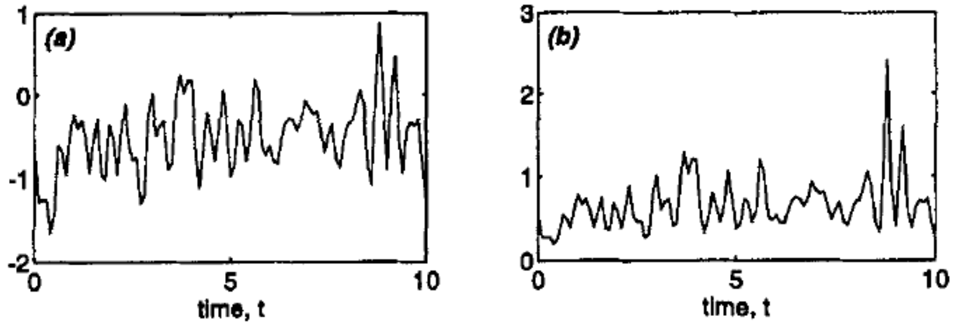

Figure. 2.8: Gaussian translation process with target distribution (Lognormal): (a)Realization of $Z(t)$; (b) Realization of $Y(t)$. Reprinted from Grigoriu (1998).

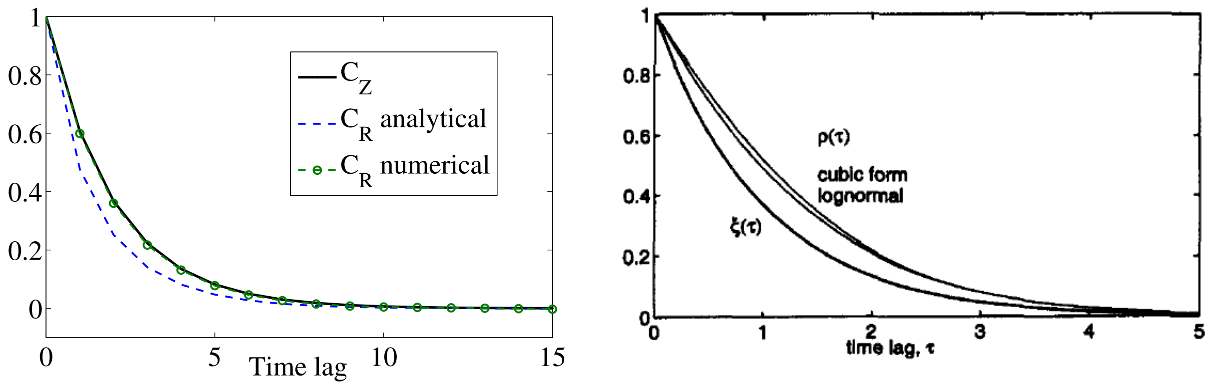

Figure. 2.9: At the left-hand side, covariance function C_Z compared with analytical and numerical approximated covariation function (C_R). At right-hand side, target covariance function $\xi(T)$ and covariance function $\rho(T)$ for translation process, reprinted from Grigoriu (1998).

Next, the case of target PDF is Gamma distribution is analysed. Figure 2.10 shows the Gamma translation process expressed as a transformation of a homogeneous Gaussian field with a zero mean, unit variance, and exponential covariance function. The memoryless transformation is used based on numerical method.

In the numerical memoryless approach, the projection of this transformation is based on Hermite polynomial degree fucntion (equation 2.42). In view that an approximation of $Y(x,\theta)$ as a function of $Z(x,\theta)$ improves as the Hermite polynomial degree increases. Figure 2.11 shows the correlation function convergence related with the $P-th$ order Hermite polynomial approximation with $P = 1, 3, 5$ and 7. The transformation with $3rd - 7th$ order shows good agreement with the input correlation. It was performed for 10000 realizations of the underlying Gaussian process $Z(x,\theta)$. Figure 2.12 illustrates the marginal PDF $p_Y(y)$ of the zero mean non-Gaussian process as obtained by a transformation of the underlying Gaussian process. The 1st order approximation of the transformation leads to a Gaussian process as higher degree the convergence with targed PDF are rise. The 5th order approximation leads to a process with an acceptable marginal PDF while with 7th order approximation is the curves practically coincident.

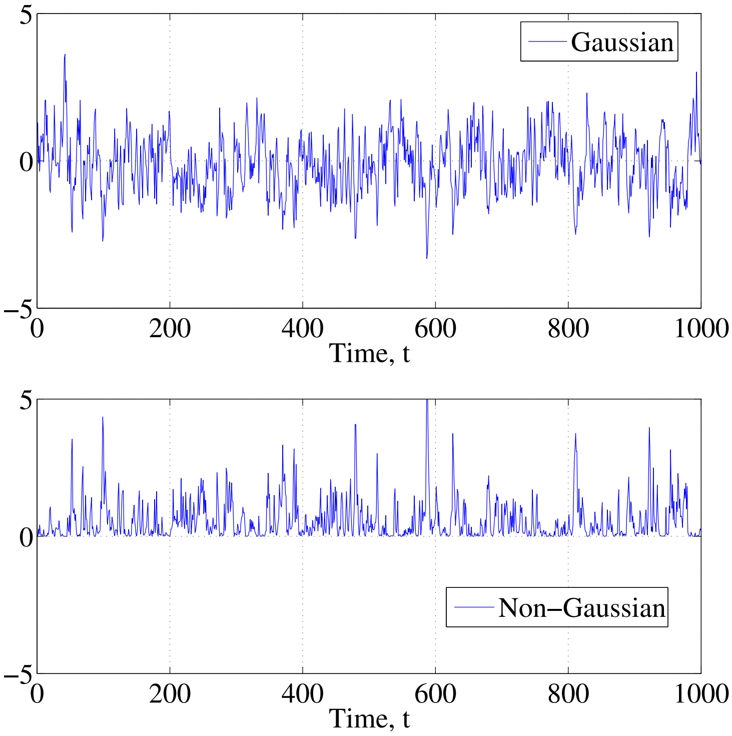

Figure. 2.10: Gaussian translation process with target (Gamma) distribution by using numerical approaches with 3rd order in Hermite polynomial.

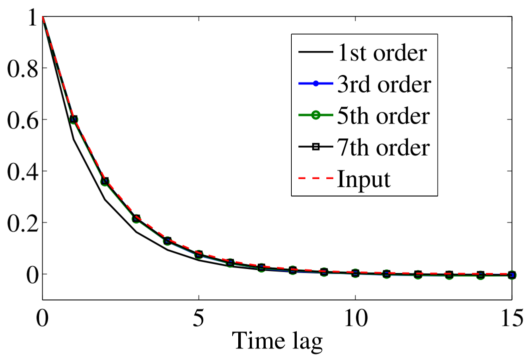

Figure. 2.11: Input covariance function compared with approximated covariance function estimated with 1, to 7 order in Hermite polynomial.

The problem of the dynamic system is analysed by using a Gaussian random field and a non-Gaussian random field target with a Gamma distribution. In this numerical test, a free-free rod structure is modelled with a two node rod spectral element. Stochastic variabilities are considered for the rod longitudinal rigidity EA. The "measured" FRF is obtained by simulating the inertance FRF with unitary force excitation at node 2 and response at node 1. The unperturbed physical and geometrical properties of the rod are given by: $L = 3.0$ m, $h = 0.02$ m, $b = 0.02$ m, $E = 71$ GPa, $\eta = 0.01$, and $\rho = 2700$ kg/m^3. It is assumed that the variations from the unperturbed value of EA can be modelled as homogeneous Gaussian random field and a non-Gaussian random field. For numerical calculations we considered 1, 10 and 20% coefficient of

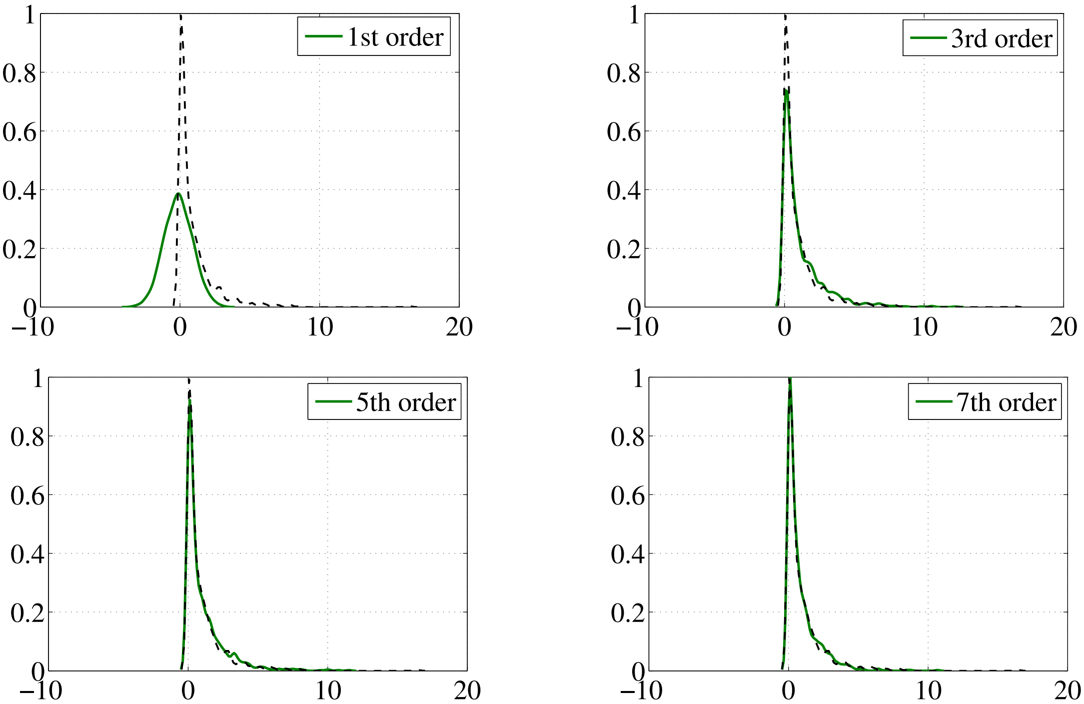

Figure. 2.12: Approximation of the $Y(t)$ PDF obtained through the Hermite polynomial expansion with P ranging from 1 to 7. In all tests the of samples is equal to 10000.

covariation with a correlation length of $\mathtt{b} = L/3$. The correlation length value is chosen associated with the number of terms, as mentioned in Section 2.4. Monte Carlo simulation is used as solver with 10000 realizations.

In the works of (Poirion and Soize, 1999) and (Schevenels et al., 2004) the authors show the implications of the assumption of a stiffness as a Gaussian distribution on the stochastic properties which has a non-Gaussian probabilistic base. According to them, the mean value of the system response does not present a high divergence. However, the discrepancy appear in the variance. Figure 2.13 shows FRF comparison among deterministic, stochastic model via Gaussian random field and stochastic model based on non-Gaussian random field. The results achieved enhance the work present by Poirion and Soize and Schevenels et al.. The mean value responses do not present difference between the models using Gaussian and non-Gaussian distribution. However, in the standard variation the results diverge between Gaussian and non-Gaussian distribution for EA which means a non-physically sound. Once that the rigidity do not assume negative values the difference is visible in the standard deviation as demonstrated.

Schevenels et al. (2004) shown analytically proof that the variance of the response of a system modelled stiffness with a Gaussian distribution the results goes to infinite. This is not physically sound as it implies that the expected value of the deformation energy of the system is undefined. In the other hand, by associating the longitudinal rigidity with Gamma marginal PDF ensures incorrect physical behaviour. Consider now the frequency response function at a given frequency (2800Hz). The longitudinal stiffness is simulated with Gaussian and Gamma

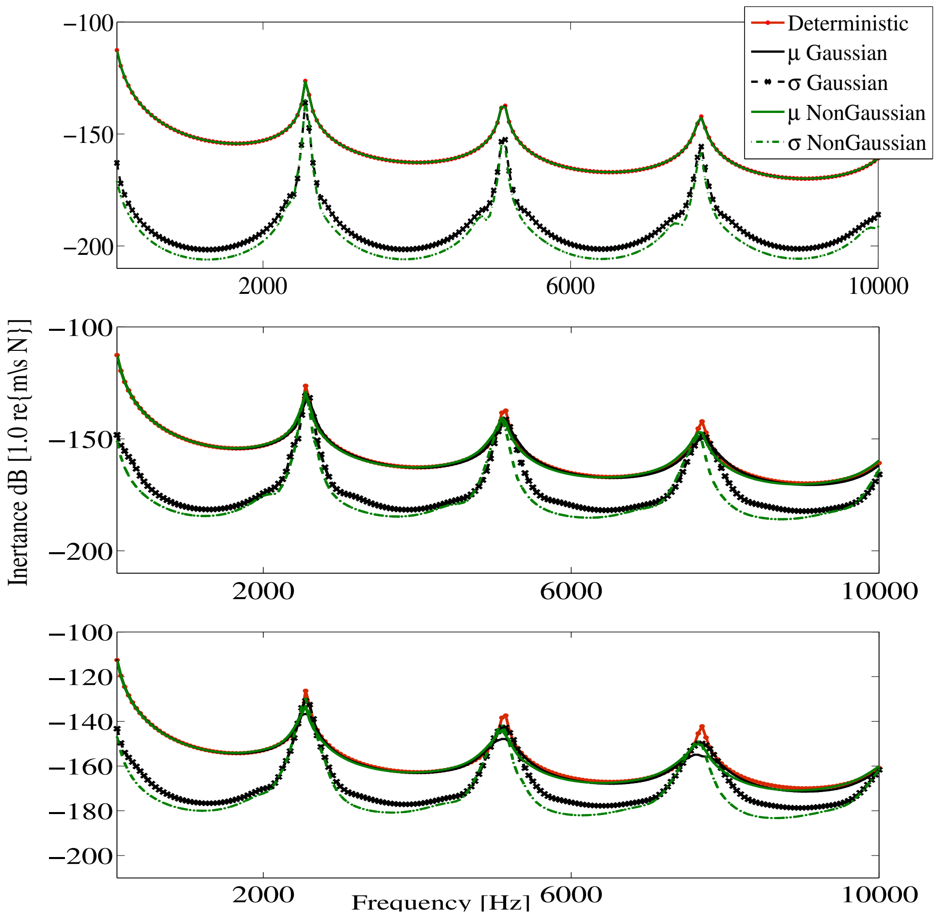

Figure. 2.13: Deterministic, mean and standard deviation Inertance FRF (H^{12}) of the rod modelled with Gaussian and non-Gaussian random field. Covariance of $1, 10$ and 20%, respectively.

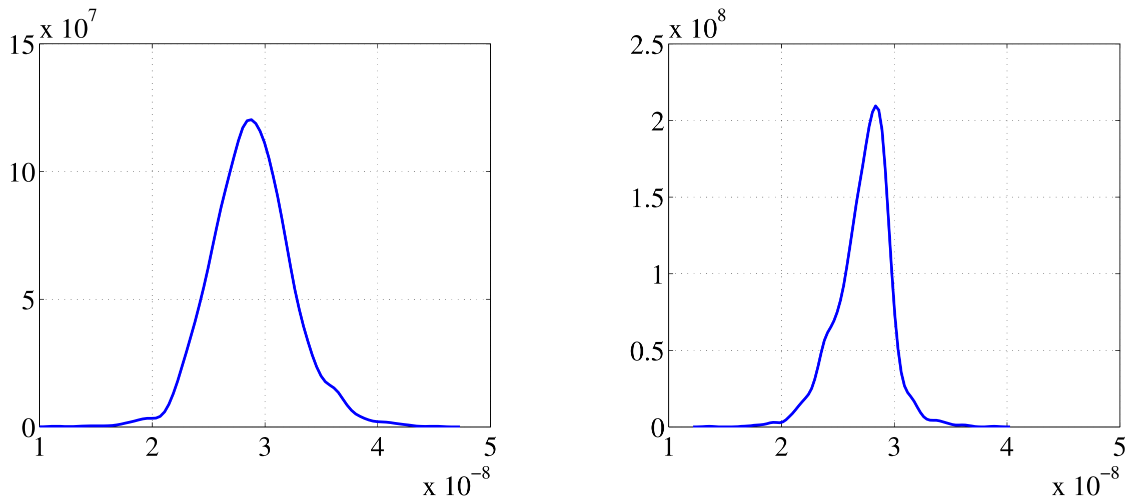

Figure. 2.14: Estimation for the PDF of the FRF ($\mathbf{H}^{21}$) at frequency (2800Hz) by using a Gaussian random field (LRS) and a non-Gaussian random field (RHS).

marginal PDFs, the estimations of PDFs for the FRF at frequency $2800Hz$ is shown in figure 2.14. The Gaussian marginal PDF of the FRF is symmetric with respect to the mean value. Consequently, the longitudinal stiffness also presents this symmetry. The results of in the analysis agreed with the outcomes presented in the literature. The mean-square convergence analysis

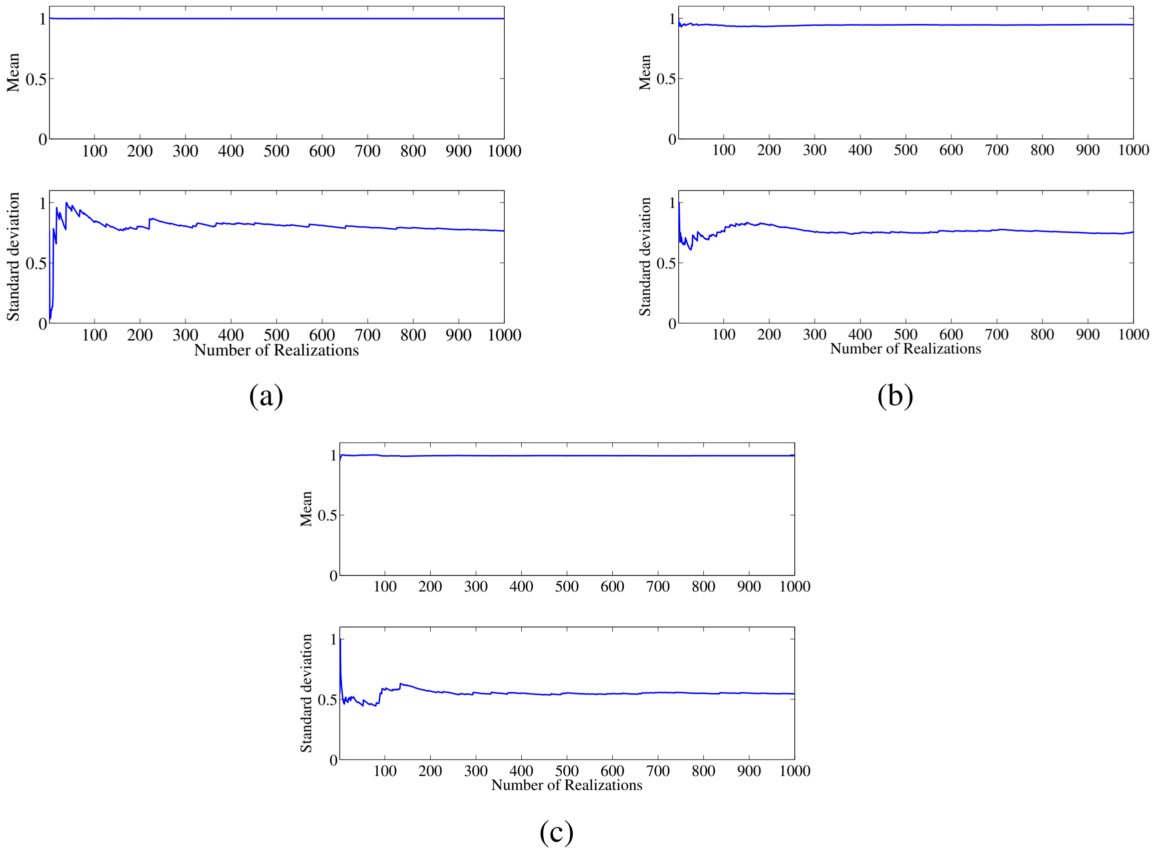

Figure. 2.15: Mean and standard deviation convergence analyse for COVs of 1%(a), 5%(b), and 10%(c)

with respect to independent realizations is calculated with equation 2.7. Mean and standard deviation square convergence are displayed in figure 2.15 for 1000 samples. The mean converges fast in all cases, using around 60 samples for COV of 1% and 180 samples for COV of 10%. However, a higher number of sample are necessary to the standard deviation convergence, it is around 300.

2.5 Polynomial Chaos expansion

The Polynomial Chaos is a stochastic solution projected on a basis of orthogonal polynomials whose variables are orthonormal. The polynomial basis properties generate a linear equation system through projections on the polynomial (Ghanem and Brzakala, 1996; Ghanem and Kruger, 1996). The stochastic problem can be formulated as in (Ghanem and Spanos, 1991; Dessombz et al., 2000), where the solution leads to the mean and variance of the system. Wiener introduced the homogeneous chaos to represent a second order Gaussian random process. Ghanem and Spanos were the first to use this technique in mechanical problems with a spectral approach (Ghanem and Spanos, 1991) in a Gaussian basis. Xiu and Karniadakis (2003) used the Askey scheme to generalize Wiener's PC expansion to non-Gaussian stochastic processes, which include various orthogonal polynomials. The work conducted here follows the approach proposed by Ghanem and Spanos (1991). The stochastic problem can be formulated as

$$\mathbf{\Lambda}(\mathbf{x},\theta)u(\mathbf{x},\theta) = [\mathbf{L}(\mathbf{x}) + \mathbf{\Pi}(\mathbf{x},\theta)]u(\mathbf{x},\theta) = \mathrm{f}(\mathbf{x},\theta), \tag{2.48}$$

where $\mathbf{L}$ represents the deterministic part and $\mathbf{\Pi}$ is stochastic part of the operator $\mathbf{\Lambda}$. The mean goal is solving the linear problem of equation (2.48) for $u(\mathbf{x},\theta)$ is a function of $F(\mathbf{x},\theta)$, where $\mathbf{x}$ belongs to the Hilbert space defined by $H = \{f/f : D \to \mathbb{R}\}$, and θ is based on probability space (Ω,Ψ,P), the space of measurable functions is given as $\Theta = \{g/g : \Omega \to \mathbb{R}\}$.

Considering $\{\xi(\theta)\}_{i=1}^{\infty}$ as a set of Gaussian orthonormal random variables and Ψ_n a polynomial chaos of order p, it can be show that any element $w(\theta)$ defined in Θ space is represented as

$$\begin{aligned} w(\theta) = a_0\Psi_0 + \sum_{i=1}^{\infty} a_{i1}\Psi_1(\xi_{i1}(\theta)) + \sum_{i_1=1}^{\infty}\sum_{i_2=1}^{i_1} a_{i_1 i_2}\Psi_2(\xi_{i1}(\theta),\xi_{i2}(\theta)) \\ + \sum_{i_1=1}^{\infty}\sum_{i_2=1}^{i_1}\sum_{i_3=1}^{i_2} a_{i_1 i_2 i_3}\Psi_3(\xi_{i1}(\theta),\xi_{i2}(\theta),\xi_{i3}(\theta)) + \dots, \end{aligned} \tag{2.49}$$

Equation 2.49 can be written in a truncated by

$$w(\theta) = \sum_{i=1}^{Q} a_i\Psi_i. \tag{2.50}$$

The polynomial chaos Ψ_i correspond to the multidimensional Hermite polynomials expressed as:

$$\Psi_n(\xi_{i1},\dots,\xi_{ip}) = (-1)^n e^{1/2\xi^t\xi}\frac{\partial^n}{\partial\xi_{i_1}\dots\partial\xi_{i_n}}e^{-1/2\xi^t\xi}, \tag{2.51}$$

where ξ consist of n orthonormal Gaussian random variable. For the polynomial chaos with order $0, 1$ and 2 it have:

$$\Psi_0 = 1 \qquad \text{Ordem } 0 \tag{2.52}$$

$$\Psi_1 = \xi_1 \quad ,\Psi_2 = \xi_2 \qquad \text{Ordem } 1 \tag{2.53}$$

$$\Psi_3 = \xi_1^2 - 1 \quad ,\Psi_4 = \xi_1\xi_2 \quad ,\Psi_5 = \xi_2^2 - 1 \qquad \text{Ordem } 2. \tag{2.54}$$

A KL expansion series is appropriated when the correlation funtion of $\mathbf{\Pi}$ is known. In general, mechanical problems can be written as:

$$([\mathbf{L}] + \sum_{q=1}^{Q} \xi_q [\Pi_q])\{u\} = \{\mathrm{f}\}. \tag{2.55}$$

A vector decomposition $\{u\}$ over polynomial chaos of $Q-$variables is given by:

$$\{u\} = \sum_{n=0}^{N} \{u_n\} \Psi_n(\{\xi_i\}_{i=1}^{Q}) \tag{2.56}$$

Substituting equation (2.56) in equation (2.55), multiplying by Ψ_m, calculating the mean values, and applying the properties of orthogonality properties of the polynomial, it has:

$$\{u_m\}\langle \Psi_m^2 \rangle = \sum_{q=1}^{Q} \sum_{n=0}^{N} \{u_n\}\langle \xi_q \Psi_n \Psi_m \rangle [\Pi_q] = \{\mathrm{f}\}\langle \Psi_m \rangle \tag{2.57}$$

It is important to observe that $\langle \Psi_m^2 \rangle$ and $\langle \xi_q \Psi_n \Psi_m \rangle$ values have to be calculated only once and applied in the whole formulation.

For all $m = 0, \ldots, N$ obtained from equation (2.57), it leads to a system of $(N+1)$ linear algebraic equations, which solution corresponds vectors $\{u_n\}$ (Dessombz et al., 2001). With all $\{u_n\}$ known, mean and variance of $\{u\}$ are given by

$$\mu = \{u_0\} \tag{2.58}$$

and

$$\sigma^2 = \sum_{n=1}^{N} \{u_n^2\}\langle \Psi_n^2 \rangle \tag{2.59}$$

2.6 Stochastic Finite Element Method (SFEM)

The stochastic finite element method (SFEM) proposed by Ghanem and Spanos (1991) is an extension of the classical deterministic FEM approach to the stochastic framework (Stefanou, 2009). In this section, a brief overview will be presented. Considering a static mechanical problem of a stochastic system solved by SFEM, where the equilibrium equations of the system are:

$$\mathbf{K}(\theta)\mathbf{u}(\theta) = \mathbf{f} \tag{2.60}$$

where $\mathbf{K}(\theta)$ is the stochastic stiffness matrix linearly dependent on a random process $(\varpi(\mathbf{x},\theta))$ defined in equation (2.22). The relation is given as $\mathbf{K}(\theta) = \kappa(\varpi(\mathbf{x},\theta))$, then stiffness matrix is decomposed accordingly:

$$\mathbf{K}(\theta) = \kappa(\varpi(\mathbf{x},\theta)) \approx \mathbf{K}_0 + \sum_{j=1}^{M} \mathbf{K}_j \xi_j(\theta) \tag{2.61}$$

Rewriting equation (2.60) in function of equation (2.61) the SFEM equation of the static problem is obtained as

$$\left(\mathbf{K}_0 + \sum_{j=1}^{M} \mathbf{K}_j \xi_j(\theta) \right) \mathbf{u}(\theta) = \mathbf{f} \tag{2.62}$$

deterministic part of the stiffness is represented by $\mathbf{K}_0$.

2.7 Closure

Statistical methods used in this thesis have been presented in this chapter. A literature review of the main methods applied was also described. Some methods that treat uncertainty quantification in the outputs of a numerical model due to uncertainty in the input parameters have been introduced. The MC simulation and Moment Equations method were formulated and commented, as well as simulation methods for Gaussian stochastic and non-Gaussian random field. The Gaussian random process translation for a target distribution was given based on a Memoryless transformation. This technique was detailed in an analytical and numerical version. The numerical application demonstrates the translation process and analysis of the correlation function convergence related with Hermite polynomial order. A numerical example presented the result of using a dynamic system modelled by Gaussian random field and non-Gaussian random field. Polynomial chaos (PC) expansion and the stochastic finite element method (SFEM) were also rescued in this section.

3 Stochastic Spectral Element Method

3.1 Introduction

The Spectral Element Method (SEM) (Doyle, 1997; Lee, 2004) is based on the analytical solution of the wave displacement equation written in the frequency domain. The element is tailored with the same matrix ideas of the Finite Element Method (FEM), where the interpolation functions are the exact solutions of wave equation. This approach has been called by different names, such as the Dynamic Stiffness Method (Paz, 1980; Banerjee and Williams, 1985; Banerjee, 1989; Banerjee and Williams, 1992; Banerjee and Fisher, 1992; Ferguson and Pilkey, 1993a,b; Banerjee and Williams, 1995; Manohar and Adhikari, 1998; Banerjee, 1997; Adhikari and Manohar, 2000), Spectral Element Method (Doyle, 1989; Lee, 2004; Gopalakrishnan et al., 2007), Spectral Finite Element Method (Finnveden, 1997) and Dynamic Finite Element Method (Hashemi et al., 1999; Hashemi and Richard, 2000). Built-up structures with geometrically uniform members can be modeled by a single spectral element (Figure 3.1), which implies into reduce significantly the total number of degrees of freedom as compared to other similar methods. It can be shown that one spectral element is equivalent to an infinite number of finite elements. The method is based on the wave equation it performs well at medium and high-frequency bands. However, there are still some drawbacks, such as difficulties to model non-uniform members, as well as apply arbitrary boundary conditions for 2D and 3D elements. The probabilistic treatment of uncertainties using Spectral Element Method is recent and some works in this sense includes the papers of Adhikari and Friswell (2010), Ajith and Gopalakrishnan (2010), and this thesis.

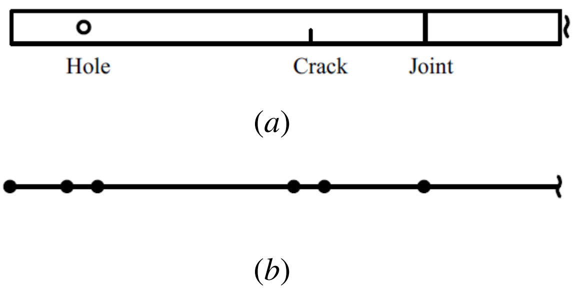

Figure. 3.1: Built-up structure representation: (a) physical structure; (b) spectral element model.

Due to the SEM being the exact solution solution of differential equations governing the problem, it became a suitable technique to model structural damage detection. In general, changes in either global or local structural properties can be associated with an imperfection or damage. Over the last decades, many works have been performed to develop vibration-based Non-Destructive Evaluation (NDE) tests and Structural Healthy Monitoring (SHM) methods, which allows a damage to be localized and quantified from variations in modal parameters and dynamic responses (Doebling et al., 1998; Montalvao et al., 2006). These techniques are well suited to detect large damages rather than small damages like a crack. A structural crack does not impose appreciable changes at low-frequency band and the global structural behavior is unaffected. However, the presence of a crack in the structure introduces a local flexibility that affects its vibration response. It also generates more evident changes in the elastic waves that propagate in the structure. Consequently, in the last two decades, damage detection researches are focused on methods that use elastic wave propagation at medium and high frequency bands (Krawczuk, 2002; Krawczuk et al., 2006a; Ostachowicz, 2008; Santos et al., 2008; Su and Ye, 2009). They use the inherent material property that discontinuities, such as a crack, generate changes in the elastic waves propagating in the structure. There are some particular advantages of elastic wave-based damage detection, such as their capacity to propagate over significant distances and high sensitivity to discontinuities near the wave propagation path. Studies related with structural damage detection including stochastic and wave propagation approaches have also been developed. In recent works of Fabro et al. (2010); NG et al. (2011); Flynn et al. (2012); Machado and Santos (2015) used wave propagation to detect damage in the presence of structural randomness.

The central theme of this Chapter is the formulation of the Spectral Element Method for stochastic and deterministic dynamic systems. A general derivation of the spectral element matrices is presented (Section 3.2). The spectral element for an undamaged rod in a deterministic and stochastic case are formulated in Section 3.3. Deterministic spectral element for a damaged rod and the new stochastic spectral element for a damaged rod are demonstrated in Section 3.4. Also described in Section 3.5 the deterministic and stochastic spectral element for an undamaged beam, deterministic spectral element for damaged beam, and the new stochastic spectral element for a damaged beam in Section 3.6.

3.2 General formulation

Stochastic SEM general derivation presented in this section is based on the formulation given by Adhikari (2011). Consider $(\Theta,\mathcal{F},P)$ a probability space with $\theta \in \Theta$ denoting a sampling point in the sampling space Θ; $\mathcal{F}$ is the complete σ-algebra over the subsets of Θ; and P is the probability measure. A distributed parameter linear damped dynamic system is governed by a linear partial differential equation (Meirovitch, 1997) given by:

$$\rho(\mathbf{r},t)\frac{\partial^2 U(\mathbf{r},t)}{\partial t^2} + L_1(\theta)\frac{\partial U(\mathbf{r},t)}{\partial t} + L_2(\theta)U(\mathbf{r},t) = q(\mathbf{r},t), \quad \mathbf{r} \in \mathcal{D}, \tag{3.1}$$

where $U(\mathbf{r},t)$ is the displacement variable, $\rho(\mathbf{r},t)$ is the random mass distribution, $q(\mathbf{r},t)$ is the distributed time-varying forcing function, L_1 is the random spatial self-adjoint damping operator, L_2 is the random spatial self-adjoint stiffness operator, $\mathbf{r} \in \mathbb{R}^d$ is the spacial position vector, $d \leq 3$ is the dimension of the model specified in some domain $\mathcal{D}$ (Figure 3.2), and t is time domain.

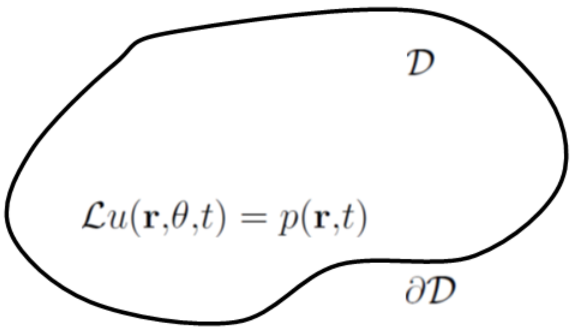

Figure. 3.2: Domain and boundary surface of differential operator describing stochastic dynamic system.

Supposing now the homogeneous deterministic system of equation (3.1) without any external force (Meirovitch, 1997) given by,

$$\rho_0 \frac{\partial^2 U(\mathbf{r},t)}{\partial t^2} + L_{10} \frac{\partial U(\mathbf{r},t)}{\partial t} + L_{20} U(\mathbf{r},t) = 0 \tag{3.2}$$

with a suitable homogeneous boundary and initial conditions. Taking the Fourier transform of equation (3.2) and considering zero initial conditions, one has

$$-\omega^2 \rho_0 u(\mathbf{r},\omega) + i\omega L_{10}\{u(\mathbf{r},\omega)\} + L_{20}\{u(\mathbf{r},\omega)\} = 0 \tag{3.3}$$

where $\omega \in [0;\Omega]$ is the circular frequency and $\Omega \in \mathbb{R}$ is the maximum frequency.

Like FEM, consider that frequency-dependent displacement within an element is interpolated from the nodal displacements as

$$u_e(\mathbf{r},\omega) = \mathbf{g}(\mathbf{r},\omega)\mathbf{d}(\omega) \tag{3.4}$$

where $\mathbf{d}(\omega) \in \mathbb{C}^n$ is the nodal displacement vector, $\mathbf{g}(\mathbf{r},\omega) \in \mathbb{C}^n$ is the vector of frequency-dependent shape functions, and n is number of the nodal degrees-of-freedom. Suppose the $s_j \in \mathbb{C}$, $j = 1,2,\ldots,m$ are the basis functions that exactly satisfy equation (3.3) where m is the order of the ordinary differential equation (3.3). The shape function vector can be expressed as

$$\mathbf{g}(\mathbf{r},\omega) = \mathbf{s}(\mathbf{r},\omega)\mathbf{\Gamma}(\omega) \tag{3.5}$$

where the vector $\mathbf{s}(\mathbf{r},\omega) = \{s_j(\mathbf{r},\omega)\}^T; \forall j = 1,2,...,m$; and the complex matrix, $\mathbf{\Gamma}(\omega) \in \mathbb{C}^{n\times m}$, depend on the boundary conditions. The derivation of $\mathbf{\Gamma}(\omega)$ for the axial vibration of rods and bending vibration of beams are given in the next sections.

Extending the weak-form of the finite-element approach to the complex domain, the frequency-dependent $n \times n$ complex random stiffness, mass, and damping element matrices can be obtained as:

$$\mathbf{K}(\omega,\theta) = \int_{\mathcal{D}} k_s(\mathbf{r},\theta)\mathcal{L}_2\{\mathbf{g}^T(\mathbf{r},\omega)\}\mathcal{L}_2\{\mathbf{g}(\mathbf{r},\omega)\}d\mathbf{r} \tag{3.6}$$

$$\mathbf{M}(\omega,\theta) = \int_{\mathcal{D}} \rho(\mathbf{r},\theta)\mathbf{g}^T(\mathbf{r},\omega)\mathbf{g}(\mathbf{r},\omega)d\mathbf{r} \tag{3.7}$$

and

$$\mathbf{C}(\omega,\theta) = \int_{\mathcal{D}} c_s(\mathbf{r},\omega)\mathcal{L}_1\{\mathbf{g}^T(\mathbf{r},\omega)\}\mathcal{L}_1\{\mathbf{g}(\mathbf{r},\omega)\}d\mathbf{r} \tag{3.8}$$

where $(\bullet)^T$ is the matrix transpose, $(k_s(\mathbf{r},\theta)) : (\mathbb{R}^d \times \Theta) \to \mathbb{R}$ is the random distributed stiffness parameter, $(c_s(\mathbf{r},\theta)) : (\mathbb{R}^d \times \Theta) \to \mathbb{R}$ is the random distributed damping, $\mathcal{L}_2\{\bullet\}$ is the strain energy operator, and $\mathcal{L}_1\{\bullet\}$ is the energy dissipation operator.

The uncertainty parameters are modelled within the framework of a random field and will be treated similar to the Stochastic Finite Element Method (SFEM) proposed by Ghanem and Spanos (1991). The random fields, $k_s(\mathbf{r},\theta)$, $c_s(\mathbf{r},\theta)$, and $\rho(\mathbf{r},\theta)$ are expanded by using the Karhunen-Loève expansion with a finite number of terms. Each complex element matrices can be expanded in a spectral series. For example, in the case of the stiffness element matrix, it can be obtained as:

$$\mathbf{K}(\omega,\theta) = \mathbf{K}_0(\omega) + \sum_{j=1}^{N_K} \xi_{Kj}(\theta)\mathbf{K}_j(\omega) \tag{3.9}$$

where N_K is the number of terms kept in the KL expansion, $\xi_{Kj}(\theta)$, are uncorrelated Gaussian random variables with zero mean and unitary standard deviation. The complex deterministic symmetric stiffness element matrix can be obtained as:

$$\begin{aligned}\mathbf{K}_0(\omega) &= \int_{\mathcal{D}} k_{s_0}(\mathbf{r},\theta)\mathcal{L}_2\{\mathbf{g}^T(\mathbf{r},\omega)\}\mathcal{L}_2\{\mathbf{g}(\mathbf{r},\omega)\}d\mathbf{r} \\ &= \mathbf{\Gamma}^T(\omega)\left(\int_{\mathcal{D}} k_s(\mathbf{r},\theta)\mathcal{L}_2\{\mathbf{s}^T(\mathbf{r},\omega)\}\mathcal{L}_2\{\mathbf{s}(\mathbf{r},\omega)\}d\mathbf{r}\right)\mathbf{\Gamma}(\omega)\end{aligned} \tag{3.10}$$

and

$$\begin{aligned}\mathbf{K}_j(\omega) &= \sqrt{\lambda_{K_j}}\int_{\mathcal{D}} \varphi_{K_j}(\mathbf{r})\mathcal{L}_2\{\mathbf{g}^T(\mathbf{r},\omega)\}\mathcal{L}_2\{\mathbf{g}(\mathbf{r},\omega)\}d\mathbf{r} \\ &= \sqrt{\lambda_{K_j}}\,\mathbf{\Gamma}^T(\omega)\left(\int_{\mathcal{D}} \varphi_{K_j}(\mathbf{r})\mathcal{L}_2\{\mathbf{s}^T(\mathbf{r},\omega)\}\mathcal{L}_2\{\mathbf{s}(\mathbf{r},\omega)\}d\mathbf{r}\right)\mathbf{\Gamma}(\omega) \\ &\forall\, j = 1,2,\ldots,M_K\end{aligned} \tag{3.11}$$

where λ_{Kj} and φ_{Kj} are the eigenvalues and eigenfunctions satisfying the integral equation of covariance function (equation 2.21). Equivalent equations corresponding to mass and damping element matrices can also be obtained in a similar manner.

The eigenfunction expressions are valid within the specific domains defined. One needs to change the coordinate to use them in equation (3.11). Once the element stiffness, mass, and damping matrices are obtained the global matrices can be achieved as in the standard FEM. Closed-form expression of the eigenfunctions are available for only a few specific correlation functions and with simple boundaries only. In these cases the integral in equation (3.11) may be obtained in a closed-form. However, in general, the integral equation governing the eigenfunctions has to be solved numerically. For such general cases, the element matrices should be obtained by using numerical integration techniques.

The spectral dynamic stiffness element matrix can be expressed as a function of the stiffness, damping and mass element matrices by,

$$\mathbf{D}(\omega,\theta) = \mathbf{K}(\omega,\theta) + i\omega\mathbf{C}(\omega,\theta) - \omega^2\mathbf{M}(\omega,\theta) \tag{3.12}$$

or applying the proposed approach,

$$\mathbf{D}(\omega,\theta) = \mathbf{D}_0(\omega) + \sum_j \xi_j(\theta)\mathbf{D}_j(\omega) \tag{3.13}$$

where $\mathbf{D}(\omega,\theta)$ is a complex random symmetric element matrix, which needs to be inverted for every ω to obtain the dynamic response. In the next sections this approach will be applied to the undamaged and damage rod and beam models.

3.3 Undamaged rod

Deterministic

In this section, the fundamental equations are derived for a longitudinal wave propagation in an undamaged rod, a more extensive formulation can be found in Doyle (1997); Lee (2004). The elementary rod theory considers this structure as long and slender, and assumes that it supports only 1-D axial stress. Figure 3.3 shows an elastic two nodes rod element with one degree-of-freedom/node, uniform rectangular cross-section subjected to dynamic forces. For this formulation all variables are assumed to be deterministic. The undamped equilibrium equation at frequency domain can be written as (Doyle, 1997):

$$EA\frac{d^2u(x)}{dx^2} + \omega^2\rho Au(x) = q(x), \tag{3.14}$$

where E is the Young's modulus, A is the cross-section area, ρ is the mass density, u is the longitudinal displacement, q is the distributed external force, and ω is the circular frequency. A structural internal damping is introduced into the rod formulation by adding into the variable

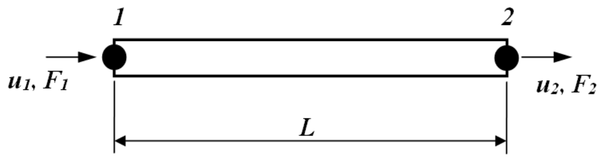

Figure. 3.3: Two nodes undamaged rod spectral element.

$(E \cdot A)$ a deterministic part $(E_0 \cdot A_0)$ weighted by a complex damping factor $(i\eta, i = \sqrt{-1})$, to obtain $EA = E \cdot A + (E_0 \cdot A_0)i\eta$. The subscripts 1 and 2 denote values at the element rod node numbers 1 and 2, respectively. The homogeneous solution of equation (3.14) is given by,

$$u(x) = a_1 e^{-ikx} + a_2 e^{-ik(L-x)} = \mathbf{s}(x,\omega)\mathbf{a}, \tag{3.15}$$

where L is the rod element length, $k = \omega/c$ is the wavenumber, which corresponds to the wave that is propagating in the a direction. The phase speed $c = \sqrt{\rho A/EA}$, in this case the propagation is said to be non-dispersive as all frequency components travel at the same speed, so that the shape of the traveling wave remains the same, and

$$\mathbf{s}(x,\omega) = \{e^{-ikx} \; e^{-ik(L-x)}\}, \tag{3.16}$$

and

$$\mathbf{a} = \begin{Bmatrix} a_1 \\ a_2 \end{Bmatrix} \tag{3.17}$$

The spectral nodal displacements of the rod can be related with the displacement field as,

$$\mathbf{d} = \begin{Bmatrix} u_1 \\ u_2 \end{Bmatrix} = \begin{Bmatrix} u(0) \\ u(L) \end{Bmatrix} \tag{3.18}$$

By substituting equation (3.15) into the right side of equation (3.18) it has

$$\mathbf{d} = \begin{bmatrix} \mathbf{s}(0,\omega) \\ \mathbf{s}(L,\omega) \end{bmatrix} \mathbf{a} = \mathbf{G}(\omega)\mathbf{a} \tag{3.19}$$

where

$$\mathbf{G}(\omega) = \begin{bmatrix} 1 & e^{-ikL} \\ e^{-ikL} & 1 \end{bmatrix} \tag{3.20}$$

The frequency-dependent displacement within an element is interpolated from the nodal displacement vector $\mathbf{d}$, by eliminating the constant vector $\mathbf{a}$ from equations (3.15) by using equation (3.19) it has

$$u(x,\omega) = \mathbf{g}(x,\omega)\mathbf{d}, \tag{3.21}$$

where the shape functions are given by,

$$\mathbf{g}(x,\omega) = \mathbf{s}(x,\omega)\mathbf{G}^{-1}(\omega) = \{g_1 \; g_2\} \tag{3.22}$$

with $g_1 = \csc(kL)\sin[k(L-x)]$ and $g_2 = \csc(kL)\sin(kx)$. A generalized longitudinal displacement at any arbitrary point in the rod element is given by,

$$u(x) = g_1(x)u_1 + g_2(x)u_2 \tag{3.23}$$

By comparing equation (3.22) with (3.5) it is obtained,

$$\mathbf{\Gamma}(\omega) = \mathbf{G}^{-1}(\omega) = \frac{1}{1-e^{-2ikL}}\begin{bmatrix} 1 & e^{ikL} \\ e^{ikL} & 1 \end{bmatrix}. \tag{3.24}$$

For the undamaged rod model, the stiffness operator is given by $\mathcal{L}_2(\bullet) = \partial(\bullet)/\partial x$ and assuming constant nominal values for the deterministic stiffness parameter, $k_{s_0}(\mathbf{r}) = EA_0$. Then, from equation (3.10), one obtains

$$\begin{aligned} \mathbf{K}_0(\omega) &= EA_0\,\mathbf{\Gamma}^T(\omega)\left[\int_0^L \mathbf{s}'^T(x,\omega)\mathbf{s}'(x,\omega)dx\right]\mathbf{\Gamma}(\omega), \qquad (3.25) \\ &= \frac{EA_0k}{2}\begin{bmatrix} \csc^2(kL)(2kL+\sin(2kL))/2 & -(kL\cot(kL)+1)\csc(kL) \\ -(kL\cot(kL)+1)\csc(kL) & \csc^2(kL)(2kL+\sin(2kL))/2 \end{bmatrix}. \end{aligned}$$

where $(\bullet)'$ is space first derivative. Applying this concept in a similar way the deterministic mass matrix is obtained as:

$$\begin{aligned} \mathbf{M}_0(\omega) &= \rho A_0\,\mathbf{\Gamma}^T(\omega)\left[\int_0^L \mathbf{s}^T(x,\omega)\mathbf{s}(x,\omega)dx\right]\mathbf{\Gamma}(\omega), \qquad (3.26) \\ &= \frac{\rho A_0}{2k}\begin{bmatrix} (\cot(kL)-kL\csc^2(kL)) & (kL\cot(kL)-1)\csc(kL) \\ (kL\cot(kL)-1)\csc(kL) & (\cot(kL)-kL\csc^2(kL)) \end{bmatrix}. \end{aligned}$$

Stochastic

The same undamaged rod analytical model considered in the deterministic formulation is used here for the stochastic formulation. Now it is assumed that cross-section area, mass density, and Young's modulus are random variables spatially distributed. Therefore, the longitudinal rigidity (EA) and mass per unit of length (ρA) are assumed as a random field respectively of the form

$$EA(x,\theta) = EA_0[1+\varepsilon_1\varpi_1(x,\theta)] \tag{3.27}$$

$$\rho A(x,\theta) = \rho A_0[1 + \varepsilon_2 \varpi_2(x,\theta)] \tag{3.28}$$

where the subscript 0 indicates the underlying baseline model and ε_i are deterministic constants ($0 < \varepsilon_i \ll 1, i = 1,2$). The random fields $\varpi_i(x,\theta), i = 1,2$ are taken to have zero mean, unit standard deviation and covariance $C_{ij}(\xi)$. Since, $EA(x,\theta)$ and $\rho A(x,\theta)$ are strictly positive, $\varpi_i(x,\theta)$ are required to satisfy the probability condition $\mathrm{P}[1+\varepsilon_i \varpi_i(x,\theta) \leq 0] = 0$. To obtain the matrices associated with the random components, for each j, two different matrices correspond to the two eigenfunctions defined in equations (2.26) and (2.27). Following equation (3.9), we can express the element stiffness and mass matrix as

$$\mathbf{K}(\omega,\theta) = \mathbf{K}_0(\omega) + \Delta\mathbf{K}(\omega,\theta) \tag{3.29}$$

$$\mathbf{M}(\omega,\theta) = \mathbf{M}_0(\omega) + \Delta\mathbf{M}(\omega,\theta) \tag{3.30}$$

where $\Delta\mathbf{K}_e(\omega,\theta)$ and $\Delta\mathbf{M}_e(\omega,\theta)$ are the random part of the stiffness and mass matrices. From the KL expansion and equations (3.27) and (3.28), this matrices can be conveniently expressed as,

$$\Delta\mathbf{K}(\omega,\theta) = \varepsilon_1 \sum_{j=1}^{N} \xi_{Kj}(\theta)\sqrt{\lambda_{Kj}}\mathbf{K}_j(\omega) \tag{3.31}$$

$$\Delta\mathbf{M}(\omega,\theta) = \varepsilon_2 \sum_{j=1}^{N} \xi_{Mj}(\theta)\sqrt{\lambda_{Mj}}\mathbf{M}_j(\omega) \tag{3.32}$$

where N is the number of terms kept in the KL expansion, $\xi_{Kj}(\theta)$ and $\xi_{Mj}(\theta)$ are uncorrelated Gaussian random variables with zero mean and unit standard deviation. From the equation (3.11) the matrices $\mathbf{K}_j(\omega)$ and $\mathbf{M}_j(\omega)$ are written as

$$\mathbf{K}_j(\omega) = EA_0\mathbf{\Gamma}^T(\omega)\left[\int_0^L \varphi_{Kj}(x_e + x)\mathbf{s}'(x,\omega)^T\mathbf{s}'(x,\omega)dx\right]\mathbf{\Gamma}(\omega), \tag{3.33}$$

$$\mathbf{M}_j(\omega) = \rho A_0\mathbf{\Gamma}^T(\omega)\left[\int_0^L \varphi_{Mj}(x_e + x)\mathbf{s}(x,\omega)^T\mathbf{s}(x,\omega)dx\right]\mathbf{\Gamma}(\omega), \tag{3.34}$$

Substituting equations (2.26) and (2.27) in equations (3.33) and (3.34) the random part of the dynamic stiffness element matrix in a closed-form expressions with odd j is

$$\begin{aligned}\mathbf{K}_j^{odd}(\omega) &= \frac{EA_0}{\sqrt{\mathsf{a} + \frac{\sin(2w_j\mathsf{a})}{2w_j}}}\mathbf{\Gamma}^T(\omega)\left[\int_0^L \cos(\omega_j(x_e + x))\mathbf{s}'(x,\omega)^T\mathbf{s}'(x,\omega)dx\right]\mathbf{\Gamma}(\omega)\\ &= \frac{EA_0}{\sqrt{\mathsf{a} + \frac{\sin(2w_j\mathsf{a})}{2w_j}}}\begin{bmatrix} Ko_{11} & Ko_{12} \\ Sym & Ko_{22}\end{bmatrix}\end{aligned} \tag{3.35}$$

$$\mathbf{M}_j^{odd}(\omega) = \frac{\rho A_0}{\sqrt{\mathsf{a} + \frac{\sin(2w_j\mathsf{a})}{2w_j}}}\mathbf{\Gamma}^T(\omega)\left[\int_0^L \cos(\omega_j(x_e+x))\mathbf{s}(x,\omega)^T\mathbf{s}(x,\omega)dx\right]\mathbf{\Gamma}(\omega)$$

$$= \frac{\rho A_0}{\sqrt{\mathsf{a} + \frac{\sin(2w_j\mathsf{a})}{2w_j}}}\begin{bmatrix} Mo_{11} & Mo_{12} \\ Sym & Mo_{22} \end{bmatrix} \tag{3.36}$$

and for even j it is given by,

$$\mathbf{K}_j^{even}(\omega) = \frac{EA_0}{\sqrt{\mathsf{a} - \frac{\sin(2w_j\mathsf{a})}{2w_j}}}\mathbf{\Gamma}^T(\omega)\left[\int_0^L \sin(\omega_j(x_e+x))\mathbf{s}'(x,\omega)^T\mathbf{s}'(x,\omega)dx\right]\mathbf{\Gamma}(\omega)$$

$$= \frac{EA_0}{\sqrt{\mathsf{a} - \frac{\sin(2w_j\mathsf{a})}{2w_j}}}\begin{bmatrix} Ke_{11} & Ke_{12} \\ Sym & Ke_{22} \end{bmatrix} \tag{3.37}$$

$$\mathbf{M}_j^{even}(\omega) = \frac{\rho A_0}{\sqrt{\mathsf{a} - \frac{\sin(2w_j\mathsf{a})}{2w_j}}}\mathbf{\Gamma}^T(\omega)\left[\int_0^L \sin(\omega_j(x_e+x))\mathbf{s}(x,\omega)^T\mathbf{s}(x,\omega)dx\right]\mathbf{\Gamma}(\omega)$$

$$= \frac{\rho A_0}{\sqrt{\mathsf{a} - \frac{\sin(2w_j\mathsf{a})}{2w_j}}}\begin{bmatrix} Me_{11} & Me_{12} \\ Sym & Me_{22} \end{bmatrix} \tag{3.38}$$

The exact closed-form expression of the elements, $Ko_{ij}, Mo_{ij}, Ke_{ij}, Me_{ij}$, of these four matrices (equations 3.35 to 3.38) are given in Appendix A.1.1.

Substituting equations (3.35 to 3.38) into the equations (3.29 to 3.32) the stochastic spectral undamaged rod element stiffness and mass matrices, $\mathbf{K}(\omega,\theta)$ and $\mathbf{M}(\omega,\theta)$, can be obtained. And then, the stochastic spectral undamaged rod element dynaic stiffness matrix is obtained as:

$$\mathbf{D}(\omega,\theta) = \mathbf{K}(\omega,\theta) - \omega^2\mathbf{M}(\omega,\theta) \tag{3.39}$$

3.4 Damaged rod

Deterministic

This section presents the formulation for a spectral rod element with a transverse, open and non-propagating crack (Krawczuk et al., 2006a,b). Figure 3.4 shows a two-nodes rod element with uniform rectangular cross-section, length L, crack position L_1, crack depth α. The crack is modelled as a dimensionless and local crack flexibility, Θ, which is calculated by Castigliano's theorem and the laws of fracture mechanics Tada et al. (1973).

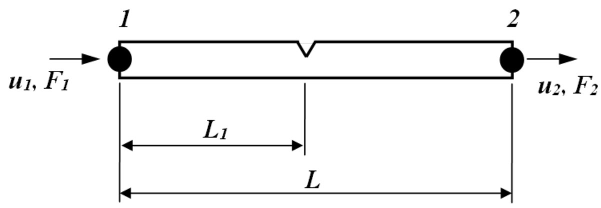

Figure. 3.4: Two-node damaged rod spectral element

The homogeneous displacement solution for equation (3.14) applied for this element must be described in two parts, one for the left-hand side of the crack and other for the right-hand side of the crack, respectively,

$$\begin{aligned} u_L(x) &= a_1 e^{-ikx} + a_2 e^{-ik(L_1-x)} \qquad (0 \leq x \leq L_1) \\ &= \mathbf{s}_L(x;\omega)\mathbf{a}_L, \end{aligned} \tag{3.40}$$

where $\mathbf{s}_L(x,\omega) = [e^{-ikx}\ e^{-ik(L_1-x)}]$; and $\mathbf{a}_L = \{a_1\ a_2\}^T$.

$$\begin{aligned} u_R(x) &= a_3 e^{-ik(x+L_1)} + a_4 e^{-ik[L-(L_1+x)]} \qquad (0 \leq x \leq L-L_1) \\ &= \mathbf{s}_R(x;\omega)\mathbf{a}_R, \end{aligned} \tag{3.41}$$

where $\mathbf{s}_R(x,\omega) = [e^{-ik(x+L_1)}\ e^{-ik[L-(L_1+x)]}$; and $\mathbf{a}_R = \{a_3\ a_4\}^T$. Writing the equations (3.40) and (3.41) in matrix form it has,

$$\left\{ \begin{array}{c} u_L(x) \\ u_R(x) \end{array} \right\} = \left[\begin{array}{cc} \mathbf{s}_L(x,\omega) & \mathbf{0} \\ \mathbf{0} & \mathbf{s}_R(x,\omega) \end{array} \right] \left\{ \begin{array}{c} \mathbf{a}_L \\ \mathbf{a}_R \end{array} \right\} = \mathbf{s}_d(x,\omega)\mathbf{a}_d \tag{3.42}$$

The coefficients vector $\mathbf{a}_d$ can be calculated as a function of the nodal spectral displacements using the element boundary and compatibility conditions:

- Element left-end $u_L(0) = u_1$
- Element cracked cross-section $u_L(L_1) - u_R(0) = \Theta \frac{\partial u}{\partial x}$
- Element non-cracked cross-section $\frac{\partial u_L(L_1)}{\partial x} = \frac{\partial u_R(0)}{\partial x}$
- Element right-end $u_R(L - L_1) = u_2$

Coupling the damaged element left and right-hand sides (equations 3.40 and 3.41) and applying boundary and compatibility conditions it has,

$$\underbrace{\begin{bmatrix} 1 & e^{-ikL_1} & 0 & 0 \\ (ik\Theta-1)e^{-ikL_1} & (ik\Theta-1) & e^{-ikL_1} & e^{-ik(L-L_1)} \\ -ike^{-ikL_1} & ik & ike^{-ikL_1} & -ike^{-ik(L-L_1)} \\ 0 & 0 & e^{-ikL} & 1 \end{bmatrix}}_{\mathbf{G}_d} \begin{Bmatrix} a_1 \\ a_2 \\ a_3 \\ a_4 \end{Bmatrix} = \begin{Bmatrix} u_1 \\ 0 \\ 0 \\ u_2 \end{Bmatrix} \tag{3.43}$$

From the equation (3.43) it can relate the coefficients vector $\mathbf{a}_d$ to the nodal spectral displacements as:

$$\begin{Bmatrix} a_1 \\ a_2 \\ a_3 \\ a_4 \end{Bmatrix} = \mathbf{G}_{dr}^{-1} \begin{Bmatrix} u_1 \\ u_2 \end{Bmatrix} \tag{3.44}$$

where $\mathbf{G}_{dr}^{-1}$ is given by

$$\mathbf{G}_d^{-1} = \begin{bmatrix} \frac{e^{ikL_1}((k\Theta-i)\cos(k(L-L_1))+\sin(k(L-L_1)))}{k\Theta(\cos(kL)+\cos(k(L-2L_1)))+2\sin(kL)} & \frac{i}{k\Theta(\cos(kL)+\cos(k(L-2L_1)))+2\sin(kL)} \\ \frac{(k\Theta+i)\cos(k(L-L_1))+\sin(k(L-L_1))}{k\Theta(\cos(kL)+\cos(k(L-2L_1)))+2\sin(kL)} & -\frac{ie^{ikL_1}}{k\Theta(\cos(kL)+\cos(k(L-2L_1)))+2\sin(kL)} \\ -\frac{ie^{ikL}}{k\Theta(\cos(kL)+\cos(k(L-2L_1)))+2\sin(kL)} & \frac{\left(1+e^{2ikL_1}\right)k\Theta+2i}{2k\Theta(\cos(kL)+\cos(k(L-2L_1)))+4\sin(kL)} \\ \frac{i}{k\Theta(\cos(kL)+\cos(k(L-2L_1)))+2\sin(kL)} & \frac{e^{ik(L-L_1)}((k\Theta-i)\cos(kL_1)+\sin(kL_1))}{k\Theta(\cos(kL)+\cos(k(L-2L_1)))+2\sin(kL)} \end{bmatrix} \tag{3.45}$$

Equation (3.44) can be rewritten in a compact form as:

$$\mathbf{a}_d = \mathbf{G}_{dr}^{-1}\mathbf{d}_d \tag{3.46}$$

Substituting equation (3.46) in (3.42) it has,

$$\begin{Bmatrix} u_L(x) \\ u_R(x) \end{Bmatrix} = \begin{bmatrix} \mathbf{s}_L(x,\omega) & \mathbf{0} \\ \mathbf{0} & \mathbf{s}_R(x,\omega) \end{bmatrix} \mathbf{G}_{dr}^{-1}\mathbf{d}_d = \mathbf{g}_d(x,\omega)\mathbf{d}_d \tag{3.47}$$

Comparing equation (3.47) with (3.5) it is obtained,

$$\mathbf{\Gamma}_d(\omega) = \mathbf{G}_{dr}^{-1} \tag{3.48}$$

For the damaged rod model, the stiffness operator is given by $\mathcal{L}_2(\bullet) = \partial(\bullet)/\partial x$ and assuming constant nominal values for the deterministic stiffness parameter, $k_{s_0}(\mathbf{r}) = EA_0$. Due spacial reference in damaged model to be different for left-hand side and right-hand side of the crack position, equation (3.10) must be integrated according to the corresponding limits, then

$$\mathbf{K}_{0_d}(\omega) = EA_0\, \mathbf{\Gamma}_d^T(\omega) \begin{bmatrix} \int_0^{L_1} \mathbf{s}'^T_L(x,\omega)\mathbf{s}'_L(x,\omega)dx & \mathbf{0} \\ \mathbf{0} & \int_0^{(L-L_1)} \mathbf{s}'^T_R(x,\omega)\mathbf{s}'_R(x,\omega)dx \end{bmatrix} \mathbf{\Gamma}_d(\omega), \tag{3.49}$$

By taking the integral,

$$\mathbf{K}_{0_d}(\omega) = \frac{EA_0}{2}\mathbf{\Gamma}_d^T(\omega) \begin{bmatrix} ik(1-e^{-2ikL_1}) & 2k^2L_1e^{-ikL_1} & 0 & 0 \\ 2k^2L_1e^{-ikL_1} & ik(1-e^{-2ikL_1}) & 0 & 0 \\ 0 & 0 & ik(e^{-2ikL_1}-e^{-2ikL}) & 2k^2(L-L_1)e^{-ikL} \\ 0 & 0 & 2k^2(L-L_1)e^{-ikL} & ik(1-e^{2ik(L_1-L)}) \end{bmatrix} \mathbf{\Gamma}_d(\omega) \tag{3.50}$$

Simplifying,

$$\mathbf{K}_{0_d}(\omega) = \begin{bmatrix} K_{0d_{11}} & K_{0d_{12}} \\ sym & K_{0d_{22}} \end{bmatrix} \tag{3.51}$$

Similarly, the damage rod deterministic mass element matrix is obtained as:

$$\mathbf{M}_{0_d}(\omega) = \rho A_0\, \mathbf{\Gamma}_d^T(\omega) \begin{bmatrix} \int_0^{L_1} \mathbf{s}^T_L(x,\omega)\mathbf{s}_L(x,\omega)dx & \mathbf{0} \\ \mathbf{0} & \int_0^{(L-L_1)} \mathbf{s}^T_R(x,\omega)\mathbf{s}_R(x,\omega)dx \end{bmatrix} \mathbf{\Gamma}_d(\omega), \tag{3.52}$$

By taking the integral

$$\mathbf{M}_{e0_d}(\omega) = \frac{\rho A_0}{2}\mathbf{\Gamma}_d^T(\omega) \begin{bmatrix} i(e^{-2ikL_1-1})/k & 2L_1e^{-ikL_1} & 0 & 0 \\ 2L_1e^{-ikL_1} & i(e^{-2ikL_1}-1)/k & 0 & 0 \\ 0 & 0 & i(e^{-2ikL}-e^{-2ikL_1})/k & 2(L-L_1)e^{-ikL} \\ 0 & 0 & 2(L-L_1)e^{-ikL} & i(e^{2ik(L_1-L)}-1)/k \end{bmatrix} \mathbf{\Gamma}_d(\omega), \tag{3.53}$$

and simplifying it has,

$$\mathbf{M}_{0_d}(\omega) = \begin{bmatrix} M_{0d_{11}} & M_{0d_{12}} \\ sym & M_{0d_{22}}. \end{bmatrix} \tag{3.54}$$

The exact closed-form expression of the elements, $K_{0d_{ij}}$ and $M_{0d_{ij}}$, of these two matrices (equations 3.51 to 3.54) are given in Appendix A.2.1.

Crack flexibility

The crack flexibility coefficient (Θ) is calculated using Castigliano's theorem, where the flexibility at the crack location for the one-dimensional rod spectral element is obtained by (Tada et al., 1973; Gdoutos, 1993):

$$c_{ij} = \frac{\partial^2 \mathtt{U}}{\partial S_i \partial S_j}, \qquad i = j = 1. \tag{3.55}$$

where $\mathtt{U}$ denotes the elastic strain energy due to the crack and S are the independent nodal force on the element. By considering that only crack mode I (Tada et al., 1973) is present in the rod element, the elastic strain energy is specified as:

$$\mathtt{U} = \frac{1}{E}\int_{\mathsf{A}} \mathtt{K}_{\mathtt{I}}^2 d\mathsf{A} \tag{3.56}$$

where $\mathsf{A} = bh$ is the damaged area and $\mathtt{K}_{\mathtt{I}}$ is the stress intensity factor corresponding to the crack mode I, which can be represented by,

$$\mathtt{K}_I = \frac{S_1}{bh}\sqrt{\pi a} f\left(\frac{a}{h}\right) \tag{3.57}$$

Figure 3.5 shows the damaged rod element cross-section at the crack position, including the new geometric definition of crack depth as $\alpha = a/h$. The crack flexibility coefficient is written

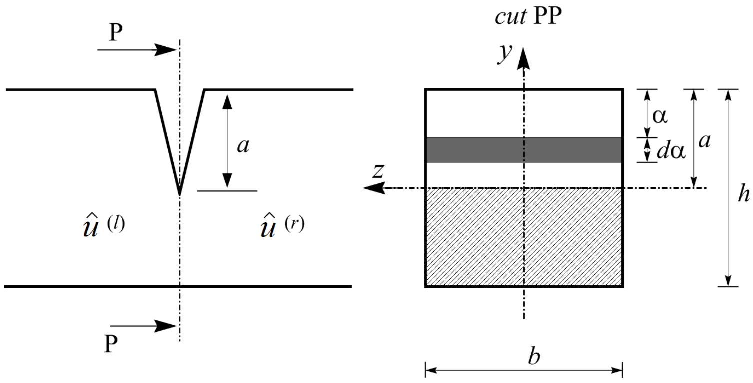

Figure. 3.5: Damaged rod cross-section at the crack position

as a function of crack depth as,

$$\mathtt{c}(\alpha) = \frac{2\pi}{Eb}\int_0^{\alpha} \alpha \mathtt{f}(\alpha)^2 d\alpha, \tag{3.58}$$

where the function $\mathtt{f}$ is given by,

$$\mathtt{f}(\alpha) = 1.122 - 0.231\alpha + 10.550\alpha^2 - 21.710\alpha^3 + 30.382\alpha^4. \tag{3.59}$$

It can be shown that the dimensionless local crack flexibility can be written as $\Theta = \mathtt{c}EA$. Then, from the equation (3.123) it has

$$\Theta = 2\pi h \int_0^{\alpha} \alpha \mathtt{f}(\alpha)^2 d\alpha \tag{3.60}$$

Stochastic

Likewise the stochastic undamaged rod formulation (Section3.5), the stochastic dynamic stiffness element matrix for the damaged rod spectral element, $\mathbf{D}_d(\omega,\theta)$, is developed. The same damaged rod analytical model considered in the deterministic formulation is used here for the stochastic formulation. Also, it is assumed that A, E, ρ are random variables, and EA and ρA are random fields. Following equation (3.9), we can express the stochastic damaged rod stiffness and mass element matrices, respectively, as:

$$\mathbf{K}_d(\omega,\theta) = \mathbf{K}_{0_d}(\omega) + \Delta\mathbf{K}_d(\omega,\theta) \tag{3.61}$$

$$\mathbf{M}_d(\omega,\theta) = \mathbf{M}_{0_d}(\omega) + \Delta\mathbf{M}_d(\omega,\theta) \tag{3.62}$$

From the KL expansion and equations (3.27) and (3.28) it has,

$$\Delta\mathbf{K}_d(\omega,\theta) = \varepsilon_1 \sum_{j=1}^{N} \xi_{Kj}(\theta)\sqrt{\lambda_{Kj}}\mathbf{K}_{j_d}(\omega) \tag{3.63}$$

$$\Delta\mathbf{M}_d(\omega,\theta) = \varepsilon_2 \sum_{j=1}^{N} \xi_{Mj}(\theta)\sqrt{\lambda_{Mj}}\mathbf{M}_{j_d}(\omega) \tag{3.64}$$

where N is the number of terms kept in the KL expansion, $\xi_{Kj}(\theta)$ and $\xi_{Mj}(\theta)$ are uncorrelated Gaussian random variables with zero mean and unit standard deviation. From the equation (3.11) and considering different limits of integration (left and right-hand sides) for the damaged rod model it has,

$$\mathbf{K}_{j_d}(\omega) = EA_0\mathbf{\Gamma}_d^T(\omega)\begin{bmatrix} \mathbf{Sk}_L & \mathbf{0} \\ \mathbf{0} & \mathbf{Sk}_R \end{bmatrix}\mathbf{\Gamma}_d(\omega), \tag{3.65}$$

$$\mathbf{M}_{j_d}(\omega) = \rho A_0\mathbf{\Gamma}_d^T(\omega)\begin{bmatrix} \mathbf{Sm}_L & \mathbf{0} \\ \mathbf{0} & \mathbf{Sm}_R \end{bmatrix}\mathbf{\Gamma}_d(\omega), \tag{3.66}$$

where

$$\begin{aligned}
\mathbf{Sk}_L &= \int_0^{L_1} \varphi_{Kj}(x_e+x)\mathbf{s}'^T_L(x,\omega)\mathbf{s}'_L(x,\omega)dx \\
\mathbf{Sk}_R &= \int_0^{(L-L_1)} \varphi_{Kj}(x_e+x)\mathbf{s}'^T_R(x,\omega)\mathbf{s}'_R(x,\omega)dx \\
\mathbf{Sm}_L &= \int_0^{L_1} \varphi_{Mj}(x_e+x)\mathbf{s}^T_L(x,\omega)\mathbf{s}_L(x,\omega)dx \\
\mathbf{Sm}_R &= \int_0^{(L-L_1)} \varphi_{Mj}(x_e+x)\mathbf{s}^T_R(x,\omega)\mathbf{s}_R(x,\omega)dx
\end{aligned} \tag{3.67}$$

Substituting equations (2.26) and (2.27) in equations (3.67) the random part of the stiffness and mass matrices as closed-form expressions can be obtained. However, these are huge closed-form expressions not easily workable. Then, equations (3.65) and (3.66) were solved with MATHEMATICA® software and exported directly to the MATLAB® code to obtain the numerical solutions. As a matter of understanding and results reproducibility it is shown here only the matrices form of $\mathbf{Sk}_L$,$\mathbf{Sk}_R$,$\mathbf{Sm}_L$,$\mathbf{Sm}_R$ for each j^{th} terms respecting the odd and even KL formulation. By considering odd j it has,

$$\mathbf{Sk}_L^{odd}(\omega) = \frac{EA_0}{\sqrt{\mathsf{a} + \frac{\sin(2w_j\mathsf{a})}{2w_j}}} \begin{bmatrix} SkLo_{11} & SkLo_{12} \\ Sym & SkLo_{22} \end{bmatrix} \tag{3.68}$$

$$\mathbf{Sk}_R^{odd}(\omega) = \frac{EA_0}{\sqrt{\mathsf{a} + \frac{\sin(2w_j\mathsf{a})}{2w_j}}} \begin{bmatrix} SkRo_{11} & SkRo_{12} \\ Sym & SkRo_{22} \end{bmatrix} \tag{3.69}$$

$$\mathbf{Sm}_L^{odd}(\omega) = \frac{\rho A_0}{\sqrt{\mathsf{a} + \frac{\sin(2w_j\mathsf{a})}{2w_j}}} \begin{bmatrix} SmLo_{11} & SmLo_{12} \\ Sym & SmLo_{22} \end{bmatrix} \tag{3.70}$$

$$\mathbf{Sm}_R^{odd}(\omega) = \frac{\rho A_0}{\sqrt{\mathsf{a} + \frac{\sin(2w_j\mathsf{a})}{2w_j}}} \begin{bmatrix} SmRo_{11} & SmRo_{12} \\ Sym & SmRo_{22} \end{bmatrix} \tag{3.71}$$

and for even j it has,

$$\mathbf{Sk}_L^{even}(\omega) = \frac{EA_0}{\sqrt{\mathsf{a} - \frac{\sin(2w_j\mathsf{a})}{2w_j}}} \begin{bmatrix} SkLe_{11} & SkLe_{12} \\ Sym & SkLe_{22} \end{bmatrix} \tag{3.72}$$

$$\mathbf{Sk}_R^{even}(\omega) = \frac{EA_0}{\sqrt{\mathsf{a} - \frac{\sin(2w_j\mathsf{a})}{2w_j}}} \begin{bmatrix} SkRe_{11} & SkRe_{12} \\ Sym & SkRe_{22} \end{bmatrix} \tag{3.73}$$

$$\mathbf{Sm}_L^{even}(\omega) = \frac{\rho A_0}{\sqrt{\mathsf{a} - \frac{\sin(2w_j\mathsf{a})}{2w_j}}} \begin{bmatrix} SmLe_{11} & SmLe_{12} \\ Sym & SmLe_{22} \end{bmatrix} \tag{3.74}$$

$$\mathbf{Sm}_R^{even}(\omega) = \frac{\rho A_0}{\sqrt{\mathsf{a} - \frac{\sin(2w_j\mathsf{a})}{2w_j}}} \begin{bmatrix} SmRe_{11} & SmRe_{12} \\ Sym & SmRe_{22} \end{bmatrix} \tag{3.75}$$

The exact closed-form expression of each element, $\{SkLo_{ij}, SmLo_{ij}, SkRo_{ij}, SmRo_{ij}\}$ and $\{SkLe_{ij}, SmLe_{ij}, SkRe_{ij}, SmRe_{ij}\}$, of these eight matrices are given in Appendix A.2.2.

Considering that all parameters and matrices of equations (3.65) and (3.66) are presented, it is easy to implement then in MATHEMATICA software to obtain the random damage rod stiffness and mass matrices $\mathbf{K}_{j_d}(\omega)$ and $\mathbf{M}_{j_d}(\omega)$.

Then, the stochastic spectral damaged rod element dynamic stiffness matrix is obtained as:

$$\mathbf{D}_d(\omega,\theta) = \mathbf{K}_d(\omega,\theta) - \omega^2\mathbf{M}_d(\omega,\theta) \tag{3.76}$$

3.5 Undamaged beam

Deterministic

The fundamental equation for the flexural motion in a beam-like structure is introduced in this section. Figure 3.6 shows an elastic two-node beam element with an uniform rectangular cross-section, where the properties are assumed to be deterministic variables. The undamped

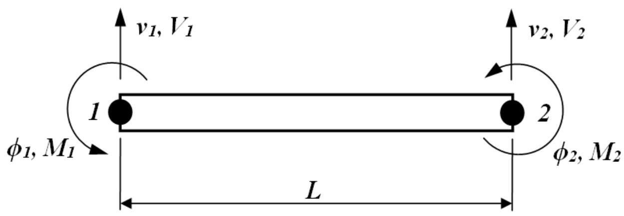

Figure. 3.6: Two-node beam spectral element

Euler-Bernoulli beam equation of motion under bending vibration can be written as (Doyle, 1997; Lee, 2004),

$$EI\frac{\partial^4 v(x,t)}{\partial x^4} + \rho A\frac{\partial^2 v(x,t)}{\partial t^2} = q(x,t) \tag{3.77}$$

where E ,I, ρ are elastic modulus, inertia moment, and mass density per unit length, respectively. Then, $v(x,t)$ is the transversal displacement and $q(x,t)$ external distributed load. A structural internal damping is introduced into the beam formulation by adding into the variable $(E \cdot I)$ a deterministic part $(E_0 \cdot I_0)$ weighted by a complex damping factor $(i\eta, i = \sqrt{-1})$, to obtain $EI = E \cdot I + (E_0 \cdot I_0)i\eta$.

By considering the homogeneous differential equation with constant properties along the beam length, the spectral form of equation (3.77) becomes:

$$\frac{d^4\hat{v}}{dx^4} - k^4\hat{v} = 0, \tag{3.78}$$

where

$$k^4 = \omega^2\frac{\rho A}{EI}. \tag{3.79}$$

The equation (3.78) can be split into a product of two terms,

$$\frac{d^2\hat{v}}{dx^2} + k^2\hat{v} = 0, \quad \frac{d^2\hat{v}}{dx^2} - k^2\hat{v} = 0 \tag{3.80}$$

Considering solutions of the form $e^{-i\beta x}$, and substituting into the equations (3.80) gives,

$$\beta_1 = \pm k, \quad \beta_2 = \pm ik \tag{3.81}$$

For the spectral Euler-Bernoulli beam element of length L, the general solution of equation (3.78) can be obtained in the form

$$v(x,\omega) = a_1 e^{-ikx} + a_2 e^{-kx} + a_3 e^{-ik(L-x)} + a_4 e^{-k(L-x)} = \mathbf{s}(x,\omega)\mathbf{a} \tag{3.82}$$

where

$$\begin{aligned} \mathbf{s}(x,\omega) &= \left\{e^{-ikx}, e^{-kx}, e^{-ik(L-x)}, e^{-k(L-x)}\right\}, \\ \mathbf{a}(x,\omega) &= \{a_1, a_2, a_3, a_4\}^T \end{aligned} \tag{3.83}$$

The spectral nodal displacements and slopes of the beam element are related to the displacement field at node 1 ($x = 0$) and node 2 ($x = L$), by

$$\mathbf{d} = \begin{bmatrix} v_1 \\ \phi_1 \\ v_2 \\ \phi_2 \end{bmatrix} = \begin{bmatrix} v(0) \\ v'(0) \\ v(L) \\ v'(L) \end{bmatrix} \tag{3.84}$$

By substituting equation (3.82) into the right-hand side of equation (3.84) ans written in a matrix form gives

$$\mathbf{d} = \begin{bmatrix} s(0,\omega) \\ s'(0,\omega) \\ s(L,\omega) \\ s'(L,\omega) \end{bmatrix} \mathbf{a} = \mathbf{G}_B(\omega)\mathbf{a} \tag{3.85}$$

where

$$\mathbf{G}_B(\omega) = \begin{bmatrix} 1 & 1 & e^{-ikL} & e{-}kL \\ -ik & -k & ie^{-ikL}k & e{-}kLk \\ e{-}ikL & e{-}kL & 1 & 1 \\ -ie{-}ikLk & -e{-}kLk & ik & k \end{bmatrix} \tag{3.86}$$

The frequency-dependent displacement within an element is interpolated from the nodal displacement vector $\mathbf{d}$ by eliminating the constant vector $\mathbf{a}$ from equation (3.84) and using equation (3.85) it is expressed as

$$v(x,\omega) = \mathbf{g}(x,\omega)\mathbf{d} \tag{3.87}$$

where the shape function is

$$\mathbf{g}(\mathbf{x},\omega) = \mathbf{s}(\mathbf{x},\omega)\mathbf{G}_B^{-1}(\omega) = \mathbf{s}(\mathbf{x},\omega)\mathbf{\Gamma}(\omega) \tag{3.88}$$

$$= \begin{bmatrix} \frac{-2\cos(kx)-2\cosh(kx)+(1-i)(\cos(k((1+i)L-x))+i\cos(k((1+i)L-ix))+\cosh(k((1+i)L-x))+i\cosh(k((1+i)L-ix)))}{4\cos(kL)\cosh(kL)} \\ -\frac{2\sin(kx)+2\sinh(kx)+(1+i)(\sin(k((1+i)L-x))-\sin(k((1+i)L-ix))+\sinh(k((1+i)L-x))-\sinh(k((1+i)L-ix)))}{4k(\cos(kL)\cosh(kL)-1)} \\ \frac{\cos(k(L-x))-\cos(kx)\cosh(kL)+\cosh(k(L-x))-\cos(kL)\cosh(kx)+\sin(kx)\sinh(kL)-\sin(kL)\sinh(kx)}{2-2\cos(kL)\cosh(kL)} \\ \frac{\sin(k(L-x))-\cos(kx)\sinh(kL)+\cosh(kx)(\sinh(kL)-\sin(kL))+\cosh(kL)(\sin(kx)-\sinh(kx))+\cos(kL)\sinh(kx)}{2k(\cos(kL)\cosh(kL)-1)} \end{bmatrix}$$

A generalized transverse displacement at any arbitrary point in the beam element is given by,

$$v(x) = g_1(x)v_1 + g_2(x)\phi_1 + g_3(x)v_2 + g_4(x)\phi_2 \tag{3.89}$$

From the generalized formulation (equations 3.6 and 3.7) the deterministic stiffness and mass matrices can be determined as:

$$\begin{aligned}\mathbf{K}_0(\omega) &= EI_0\mathbf{\Gamma}^T(\omega)\left[\int_0^L \mathbf{s}''^T(x,\omega)\mathbf{s}''(x,\omega)dx\right]\mathbf{\Gamma}(\omega) \\ &= EI_0\mathbf{\Gamma}^T(\omega)\begin{bmatrix} K_{11} & K_{12} & K_{13} & K_{14} \\ & K_{22} & K_{23} & K_{24} \\ & & K_{33} & K_{34} \\ \text{sym} & & & K_{44}\end{bmatrix}\mathbf{\Gamma}(\omega)\end{aligned} \tag{3.90}$$

and

$$\begin{aligned}\mathbf{M}_0(\omega) &= \rho A_0\mathbf{\Gamma}^T(\omega)\left[\int_0^L \mathbf{s}^T(x,\omega)\mathbf{s}(x,\omega)dx\right]\mathbf{\Gamma}(\omega) \\ &= \rho A_0\mathbf{\Gamma}^T(\omega)\begin{bmatrix} M_{11} & M_{12} & M_{13} & M_{14} \\ & M_{22} & M_{23} & M_{24} \\ & & M_{33} & M_{34} \\ \text{sym} & & & M_{44}\end{bmatrix}\mathbf{\Gamma}(\omega)\end{aligned} \tag{3.91}$$

where the closed-form expressions for the elements of stiffness and mass matrices, K_{ij} and M_{ij}, are presented in Appendix A.3.1.

Stochastic

The stochastic beam spectral element is formulated as a random process expanded in a spectral KL decomposition. Flexural bending ($EI(x)$) and mass per unit of length ($\rho A(x)$) are considered as spatially distributed random variables. Therefore, the flexural bending is assumed as a random field of the form:

$$EI(x,\theta) = EI_0[1 + \varepsilon_1 \varpi_1(x,\theta)] \tag{3.92}$$

and the mass per unit of length is assumed a random field as

$$\rho A(x,\theta) = \rho A_0[1 + \varepsilon_2 \varpi_2(x,\theta)] \tag{3.93}$$

Likewise, the subscript 0 indicates the mean value, $0 < \varepsilon_i \ll 1(i = 1,2,...)$ are deterministic constants and the random field $\varpi_i(x,\theta)$ is taken to have zero mean, unit standard deviation and covariance $C_{ij}(\xi)$. Since, $EI(x,\theta)$ and $\rho A(x,\theta)$ are strictly positive, $\varpi_i(x,\theta)(i = 1,2,...)$ is required to satisfy the probability condition $\mathrm{P}[1 + \varepsilon_i \varpi_i(x,\theta) \leq 0] = 0$. Expanding the random fields $\varpi_1(x,\theta)$ and $\varpi_2(x,\theta)$ in a KL spectral decomposition one obtains the stochastic dynamic stiffness and stochastic mass matrices as,

$$\mathbf{K}(\omega,\theta) = \mathbf{K}_0(\omega) + \Delta\mathbf{K}(\omega,\theta) \tag{3.94}$$

$$\mathbf{M}(\omega,\theta) = \mathbf{M}_0(\omega) + \Delta\mathbf{M}(\omega,\theta) \tag{3.95}$$

where ($\Delta\mathbf{K}(\omega,\theta)$) and mass ($\Delta\mathbf{M}(\omega,\theta)$) are the random part of the matrices. Expanding the random matrices in a KL decomposition we have

$$\Delta\mathbf{K}(\omega,\theta) = \varepsilon_1 \sum_{j=1}^{N_K} \xi_{Kj}(\theta)\sqrt{\lambda_{Kj}}\mathbf{K}_j(\omega) \tag{3.96}$$

and

$$\Delta\mathbf{M}(\omega,\theta) = \varepsilon_2 \sum_{j=1}^{N_M} \xi_{Mj}(\theta)\sqrt{\lambda_{Mj}}\mathbf{M}_j(\omega) \tag{3.97}$$

where N_k and N_M are the numbers of terms kept in the KL expansion; $\xi_{Kj}(\theta)$ and $\xi_{Mj}(\theta)$ are uncorrelated Gaussian random variables with zero mean and unit standard deviation. The matrices $\mathbf{K}_j(\omega)$ and $\mathbf{M}_j(\omega)$ are

$$\mathbf{K}_j(\omega) = EI_0\mathbf{\Gamma}^T(\omega)\left[\int_0^L \varphi_{Kj}(x_e + x)\mathbf{s}''(x,\omega)^T\mathbf{s}''(x,\omega)dx\right]\mathbf{\Gamma}(\omega) \tag{3.98}$$

$$\mathbf{M}_j(\omega) = \rho A_0\mathbf{\Gamma}^T(\omega)\left[\int_0^L \varphi_{Kj}(x_e + x)\mathbf{s}(x,\omega)^T\mathbf{s}(x,\omega)dx\right]\mathbf{\Gamma}(\omega) \tag{3.99}$$

Substituting equations (2.26) and (2.27) in equations (3.98) and (3.97), the closed-form expressions for the random part of the stiffness and mass matrices in odd j are

$$\mathbf{K}_j^{odd}(\omega) = \frac{EI_0}{\sqrt{\mathsf{a} + \frac{\sin(2\omega_j \mathsf{a})}{2\omega_j}}}\mathbf{\Gamma}^T(\omega)\left[\int_0^L \cos(\omega_j(x_e+x))\mathbf{s}''(x)^T\mathbf{s}''(x)dx\right]\mathbf{\Gamma}(\omega)$$

$$= \frac{EI_0}{\sqrt{\mathsf{a} + \frac{\sin(2\omega_j \mathsf{a})}{2\omega_j}}}\mathbf{\Gamma}^T(\omega)\begin{bmatrix} Ko_{11} & Ko_{12} & Ko_{13} & Ko_{14} \\ & Ko_{22} & Ko_{23} & Ko_{24} \\ & & Ko_{33} & Ko_{34} \\ \text{sym} & & & Ko_{44} \end{bmatrix}\mathbf{\Gamma}(\omega) \qquad (3.100)$$

$$\mathbf{M}_j^{odd}(\omega) = \frac{\rho A_0}{\sqrt{\mathsf{a} + \frac{\sin(2\omega_j \mathsf{a})}{2\omega_j}}}\mathbf{\Gamma}^T(\omega)\left[\int_0^L \cos(\omega_j(x_e+x))\mathbf{s}(x)^T\mathbf{s}(x)dx\right]\mathbf{\Gamma}(\omega)$$

$$= \frac{\rho A_0}{\sqrt{\mathsf{a} + \frac{\sin(2\omega_j \mathsf{a})}{2\omega_j}}}\mathbf{\Gamma}^T(\omega)\begin{bmatrix} Mo_{11} & Mo_{12} & Mo_{13} & Mo_{14} \\ & Mo_{22} & Mo_{23} & Mo_{24} \\ & & Mo_{33} & Mo_{34} \\ \text{sym} & & & Mo_{44} \end{bmatrix}\mathbf{\Gamma}(\omega) \qquad (3.101)$$

and for even j are

$$\mathbf{K}_j^{even}(\omega) = \frac{EI_0}{\sqrt{\mathsf{a} - \frac{\sin(2\omega_j \mathsf{a})}{2\omega_j}}}\mathbf{\Gamma}^T(\omega)\left[\int_0^L \sin(\omega_j(x_e+x))\mathbf{s}''(x)^T\mathbf{s}''(x)dx\right]\mathbf{\Gamma}(\omega)$$

$$= \frac{EI_0}{\sqrt{\mathsf{a} - \frac{\sin(2\omega_j \mathsf{a})}{2\omega_j}}}\mathbf{\Gamma}^T(\omega)\begin{bmatrix} Ke_{11} & Ke_{12} & Ke_{13} & Ke_{14} \\ & Ke_{22} & Ke_{23} & Ke_{24} \\ & & Ke_{33} & Ke_{34} \\ \text{sym} & & & Ke_{44} \end{bmatrix}\mathbf{\Gamma}(\omega) \qquad (3.102)$$

$$\mathbf{M}_j^{even}(\omega) = \frac{\rho A_0}{\sqrt{\mathsf{a} - \frac{\sin(2\omega_j \mathsf{a})}{2\omega_j}}}\mathbf{\Gamma}^T(\omega)\left[\int_0^L \sin(\omega_j(x_e+x))\mathbf{s}(x)^T\mathbf{s}(x)dx\right]\mathbf{\Gamma}(\omega)$$

$$= \frac{\rho A_0}{\sqrt{\mathsf{a} - \frac{\sin(2\omega_j \mathsf{a})}{2\omega_j}}}\mathbf{\Gamma}^T(\omega)\begin{bmatrix} Me_{11} & Me_{12} & Me_{13} & Me_{14} \\ & Me_{22} & Me_{23} & Me_{24} \\ & & Me_{33} & Me_{34} \\ \text{sym} & & & Me_{44} \end{bmatrix}\mathbf{\Gamma}(\omega) \qquad (3.103)$$

Mass and stiffness matrices components for undamaged beam stochastic stiffness matrix components (Ko_{ij},Ke_{ij}), and stochastic mass matrix components (Mo_{ij},Me_{ij}) of equations (3.100- 3.103) are fully expressed in Appendix A.3.2.

3.6 Damaged beam

Deterministic

A spectral Euler Bernoulli beam element with a transverse, open and non-propagating crack (Krawczuk, 2002; Krawczuk et al., 2002) is addressed. Figure 3.7 shows a two-nodes beam element with uniform rectangular cross-section, length L, crack position L_1, crack depth α. The crack is modelled by a dimensionless and local crack flexibility, Θ_b. Castigliano's theorem and the laws of fracture mechanics (Tada et al., 1973) are used to calculate crack flexibility. The displacement field with the element is represented by a linear combination of the basic

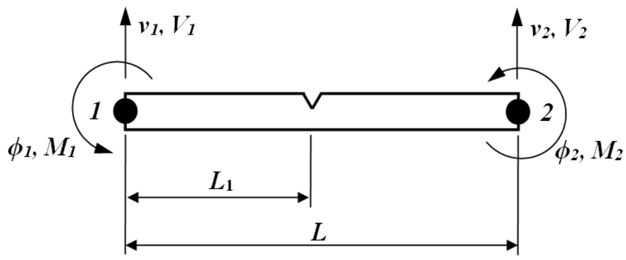

Figure. 3.7: Two-node damaged (damaged) rod spectral element

functions $e^{\pm ikx}$ and $e^{\pm kx}$ similar to undamaged beam, however in this case displacements field are considered at the left-hand side of the crack ($\mathbf{s}_L(x,\omega)$) and right-hand side of the crack ($\mathbf{s}_R(x,\omega)$). These elements are defined by a linear combination of the basic functions,

$$\begin{aligned} v_L(x) &= a_1e^{-i(kx)} + a_2e^{-(kx)} + a_3e^{-ik(L_1-x)} + a_4e^{-k(L_1-x)} \quad (0 \leq x \leq L_1) \\ &= \mathbf{s}_L(x,\omega)\mathbf{a}_L \end{aligned} \tag{3.104}$$

where $\mathbf{s}_L(x,\omega) = \left[e^{-i(kx)}, e^{-(kx)}, e^{-ik(L_1-x)}, e^{-k(L_1-x)}\right]$, and $\mathbf{a}_L = \{a_1,a_2,a_3,a_4\}^T$.

$$\begin{aligned} v_R(x) &= a_5e^{-ik(L_1+x)} + a_6e^{-k(L_1+x)} + a_7e^{-ik(L-(L_1+x))} + a_8e^{-k(L-(L_1+x))} \quad (0 \leq x \leq L - L_1) \\ &= \mathbf{s}_R(x,\omega)\mathbf{a}_R \end{aligned} \tag{3.105}$$

where $\mathbf{s}_R(x,\omega) = \left[e^{-ik(L_1+x)}, e^{-k(L_1+x)}, e^{-ik(L-(L_1+x))}, e^{-k(L-(L_1+x))}\right]$, and $\mathbf{a}_R = \{a_5,a_6,a_7,a_8\}^T$. Writing equation (3.104) in equation (3.105) in a matrix form,

$$\left\{\begin{array}{c} v_L(x) \\ v_R(x) \end{array}\right\} = \left[\begin{array}{cc} \mathbf{s}_L(x,\omega) & \mathbf{0} \\ \mathbf{0} & \mathbf{s}_R(x,\omega) \end{array}\right] \left\{\begin{array}{c} \mathbf{a}_L \\ \mathbf{a}_R \end{array}\right\} = \mathbf{s}_d(x,\omega)\mathbf{a}_d \tag{3.106}$$

The coefficients vector $\mathbf{a}_d$ can be calculated as a function of the nodal spectral displacements using the element boundary and compatibility conditions:

- Element left-end $v_L(0) = v_1$
- Element cracked cross-section $v_L(L_1) - v_R(0) = \Theta_b \frac{\partial v}{\partial x}$
- Element non-cracked cross-section $\frac{\partial v_L(L_1)}{\partial x} = \frac{\partial v_R(0)}{\partial x}$
- Element right-end $v_R(L - L_1) = v_2$

Coupling the damaged element left and right-hand sides (equations 3.104 and 3.105) and applying boundary and compatibility conditions it has,

$$\underbrace{\left[\begin{array}{cccccccc} 1 & 1 & \mathsf{m} & \mathsf{n} & 0 & 0 & 0 & 0 \\ -ik & -k & ik\mathsf{m} & k\mathsf{n} & 0 & 0 & 0 & 0 \\ -\mathsf{m} & -\mathsf{n} & -1 & -1 & \mathsf{m} & \mathsf{n} & \mathsf{o} & \mathsf{p} \\ i\mathsf{m}k - \mathsf{m}\Theta_b k^2 & \mathsf{n}k + \mathsf{n}\Theta_b k^2 & -ik - \Theta_b k^2 & -k + \Theta_b k^2 & -ik\mathsf{m} & -k\mathsf{n} & ik\mathsf{o} & k\mathsf{p} \\ -k^2\mathsf{m} & k^2\mathsf{n} & -k^2 & k^2 & k^2\mathsf{m} & -k^2\mathsf{n} & k^2\mathsf{o} & -k^2\mathsf{p} \\ ik^3\mathsf{m} & -k^3\mathsf{n} & -ik^3 & k^3 & -k^3\mathsf{m} & k^3\mathsf{n} & ik^3\mathsf{o} & -k^3\mathsf{p} \\ 0 & 0 & 0 & 0 & \mathsf{r} & \mathsf{t} & 1 & 1 \\ 0 & 0 & 0 & 0 & -ik\mathsf{r} & -k\mathsf{t} & ik & k \end{array}\right]}_{\mathbf{G}_{Bd}} \left\{\begin{array}{c} a_1 \\ a_2 \\ a_3 \\ a_4 \\ a_5 \\ a_6 \\ a_7 \\ a_8 \end{array}\right\} = \left\{\begin{array}{c} v_1 \\ \phi_1 \\ 0 \\ 0 \\ 0 \\ 0 \\ v_2 \\ \phi_2 \end{array}\right\} \tag{3.107}$$

where: $\mathsf{m} = e^{-ikL_1}, \mathsf{n} = e^{-kL_1}, \mathsf{o} = e^{-ik(L-L_1)}, \mathsf{p} = e^{k(L-L_1)}, \mathsf{r} = e^{-ikL}, \mathsf{t} = e^{-kL}$.

From the equation (3.107) it can relate the coefficients vector $\mathbf{a}_d$ to the nodal spectral displacements as:

$$\left\{\begin{array}{c} a_1 \\ a_2 \\ a_3 \\ a_4 \\ a_5 \\ a_6 \\ a_7 \\ a_8 \end{array}\right\} = \mathbf{G}_{Bdr}^{-1} \left\{\begin{array}{c} v_1 \\ \phi_1 \\ v_2 \\ \phi_2 \end{array}\right\} \tag{3.108}$$

where $\mathbf{G}_{Bdr}^{-1}$ is given by

$$\mathbf{G}_{Bdr}^{-1} = \begin{bmatrix} G_{Bd_{11}}^{-1} & G_{Bd_{12}}^{-1} & G_{Bd_{17}}^{-1} & G_{Bd_{18}}^{-1} \\ G_{Bd_{21}}^{-1} & G_{Bd_{22}}^{-1} & G_{Bd_{27}}^{-1} & G_{Bd_{28}}^{-1} \\ G_{Bd_{31}}^{-1} & G_{Bd_{32}}^{-1} & G_{Bd_{37}}^{-1} & G_{Bd_{38}}^{-1} \\ G_{Bd_{41}}^{-1} & G_{Bd_{42}}^{-1} & G_{Bd_{47}}^{-1} & G_{Bd_{48}}^{-1} \\ G_{Bd_{51}}^{-1} & G_{Bd_{52}}^{-1} & G_{Bd_{57}}^{-1} & G_{Bd_{58}}^{-1} \\ G_{Bd_{61}}^{-1} & G_{Bd_{62}}^{-1} & G_{Bd_{67}}^{-1} & G_{Bd_{68}}^{-1} \\ G_{Bd_{71}}^{-1} & G_{Bd_{72}}^{-1} & G_{Bd_{77}}^{-1} & G_{Bd_{78}}^{-1} \\ G_{Bd_{81}}^{-1} & G_{Bd_{82}}^{-1} & G_{Bd_{87}}^{-1} & G_{Bd_{88}}^{-1} \end{bmatrix} \tag{3.109}$$

Equation (3.108) can be rewritten in a compact form as:

$$\mathbf{a}_d = \mathbf{G}_{Bdr}^{-1}\mathbf{d}_d \tag{3.110}$$

Substituting equation (3.110) in (3.106) it has,

$$\left\{ \begin{array}{c} v_L(x) \\ v_R(x) \end{array} \right\} = \begin{bmatrix} \mathbf{s}_L(x,\omega) & \mathbf{0} \\ \mathbf{0} & \mathbf{s}_R(x,\omega) \end{bmatrix} \mathbf{G}_{Bdr}^{-1}\mathbf{d}_d = \mathbf{g}_B d(x,\omega)\mathbf{d}_d \tag{3.111}$$

Comparing equation (3.47) with (3.5) it is obtained,

$$\mathbf{\Gamma}_d(\omega) = \mathbf{G}_{Bdr}^{-1} \tag{3.112}$$

Same procedure demonstrated for the damaged rod model is applied here, the stiffness operator is given by $\mathcal{L}_2(\bullet) = \partial(\bullet)/\partial x$ and assuming constant nominal values for the deterministic stiffness parameter, $k_{s_0}(\mathbf{r}) = EI_0$. Due spacial reference in damaged model equation (3.10) must be integrated according to the corresponding limits, then

$$\mathbf{K}_{0_d}(\omega) = EI_0\, \mathbf{\Gamma}_d^T(\omega) \begin{bmatrix} \mathbf{Sk}_{0L} & \mathbf{0} \\ \mathbf{0} & \mathbf{Sk}_{0R} \end{bmatrix} \mathbf{\Gamma}_d(\omega), \tag{3.113}$$

$$\mathbf{M}_{0_d}(\omega) = \rho A_0\, \mathbf{\Gamma}_d^T(\omega) \begin{bmatrix} \mathbf{Sm}_{0L} & \mathbf{0} \\ \mathbf{0} & \mathbf{Sm}_{0R} \end{bmatrix} \mathbf{\Gamma}_d(\omega), \tag{3.114}$$

where

$$\mathbf{Sk}_{0L} = \int_0^{L_1} \mathbf{s}''^T_L(x,\omega)\mathbf{s}''_L(x,\omega)dx \tag{3.115}$$

$$\mathbf{Sk}_{0R} = \int_0^{(L-L_1)} \mathbf{s}''^T_R(x,\omega)\mathbf{s}''_R(x,\omega)dx \tag{3.116}$$

$$\mathbf{Sm}_{0L} = \int_0^{L_1} \mathbf{s}_L^T(x,\omega)\mathbf{s}_L(x,\omega)dx \tag{3.117}$$

$$\mathbf{Sm}_{0R} = \int_0^{(L-L_1)} \mathbf{s}_R^T(x,\omega)\mathbf{s}_R(x,\omega)dx \tag{3.118}$$

Substituting equations (3.115) and (3.116) in equations (3.113), and equations (3.117) and (3.118) in equations (3.114) the deterministic stiffness and mass matrices as closed-form expressions can be obtained. However, these are huge closed-form expressions not easily workable. As a matter of understanding and results reproducibility it is shown here only the matrices form of $\mathbf{Sk}_{0L}$, $\mathbf{Sk}_{0R}$, $\mathbf{Sm}_{0L}$ and $\mathbf{Sm}_{0R}$. The exact closed-form expression of these four matrices are given in Appendix A.4.1.

Bending crack flexibility

The crack flexibility coefficient (Θ_b) is calculated by using Castigliano's theorem, so that the flexibility at the crack location for the one-dimensional beam spectral element is:

$$\mathtt{c} = \frac{\partial^2 U}{\partial P^2}, \tag{3.119}$$

where $\mathtt{U}$ denotes the elastic strain energy due to the crack and P is the nodal force on the element. By considering that only crack mode I is present in the beam element, the elastic strain energy is given by

$$\mathtt{U} = \frac{1-\nu^2}{E}\int_{S_c} K_I^2 dS_c, \tag{3.120}$$

where ν is the Poisson's ratio, S_c is the damaged area and $\mathtt{U}_I$ is the stress intensity factor corresponding to the crack mode I, which is represented by:

$$\mathtt{U}_I = \frac{6\mathtt{M}}{bh^2}\sqrt{\pi\alpha}f(\frac{\alpha}{h}), \tag{3.121}$$

where b is the cross section base, h is the cross section height, α is the crack depth variation (Fig.3.5), $\mathtt{M}$ is the bending moment at crack position, and $\mathtt{f}$ is the following correction function:

$$\mathtt{f}(\frac{\alpha}{h}) = \sqrt{\frac{2h}{\pi\alpha}\tan(\frac{\pi\alpha}{2h})}\frac{0.923 + 0.199(1-\sin(\frac{\pi\alpha}{2h}))^4}{\cos(\frac{\pi\alpha}{2h})}. \tag{3.122}$$

The coefficient $\mathtt{c}$ used to calculate the crack flexibility is

$$\mathtt{c} = \frac{72\pi}{bh^2}\int_0^{\bar{a}} \bar{\alpha}\mathtt{f}^2(\bar{\alpha})d\bar{\alpha}, \tag{3.123}$$

where $\bar{a} = \frac{a}{h}$ and $\bar{\alpha} = \frac{\alpha}{h}$. The dimensionless and local bending flexibility is given by:

$$\Theta_b = \frac{EI\mathsf{c}}{L} \tag{3.124}$$

Stochastic

Similarly the stochastic undamaged beam formulation (Section3.5), the stochastic dynamic stiffness element matrix for the damaged beam spectral element, $\mathbf{D}_d(\omega,\theta)$, is developed. Also, it is assumed that A, E, ρ are random variables, and EI and ρA are random fields. Following equation (3.9), we can express the stochastic damaged rod stiffness and mass element matrices, respectively, as:

$$\mathbf{K}_d(\omega,\theta) = \mathbf{K}_{0_d}(\omega) + \Delta\mathbf{K}_d(\omega,\theta) \tag{3.125}$$

$$\mathbf{M}_d(\omega,\theta) = \mathbf{M}_{0_d}(\omega) + \Delta\mathbf{M}_d(\omega,\theta) \tag{3.126}$$

From the KL expansion and equations (3.92) and (3.93) it has,

$$\Delta\mathbf{K}_d(\omega,\theta) = \varepsilon_1 \sum_{j=1}^{N} \xi_{Kj}(\theta)\sqrt{\lambda_{Kj}}\mathbf{K}_{j_d}(\omega) \tag{3.127}$$

$$\Delta\mathbf{M}_d(\omega,\theta) = \varepsilon_2 \sum_{j=1}^{N} \xi_{Mj}(\theta)\sqrt{\lambda_{Mj}}\mathbf{M}_{j_d}(\omega) \tag{3.128}$$

where N is the number of terms kept in the KL expansion, $\xi_{Kj}(\theta)$ and $\xi_{Mj}(\theta)$ are uncorrelated Gaussian random variables with zero mean and unit standard deviation. From the equation (3.11) and considering different limits of integration (left and right-hand sides) for the damaged beam model it has,

$$\mathbf{K}_{j_d}(\omega) = EI_0\mathbf{\Gamma}_d^T(\omega)\begin{bmatrix} \mathbf{Sk}_L & \mathbf{0} \\ \mathbf{0} & \mathbf{Sk}_R \end{bmatrix}\mathbf{\Gamma}_d(\omega), \tag{3.129}$$

$$\mathbf{M}_{j_d}(\omega) = \rho A_0\mathbf{\Gamma}_d^T(\omega)\begin{bmatrix} \mathbf{Sm}_L & \mathbf{0} \\ \mathbf{0} & \mathbf{Sm}_R \end{bmatrix}\mathbf{\Gamma}_d(\omega), \tag{3.130}$$

where

$$\mathbf{Sk}_L = \int_0^{L_1} \varphi_{Kj}(x_e+x)\mathbf{s}''^T_L(x,\omega)\mathbf{s}''_L(x,\omega)dx$$
$$\mathbf{Sk}_R = \int_0^{(L-L_1)} \varphi_{Kj}(x_e+x)\mathbf{s}''^T_R(x,\omega)\mathbf{s}''_R(x,\omega)dx$$
$$\mathbf{Sm}_L = \int_0^{L_1} \varphi_{Mj}(x_e+x)\mathbf{s}^T_L(x,\omega)\mathbf{s}_L(x,\omega)dx$$
$$\mathbf{Sm}_R = \int_0^{(L-L_1)} \varphi_{Mj}(x_e+x)\mathbf{s}^T_R(x,\omega)\mathbf{s}_R(x,\omega)dx \tag{3.131}$$

Substituting equations (2.26) and (2.27) in equations (3.131) the random part of the stiffness and mass matrices as closed-form expressions can be obtained. Again extensive closed-form expressions are found. Then, equations (3.129) and (3.130) were solved with MATHEMATICA® software. Thus, only the matrices form of $\mathbf{Sk}_L$,$\mathbf{Sk}_R$,$\mathbf{Sm}_L$,$\mathbf{Sm}_R$ for each j^{th} terms respecting the odd and even KL formulation. By considering odd j it has,

$$\mathbf{Sk}_L^{odd}(\omega) = \frac{EI_0}{\sqrt{\mathsf{a}+\frac{\sin(2w_j\mathsf{a})}{2w_j}}}\begin{bmatrix} SkLo_{11} & SkLo_{12} & SkLo_{13} & SkLo_{14} \\ & SkLo_{22} & SkLo_{23} & SkLo_{24} \\ & & SkLo_{33} & SkLo_{34} \\ Sym & & & SkLo_{44} \end{bmatrix} \tag{3.132}$$

$$\mathbf{Sk}_R^{odd}(\omega) = \frac{EI_0}{\sqrt{\mathsf{a}+\frac{\sin(2w_j\mathsf{a})}{2w_j}}}\begin{bmatrix} SkRo_{11} & SkRo_{12} & SkRo_{13} & SkRo_{14} \\ & SkRo_{22} & SkRo_{23} & SkRo_{24} \\ & & SkRo_{33} & SkRo_{34} \\ Sym & & & SkRo_{44} \end{bmatrix} \tag{3.133}$$

$$\mathbf{Sm}_L^{odd}(\omega) = \frac{\rho A_0}{\sqrt{\mathsf{a}+\frac{\sin(2w_j\mathsf{a})}{2w_j}}}\begin{bmatrix} SmLo_{11} & SmLo_{12} & SmLo_{13} & SmLo_{14} \\ & SmLo_{22} & SmLo_{23} & SmLo_{24} \\ & & SmLo_{33} & SmLo_{34} \\ Sym & & & SmLo_{44} \end{bmatrix} \tag{3.134}$$

$$\mathbf{Sm}_R^{odd}(\omega) == \frac{\rho A_0}{\sqrt{\mathsf{a}+\frac{\sin(2w_j\mathsf{a})}{2w_j}}}\begin{bmatrix} SmRo_{11} & SmRo_{12} & SmRo_{13} & SmRo_{14} \\ & SmRo_{22} & SmRo_{23} & SmRo_{24} \\ & & SmRo_{33} & SmRo_{34} \\ Sym & & & SmRo_{44} \end{bmatrix} \tag{3.135}$$

and for even j it has,

$$\mathbf{Sk}_L^{even}(\omega) = \frac{EI_0}{\sqrt{\mathtt{a} - \frac{\sin(2w_j\mathtt{a})}{2w_j}}} \begin{bmatrix} SkLe_{11} & SkLe_{12} & SkLe_{13} & SkLe_{14} \\ & SkLe_{22} & SkLe_{23} & SkLe_{24} \\ & & SkLe_{33} & SkLe_{34} \\ Sym & & & SkLe_{44} \end{bmatrix} \tag{3.136}$$

$$\mathbf{Sk}_R^{even}(\omega) = \frac{EI_0}{\sqrt{\mathtt{a} - \frac{\sin(2w_j\mathtt{a})}{2w_j}}} \begin{bmatrix} SkRe_{11} & SkRe_{12} & SkRe_{13} & SkRe_{14} \\ & SkRe_{22} & SkRe_{23} & SkRe_{24} \\ & & SkRe_{33} & SkRe_{34} \\ Sym & & & SkRe_{44} \end{bmatrix} \tag{3.137}$$

$$\mathbf{Sm}_L^{even}(\omega) = \frac{\rho A_0}{\sqrt{\mathtt{a} - \frac{\sin(2w_j\mathtt{a})}{2w_j}}} \begin{bmatrix} SmLe_{11} & SmLe_{12} & SmLe_{13} & SmLe_{14} \\ & SmLe_{22} & SmLe_{23} & SmLe_{24} \\ & & SmLe_{33} & SmLe_{34} \\ Sym & & & SmLe_{44} \end{bmatrix} \tag{3.138}$$

$$\mathbf{Sm}_R^{even}(\omega) = \frac{\rho A_0}{\sqrt{\mathtt{a} - \frac{\sin(2w_j\mathtt{a})}{2w_j}}} \begin{bmatrix} SmRe_{11} & SmRe_{12} & SmRe_{13} & SmRe_{14} \\ & SmRe_{22} & SmRe_{23} & SmRe_{24} \\ & & SmRe_{33} & SmRe_{34} \\ Sym & & & SmRe_{44} \end{bmatrix} \tag{3.139}$$

The exact closed-form expression of each element, $\{SkLo_{ij}, SmLo_{ij}, SkRo_{ij}, SmRo_{ij}\}$ and $\{SkLe_{ij}, SmLe_{ij}, SkRe_{ij}, SmRe_{ij}\}$, of these eight matrices are given in Appendix A.4.2. Considering that all parameters and matrices of equations (3.129) and (3.130) are calculated, it is easy to obtain the random damage bean stiffness and mass matrices $\mathbf{K}_{j_d}(\omega)$ and $\mathbf{M}_{j_d}(\omega)$. Then, the stochastic spectral damaged beam element dynamic stiffness matrix is obtained as:

$$\mathbf{D}_d(\omega,\theta) = \mathbf{K}_d(\omega,\theta) - \omega^2\mathbf{M}_d(\omega,\theta) \tag{3.140}$$

3.7 Closure

This chapter presents the general formulation of the SEM for undamaged and damaged structures like-rod and like-beam. Intrinsic to all real structures, parameter uncertainty can be found in material properties and geometries. To handle such randomness, stochastic methods have been used to include this uncertainty into structure numerical model. Many structural parameters, such as Elastic modulus, Poisson's rate, thickness, density, etc., are spatially distributed by nature. Thus, a stochastic spectral element method is developed to express these parameters as a spatially correlated random field. The random field is expanded in a spectral decomposition known as the Karhunen-Loève expansion. A deterministic and stochastic spectral element formulation for an undamaged structure (rod and beam) were demonstrated. Deterministic spectral element for a damaged structure (rod and beam) were also presented.A new formulation for damaged spectral element (rod and beam) with a stochastic basis were developed. We compared our results with the ones presented literature. However, in the literature just a deterministic approach can be found.

4 Parameter estimation in stochastic dynamic systems

4.1 Introduction

Model updating methods in dynamic structural analysis are basically a process of minimizing the differences between the numerical model predictions and measured responses obtained in experimental tests using a parameter estimation procedure (Mottershead and Friswell, 1993; Friswell and Mottershead, 1995). The model updating procedure starts with the parameters choice (parametrisation), followed by correction procedure based on the available measured data. The parametrisation is an important topic in model updating which requires considerable physical knowledge regarding the system, more details can be found in references (Link and Santiago, 1991; Mottershead et al., 1996; Gladwell and Ahmadian, 1996; Friswell et al., 1998; Adhikari and Friswell, 2010; Mottershead et al., 2011).

Based on the system variability, some authors proposed the stochastic model updating techniques (Khodaparast and Mottershead, 2008; Khodaparast et al., 2008; Vanli and Jung, 2013). The main advantage in this approach is to add randomness in the model updating process. Generally, the numerical model is corrected related to uncertain measured data. Statistical techniques combined with model updating can improve the parameter estimation accuracy. In the field of structural dynamic, some authors traditionally use modal parameters (natural frequencies and mode shapes) to updating the model. However, in a structural dynamic test, it is a common practice to measure the data in the form of Frequency Response Functions (FRF), which requires an additional Experimental Modal Analysis procedure (Ewins, 1984; Maia and Silva, 1997) to extract modal parameters. Natke (1977) presented a model updating procedure using measured FRF's instead of modal parameters. After that, a growing number of researchers focused on model updating algorithms using the measured data directly (Natke, 1988b; Cottin et al., 1984; Link, 1990; Ibrahim et al., 1992; Natke, 1992; Arruda and Santos, 1993; Grafe, 1998). The book of Friswell and Mottershead (1995) compiles different model updating techniques. Model updating procedure using measured FRF's will be applied in this work .

In a deterministic point of view, the model updating can be classified in two groups: Direct methods using experimental modal data; and Iterative methods using experimental modal or FRF data. Direct methods or representational methods do not require iteration procedure and seek to produce the reference data set exactly, which can be an advantage in certain cases. On the other hand, the direct approach can generate inaccurate parameters, that comes from noise present in measured data. Then, the applicability of this methods requires precise modelling and very high quality measurement. The direct methods most widely used are Lagrange Multiplier methods, Matrix Mixing methods, and Control Theory Based methods. The works of Baruch and Itzhac (1978); Baruch (1978, 1982); Berman and Nagy (1983); Caesar (1986, 1987); Link et al. (1987); Carvalho et al. (2007) show application of direct methods for model updating.

The general concept of model updating is to minimize the error between measured experimental data and predicted analytical/numerical result via an optimization procedure. Iterative methods are based in the minimization of an objective function. Frequently, these objective functions are non-linear, which can generate convergence to local minimums. In these cases some form of regularization must be applied (Titurus and Friswell, 2008). Advantages related to these methods include the wide range of parameters that can be updated simultaneously, and both measured and analytical data can be weighted, a feature which can accommodate engineering insight.

In the practical applications of model updating the measured data are often incomplete and include randomness. In this manner, the importance of including statistical techniques to improve the method performance (Khodaparast, 2010). The interpretation of variability in experimental results can be classified as reducible and irreducible uncertainty. Reducible uncertainty is such that can be minimised by gathering more/further information, e.g. repeating the measurement, reducing measurement noise, avoiding the use of sensors that affect the measurement or signal processing. The beginning researches which incorporated statistical methods for the treatment of measurement noise in model updating were presented by Collins et al. (1974) and later by Friswell (1989). Errors in measured data and initial parameters may arise due to randomness. Such errors can be expressed in terms of a weighting matrix constructed with the inverse of the variances. Another technique is the model updating in the Bayesian probabilistic framework presented by Beck and Katafygiotis (1998); Katafygiotis and Beck (1998); Mares et al. (2006). Haag et al. (2010) proposed an inverse approach based on the fuzzy arithmetic for the model updating. Soize (2008) presented a methodology for robust model updating by using a non-parametric probabilistic approach.

Uncertainty in structural properties, such as Poisson's ratio, Young's modulus, mass density, modal damping, etc., are considered irreducible uncertainty data and require different mathematical approaches of the updating parameters. The distributions of the updating parameters are then modified in order to improve the correlation between model-predicted distributions and measured data distributions. This is a technique developed by Mottershead et al. (2006); Mares et al. (2006) and it is called stochastic model updating or uncertainty identification. The stochastic model updating is efficient, not only because it includes variability in measurement signals due to noise for example, but also includes the variability already existing in the structural property (Mottershead et al., 2006; Mares et al., 2006; Khodaparast and Mottershead, 2008; Khodaparast et al., 2008; Khodaparast, 2010). Govers and Link (2010) presented an approach of stochastic model updating with covariance matrix adjustment from uncertain experimental modal data. Therefore methods proposed by Collins et al. (1974); Friswell (1989); Beck and Au (2002); Fonseca et al. (2005); Hua et al. (2008) investigated different problems using stochastic model updating.

This Chapter presents a general review of the model updating techniques for a deterministic case and in the presence of uncertain measured data with reducible and irreducible uncertainty. The studies main goal is to use sensitivity-based model updating with measured FRF's to estimate spatially distributed parameters of the structure, then a brief description of the techniques in model updating and sensitivity-based updating method are given. Thus, numerical and experimental tests in two different types of structures demonstrate the performance of the proposed technique.

4.2 Model updating using frequency response function

In a structural dynamic test, it is a common practice to measure the data in the form of Frequency Response Function (FRF). Advantages in use directly FRF data are vast. Some of them are that no experimental modal analysis is required and identification errors are avoided. Since the problem is over-determined due to the availability of FRF data, it is possible to check a given solution by generating another one. The technique is applicable to structures with non-modal behaviour such as cases of high damping and/or modal density, and when the accurate determination of modal parameters can be difficult.

Natke (1992) and Friswell and Mottershead (1995) published a good survey about the subject and discriminate FRF model updating methods based on the types of error in the objective function: *input residual* and *output residual*. Input residual error formulations are different from many other FRF model updating formulations in the sense of linear design parameters. Comprehensive discussions of methods based on input residuals were presented by Cottin et al. (1984); Fritzen (1986); Link (1990); Ibrahim et al. (1992). Both approaches are based on the equations of motion written in terms of the dynamic stiffness matrix as,

$$\underbrace{\left[-\omega^2\mathbf{M} + i\omega\mathbf{C} + \mathbf{K}\right]}_{\mathbf{D}(\boldsymbol{\psi}),\omega} \mathbf{u}(\omega) = \mathbf{f}(\omega) \tag{4.1}$$

where $\boldsymbol{\psi}$ is the parameter vector, $\mathbf{u}$ and $\mathbf{f}$ are frequency dependent displacement and force vectors, respectively. Model updating methods originate from an input residual error (or equation error) given by the difference between measured and predicted (input) forces given by:

$$\varepsilon_{input} = \mathbf{f}(\omega) - \mathbf{D}(\omega)\mathbf{x}(\omega) \tag{4.2}$$

The output residual error is often based on minimising the difference between the measured and estimated response. Cottin et al. (1984); Fritzen (1986) and Natke (1988b) discussed output residual in detail. Fritzen (1992); Imregun et al. (1995b,a) presented theoretical and experimental application. Ibrahim et al. (1992) showed a comparison between input and output residual formulations. The minimised output residual error is

$$\boldsymbol{\varepsilon}_{output} = \mathbf{D}^{-1}(\omega)\mathbf{f}(\omega) - \mathbf{u}(\omega) \tag{4.3}$$

This approach has the advantage of minimising the error between directly measured responses, although it becomes a non-linear treatment of the updating parameters caused by the inverse relationship between the design parameters and the response matrix.

4.2.1 Least squares estimator

An objective function involving modal or dynamic frequency response data determine the correlation between the measured and predicted responses. In general, the objective function is non-linear functions with respect to the model parameters, and then the possibly associated convergence problems require an iterative procedure (Friswell and Mottershead, 1995). The methods generally are based on the use of a truncated Taylor series expansion of the modal or response data in terms of the unknown parameters, which is often limited to the first two terms. Considering the FRF's as measured output this linear approximation is given by:

$$\delta\mathbf{H} = \mathbf{S}_j\delta\boldsymbol{\psi}, \tag{4.4}$$

where $\delta\mathbf{H} = \mathbf{H}_m - \mathbf{H}_j$ is the residual of the measured FRF's, $\delta\boldsymbol{\psi} = \boldsymbol{\psi} - \boldsymbol{\psi}_j$ is the perturbation in the parameters, and $\mathbf{S}_j$ is the sensitivity matrix (see Section 4.3). It contains the derivatives of the FRF's with respect to the parameters ($\partial\mathbf{H}_j/\boldsymbol{\psi}_j$), evaluated at the current parameter j. The iteration is initialized with *guess values* for the initial parameter vector ($\boldsymbol{\psi}_0$). It is assumed that the number of measured data is bigger than the number of unknown parameters, which produces an overdetermined set of simultaneous equations that can be solved using the least squares solution technique. The objective function is defined as,

$$J(\delta\boldsymbol{\psi}) = \boldsymbol{\varepsilon}^T\boldsymbol{\varepsilon}, \tag{4.5}$$

where $\boldsymbol{\varepsilon}$ is the error in the predicted measurements based on the updated parameters given by,

$$\boldsymbol{\varepsilon} = \delta\mathbf{H} - \mathbf{S}_j\delta\boldsymbol{\psi} \tag{4.6}$$

Substituting equation (4.6) in equation (4.5) leads to

$$\begin{aligned} J(\delta\boldsymbol{\psi}) &= \{\delta\boldsymbol{\psi} - \mathbf{S}\delta\mathbf{H}\}^T\{\delta\boldsymbol{\psi} - \mathbf{S}\delta\mathbf{H}\} \\ &= \delta\mathbf{H}^T\delta\mathbf{H} - 2\delta\boldsymbol{\psi}^T\mathbf{S}_j^T\delta\mathbf{H} + \delta\boldsymbol{\psi}^T\mathbf{S}_j^T\mathbf{S}_j\delta\boldsymbol{\psi}, \end{aligned} \tag{4.7}$$

By minimizing J with respect to $\delta\boldsymbol{\psi}$ it has,

$$\delta\boldsymbol{\psi} = [\mathbf{S}^T\mathbf{S}]^{-1}\mathbf{S}^T\delta\mathbf{H}, \tag{4.8}$$

or in full,

$$\boldsymbol{\psi}_{j+1} = \boldsymbol{\psi}_j + [\mathbf{S}_j^T\mathbf{S}_j]^{-1}\mathbf{S}_j^T(\mathbf{H}_m - \mathbf{H}_j). \tag{4.9}$$

In this approach equal weighting is given to the measured components. However, in certain types of problem, e.g. in vibration test, components like natural frequencies and mode shape may have different reliability. To incorporate this relative accuracy the updating algorithm adopt the weighting objective function:

$$J(\delta\boldsymbol{\psi}) = \boldsymbol{\varepsilon}^T\mathbf{W}_e\boldsymbol{\varepsilon}, \tag{4.10}$$

where $\mathbf{W}_e$ is a positive definite weighting measurement error matrix. Substituting equation (4.6) in equation (4.10) and operating, leads to

$$J(\delta\boldsymbol{\psi}) = \mathbf{W}_e\delta\mathbf{H}\delta\mathbf{H}^T - \mathbf{W}_e(\mathbf{S}\delta\mathbf{H}^T\delta\boldsymbol{\psi} + \mathbf{S}^T\delta\mathbf{H}\delta\boldsymbol{\psi}^T) + \delta\boldsymbol{\psi}\mathbf{S}\mathbf{W}_e\mathbf{S}^T\delta\boldsymbol{\psi}^T. \tag{4.11}$$

Minimizing J with respect to $\delta\boldsymbol{\psi}$ it has

$$\nabla J(\delta\boldsymbol{\psi}) = 0 = -\mathbf{S}\mathbf{W}_e\delta\mathbf{H}^T + \mathbf{S}\mathbf{S}^T\mathbf{W}_e\delta\boldsymbol{\psi}, \tag{4.12}$$

and solving equation (4.12) for $\delta\boldsymbol{\psi}$ results,

$$\delta\boldsymbol{\psi} = [\mathbf{S}^T\mathbf{W}_e\mathbf{S}]^{-1}\mathbf{S}^T\mathbf{W}_e\delta\mathbf{H}. \tag{4.13}$$

Thus, the updated parameter can be obtained as:

$$\boldsymbol{\psi}_{j+1} = \boldsymbol{\psi}_j + [\mathbf{S}_j^T\mathbf{W}_e\mathbf{S}_j]^{-1}\mathbf{S}_j^T\mathbf{W}_e(\mathbf{H}_m - \mathbf{H}_j). \tag{4.14}$$

An alternative approach to obtaining a well conditioned set of equations is to weight the initial estimate of the unknown parameters and the errors in the measurements. Thus the objective function is given by

$$\begin{aligned} J(\delta\boldsymbol{\psi}) &= \boldsymbol{\varepsilon}^T\mathbf{W}_e\boldsymbol{\varepsilon} + (\boldsymbol{\psi}_j - \boldsymbol{\psi}_0)^T\mathbf{W}_p(\boldsymbol{\psi}_j - \boldsymbol{\psi}_0) \\ &= \boldsymbol{\varepsilon}^T\mathbf{W}_e\boldsymbol{\varepsilon} + \left\{\delta\boldsymbol{\psi} + (\boldsymbol{\psi}_j - \boldsymbol{\psi}_0)\right\}^T\mathbf{W}_p\left\{\delta\boldsymbol{\psi} + (\boldsymbol{\psi}_j - \boldsymbol{\psi}_0)\right\}. \end{aligned} \tag{4.15}$$

where $\mathbf{W}_p$ is the weighting parameter matrix and $\boldsymbol{\psi}_0$ is the initial parameter vector. Expanding the second term and substituting equation (4.6) in equation (4.15), leads to

$$\begin{aligned} J(\delta\boldsymbol{\psi}) &= \delta\mathbf{H}^T\mathbf{W}_e\delta\mathbf{H} + (\boldsymbol{\psi}_j - \boldsymbol{\psi}_0)^T\mathbf{W}_p(\boldsymbol{\psi}_j - \boldsymbol{\psi}_0) \\ &\quad - 2\delta\boldsymbol{\psi}^T\left\{\mathbf{S}^T\mathbf{W}_e\delta\mathbf{H} - \mathbf{W}_p(\boldsymbol{\psi}_j - \boldsymbol{\psi}_0)\right\} + \delta\boldsymbol{\psi}^T\left[\mathbf{S}^T\mathbf{W}_e\mathbf{S} + \mathbf{W}_p\right]\delta\boldsymbol{\psi}. \end{aligned} \tag{4.16}$$

Minimizing J with respect to $\delta\boldsymbol{\psi}$ gives

$$\delta\boldsymbol{\psi} = [\mathbf{S}^T\mathbf{W}_e\mathbf{S} + \mathbf{W}_p]^{-1}\left\{\mathbf{S}^T\mathbf{W}_e\delta\mathbf{H} - \mathbf{W}_p(\boldsymbol{\psi}_j - \boldsymbol{\psi}_0)\right\}. \tag{4.17}$$

or in full as,

$$\boldsymbol{\psi}_{j+1} = \boldsymbol{\psi}_j + [\mathbf{S}_j^T\mathbf{W}_e\mathbf{S}_j + \mathbf{W}_p]^{-1}\left\{\mathbf{S}_j^T\mathbf{W}_e\left(\mathbf{H}_m - \mathbf{H}_j\right) - \mathbf{W}_p(\boldsymbol{\psi}_j - \boldsymbol{\psi}_0)\right\}. \tag{4.18}$$

The weighted least squares method is a good practice in case it is difficult to obtain a convergent solution because of an ill-conditioned sensitivity matrix Mottershead et al. (2011). The choice of weighting matrices is a difficult subject, and estimated statistical properties can be employed (Friswell and Mottershead, 1995; Natke, 1988a; Link, 1998). Titurus and Friswell presented a regularization treatment within the context of sensitivity-based finite element model updating. In this work we use a diagonal error measurement weighting matrix presented by Grafe (1998). No explicit statistical calculations of the weighting factors are required and the correlation coefficient $(X_s(\omega))$ is directly applied as,

$$[^\setminus\mathbf{W}_{e\setminus}] = [^\setminus X_s(\omega)_\setminus] \tag{4.19}$$

The Correlation coefficient is based on the Modal Assurance Criterion - MAC (Allemang and Brown, 1982; Allemang, 2002), where for any measured frequency point a correlation between the measured and predicted value is give by

$$X_s(\omega) = \frac{\left|\{\mathbf{H}_m(\omega)\}^H\{\mathbf{H}_{an}(\omega)\}\right|^2}{(\{\mathbf{H}_m(\omega)\}^H\{\mathbf{H}_m(\omega)\})(\{\mathbf{H}_{an}(\omega)\}^H\{\mathbf{H}_{an}(\omega)\})} \tag{4.20}$$

where $\mathbf{H}_m(\omega)$ and $\mathbf{H}_{an}(\omega)$ are the measured and predicted FRF vectors at matching excitation/response locations, respectively. Proposed by Mottershead and Foster (1991) and Link (1998) the parameter weighting matrix, $(\mathbf{W}_p)$, used here is expressed as

$$[^\setminus\mathbf{W}_{p\setminus}] = \frac{\|[\mathtt{W}_e]\|_2}{\max(\mathrm{diag}([\mathtt{W}_e]))}[\mathrm{diag}([\mathtt{W}_e])] \tag{4.21}$$

where $[\mathtt{W}_e] = [\mathbf{S}[^\setminus\mathbf{W}_{e\setminus}]\mathbf{S}^T]^{-1}$. The weighting matrix varies from one iteration to the next. Solution of equation (4.18) represents the standard weighted least-square solution when equation (4.21) is zero. In all other cases, the diagonal elements constrain their corresponding updating parameters in proportion to their sensitivity. Mottershead and Foster (1991) proposed an alternative definition of weighting matrix equation (4.21) for the case when a parameter remains unchanged if its corresponding sensitivity approaches zero.

4.3 Sensitivity calculation for deterministic system

The sensitivity calculations is a procedure that usually linearise some non-linear relationship between measured outputs (modal data or FRF's) and the model parameters (Grafe, 1998; Mottershead et al., 2011). Hua et al. (2008) presented the computation of second-order sensitivities. The problem solution is obtained by an iterative procedure. During the iterations the gradient or system's sensitivity related to the parameters is the main consideration. In this work the system's components adjusted by model updating technique are the FRF predictions, $\mathbf{H} = \mathbf{D}^{-1}(\boldsymbol{\psi},\omega)$. There are some ways to compute the FRF sensitivity. All of them require the derivative of the dynamic stiffness matrix in one way or another. Some description about how to calculate the sensitivity matrix can be founded in the references (Vanhonacker, 1989; Sutter, 1988; Sutter and Brooks, 1988; Adelman and Haftka, 1986; Wolfe, 1978). Three of them are described in the following.

4.3.1 Linear scale

Considering that $\mathbf{H}(\omega) = \mathbf{D}^{-1}(\omega)$ an it is written in a linear scale, the first derivative of the FRF related to the model parameters can be written as:

$$
\begin{aligned}
\frac{\partial \mathbf{H}(\omega)}{\partial \boldsymbol{\psi}} &= \frac{\partial}{\partial \boldsymbol{\psi}}[\mathbf{H}(\omega)\underbrace{\mathbf{D}(\omega)\mathbf{H}(\omega)}_{\mathbf{I}}] \\
&= \frac{\partial \mathbf{H}(\omega)}{\partial \boldsymbol{\psi}}\underbrace{\mathbf{D}(\omega)\mathbf{H}(\omega)}_{\mathbf{I}} + \mathbf{H}(\omega)\frac{\partial \mathbf{D}(\omega)}{\partial \boldsymbol{\psi}}\mathbf{H}(\omega) + \underbrace{\mathbf{H}(\omega)\mathbf{D}(\omega)}_{\mathbf{I}}\frac{\partial \mathbf{H}(\omega)}{\partial \boldsymbol{\psi}} \\
&= 2\frac{\partial \mathbf{H}(\omega)}{\partial \boldsymbol{\psi}} + \mathbf{H}(\omega)\frac{\partial \mathbf{D}(\omega)}{\partial \boldsymbol{\psi}}\mathbf{H}(\omega) \\
&= -\mathbf{H}(\omega)\frac{\partial \mathbf{D}(\omega)}{\partial \boldsymbol{\psi}}\mathbf{H}(\omega)
\end{aligned}
\tag{4.22}
$$

The sensitivity of the FRF developed in equation (4.22) is valid for generally damped systems yielding complex responses. It reduces the computational effort to the evaluation of dynamic stiffness derivative. In fact this mathematical approximation of $\partial \mathbf{H}(\omega)\ \partial \boldsymbol{\psi}$ calculated from the derivatives of $\mathbf{D}(\omega)$ is easier and more accurate to compute than the partial derivative directly.

Often the FRF has real $\Re()$ and imaginary $\Im$ parts. In this case the elements of the response matrix become complex as $\mathbf{H}(\omega) = \Re(\mathbf{H}(\omega)) + i\Im(\mathbf{H}(\omega))$, and the sensitivities can be written as a complex variable by

$$\frac{\partial \mathbf{H}(\omega)}{\partial \psi} = \frac{\partial \Re(\mathbf{H}(\omega))}{\partial \psi} + \frac{\partial \Im(\mathbf{H}(\omega))i}{\partial \psi} \tag{4.23}$$

4.3.2 Logarithmic scale

It is a common practice to use FRF's in dB scale or logarithmic. Besides, in order to improve convergence of iterative model updating procedure some authors proposed to use $\delta\mathbf{H}$ in equation (4.4) in dB scale instead of linear scale. Also the difference between the measurements ($\mathbf{H}_m(\omega)$) and the predictions ($\mathbf{H}_{an}(\omega)$) using a norm in the form of the objective function as (Balmes, 1993):

$$J(\vartheta) = \|20\log|\mathbf{H}_{an}(\omega,\vartheta)| - 20\log|\mathbf{H}_m(\omega)|\| \tag{4.24}$$

Based on these arguments Arruda and Duarte (1990); Arruda (1992) proposed the sensitivity calculation of FRFs written in dB scale as:

$$\begin{aligned}
\frac{\partial(20\log|\mathbf{H}(\omega)|)}{\partial\psi} &= \frac{\partial(20\log\sqrt{\Re(\mathbf{H}(\omega))^2 + \Im(\mathbf{H}(\omega))^2})}{\partial\psi} \\
&= \frac{20}{\ln(10)}\left(\frac{\Re(\mathbf{H}(\omega))\frac{\partial\Re(\mathbf{H}(\omega))}{\partial\psi} + \Im(\mathbf{H}(\omega))\frac{\partial\Im(\mathbf{H}(\omega))}{\partial\psi}}{\Re(\mathbf{H}(\omega))^2 + \Im(\mathbf{H}(\omega))^2}\right) \\
&\approx 8.6859\left(\frac{\Re(\mathbf{H}(\omega))\frac{\partial\Re(\mathbf{H}(\omega))}{\partial\psi} + \Im(\mathbf{H}(\omega))\frac{\partial\Im(\mathbf{H}(\omega))}{\partial\psi}}{\Re(\mathbf{H}(\omega))^2 + \Im(\mathbf{H}(\omega))^2}\right)
\end{aligned} \tag{4.25}$$

Balmes (1993) shown a comparison between the logarithmic least-squares cost function (equation 4.24) with the equivalent linear least-squares objective function. The logarithmic approach found to be locally convex in much larger regions than the equivalent linear formulation. Since the level of response change in dB scale is naturally much smaller than that in a linear scale, the sensitivitie calculation in logarithmic scale will be smaller in magnitude (Grafe, 1998). Furthermore, in terms of physical meaning the sensitivity in logarithmic scale is more accessible than sensitivity in linear scale, because it works with absolute values.

4.3.3 Sensitivity calculation for stochastic system

Some authors have presented eigen-sensitivity or FRF-sensitivity for stochastic systems. Mottershead et al. (2015) published a brief overview of sensitivity calculation for stochastic model updating. Govers and Link (2010) defined an objective function for the identification of updating-parameter covariances with the forward propagation of parameters in each iteration. Rui et al. (2013) presented a computationally efficient approach to stochastic model updating by using the Polynomial Chaos expansion. Fang et al. (2012) proposed a stochastic model updating method for parameter variability quantification based on Response Surface models and Monte Carlo simulation. Adhikari and Friswell (2010) proposed a distributed parameter model updating using the Karhunen-Loève expansion, where they used eigen-sensitivities procedure and the Karhunen-Loève expansion to represent distributed parameters. This section presents a treatment of the sensitivity using FRF and KL expansion. It is a new approach, when the coefficients of the KL expansion assumed as uncertain parameters will be estimated using the equation (4.14). For that a FRF sensitivity in the stochastic context is developed along this section.

Natke (1977); Cottin et al. (1984); Arruda and Santos (1993); Grafe (1998) used the deterministic FRF sensitivity related to the model parameter vector $\boldsymbol{\psi}$ which is expressed as:

$$\frac{\partial \mathbf{H}(\omega)}{\partial \boldsymbol{\psi}} = -\mathbf{H}(\omega)\frac{\partial \mathbf{D}_0(\omega)}{\partial \boldsymbol{\psi}}\mathbf{H}(\omega) \tag{4.26}$$

where $\mathbf{H}(\omega) = \mathbf{D}_0^{-1}(\omega)$ is inverse of the deterministic dynamic stiffness matrix.

In the stochastic context, two techniques are used. The first one estimates $\boldsymbol{\psi}(\theta)$ as random variable vector. The second one estimates $\boldsymbol{\psi}(\theta) = \boldsymbol{\xi}(\theta)$ which is a random field parameter vector in the KL expansion (equation 2.19). In the first approach equation (4.26) becomes:

$$\frac{\partial \mathbf{H}(\omega,\theta)}{\partial \boldsymbol{\xi}(\theta)} = -\mathbf{H}(\omega,\theta)\frac{\partial \mathbf{D}(\omega,\theta)}{\partial \boldsymbol{\xi}(\theta)}\mathbf{H}(\omega,\theta) \tag{4.27}$$

where $\mathbf{H}(\omega,\theta) = \mathbf{D}^{-1}(\omega,\theta)$, which is inverse of the stochastic dynamic stiffness matrix. Then, equation (4.27) becomes:

$$\frac{\partial \mathbf{H}(\omega,\theta)}{\partial \boldsymbol{\xi}} = -\mathbf{H}(\omega,\theta)\left[\frac{\partial \mathbf{K}(\omega,\theta)}{\partial \boldsymbol{\xi}_{Kj}} - \omega^2\frac{\partial \mathbf{M}(\omega,\theta)}{\partial \boldsymbol{\xi}_{Mj}}\right]\mathbf{H}(\omega,\theta) \tag{4.28}$$

the derivative of $\mathbf{K}(\omega,\theta)$ and $\mathbf{M}(\omega,\theta)$ related to the parameter $\boldsymbol{\xi}_{Kj}$ and $\boldsymbol{\xi}_{Mj}$, respectively, produces:

$$\frac{\partial \mathbf{K}(\omega,\theta)}{\partial \boldsymbol{\xi}_{Kj}(\theta)} = \varepsilon_1\sqrt{\lambda_{Kj}}\mathbf{K}_j(\omega) \tag{4.29}$$

and

$$\frac{\partial \mathbf{M}(\omega,\theta)}{\partial \boldsymbol{\xi}_{Mj}(\theta)} = \varepsilon_2\sqrt{\lambda_{Mj}}\mathbf{M}_j(\omega) \tag{4.30}$$

Substituting equations (4.29) and (4.30) in equation (4.28) it has,

$$\frac{\partial \mathbf{H}(\omega,\theta)}{\partial \boldsymbol{\xi}(\theta)} = s_{ij} = -\mathbf{H}(\omega,\theta)\left[\varepsilon_1\sqrt{\lambda_{Kj}}\mathbf{K}_j(\omega) - \omega^2\varepsilon_2\sqrt{\lambda_{Mj}}\mathbf{M}_j(\omega)\right]\mathbf{H}(\omega,\theta) \tag{4.31}$$

In this work the sensitivity of the receptance FRFs $\frac{\partial \mathbf{H}(\omega,\theta)}{\partial \boldsymbol{\xi}(\theta)}$ were taken in dB scale (Arruda, 1992) with 1.0 [m/N] as reference. It can be shown by,

$$\frac{\partial 20 \log |\mathbf{H}(\omega,\theta)|}{\partial \boldsymbol{\xi}(\theta)} \approx 8.6859 \left(\frac{\Re(\mathbf{H}(\omega,\theta))\frac{\partial(\mathbf{H}(\omega,\theta))}{\partial \boldsymbol{\xi}(\theta)} + \Im(\mathbf{H}(\omega,\theta))\frac{\partial(\mathbf{H}(\omega,\theta))}{\partial \boldsymbol{\xi}(\theta)}}{\Re(\mathbf{H}(\omega,\theta))^2 + \Im(\mathbf{H}(\omega,\theta))^2} \right) \tag{4.32}$$

Equation (4.32) represents the elements of the sensitivity matrix S_{ij}, and the $N_K + N_M$ dimensional vector of updating parameters

$$\boldsymbol{\xi} = [\xi_{K_1},\xi_{K_2}...,\xi_{K_{N_K}} \quad \xi_{M_1},\xi_{M_2}...,\xi_{M_{N_M}}]^T \tag{4.33}$$

The elements of the vector $\boldsymbol{\xi}$ are sampled from independent and identically distributed standard Gaussian random variables (i.e., with zero-mean and unit standard deviation) from the KL expansion. The parameter vector $\boldsymbol{\xi}$ will be estimated from the measured FRF and used to reconstruct the $EA(x,\theta)$ and $\rho A(x,\theta)$ random fields. Once obtained the parameters $\boldsymbol{\xi}$ the estimated FRF is

$$\mathbf{H} = \mathbf{H}_0 + \mathbf{S}\boldsymbol{\xi} \tag{4.34}$$

where $\mathbf{H}_0$ is the vector of deterministic FRF measured at a specified point, S is the sensitivity matrix calculated with equation (4.31), and vector $\boldsymbol{\xi}$ is parameter obtained of equation (4.33).

4.4 Numerical and experimental application

4.4.1 Numerical test in rod

In the numerical test, a free-free rod structure is modelled by a two nodes rod spectral element with variabilities considered at the longitudinal rigidity EA and at the mass per unit of length ρA. The measured FRF simulates the inertance FRF with force excitation in node 2 and response in node 1. The unperturbed physical and geometrical properties of the rod are; length of $L = 3.0$ m, high of $h = 0.02$ m, base of $b = 0.02$ m, $E = 71$ GPa, $\eta = 0.01$, and $\rho = 2700$ kg/m^3. It assumed that the variations from the unperturbed value of EA and ρA can be modelled by homogeneous Gamma random field and then transposed to a Gamma distribution by using a memoryless transformation. For numerical calculations we considered 10% of variation with a correlation length of $\mathtt{b} = L/3$. The correlation length value is a chosen referent with the number of terms, as mentioned in Section 2.4.

Two analysis verify the presented theory. The main goal of them is to show the efficiency of the developed technique in parameter estimation and random field reconstruction, both using a direct FRF based on a stochastic model. In the first analysis the objective is to be estimate a single variable, it is longitudinal rigidity and mass per unit of length. Figure 4.1 shows EA and

ρA parameters convergence from three different input variable with initial values about 10%, 20% and 30% of the exact value. In all cases analysed results were satisfactory and minimal error associated. The error and iteration number increase as the input values are far from the exact value. Figure 4.2 shows the comparison of initial, measured, and estimated FRF with an initial parameter of 30% of the exact value. Estimated FRF calculated by using the updated parameter seems close to the measured FRF, because the updated parameters EA and ρA were predicted with a small error.

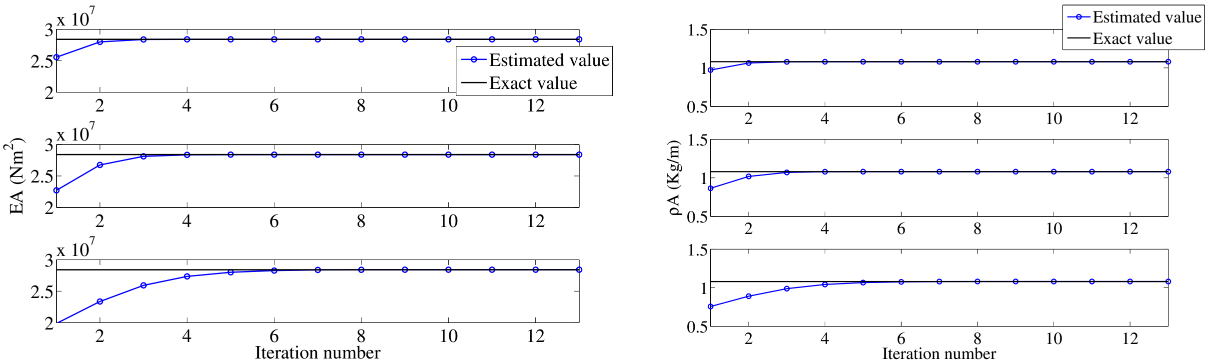

Figure. 4.1: Parameters estimation from initial values with error of 10%, 20% and 30%.

Additionally to the first analysis, considering that the measured FRF contaminated with additive random noise, having zero mean and with mutually independent entries. Parameter starts with 30% of error of exact parameter value. Figure 4.3 shows the estimation of EA and ρA calculated from a measured FRF with additive random noise related with iteration number. Also, it shows approximated results for EA and ρA with a small error associated, and estimated FRF calculated by using the updated parameter close to the measured FRF. Figure 4.4 shows the comparison of an initial, measured with additive noise, and estimated FRF's.

Tables 4.1 and 4.2 summarized the results of initial, exact and estimated values with associated errors. Good results presented in this first tests demonstrated the efficiency of the technique in parameter estimation. Noting that the FRFs were obtained using stochastic models

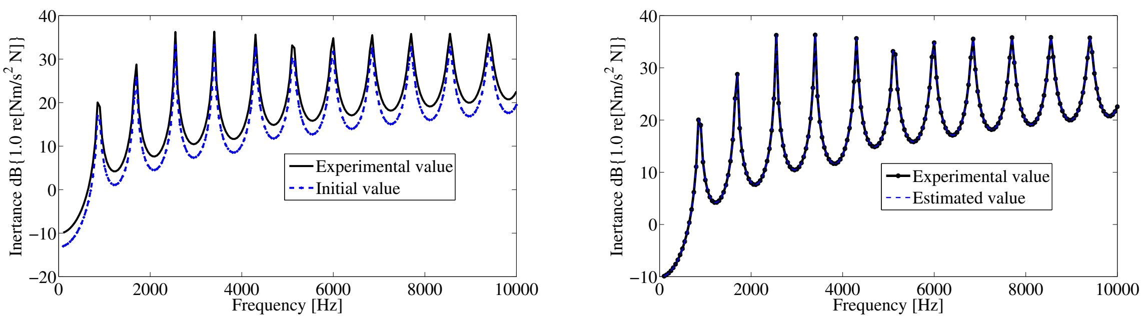

Figure. 4.2: Comparison between an initial value and the "measured" FRF (LHS) and between the "measured" and estimated FRF (RHS).

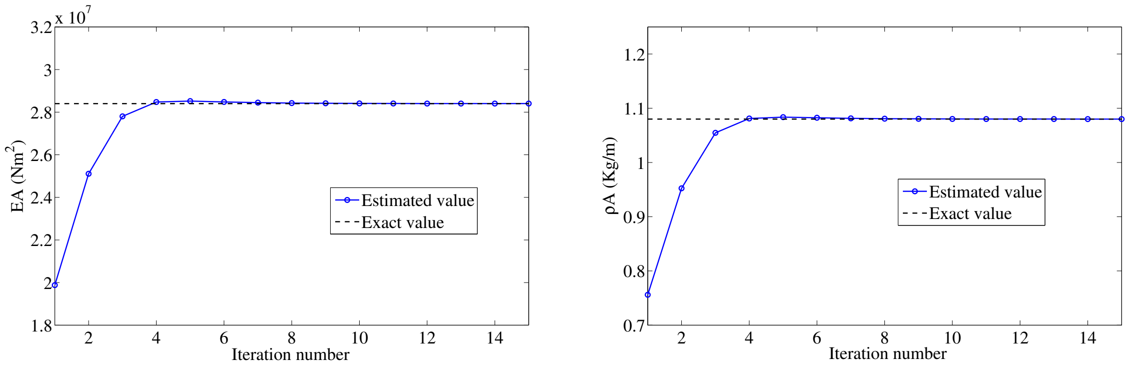

Figure. 4.3: Longitudinal rigidity and mass estimation compared with the exact values.

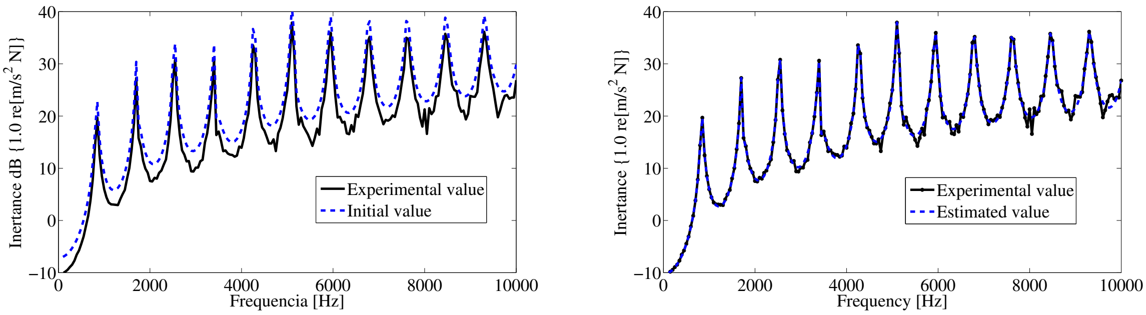

Figure. 4.4: Comparison between an initial value and the "measured" FRF contaminated with Gaussian random noise at left-hand side and between the "measured" FRF contaminated with Gaussian random noise and estimated FRF.

Table 4.1: Results of initial, exact and estimated values with error associated for the longitudinal rigidity EA.

Parameter	EA			
Exact value	$2.84\text{x}10^7$			
Initial value (Error[%])	$2.56\text{x}10^7$(10)	$2.27\text{x}10^7$(20)	$1.98\text{x}10^7$(30)	$1.98\text{x}10^7$(30)*
Estimated value (Error[%])	$2.84\text{x}10^7$(0.002)	$2.839\text{x}10^7$(0.016)	$2.837\text{x}10^7$(0.1)	$2.845\text{x}10^7$(0.17)

*"Measured" FRF contaminated with Gaussian random noise.

Table 4.2: Results of initial, exact and estimated values with error associated for the mass per unit of length ρA.

Parameter	ρA			
Exact value	1.08			
Initial value (Error[%])	0.972(10)	0.864(20)	0.756(30)	0.756(30)*
Estimated value (Error[%])	1.0799(0.0092)	1.0802(0.0185)	1.0789(0.1019)	1.0804(0.0370)

*"Measured" FRF contaminated with Gaussian random noise.

presented in Section 3.

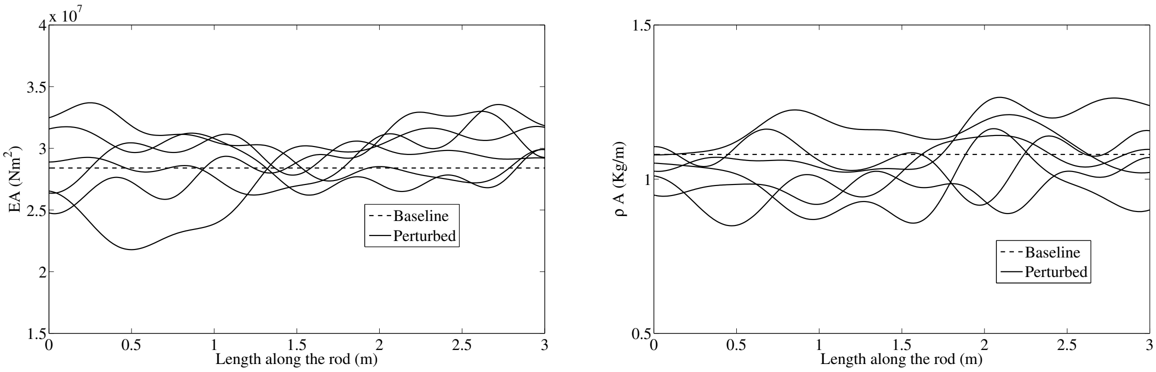

Figure. 4.5: Random realizations of the rod longitudinal rigidity EA (LHS) and random realizations of the rod mass per unit of length ρA (RHS), for both correlation length $\mathtt{b} = L/3$, strength parameter $\varepsilon_1 = 0.1$ and number of terms $N = 12$.

The second analysis carry out the parameter estimation of the random fields. Generated data using 12 terms in the KL expansion compared with the baseline value showed in figure 4.5. These random realisations of the variability type simulating a physical structure behaviour. In the present example, we treat the FRF obtained at node 2 of the perturbed rod element as "measured". This analysis tries to simulate a realistic situation where the true model parameters, EA and ρA can deviate from the baseline assumed values in a priori unknown manner. The objective is to reconstruct the distributed longitudinal rigidity EA function and mass ρA from the "measured FRF obtained with a stochastic model of a sample rod. Previously, a study realised in the sensitivity matrix demonstrate any likely ill-conditioning problems. A test performed in EA and ρA versus KL mode shows the parameter sensitivity. Figure 4.6 shows one FRF sensitivity vector calculated for 12 modes in the KL expansion. Adhikari and Friswell (2010) realised similar test although using modal parameters. In this work they found several orders of magnitude difference in some sensitivities, and in particular the natural frequencies are much more sensitive to the odd terms in the KL expansion than the even terms. They concluded that it is highly unlikely that the distributed parameter can be accurately reconstructed from the lower measured natural frequencies. Returning to our approach, by analysing along the FRF sensitivity vector, it can be seen that resonance peaks present close amplitudes among them. Also, the FRF's do not show different sensitivities related to odd or even terms in KL expansion, which prove the sensitivity in parameter and an estimation accurate. The amplitudes analysis in each resonance frequency related to the FRF sensitivity vector obtained with the odd and even coefficients in the KL expansion can be seen more clearly at the figure 4.7. The FRF sensitivities vary with the parameter number and in certain FRF vector points. These features mean that the distributed longitudinal rigidity EA and mass ρA have a high sensitivity which may enhance the accuracy at parameter reconstruction.

The longitudinal rigidity and mass based on updating of 12 parameters ($\boldsymbol{xi}$) and the re-

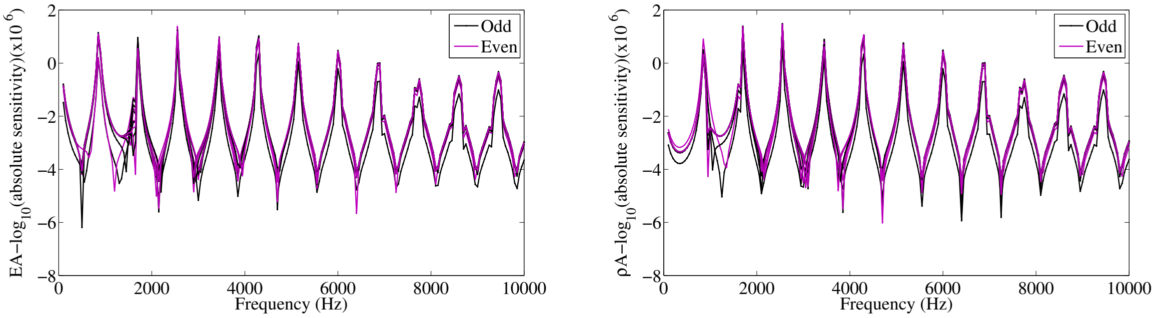

Figure. 4.6: FRF sensitivity vector of EA (LHS) and ρA (RHS) in the KL expansion, both with multiplied by 10^6.

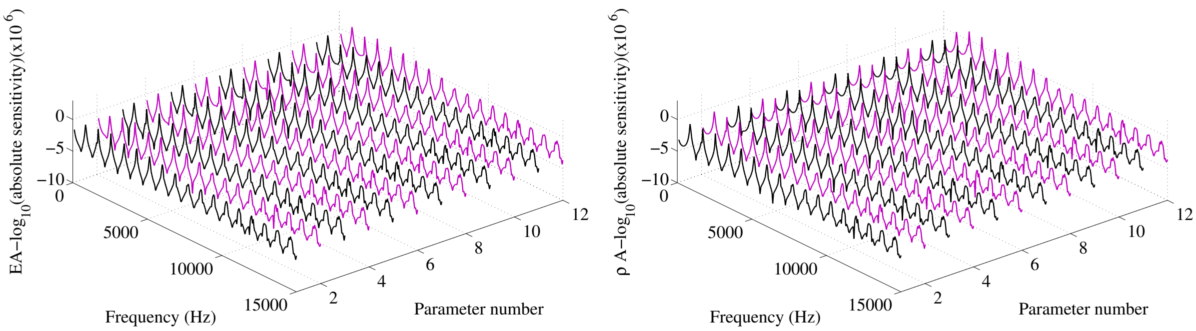

Figure. 4.7: FRF sensitivity vector for the EA (LHS) and ρA (RHS) in the KL expansion multiplied by 10^6.

constructed variables random field evaluated with 4, 8 and 12 terms of KL expansion are shown in figure 4.8. In both cases, the variables function are smoother than the simulated function that generated the data. This is because the higher terms in the KL expansion cannot be precisely estimated from the data, although a good approximation result is found for the reconstructed longitudinal rigidity and mass as compared with the generated sample.

Next, the reconstructed longitudinal rigidity EA and mass per unit of length ρA are used to calculate the frequency response function of the stochastic rod in each iteration of the optimization procedure. Figure 4.9 shows the comparison among initial, measured, and estimated FRF. The responses used 8 and 12 terms in KL expansion, it is clear that the FRF calculated using 12 terms is more accurate than the FRF calculated with 8, however in both cases the estimated FRF do not present close results of the measured FRF as a consequence of the variables random field could not be precisely reconstructed.

In a brief overview of this numeral test using a rod, it was proposed a technique for estimation of the distributed parameters in structural dynamics by using FRF. Randomness included in the rod longitudinal rigidity (EA) and mass per unit of length (ρA) has the aim to obtain a more realistic model. As the distributed parameters are the parameters updated target, the formulation is based on stochastic model expanded in KL expansion and sensitivity analysis using FRF.

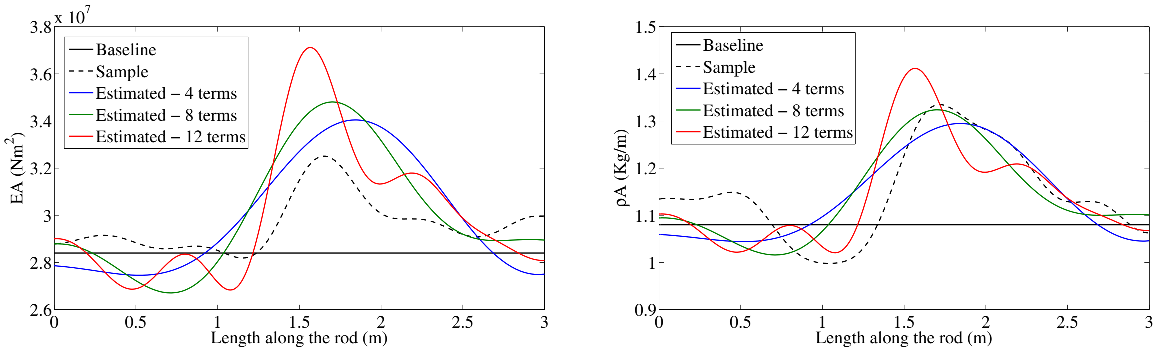

Figure. 4.8: Baseline, actual and reconstructed values of the longitudinal rigidity along the length of the rod (LHS) and mass per unit of length (RHS)

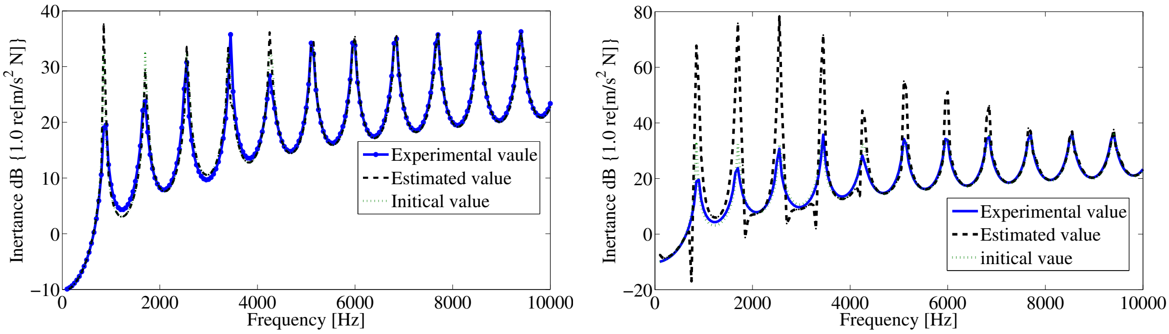

Figure. 4.9: Comparison between an initial value and the "measured" FRF computed with 12 modes in KL expansion at left-hand side and between the "measured" and estimated FRF at right-hand side with computed with 8 modes in KL expansion

Sensitivity method based on the frequency response function is also developed for a stochastic proposal. To verify the efficiency of the technique presented two analysis are performed. In the first case, a single value estimation of longitudinal rigidity and mass per unit of length from a stochastic model is the main goal. Initial parameters values are 10%, 20% and 30% of the exact value. In all cases, results obtained for EA and ρA estimation were satisfactory in view of the minimal percent error associated. Another parameter estimation was evaluated from measured FRF contaminated with additive random noise. Initial parameter starts with an error of 30%. Since in the presence of noise, it presents approximated results in the estimation of EA and ρA, and the small percent error justified the analysis. Second case calculated variables of the random field. This analyse try to simulate a realistic situation where the true model parameters, EA and ρA can deviate from the baseline assumed values in an a priori unknown manner. The objective is to reconstruct the distributed longitudinal rigidity and mass from the stochastic model of a sample rod. The random field is discretized into random variables using the Karhunen Loève (KL) expansion. For such distributed deviations (ξ) are a priori unknown and therefore can be considered to be samples from a random field, also it is the updated parameter predicted from the measured FRF through an optimization procedure. A subset of these random variables are in turn considered as parameters to reconstruct the random field of the longitudinal rigidity and mass. The longitudinal rigidity sample has 12 parameters in KL expansion and the reconstructed longitudinal rigidity used 4, 8 and 12 terms of KL expansion. The results presented a smoother response, specially for the lowest number of coefficients in comparison to the simulated function that generated the data. This smoother behaviour is because the higher terms in the KL expansion cannot be estimated from the data, although approximated results were found in all cases simulated. The FRF of the stochastic model uses reconstructed EA and ρA in each iteration of the optimization procedure. The FRF calculated with 12 terms is more accurate than calculated with 8 terms in KL expansion, however in both cases the estimated FRF do not present close results of the measured FRF in reason of the variables random field could not be completely reconstructed.

4.4.2 Numerical and experimental tests in beam

Numerical results

Now, a free-free beam structure is modelled by a two nodes beam spectral element with variabilities considered at the beam flexural rigidity EI and at the mass per unit of length ρA, both structural variabilities are of the Gamma marginal type. The measured FRF simulates the transfer receptance FRF with force excitation at node 1 and displacement response in node 1 and node 2. The unperturbed physical and geometrical properties of the beam are: $L = 0.33$ m, $h = 0.006$ m, $b = 0.018$ m, $\eta = 0.1$, and $\rho = 1140$ kg/m^3. It assumed that a variation of the unperturbed value of EI and ρA can be modelled by a homogeneous Gaussian random field and then transposed to a Gamma distribution by using a memoryless transformation. For numerical calculations we considered 20% of variation with a correlation length of $\mathtt{b} = L/3$.

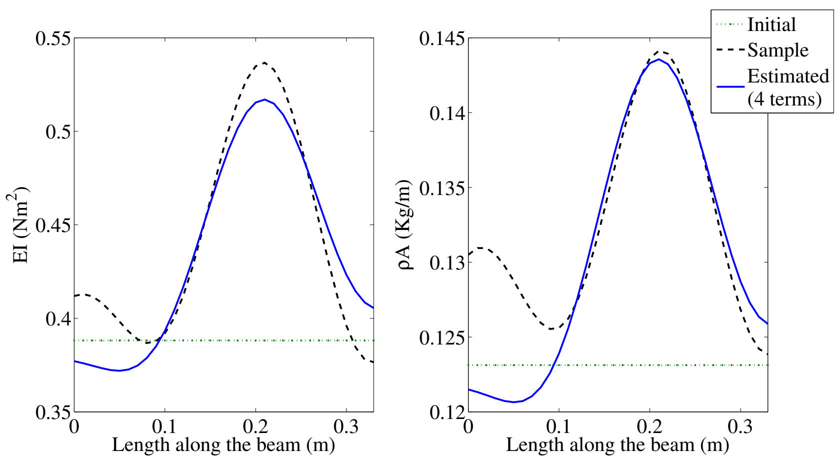

Figure. 4.10: Initial, actual and reconstructed values of the flexural rigidity along the length (LHS) and mass per unit of length (RHS).

A random field estimation of the beam flexural rigidity and mass per unit of length was performed. The data was generated using 4 terms in the KL expansion and the deviations from the initial value is distributed, simulating a physically realistic property. In this numerical test, we use the FRFs obtained at node 1 and 2 of the perturbed beam element as "measured". Two FRF's are considered in order to increase the information of the response and accurate the parameter estimation. The objective is to reconstruct the distributed flexural rigidity EI function and mass ρA from the "measured" FRFs obtained with a sample of a stochastic beam model.

The random field samples estimated using two FRFs with 4 parameters (ξ) of the KL expansion are shown in figure 4.10. In both cases, the functions are smoother than the simulated functions that generated the "measured" data. This is due to the use of just small number of FRF, therefore with poor spatial information. The reconstructed random fields are used to calculate the FRF of the stochastic beam at each iteration of the optimization procedure. The comparison between the "measured", initial and updated FRF is shown in figure 4.11. The FRF with the estimated parameters is closer to the "measured" FRF, as expected.

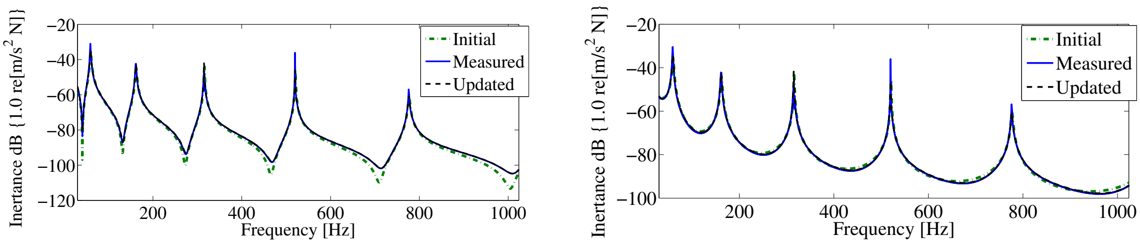

Figure. 4.11: Comparison among an initial value, updated and the "measured" FRF at node 1(LHS) and at node 2 (RHS)

Experimental results

A beam made of polyamide (PA) with uniform rectangular cross-section was used in the experiment tests. The beam is 18mm wide, 6mm thick, with a mass per unit length of 0.02343kg/m. The average flexural rigidity (EI) was obtained experimentally. The beam was manufactured using the Selective Laser Sintering (SLS) technology. As a consequence of the manufacturing process, a variability of the beam properties along its length can be expected. In order to verify the efficiency of the proposed method it was applied to a measured FRF and results were compared with measurements of the flexural rigidity at many points along the beam using an ultrasound apparatus. The Young's modulus (E) was measured at 22 points along the beam with an ultrasonic pulse-echo device. The experimental setup is shown in figure 4.12. In this experiment a shear wave transducer $(U8403072/U8403071)$ was used. The signals were measured and analysed using an Olympus Panametrics NDT EPOCH 4 Ultrasonic Flaw Detector. The measured Young's modulus E along the beam is shown in figure 4.14, where it is compared with the predicted values using the KL expasion with 4 estimated parameters.

Figure. 4.12: Procedure for experimental measure of Nylon beam properties.

Figure 4.13 shows the second experimental test setup, used to measure the FRF. The signals were acquired and analysed using LMS Test Lab. The FRFs were estimated with a bandwidth of 1024Hz and 1024 spectral lines. An impact hammer was used to excite the structure and a micro accelerometer to measure the response. The experimental FRFs were obtained by impact force excitation at node 1 and acceleration response at the point 1 and point 2.

The FRF's reconstructed with the estimated flexural rigidity with 4 terms (ξ) of the KL expansion is illustrated in figure 4.15. The reconstructed $EI(x)$ presents a good agreement with the values measured by ultrasound. The FRF's obtained with the initial constant value of EI, with the estimated $EI(x)$ and the measured FRF's are shown in figure 4.14. As the random field could not be reconstructed accurately, an acceptable difference between updated and measured FRF's can be observed.

In the present tests for beam, a technique to estimate spatially distributed parameters of samples of a stochastic structure using a KL expansion and sensitivity-based FRF model updating was proposed. Randomness was included in the flexural rigidity (EI) and mass per unit length (ρA) of a beam structure. As a stochastic model is employed, the sensitivity-based

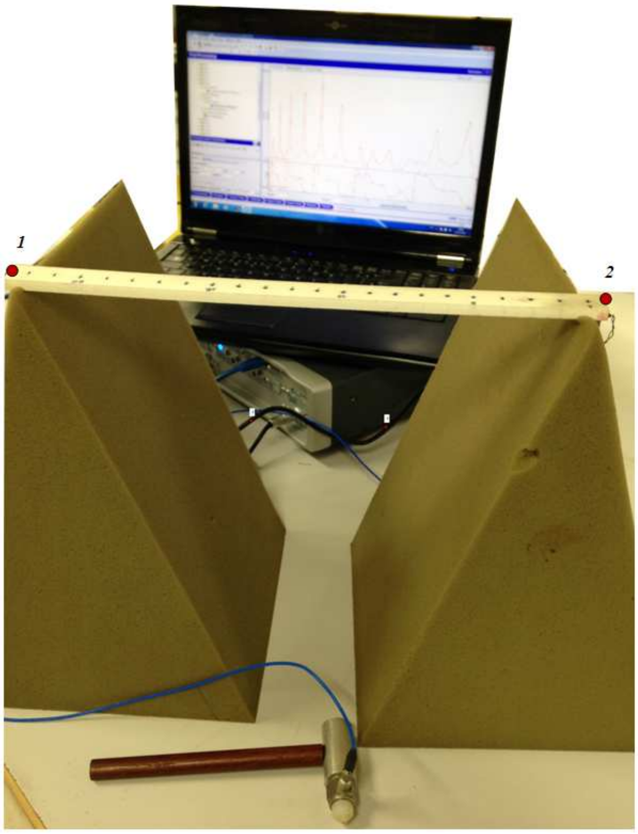

Figure. 4.13: The test rig for the free-free beam.

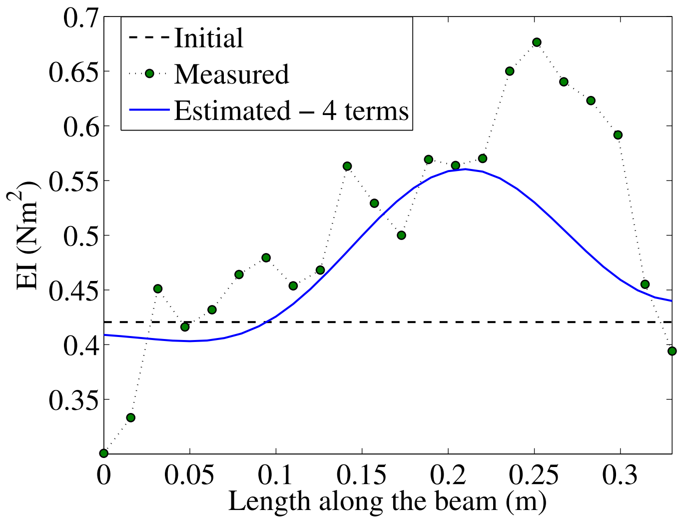

Figure. 4.14: Initial, measured experientially and reconstructed values of the flexural rigidity $(EI(x))$ along the length

method using FRF is also developed for a stochastic model based on spectral beam elements. To verify the efficiency of the presented technique a numerical test and an experimental test were performed. In the first case, random field estimation of the beam flexural rigidity and mass per unit length was performed. This analysis tries to simulate a realistic situation where the

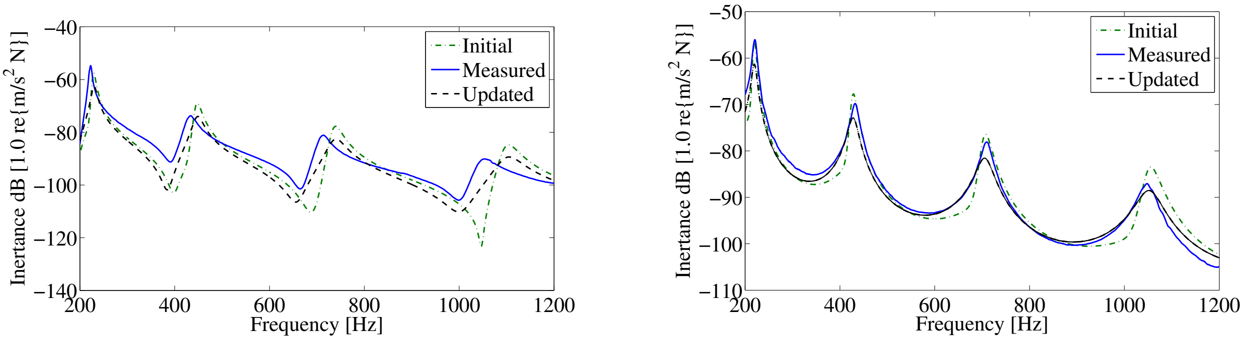

Figure. 4.15: Comparison among an initial value, updated and the measured experientially FRF at node 1(LHS) and at node 2 (RHS)

true model parameters, EI and ρA can deviate from the baseline homogeneous values. The objective is to reconstruct the distributed random field from the measured FRF, obtained for a sample of a stochastic model of the beam. The discretized variables (ξ) were estimated from the measured FRF through a non-linear least squares curve fit procedure. A subset of these random variables can be considered as parameters to reconstruct the random field of the flexural rigidity and mass per unit of length. In the experimental test, an experimentally obtained FRF was used. In this case only the flexural rigidity was predicted. An experimental measurement of the Young's modulus at 22 point along the beam was performed using ultrasound. By comparing the reconstructed and experimentally measured of $EI(x)$ the proposed method proved to work reasonably well. Ongoing work consist of improving these preliminary results by curve fitting many measured FRF, instead of just one, to enrich the spatial information of the measured data.

4.5 Closure

This chapter presented a model updating literature review, the model updating using FRF theory, frequency response function sensitivities, numerical and experimental tests. It showed a proposed method to estimate spatially distributed parameters of samples of a stochastic structure using a KL expansion and sensitivity-based FRF model updating. Two numerical and one experimental tests to verify the developed theory were demonstrated. In brief, the proposed methodology showed acceptable performance by comparing numerical and experimental results.

5 Damage detection in stochastic dynamic system

5.1 Introduction

Mechanical, aerospace, and/or civil structures may be subject to harsh environments such as corrosion, high pressure, earthquakes, hurricanes, and overloads. This kind of environment may cause deterioration the structure. Many methods have been developed to analyse the occurrence, detection and quantification of the damage. Changes in local and global properties of a structure can be induced by damage. This changes under inspection are associated with damage parameters, e.g. changing of stiffness. Among other methods, these changes can detected from dynamic response signals captured from the structure.

During the last decades, modern techniques to detect damage were developed, such as modal-data-based, electro-mechanical-impedance-based, static-parameter-based, acoustic emission, and elastic-wave-based (Su and Ye, 2009). Comprehensive surveys focus on damage identification methods were proposed by Doebling et al. (1996, 1998); Sinou (2013). Sohn et al. (2003) published a survey in structural health monitoring and damage detection techniques for civil and mechanical engineering areas. Structural health monitoring (SHM) can be defined as a process that involves the observation of a structure over time using periodically spaced measurements (Farrar and Worden, 2007; Doebling et al., 1996). These measurements determine the current state of the undamaged system. Dimarogonas (1996) gave an extensive review of damaged structures including beam, rotor, shell and blades, plates and pipelines under vibration. The inverse problem is a technique where the structural model parameters can be identified based on measured frequency response data (Aster and Thurber, 2012). In general, the structural damage is a local phenomenon and produces a stiffness reduction, which changes the frequency response of the system. Friswell (2007) presented a brief overview of the use of inverse methods for damage detection and location from measured data. Some authors (Mottershead and Friswell, 1993; Fritzen and Jennewein, 1998; Friswell and Mottershead, 1995; Morassi and Vestroni, 2008; Santos and Zimmerman, 1996) presented damage estimation methods based on solving the inverse problem. These techniques consist in minimizing the differences between the numerical model and experimental test responses by using a parameter estimation procedure.

Statistical methods were incorporated in damage location as susceptible to measurement error by Cawley et al. (1978); Cawley and Adams (1979). Since then, the number of research including statistical treatment in damage detection has increased (Friswell, 1994; Sohn et al., 2002). Messina et al. (1998) described a structural damage detection through a sensitivity and statistical-based method, they do an assessment of the amount of damage present and validates the method with an experimental investigation. Sohn et al. (2001) and Farrar and Worder (2013) used a combination of time-series analysis, neural networks, and statistical tools to determine the damage state for structures affected the environmental conditions. In order to include parameter variability in damage detection and parameter estimation methods, researchers have recently started to use stochastic models. Xu et al. (2011); NG et al. (2011); Fabro et al. (2010) have proposed stochastic methods to characterize and identify the damage including random parameters based on probabilistic approaches. Vanli and Jung (2013), and Khodaparast and Mottershead (2008) present a probabilistic and stochastic model updating method to improve damage location and damage quantification prediction of a structural health monitoring system.

The presence of a crack in a structure introduces a local flexibility that affects its vibration response. Also, it generates changes in elastic waves that propagate in the structure. Research on damage detection based on elastic wave propagation in structures is concentrated on methods at medium and high frequencies (Krawczuk, 2002; Krawczuk et al., 2006a; Su and Ye, 2009). They utilize the evidence that material discontinuities, such as a crack, generate changes in elastic waves propagating in the structure (Santos et al., 2008). Elastic wave-based damage detection presents some particular advantages like the capability of propagation over significant distances and high sensitivity to discontinuities near the wave propagation path. This research concentrates on methods that use elastic wave propagation in structures at medium and high frequencies (Krawczuk et al., 2006a). Uncertainties such as parameters, modelling, and measurement errors are inherently involved in the damage detection procedure (Xu et al., 2011). Stochastic approaches as the Bayesian methods, the Monte Carlo simulation (MC), and the perturbation methods stand out as the methods being used to detect structural damage considering uncertainties. However, a small number of works found in the literature treat elastic wave propagation under randomness environment. Based on these arguments, this study intends to develop an inverse damage detection method using elastic wave propagation with parameter uncertainties.

The basic issue presented here is to detect and quantify damage in a dynamic system containing uncertain properties. The technique proposed for damage detection is shown in Section 5.2, followed by theory, numerical simulations and experimental test. The method developed for damage detection based on energy method with uncertain parameters with theory and numerical test are presented in Section 5.3.

5.2 Damage detection via explicit formulation

Techniques such as Global Shape Correlation function (GSC), Global Amplitude Correlation function (GAC), the first Global Amplitude Correlation function (AIGSC) and the second Global Amplitude Correlation function (AIGAC) (Zang and Imregun, 2001; Zang et al., 2003), Frequency Response Assurance Criterion (FRAC) (Heylen and Lammens, 1996), Frequency Domain Assurance Criterion (FDAC) and Response Vector Assurance Criterion (RVAC)

(Pascual et al., 1997, 1999), and Frequency response curvature method (Palacz and Krawczuk, 2002) use the difference between damaged and undamaged FRF structures to locate or to estimate damage (Sinou, 2013). Owolabi et al. (2003) and Kin and Stubbs (2003) utilised measured dynamic responses of damaged beams to detect the presence of a crack and to determine its location and size. Maia et al. (2003) proposed a relative damage quantification indicator by using an adaptation of the RVAC. A general overview of research in SHM and damage detection may be found in (Doebling et al., 1998; Friswell, 2007; Sinou, 2013).

In this study, we employed a rod structure modelled by damaged spectral elements to assess damage. The reason for use a rod structure in this first analysis was to avoid the effects of evanescent waves present other kinds of structures, e.g. in beams. To consider the parameter variability in the system response, we include uncertainty related with material property and geometry. The cross section area and Young's modulus of an undamaged and a damaged rod will be assumed as non-Gaussian random variables. These parameters will be expressed as non-Gaussian random fields expanded by using KL. The KL expansion has an underlying Gaussian process, a non-Gaussian process will be expressed through a memoryless transformation of the Gaussian process. The goal is mainly to detect damage by using an explicit euqation. The equation proposed is derived from a relative change between a damaged and undamaged response of the structure. This method allows improving the control over the dispersion in damage quantification obtained from the dynamic response by introducing the uncertainty into the most sensitive parameters of the model. The originality of the method consists in obtaining the crack depth from a structural response obtained of a model taking into account uncertainty in the structural spatially distributed parameters. Analysis using random variables and random field, as well as three different approaches to handling the average of the response being performed.

5.2.1 Explicit crack depth quantification

Regarding the formulation of the crack flexibility coefficient (Θ) showed in Section 3.4, when the integral solution of equation (3.60) may be shown to be

$$\Theta(\alpha) = 2\pi h(0.63\alpha^2 - 0.17\alpha^3 + 5.93\alpha^4 - 10.72\alpha^5 + 31.58\alpha^6 - 67.44\alpha^7 + 139.05\alpha^8 - 146.58\alpha^9 + 92.30\alpha^{10})$$

Since the rod crack depth is a variable that physically quantifies the damage, it is important to find out an explicit equation to obtain α. Nevertheless, the dynamic spectral matrix for the damaged rod element (equation 3.45) is as a function of Θ, which in turn is a polynomial of degree 10 in α. To obtain a simple and feasible explicit solution for α, in this study a priori the crack flexibility polynomial is approximated by its first term.

In structural dynamic testing, it is a common practice to measure the data in the form of frequency response function (FRF). The knowledge about a particular structure will be contained in an analytical (or numerical) model. The theoretical FRF obtained from the analytical model here is the inverse of the dynamic stiffness matrix for structural systems. Many damage quantification methods use of comparing the undamaged with the damaged response of the system. One of them, called Damage Index (DI) define the average power reduction between the damaged and undamaged state signals (Su and Ye, 2009). Others authors (Sinou, 2007; Narkis, 1994; Doebling et al., 1996; Sinou, 2013) proposed the percentage changes in the natural frequencies between the system undamaged and damaged states. Regarding this principle, we used a damage indicator defined by a *relative change* between the damaged and undamaged FRF's system

$$\mathbf{\Lambda}(\omega) = \frac{\mathbf{H}_d(\omega) - \mathbf{H}_u(\omega)}{\mathbf{H}_u(\omega)} \tag{5.1}$$

where $\mathbf{H}_d(\omega) = [\mathbf{K}_{d0}(\omega)]^{-1}$ is the damaged rod frequency response function (FRF), and $\mathbf{H}_u(\omega) = [\mathbf{K}_0(\omega)]^{-1}$ is the undamaged rod frequency response function. Where $\mathbf{H}^{(\mathrm{ij})}$ is a FRF with response at node i and excitation at node j. The rod FRF matrix with respective terms can be obtained as,

$$\mathbf{H} = \begin{bmatrix} H^{(11)} & H^{(12)} \\ H^{(21)} & H^{(22)} \end{bmatrix} \tag{5.2}$$

To formulate the explicit equation, we started by considering a point receptance FRF, e.g $\mathbf{H}^{(11)}$, for a damaged and undamaged rod models. The analytical and measured FRF are used to calculate the relative change as

$$\mathbf{\Lambda}_{an}(\omega) = \frac{\mathbf{H}^{(11)}_{d_{an}} - \mathbf{H}^{(11)}_{u_{an}}}{\mathbf{H}^{(11)}_{u_{an}}}, \quad \mathbf{\Lambda}_{m}(\omega) = \frac{\mathbf{H}^{(11)}_{d_{m}} - \mathbf{H}^{(11)}_{u_{m}}}{\mathbf{H}^{(11)}_{u_{m}}} \tag{5.3}$$

where measured FRF is the effect data which can be obtained experimentally or numerically, and the analytical FRF means the symbolic mathematical expression. The relative change using analytical FRF for a red with tow node is

$$\mathbf{\Lambda}_{an}(\omega) = \frac{\Theta k\left(-2\sin^2\left(k\left(L-L_1\right)\right) - \cos(kL) + \cos\left(k\left(L-2L_1\right)\right)\right)}{\left(\cos(kL)\right)\left(\Theta k\left(\cos(kL) - \cos\left(k\left(L-2L_1\right)\right)\right) - 2\sin(kL)\right)} \tag{5.4}$$

Similarly to the model updating approach, the inverse problem will be applied here as a technique where the structural damage parameter (α) will be quantified based on the minimization of the difference between analytical and measured FRF relative change (Friswell and Mottershead, 1995; Morassi and Vestroni, 2008; Doebling et al., 1998) expressed by,

$$\mathbf{\Lambda}_{an}(\omega) - \mathbf{\Lambda}_{m}(\omega) = \varepsilon_{\mathbf{\Lambda}} \tag{5.5}$$

By neglecting modelling and measurements errors, so that $\varepsilon_\Lambda = 0$. The crack flexibility polynomial is approximated by its first term, so that $\Theta = 2\pi h(0.63\alpha^2)$. Substituting equation (5.4) in (5.5) and the consideration for ε_Λ and Θ it has

$$\frac{(2\pi h(0.63\alpha^2))k\left(-2\sin^2\left(k\left(L-L_1\right)\right)-\cos(kL)+\cos\left(k\left(L-2L_1\right)\right)\right)}{(\cos(kL))\left((2\pi h(0.63\alpha^2))k\left(\cos(kL)-\cos\left(k\left(L-2L_1\right)\right)\right)-2\sin(kL)\right)}-\mathbf{\Lambda}_m(\omega)=0 \quad (5.6)$$

It is possible to obtain an explicit equation for the crack depth, $\alpha(\omega)$, in function of the analytical and measured relative change by using equation (5.6) and solving into the MATHEMATICA software. We obtain the crack depth as

$$\boldsymbol{\alpha}(\omega)=\frac{0.710812\sqrt{\mathbf{\Lambda}_m(\omega)\sin(2kL)}}{\sqrt{hk\mathbf{\Lambda}_m(\omega)[\cos(2kL)-\cos(2k(L-L_1))-\cos(2kL_1)]-2hk\cos(2k(L-L_1))+hk\mathbf{\Lambda}_m(\omega)+2hk}} \quad (5.7)$$

The relative error between the crack depth calculated with the equation (5.1) and with the approximation by its first term can be evaluated by,

$$\varepsilon_\alpha=\left|\frac{\alpha_{no}(\omega)-\alpha_C(\omega)}{\alpha_{no}(\omega)}\right|\times 100 \quad (5.8)$$

where nominal crack depth (α_{no}) is a given value at a crack position L_1. It is used to obtain a measured FRF relative change (Λ_m) using the complete equation of crack flexibility (equation 5.1). Then, Λ_m is substituted into equation (5.7) and calculated the crack depth (α). By substituting α_{no} and α into the equation (5.8) the crack depth error in percentage is obtained.

5.2.2 Average crack depth estimation

In the procedure to estimate the crack depth (equation 5.7) presented in the Section 5.2.1, it will be required to obtain a measured FRF relative change. In this paper, it is proposed to use stochastic rod models (Sections 3.5 and 3.4) to calculate the measured FRF's to obtain $\Lambda_m(\omega,\theta)$. Three statistical approaches are used:

- Mathematical expectation of the measured FRF relative change, which can be expressed as,

$$\mathbf{\Lambda}_m^{(1)}(\omega)=\mathbb{E}\left[\frac{\mathbf{H}_{d_m}(\omega,\theta)-\mathbf{H}_{u_m}(\omega,\theta)}{\mathbf{H}_{u_m}(\omega,\theta)}\right] \quad (5.9)$$

- Mathematical expectation of the difference between measured damage and undamaged FRF's, divided by the mathematical expectation of the measured undamaged FRF. It can be expressed as,

$$\mathbf{\Lambda}_m^{(2)}(\omega)=\frac{\mathbb{E}[\mathbf{H}_{d_m}(\omega,\theta)-\mathbf{H}_{u_m}(\omega,\theta)]}{\mathbb{E}[\mathbf{H}_{u_m}(\omega,\theta)]} \quad (5.10)$$

- Mathematical expectation of the measured crack depth, $\mathbb{E}\left[\alpha(\omega)\right]$, calculated by,

$$\boldsymbol{\Lambda}_m^{(3)}(\omega,\theta) = \frac{\mathbf{H}_{d_m}(\omega,\theta) - \mathbf{H}_{u_m}(\omega,\theta)}{\mathbf{H}_{u_m}(\omega,\theta)} \tag{5.11}$$

  using all samples of $\mathbf{H}_{d_m}(\omega,\theta)$ and $\mathbf{H}_{u_m}(\omega,\theta)$ generated by the stochastic process.

These three different ways to calculate the crack depth statistics were used because this is a non-linear problem. Thus, different results are expected for each formulation. An illustration of that non-linearity will be seen in Section , these results change in function of the frequency vary. Nevertheless, a physical crack reminds a single value, then these formulations are modified by integrating the measured FRF relative change ($\boldsymbol{\Lambda}_m$) over the frequency to estimate single value for α. By applying to the Equations (5.9-5.11) we get:

$$\bar{\Lambda}_m^{(1)} = \int_\omega \mathbb{E}\left[\frac{\mathbf{H}_{d_m}(\omega,\theta) - \mathbf{H}_{u_m}(\omega,\theta)}{\mathbf{H}_{u_m}(\omega,\theta)}\right] d\omega \tag{5.12}$$

$$\bar{\Lambda}_m^{(2)} = \int_\omega \frac{\mathbb{E}[\mathbf{H}_{d_m}(\omega,\theta) - \mathbf{H}_{u_m}(\omega,\theta)]}{\mathrm{E}[\mathbf{H}_{u_m}(\omega,\theta)]} d\omega \tag{5.13}$$

and the third is obtained as $\int_\omega \mathbb{E}[\alpha(\omega)]d\omega$, which is the integral of the mathematical expectation of the measured crack depth, $\mathbb{E}\left[\alpha(\omega)\right]$, calculated by,

$$\bar{\Lambda}_m^{(3)}(\omega,\theta) = \frac{\mathbf{H}_{d_m}(\omega,\theta) - \mathbf{H}_{u_m}(\omega,\theta)}{\mathbf{H}_{u_m}(\theta)} \tag{5.14}$$

Next section shows a series of numerical and experimental cases to test the efficiency of the present study.

5.2.3 Numerical and experimental tests

Deterministic damage quantification

The system used in all examples consists of a free-free rod modelled with a two nodes spectral element. It is excited by a unit longitudinal harmonic force applied at the rod element node 1, and the response is obtained at node 2, figure 3.4. Geometries and material properties are: $L = 1.0$ m, $h = 0.018$ m, $b = 0.006$ m, $E = 71$ GPa, $\eta = 0.01$, and $\rho = 2700$ kg/m^3. We started with the analyses of relative change sensitivity , $\boldsymbol{\Lambda}(\omega)$, related with the crack depth, (α), and crack position, (L_1). Two simulations using different crack depth values and crack positions as ($\alpha = 0.10, 0.20, 0.30$ and $L_1 = 0.35L, 0.5L, 0.7L$) are presented. The first one fixes a crack position value, varies for all other values of crack depth, and calculates FRF relative change. This procedure is repeated for all other values of L_1, and the results presented in figure 5.1. For values of L_1, it can bee seen that FRF relative change sensitivity increases ($\mathbf{\Lambda}(\omega) \approx 5\%, 20\%$ and 60% in average) as the crack depth value increases, which means a high sensitivity of FRF relative change to the crack depth parameter. The second fixes the value of α, varies L_1 for all values, and calculates $\mathbf{\Lambda}(\omega)$. This procedure is repeated for all other values of α and the results showed in figure 5.2. The results show no significant variations in FRF relative change as the L_1 values change. It means the very low sensitivity of FRF relative change to the crack position. Based on this results, from now on our analysis will regard on the crack depth parameter.

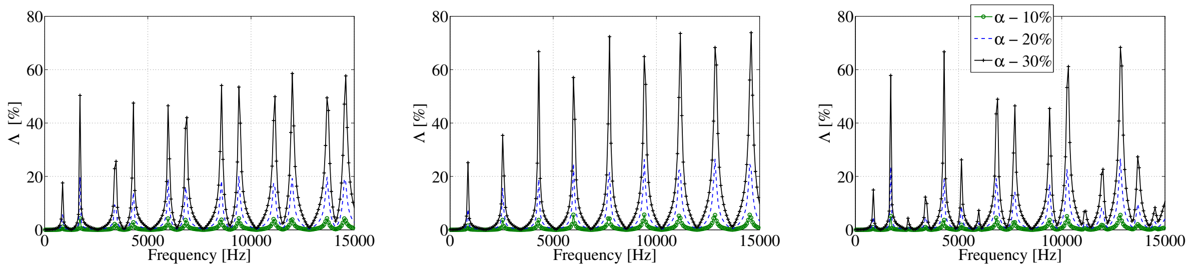

Figure. 5.1: Sensitivity analysis of FRF relative change varying crack depth values ($\alpha = 0.10, 0.20, 0.30$) at the crack position: $L_1 = 0.35L$ (LHS); $L_1 = 0.5L$ (middle); and $L_1 = 0.7L$ (RHS).

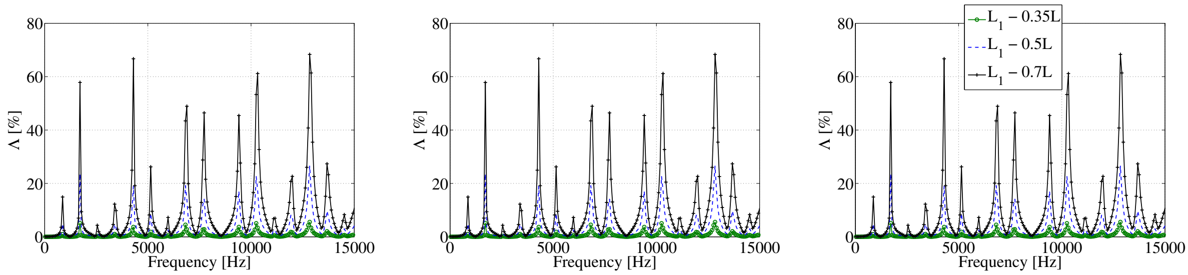

Figure. 5.2: Sensitivity analysis of FRF relative change varying crack position values ($L_1 = 0.35L, 0.5L, 0.7L$) with crack depth: $\alpha = 0.10$ (LHS); $\alpha = 0.20$ (middle); and $\alpha = 0.30$ (RHS).

To verify the crack depth analytical expression (equation 5.7), a measured FRF relative change (equation 5.3) is obtained using the damage model with the crack flexibility (equation 5.1), then substituted in the equation (5.7). In pratical application the nominal crack depth values assumed are $\alpha_{no} = \{0.02, 0.10, 0.30\}$, at crack position value of $L_1 = 0.35L$. By introducing $\mathbf{\Lambda}_m$ in equation (5.7), a crack depth (α) is estimated. Figure 5.3 shows the calculated crack depth with the percentage relative error (equation 5.8).

The results show a good approximation in using the first term of Eq.(5.1). The crack depth estimation with $\alpha_{no} = 0.30$ shows error of 21%, it can be related with the reduction of the term in crack flexibility polynomial used to estimate α. Although a crack depth of 30% of high section is a quite considerable size, the efficiency of the method is in quantify the a small size crack with accurate estimation. Based on percentage errors (ε_α) and a good crack depth estimation obtained in a small crack depth, an increase of polynomial degree is not considered. With regards to the uncertainty sources that a structure can contain, the following sections will

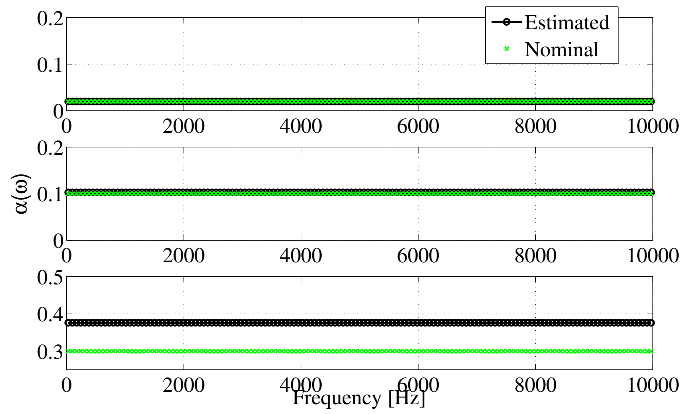

Figure. 5.3: Estimation of crack depth for $\alpha_{no} = \{0.02, 0.10, 0.30\}$. Relative error ($\varepsilon_\alpha$) are equals to 0.1%,2.7% and 21%, respectively.

be dedicated to verify the efficiency of the present technique for damage detection considering a stochastic system.

Stochastic damage quantification

To start with a numerical test depth crack estimation are considered stochastic dynamic responses for the undamaged and damage models presented in Section 3. It was assumed a rod structure with the same geometries and material properties of the Section. The crack depth value is of $\alpha_{no} = 0.10$ and crack positions is $L_1 = 0.35L$). The variability will be considered in cross section area and Young's modulus. For the random variable (RV) cases, both are assumed as a Gamma distribution with means, $\mu_A = 0.004$ m^2 and $\mu_E = 71$ GPa, and coefficients of variation $COV_A = COV_E = \{0.01, 0.05, 0.1\}$. For the random field (RF) cases, the longitudinal rigidity $EA(x,\theta)$ has a Gamma marginal PDF. The covariance function of the random field is exponential with correlation length $\mathtt{b} = L/3$ and 4 modes. Monte Carlo simulation is evaluated with 500 samples. For the equations (5.9-5.11), $\mathbf{H}_{d_m}(\omega,\theta) = [\mathbf{K}_d(\omega,\theta)]^{-1}$ and $\mathbf{H}_{u_m}(\omega,\theta) = [\mathbf{K}(\omega,\theta)]^{-1}$.

Figure 5.4 shows the mean and standard deviation receptance FRF's for an undamaged rod, modelled as random variables (RV) with damping factor of 0.01 and 0.05, and different COV's. Figure 5.6 shows the mean and standard deviation receptance FRF's for an undamaged rod, modelled as random variables (RF) with damping factor of 0.01 and 0.05, and different COV's. For RV and RF cases, the mean responses are slightly different from the deterministic response. As the frequency and coefficient of variation increase, the stochastic responses presents an increasing damping behaviour. It comes from the average process which flattens curve peaks as the dispersion increases. These results agree with those presented in the literature by Adhikari (2011).

For the damaged rod case the results presented similar behaviour as the undamaged

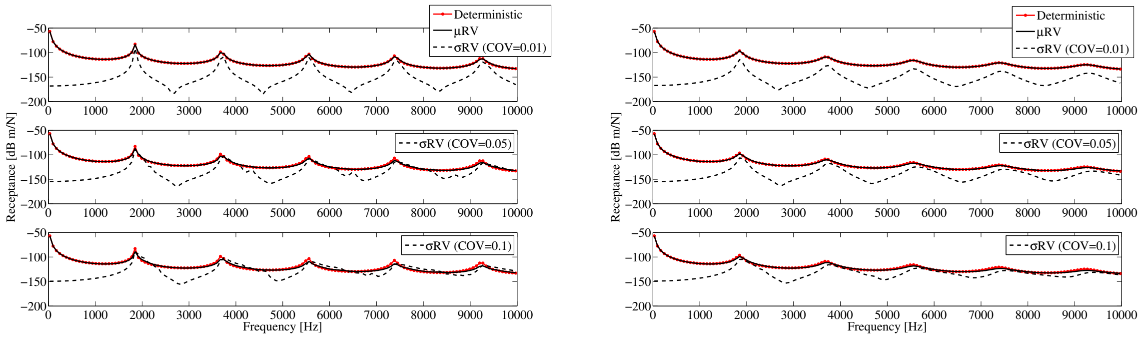

Figure. 5.4: Mean receptance FRF ($\mathbf{H}^{12}$) and standard deviation for undamaged rod modelled by using RV with $\eta = 0.01$ (LHS) and $\eta = 0.05$ (RHS) for $COV = \{0.01, 0.05, 0.1\}$.

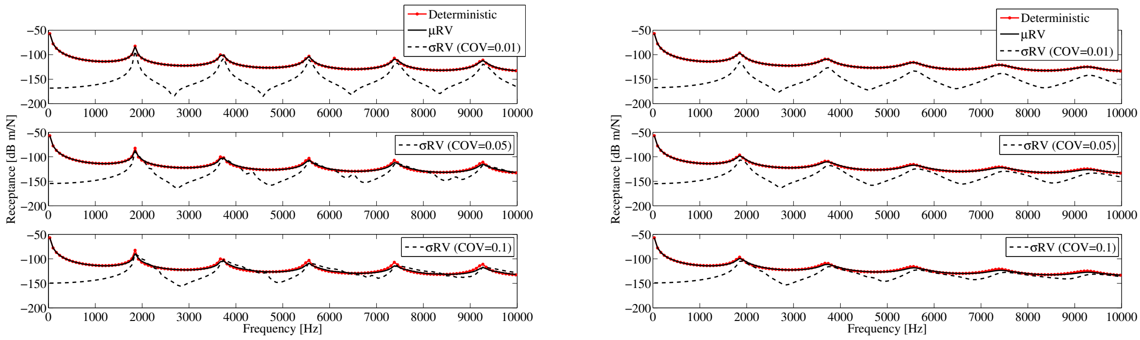

Figure. 5.5: Mean receptance FRF ($\mathbf{H}^{12}$) and standard deviation for damaged rod modelled by using RV with $\eta = 0.01$ (LHS) and $\eta = 0.05$ (RHS) for $COV = \{0.01, 0.05, 0.1\}$.

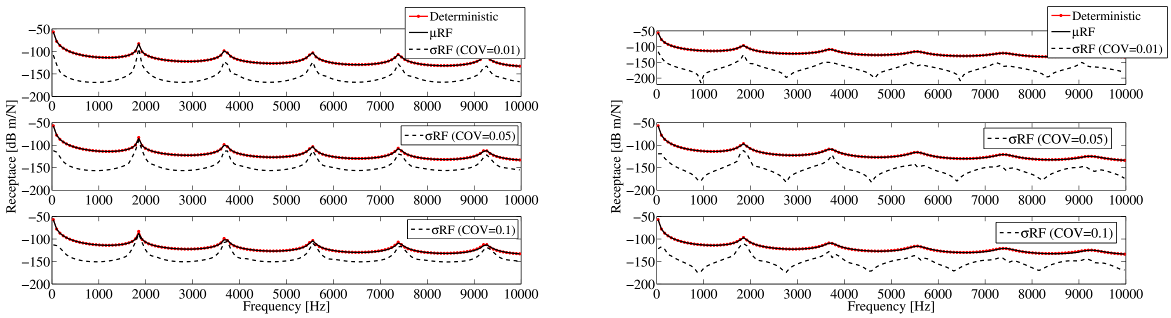

Figure. 5.6: Mean receptance FRF ($\mathbf{H}^{12}$) and standard deviation for undamaged rod modelled by using RF with $\eta = 0.01$ (LHS) and $\eta = 0.05$ (RHS) for $COV = \{0.01, 0.05, 0.1\}$.

model. Figure 5.5 shows the mean and standard deviation receptance FRF's for the damaged rod, modelled as random variables (RV) with damping factor of 0.01 and 0.05 with different COV's. Figure 5.7 shows the mean and standard deviation receptance FRF's for the damaged rod, modelled as random variables (RF) with damping factor of 0.01 and 0.05 and different COV's.

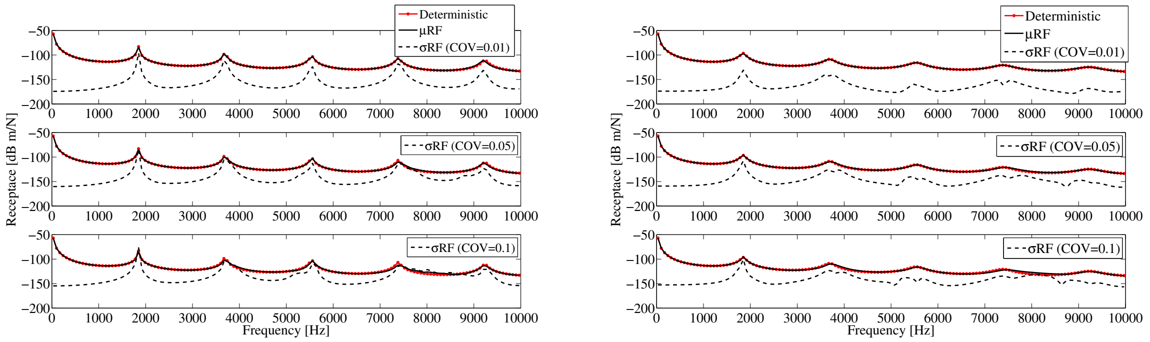

Figure. 5.7: Mean receptance FRF ($\mathbf{H}^{12}$) and standard deviation for damaged rod modelled by using RF with $\eta = 0.01$ (LHS) and $\eta = 0.05$ (RHS) for $COV = \{0.01, 0.05, 0.1\}$.

Crack depth quantification using random variables

By using the same numerical example, parameters variability, number of samples and measured FRF relative change as in the Section , the crack depth (α) is calculated by using random variable (RV) model in relation with $\mathbf{\Lambda}_m^{(1)}$, $\mathbf{\Lambda}_m^{(2)}$, and $\mathbf{\Lambda}_m^{(3)}$ (equations 5.9-5.11). By evaluating the structural damping effects on the stochastic damage quantification, two values of damping factor $\eta = 0.01$ and $\eta = 0.05$ are used.

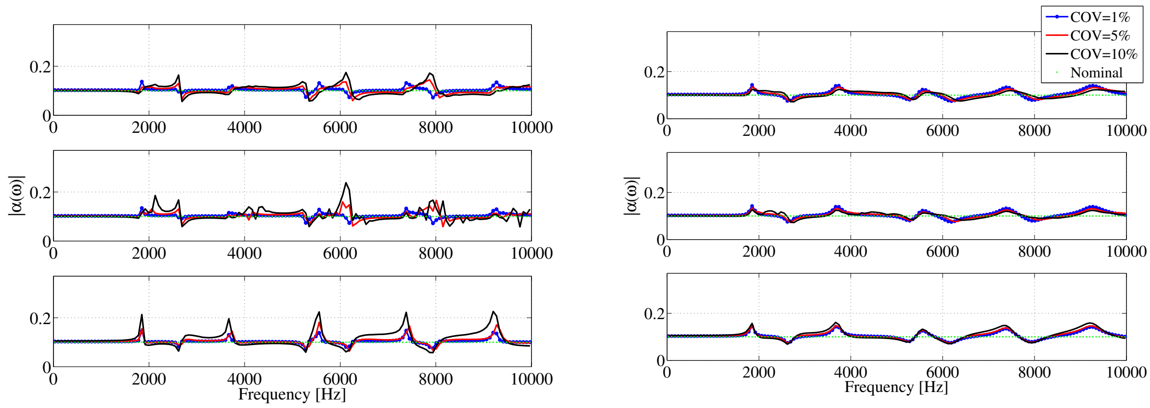

Figure. 5.8: Mean of crack depth with RV model, for $COV = \{0.01, 0.05, 0.1\}$ using the approaches: $\Lambda_m^{(1)}$, $\Lambda_m^{(2)}$, and $\Lambda_m^{(3)}$, with damping factor $\eta = 0.01$ (LHS) and $\eta = 0.05$ (RHS).

Figure 5.8 shows the mean of crack depth for a given frequency band. By considering damping factor $\eta = 0.01$ (LHS figure) with low coefficient of variation $(COV = 1\%)$, all approaches present good approximation between calculated and nominal crack depth. However, as the COV's increase α obtained by all approaches shows high dispersion around the value of α_{no} with $\Lambda_m^{(1)}$ and lower dispersion when compared to the others. By increasing the damping factor to $\eta = 0.05$ (RHS figure), the α converges to α_{no} much better, although it still has a moderate dispersion around the α_{no} at high values of COV. This comes from the fact that damping greatly influences the behaviour of the stochastic system Pavlovic et al. (2005); Adhikari (2013).

Figure 5.9 illustrates the crack depth error (ε_α) variation based on the approaches $\mathbf{\Lambda}_m^{(1)}$, $\mathbf{\Lambda}_m^{(2)}$, and $\mathbf{\Lambda}_m^{(3)}$ with damping factor $\eta = 0.01$ and $\eta = 0.05$, respectively.

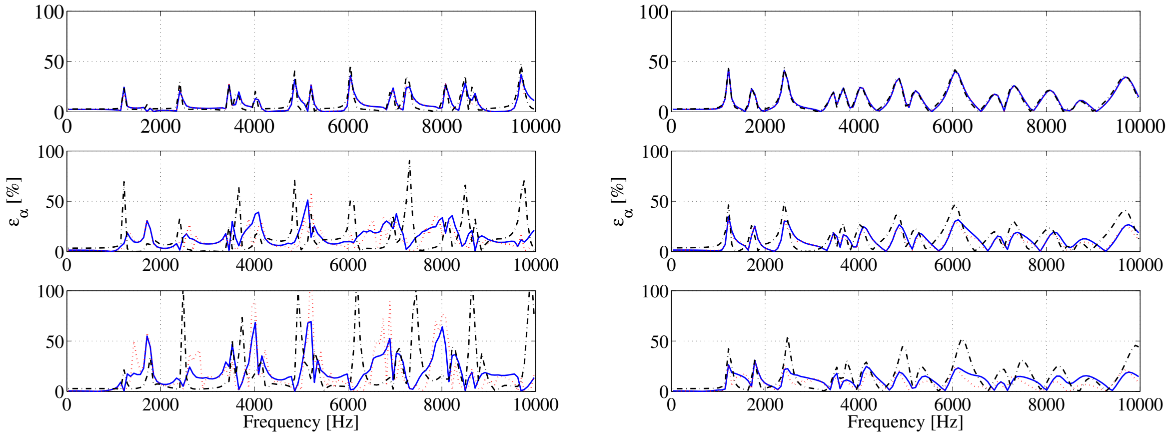

Figure. 5.9: Crack depth error with RV model, damping factor $\eta = 0.01$(LHS) and $\eta = 0.05$(RHS), approaches $\mathbf{\Lambda}_m^{(1)}$ ($- \cdot - \cdot -$), $\mathbf{\Lambda}_m^{(2)}$ (——), and $\mathbf{\Lambda}_m^{(3)}$ ($\cdots$), for $COV = 1\%$ (top), $COV = 5\%$ (middle) and $COV = 10\%$ (bottom)

Thus, the result obtained from the RV model shows the influence of the different COV's where the ε_α increases as the COV increase. By comparing the three FRF relative change, $\mathbf{\Lambda}_1(\omega)$ exhibited the best outcome. With the increasing damping factor reduction of error is observed in all study cases, following the analogy, the error parameter increases with higher coefficient of variation.

Crack depth quantification using random field

By supposing that random material properties will change continuously over the structural space. In this situation the dynamic stiffness matrix for the two-node damaged and undamaged rod elements are modelled within the random field framework. By using the same numerical example, parameters variability, number of samples and measured FRF relative change as in the Section , the crack depth $(\alpha(\omega))$ calculated using RF model is based on the approaches $\mathbf{\Lambda}_m^{(1)}$, $\mathbf{\Lambda}_m^{(2)}$, and $\mathbf{\Lambda}_m^{(3)}$ (Equations 5.9-5.11). Figure 5.10 illustrates nominal crack depth values and crack depth mean of the respective COV's for two values of damping factor ($\eta = 0.01$ and $\eta = 0.05$). In the response with damping factor $\eta = 0.01$ (LHS figure), mean of calculated crack depth (α) obtained with $\mathbf{\Lambda}_m^{(1)}(\omega)$ and $\mathbf{\Lambda}_m^{(2)}(\omega)$ shows better approximation to the nominal crack depth (α_N) when compared with other approaches. These results become better as the frequency raises and for small COV's. The means obtained with the approaches $\mathbf{\Lambda}_m^{(1)}(\omega,\theta)$ and $\mathbf{\Lambda}_m^{(2)}(\omega)$ present similar results for all values of COV's, with the α values varying around (α_N) value. Based on the results, it can be seen that the crack depth estimation presents a great oscillation due to the randomness in wave numbers. Also, like the random variable case, as the damping

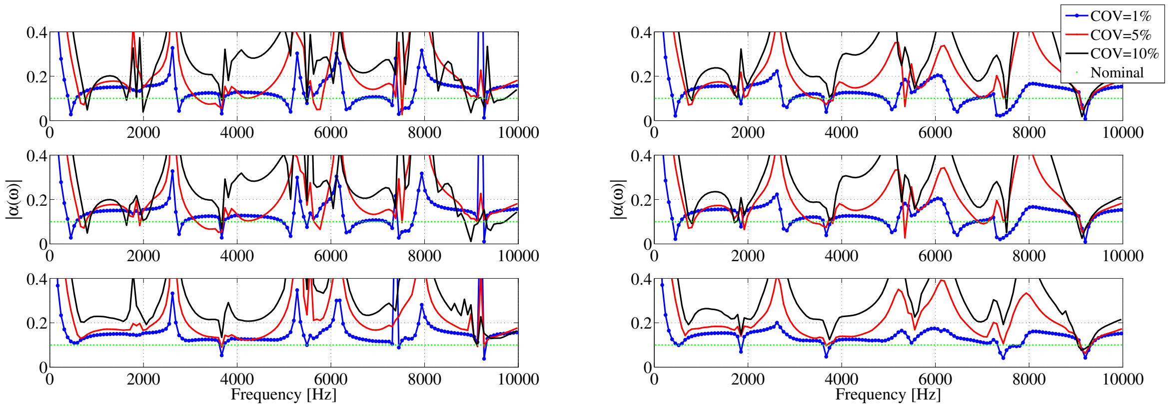

Figure. 5.10: Mean of crack depth with RF model, for $COV = \{0.01, 0.05, 0.1\}$ using the approaches: $\mathbf{\Lambda}_m^{(1)}$, $\mathbf{\Lambda}_m^{(2)}$, and $\mathbf{\Lambda}_m^{(3)}$, with damping factor $\eta = 0.01$ (LHS) and $\eta = 0.05$ (RHS).

factor increases, the calculated crack depth responses approximates more to the nominal crack depth value.

The results for the crack depth in this section were obtained in the frequency domain. In the first analyse using deterministic system, the crack depth value was constant along the frequency. However, in a stochastic model it presented a random behaviour along the frequency. The crack depth shown high oscillations in the frequency domain, which became difficult to quantify the damage. For this reason an alternative technique to obtain a single value for the crack depth is presented in the next section.

Single crack depth quantification

A single crack depth value was estimated using stochastic response obtained from RV and RF of the same numerical example. Parameter variability and a number of samples exposed in the cases shown previous. However, the measured FRF relative change are obtained by the equations (5.12-5.14). Predicted crack depth and crack depth error obtained for different approaches ($\bar{\Lambda}_m^{(1)}$, $\bar{\Lambda}_m^{(2)}$ and $\bar{\Lambda}_m^{(3)}$) are presented in Table 5.1.

Also in the Table 5.1 for all COV's values with a damping factor $\eta = 0.01$ the calculated crack depths modelled as RV present crack depth error very low ($\varepsilon_\alpha = 4 - 11\%$) can be seen. However, for the calculated crack depths modelled as RF, these errors are high ($\varepsilon_\alpha = 6 - 86\%$). For all cases, ε_α increases as the coefficient of variation increases. Related with a greater damping factor ($\eta = 0.05$), and the RV model the ε_α presents almost the same value ($4.2 - 4.4\%$) for all COV's. For the RF model the ε_α presents similar results as obtained with $\eta = 0.01$, i.e. very high values for ε_α. Nonetheless, some conflicting results have been founded related with the COV, where with $\eta = 0.05$ for a $COV = 1\%$ the ε_α increases and for

Table 5.1: Calculated crack depth results using $\bar{\Lambda}_m^{(1)}$, $\bar{\Lambda}_m^{(2)}$, and $\bar{\Lambda}_m^{(3)}$ with $\alpha_{no} = 0.1$, modelled as RV and RF for different coefficient of variation (COV) and damping factor (η) values.

	COV [%]	Calculated crack depth (Error ε_α [%])			
		$\eta = 0.01$		$\eta = 0.05$	
		RV	RF	RV	RF
$\bar{\Lambda}_m^{(1)}$	1	0.1027 (2.7)	0.1026 (2.6)	0.1016 (1.6)	0.1061 (6.1)
	5	0.1046 (4.6)	0.1419 (41.0)	0.1018 (1.8)	0.1277 (27.7)
	10	0.1055 (5.5)	0.1890 (89.0)	0.1023 (2.2)	0.1703 (70.3)
$\bar{\Lambda}_m^{(2)}$	1	0.1027 (4.0)	0.1026 (2.6)	0.1023 (2.3)	0.1061 (6.1)
	5	0.1055 (7.0)	0.1419 (41.0)	0.1021 (2.2)	0.1277 (27.7)
	10	0.1134 (11.0)	0.1890 (89.0)	0.1025 (2.5)	0.1703 (70.3)
$\bar{\Lambda}_m^{(3)}$	1	0.1031 (5.0)	0.1077 (7.66)	0.1030 (3.0)	0.1031 (3.05)
	5	0.1084 (11.0)	0.1816 (81.57)	0.1068 (6.8)	0.1588 (58.8)
	10	0.1128 (12.0)	0.2437 (143.7)	0.1097 (9.7)	0.2122 (112.2)

$COV = 5\%$ and 10% the ε_α decrease as compared with the results obtained with $\eta = 0.01$. It can be concluded that there are no significant differences in the approaches calculated with the equations of $\bar{\Lambda}_1$ and $\bar{\Lambda}_2$. Although the values of ε_α for $\bar{\Lambda}_3$ are higher than the ones of the other approaches. They do not present conflicting results for ε_α as the COV and η changes. Also, the results obtained confirms the expected behaviour, where ε_α should be increasing as COV increases, and should be decreasing as η increases.

Based on these results it can be concluded that for the damage quantification point of view that calculated crack depth using the approach $\bar{\Lambda}_m^{(3)}$ with RV model presents a good performance. The α using the approaches $\bar{\Lambda}_m^{(1)}$ and $\bar{\Lambda}_m^{(2)}$ with RF model present some conflicting results as the damping factor increases, which requires more investigation. Finally, the random field (RF) model reveals to be unable to estimate the crack depth (α) for high COV independently of the approach used to calculate the FRF relative change.

Experimental test

Experiment tests used a rod structure made of polyamide (PA) with a uniform rectangular cross-section. The rod manufactured using the Selective Laser Sintering (SLS) technology is 18mm wide, 6 mm thick, 250 mm of length, and properties with mean Young's modulus value of $E = 0.94$ GPa, $\eta \approx 0.02$, mean material density value of $\rho = 625$ kg/m^3. As a consequence of the manufacturing process, a variability of the rod properties along its length can be expected. The damage is located at position $L_1 = 0.3L$, and damage depth of $\alpha = \{0.1{,}0.2\}$. Figure 5.11 shows the experimental test setup, used to measure the FRF. The signals were acquired and analysed using LMS Test Lab. The FRFs measured with a bandwidth of 8192Hz and 8192 spectral lines. An impact hammer was used to excite the structure and a micro accelerometer to measure the response. The experimental FRFs were obtained by impact force excitation at node 1 and acceleration response at the node 2. The test consists of quantifying the damaged by applying the developed theory. For this, we firstly measured the rod without damage, then introduced a damage with 10% of the high section, and the measurement obtained. Afterwards the same procedure has been applied to a damage with 20% of the cross section.

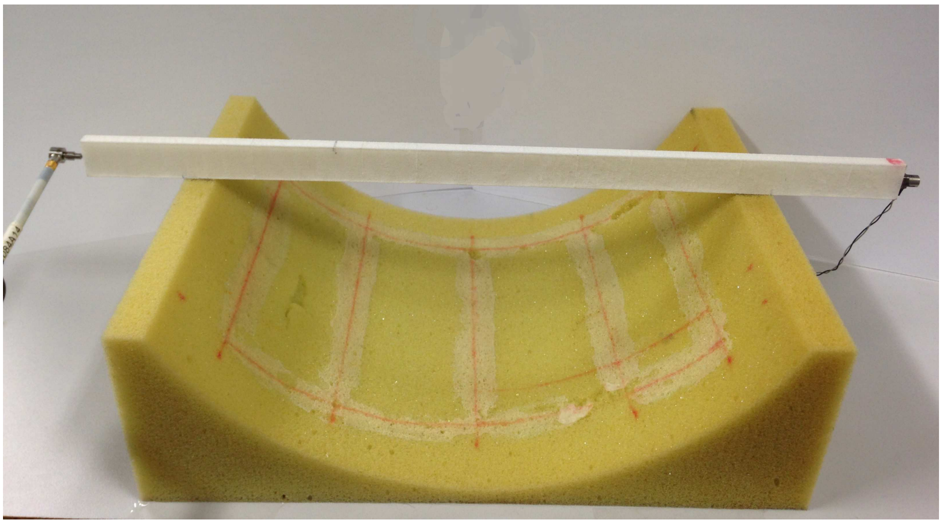

Figure. 5.11: The test rig for the free-free rod.

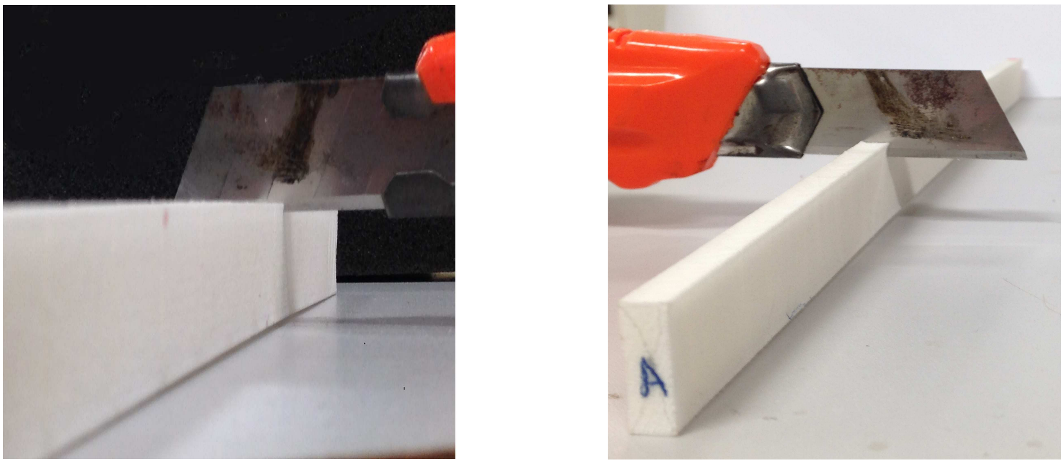

Figure. 5.12: Rod damaged with α of 0.1 (LHS) and with α of 0.2 (RHS).

Figure 5.12 shows the rod with crack depth of 10% and 20%. As mentioned before, α is measured in percentage of the high cross section. The experimental measures of the Inertance correspondent of an undamaged and a damaged rod compared with a numerical undamaged model are presented in Figure 5.13 and 5.14.

The experimental FRF is used to calculate measured the FRF relative change (equation 5.1), and then introduced in equation (5.7) to estimate the crack depth. Figure 5.15 shows

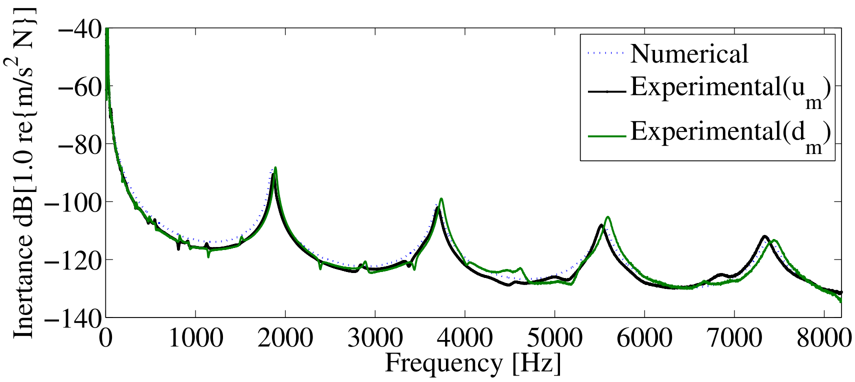

Figure. 5.13: Undamaged and damaged, with crack depth equals 10%, experimental measured FRF's of the rod.

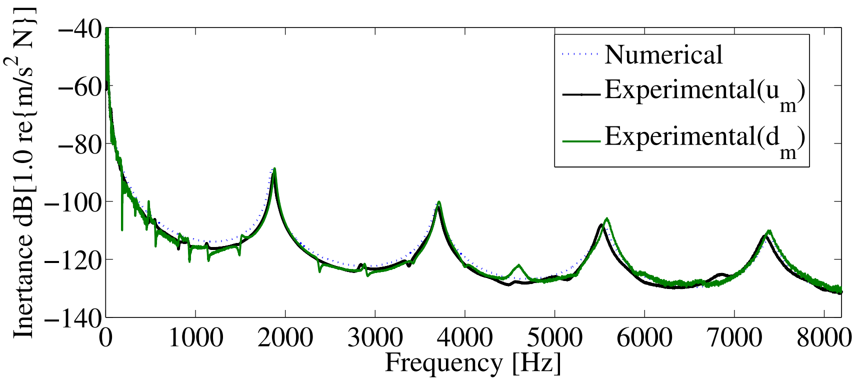

Figure. 5.14: Undamaged and damaged, with crack depth equals 20%, experimental measured FRF's of the rod.

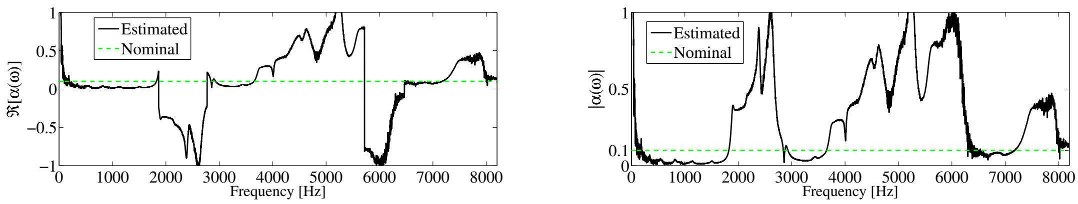

Figure. 5.15: Real(LRS) and absolute(RHS) estimation of crack depth using experimental measured FRF's compared with the nominal of $\alpha = 0.1$.

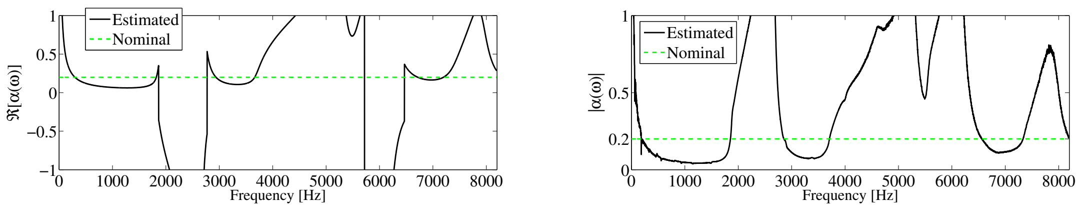

Figure. 5.16: Real(LRS) and absolute(RHS) estimation of crack depth using experimental measured FRF's compared with the nominal of $\alpha = 0.2$.

the results of $\alpha(\omega)$ in the frequency domain for a crack depth with 10% of the high cross section and figure 5.16 shows the results for a crack depth with 20%. The single crack depth value established in equation (5.12) is also calculated and given in Table 5.2.

Table 5.2: Calculated crack depth results using $\bar{\Lambda}_m$.

$\alpha_{Nominal}$	Calculated crack depth (Error ε_α [%])
0.1	0.1043 (4)
0.2	0.1937 (6)

Crack depth estimation does not present a constant value along of the frequency domain, which leads to an inaccurate estimation in the first moment. As supposed, the rod does not present constant properties along with its length, which can be compared to the RF study case. To estimate a single crack depth value, a good approximation is found in relation to the inducted damaged. In case of the value damage equals 10%, the error associated with the prediction is around 4%, and for damage equal of 20% the error is of around 6%. Those results demonstrate the performance of the presented theory, although more tests should be done for other kinds of structures.

This section presented a damage detection procedure considering a system with randomness. The stochastic model assumed such uncertainty in parameters as random variables (RV) and spatially distributed random field (RF). Furthermore, a new formulation developed to obtain a closed-form analytical expression of crack depth estimation, $\alpha(\omega)$, based on SEM formulation and measured FRF relative change ($\mathbf{\Lambda}_m$), including model parameter as RV and RF. The random field was expanded in a spectral decomposition, known as the Karhunen-Loève expansion. Since some parameters cannot be assumed with a Gaussian marginal, e.g. Young's modulus, and KL expansion obeys a Gaussian distribution a transformation is needed. To obtain a Gaussian translation random field to a non-Gaussian we used the memoryless nonlinear transformations. All stochastic models used the Monte Carlo simulation as a solver. To calculate crack depth we presented three different average treatment for estimation throughout the frequency band. Also, it demonstrates a single value estimation for α calculated by integrating the measured FRF relative change over the frequency band.

All simulated examples used a two node rod spectral element in a free-free boundary condition. A sensitivity analysis was performed for the FRF relative change $(\mathbf{\Lambda})$ related with crack depth (α) and crack position (L_1). The results show a very low sensitivity of FRF relative change to the crack position; the analysis was made exclusively for the crack depth parameter. Crack depth analytical expression was verified and the percentage errors between nominal and calculated crack depth where lower than 10 %, using the first term of Equation 5.1. By analysing mean and standard deviation of receptance FRF's with different COV's, it presented a verification of the damaged and undamaged rod spectral element formulation using parameters as RF and RV. Results show that as the frequency and COV increase the stochastic responses will increase damping behaviour. It agrees with Adhikari (2011) and can be explained by the average process which flattens curve peaks as the COV value increases, and at lower frequencies the standard deviation is biased by the mean. For the damaged rod, it presented mean and standard deviation of receptance FRF's modelled as RV and RF with different COV's. Results showed similar behaviour as the undamaged cases. Crack depth estimation using RV evaluated in a frequency band for three statistical approaches to obtain $\mathbf{\Lambda}_m$. For $\eta = 0.01$ and $(COV = 1\%)$, all approaches present good approximation between calculated and nominal crack depth. Although, as the COV's increases α obtained by all approaches show high dispersion around the value of α_N with $\mathbf{\Lambda}_m^{(1)}$ showing the lowest dispersion. For $\eta = 0.05$ the α converges to α_N much better, but still keeping a moderate dispersion around the α_N at high COV's. These results agree with Pavlovic et al. (2005); Adhikari (2013) and derives from the influence of damping in the stochastic system behaviour. A single crack depth value is obtained of the stochastic response using RV and RF models. Calculated crack depth and its error obtained from $\bar{\Lambda}_m^{(1)}$, $\bar{\Lambda}_m^{(2)}$ and $\bar{\Lambda}_m^{(3)}$ show that α using the approach $\bar{\Lambda}_3$ with RV model presents a good performance. α using $\bar{\Lambda}_1$ and $\bar{\Lambda}_2$ with RF model present some conflicting results as the damping factor increases. Finally, random field (RF) model reveals a reasonable result for small COV (1%) and an approximate result for α when theCOV's increase, but with a great error associated.

Experimental test used a polyamide (PA) rod manufactured using the Selective Laser Sintering (SLS) technology. The test consisted of quantifying the damage by applying the developed theory. Results obtained for crack depth estimation do not present accurate estimation. Although, to estimate a single crack depth value, good approximation is found in a relation to the inducted damaged. The rod does not present constant properties along of its length, which can be compared to the RF study case. In summary, either numerical and experimental tests presented in this section showed satisfying results in damage assessment for this kind of structure. More tests should be realised in order to verify the damaged location sensitivity and the influence of the other kind of waves (e.g. evanescent waves) can generate in the results. It is an open topic or a suggestions for future researches, which should be extend this theory for structures like beams and plates.

5.3 Damage detection using energy flow patterns

The approach in this section is of the energy flow patterns caused by localised damage in rod structures, including uncertainties in a geometric parameter. The problem is solved in two steps. In the first step the structure is modelled by the Spectral Element Method, and the mean and variance of displacement responses are obtained by using the Polynomial Chaos expansion. In the second step, by using the displacements obtained in the step before, the mean and variance of energies are calculated by applying the statistical moments (expected value and variance) directly into the energy density and energy flow equations. This approach produces unusual equations for expected values and covariances. For example, the expected value of a product of three random correlated variables whose solution includes the covariance between one variable and a product of two others variables. A new formulation using the direct method is proposed to solve this problem. The Monte Carlo Simulation is also performed in order to validate the results obtained by the proposed solution. Numerical examples analysing different cases related to PC degree and values of COVs compared with MC results.

5.3.1 Theoretical basis

Energy flow analysis (EFA) is a method for predicting the frequency-averaged vibrational response of structures at high audible frequencies range. EFA is governed by differential equations related to the amount of energy density propagation at the structure. The power flow equations and the energy density of the analytical solution of displacement for different structural elements are presented in detail in J.C. Wohlever (1992); Cho and Bernhard (1998); Santos et al. (2008). For harmonic excitation, the time-averaged energy density for longitudinal waves in a rod can be written as the sum of the potential and kinetic energy densities,

$$e = \frac{1}{4}EA\left\{\frac{\partial u \partial u^*}{\partial x \partial x}\right\} + \frac{1}{4}\rho A\left\{\frac{\partial u \partial u^*}{\partial t \partial t}\right\} \tag{5.15}$$

where $*$ represent the time-averaged quantity and the complex conjugate, respectively. The time-averaged energy flow for longitudinal waves in a rod is given by

$$\mathrm{q} = \frac{1}{2}\Re\left\{-\mathrm{f}\frac{\partial u^*}{\partial t}\right\} \tag{5.16}$$

where $\Re$ is the real part of a complex number, and u is the structural displacement.

5.3.2 Moment equations

In this approach, the statistical moments of the random solution (expected value and variance) are calculated directly for the energy density and energy flow. In order to make this development easy to manage, the equation(5.15) is rewritten in two parts, potential and kinetic energy density, and equation(5.16) requested to obtain as

$$e_p = \frac{1}{4}EA\left\{u'u'^*\right\} \tag{5.17}$$

$$e_k = -\frac{1}{4}\rho\omega^2 A\left\{uu^*\right\} \tag{5.18}$$

$$\mathrm{q} = \frac{1}{2}\Re\left\{-i\omega EA\left\{u'u^*\right\}\right\} \tag{5.19}$$

where $u' = \partial u/\partial x$. Based on the similarities of equations(5.17- 5.19) in terms of the relationship of the random variables (A, u', u), and for the motive of conciseness it will be shown in more detail only the development for expected value and variance for the potential energy density. Considering that A and u' are correlated random variables the expected value of potential energy density can be written as,

$$\mathbb{E}[e_p] = \frac{1}{4}E\mathbb{E}[Au'u'^*] = \frac{1}{4}E\mathbb{E}[AD] \tag{5.20}$$

where $D = u'u'^*$. From the properties of expected value and variance of a product of two correlated random variables Goodman (1960),

$$\begin{aligned} \mathbb{E}[AD] &= \mathrm{C}(A,D) + \mathbb{E}[A]\mathbb{E}[D] \qquad \text{or} \\ \mathbb{E}[Au'u'^*] &= \mathrm{C}(A, u'u'^*) + \mathbb{E}[A]\mathbb{E}[u'u'^*] \end{aligned} \tag{5.21}$$

where C is the covariance. Under multivariate normality Bohrnstedt and Goldberger (1969) show that $\mathrm{C}(x,yz) = \mathbb{E}[y]\mathrm{C}(x,z) + \mathbb{E}[z]\mathrm{C}(x,y)$, and from Miller and Childers (2012) the variance of a complex random variable is $\mathrm{V}(z) = \mathrm{C}(z,z^*) = \mathbb{E}[zz^*] - \mathbb{E}[z]\mathbb{E}[z^*]$, then

$$\mathbb{E}[Au'u'^*] = \mathbb{E}[u']\mathrm{C}(A, u'^*) + \mathbb{E}[u'^*]\mathrm{C}(A, u') + \mathbb{E}[A](\mathrm{V}(u') + \mathbb{E}[u']\mathbb{E}[u'^*]) \tag{5.22}$$

where V is the variance. It shows that $\mathrm{C}(x,y) = \gamma_{x,y}[\mathrm{V}(x)\mathrm{V}(y)]^{1/2}$, where $\gamma_{x,y}$ is the linear correlation coefficient. By inserting it into equation (5.22) we obtain

$$\mathbb{E}[Au'u'^*] = \mathbb{E}[u']\gamma_{A,u'}[\mathrm{V}(A)\mathrm{V}(u'^*)]^{1/2} + \mathbb{E}[u'^*]\gamma_{A,u'}[\mathrm{V}(A)\mathrm{V}(u')]^{1/2} + \mathbb{E}[A](\mathrm{V}(u') + \mathbb{E}[u']\mathbb{E}[u'^*]) \tag{5.23}$$

Considering that $\mathbb{E}[x] = \mu_x$ and $\mathrm{V}(x) = \sigma_x^2$, the equation (5.23) becomes,

$$\mathbb{E}[Au'u'^*] = \gamma_{A,u'}\sigma_A(\mu_{u'}\sigma_{u'}^* + \mu_{u'}^*\sigma_{u'}) + \mu_A(\sigma_{u'}^2 + \mu_{u'}\mu_{u'}^*) \tag{5.24}$$

Substituting equation (5.24) into equation (5.20) we obtain the mean of potential energy density,

$$\mu_{e_p} = \mathbb{E}[e_p] = \frac{1}{4}E\{\gamma_{A,u'}\sigma_A\sigma_{u'}(\mu_{u'} + \mu_{u'}^*) + \mu_A(\sigma_{u'}^2 + \mu_{u'}\mu_{u'}^*)\} \tag{5.25}$$

By using the same development for the kinetic energy density and energy flow equations, we obtain their corresponding means as

$$\mu_{e_k} = \mathbb{E}[e_k] = \frac{1}{4}\rho\omega^2\{\gamma_{A,u}\sigma_A\sigma_u(\mu_u + \mu_u^*) + \mu_A(\sigma_u^2 + \mu_u\mu_u^*)\} \tag{5.26}$$

$$\mu_{\mathrm{q}} = \mathbb{E}[\mathrm{q}] = \frac{1}{2}\Re\{-i\omega E\sigma_A(\gamma_{A,u}\mu_{u'}\sigma_u^* + \gamma_{A,u'}\mu_u^*\sigma_{u'}) + \mu_A(\gamma_{u',u}\sigma_{u'}\sigma_u^* + \mu_{u'}\mu_u^*)\} \tag{5.27}$$

The mean value of total energy density can be written as $\mu_e = \mu_{e_p} + \mu_{e_k}$, and the variance of potential energy density can be written as,

$$\mathrm{V}(e_p) = \mathbb{E}[e_p^2] - \mathbb{E}^2[e_p] \tag{5.28}$$

where the expected value of squared potential energy density can be written as,

$$\mathbb{E}[e_p^2] = \frac{1}{16}E_c^2\mathbb{E}[A^2u'^2u'^{*2}] = \frac{1}{16}E_c^2\mathbb{E}[A^2D^2] \tag{5.29}$$

where $D = u'u'^*$. From the properties of expected value of a product of two squared correlated random variables Bohrnstedt and Goldberger (1969), one has

$\mathbb{E}[x^2v^2] = \mathrm{V}(xv) + \mathbb{E}^2[xv]$.

Considering that the variance and squared expected value of a product of two correlated random variables, where

$\mathrm{V}(xv) = \mathbb{E}^2[x]\mathrm{V}(v) + \mathbb{E}^2[v]\mathrm{V}(x) + 2\mathbb{E}^2[x]\mathbb{E}^2[v]\mathrm{C}(x,v) + \mathrm{V}(x)\mathrm{V}(v) + \mathrm{C}^2(x,v)$,

and

$\mathbb{E}^2[xv] = (\mathrm{C}(x,v) + \mathbb{E}[x]\mathbb{E}[v])^2$,

we obtain

$$\mathbb{E}[x^2v^2] = \mathbb{E}^2[x]\mathrm{V}(v) + \mathbb{E}^2[v]\mathrm{V}(x) + 4\mathbb{E}[x]\mathbb{E}[v]\mathrm{C}(x,v) + \mathrm{V}(x)\mathrm{V}(v) + 2\mathrm{C}^2(x,v) + \mathbb{E}^2[x]\mathbb{E}^2[v]. \tag{5.30}$$

By doing $x = A$, $v = D = u'u'^*$, and simplifying, we have

$$\mathbb{E}[A^2u'^2u'^{*2}] = \{\mathbb{E}^2[A]+\mathrm{V}(A)\}\{\mathrm{V}(u'u'^*)+\mathbb{E}^2[u'u'^*]\}+4\mathbb{E}[A]\mathbb{E}[u'u'^*]\mathrm{C}(A,u'u'^*)+2\mathrm{C}^2(A,u'u'^*) \tag{5.31}$$

Then, by using the properties for variance and covariance of a product of two variable multi-variate Gaussian, substituting into de equatoin(5.31) and simplifying, we get:

$$\begin{aligned}\mathbb{E}[e_p^2] = \frac{1}{16}E_c^2\{(\mu_A^2 + \sigma_A^2)[\sigma_{u'}{}^2(\mu_{u'}{}^2 + \mu_{u'}^*{}^2 + 4\mu_{u'}\mu_{u'}^*) + 3\sigma_{u'}{}^4 + \mu_{u'}{}^2\mu_{u'}^*{}^2] + 2\gamma_{A,u'}{}^2\sigma_A{}^2\sigma_{u'}{}^2(\mu_{u'} + \mu_{u'}^*)^2 \\ + 4\gamma_{A,u'}\mu_A\sigma_A\sigma_{u'}(\mu_{u'} + \mu_{u'}^*)(\sigma_{u'}{}^2 + \mu_{u'}\mu_{u'}^*)\}\end{aligned} \tag{5.32}$$

Substituting equation (5.25) and (5.32) into the equation (5.28) the variance of potential energy density is obtained. Similar developments will produce the expected values of squared kinetic energy density and energy flow as,

$$\mathbb{E}[e_k^2] = \frac{1}{16}\rho^2\omega^4\{(\mu_A^2+\sigma_A^2)[\sigma_u{}^2(\mu_u{}^2+\mu_u^{*2}+4\mu_u\mu_u^*)+3\sigma_u{}^4+\mu_u{}^2\mu_u^{*2}]+2\gamma_{A,u}{}^2\sigma_A{}^2\sigma_u{}^2(\mu_u+\mu_u^*)^2 \\ +4\gamma_{A,u}\mu_A\sigma_A\sigma_u(\mu_u+\mu_u^*)(\sigma_u{}^2+\mu_u\mu_u^*)\} \tag{5.33}$$

$$\mathbb{E}[\mathrm{q}^2] = \frac{1}{4}\omega^2E_c^2\{(\mu_A^2+\sigma_A^2)(\mu_{u'}{}^2\sigma_u^{*2}+\mu_u^{*2}\sigma_{u'}{}^2+2\gamma_{u',u}\mu_{u'}\mu_u^*+(1+\gamma_{u',u})\mu_{u'}{}^2\sigma_{u'}{}^2\sigma_u^{*2}+\mu_u{}^2\mu_u^{*2}) \\ +4\mu_A\sigma_A(\gamma_{u',u}\sigma_{u'}\sigma_u^*+\mu_u\mu_u^*)(\gamma_{A,u}\mu_{u'}\sigma_u^*+\gamma_{A,u'}\mu_u^*\sigma_{u'})+2\sigma_A^2(\gamma_{A,u}\mu_{u'}\sigma_u^*+\gamma_{A,u'}\mu_u^*\sigma_{u'})^2\} \tag{5.34}$$

Finally the variances of kinetic energy density and energy flow are obtained by:

$$\sigma_{e_k}^2 = \mathrm{V}(e_k) = \mathbb{E}[e_k^2] - \mathbb{E}^2[e_k] \tag{5.35}$$

$$\sigma_{\mathrm{q}}^2 = \mathrm{V}(\mathrm{q}) = \mathbb{E}[\mathrm{q}^2] - \mathbb{E}^2[\mathrm{q}] \tag{5.36}$$

The variance of total energy density can be obtained using (Bohrnstedt and Goldberger, 1969):

$$\sigma_e^2 = \sigma_{e_p}^2 + \sigma_{e_k}^2 - 2\gamma_{e_p,e_k}\sigma_{e_p}\sigma_{e_k}$$

5.3.3 Numerical simulation

The numerical example is a free-free rod with the following dimensions and material properties: $L1 = 0.9$ m, $L = 3.0$ m, $h = 0.02$ m, $b = 0.02$ m, $E = 71$ GPa, $\eta = 0.01$, and $\rho = 2700kg/m3$. The spectral model is excited with a longitudinal harmonic point force applied at left-hand side of the rod, with magnitude $F = 1N$, and the crack imposed at the position $x = L1$, with a crack depth of 25% of the cross section height. The cross section area (A) was assumed as a Gaussian random variable with mean $\mu_A = 0.004m^2$, and coefficient of variation $COV_A = 0.1$. The correlation coefficients (γ) were randomly assumed.

The polynomial basis properties generate a linear equation system through projections on the polynomial as presented in Section 2.5. The displacement of the rod can be calculated by the system:

$$[\mathrm{K}]\{u\} = \{\mathrm{f}\}. \tag{5.37}$$

A vector decomposition $\{u\} = \sum_{n=0}^{N}\{u_n\}\Psi_n(\{\xi_i\}_{i=1}^{Q})$ over polynomial chaos of $Q-$variables is given equation (2.56). Substituting equation (2.56) in equation (2.55), multiplying by Ψ_m, calculating the mean values, and applying the properties of orthogonality properties of the polynomial, it has:

$$\{u_m\}[\mathrm{D}_0]\langle\Psi_m^2\rangle = \sum_{q=1}^{Q}\sum_{n=0}^{N}\{u_n\}\langle\xi_q\Psi_n\Psi_m\rangle[\sigma\mathrm{D}_0] = \{\mathrm{f}\}\langle\Psi_m\rangle \tag{5.38}$$

Replacing $\{u\}$ and considering random Gaussian variables ξ_1 and with null mean, unitary standard deviation, and Hermite Polynomial with degree one we obtain

$$\begin{aligned}
\{u_0\}[\mathrm{D}_0]\langle\Psi_0^2\rangle + \{u_0\}\langle\xi_1\Psi_0^2\rangle\sigma A[\mathrm{D}_0] + \{u_1\}\langle\xi_1\Psi_1\Psi_0\rangle\sigma A[\mathrm{D}_0] = \{\mathrm{f}\}\langle\Psi_0\rangle\\
\{u_1\}[\mathrm{D}_0]\langle\Psi_1^2\rangle + \{u_0\}\langle\xi_1\Psi_0\Psi_1\rangle\sigma A[\mathrm{D}_0] + \{u_1\}\langle\xi_1\Psi_1^2\rangle\sigma A[\mathrm{D}_0] = \{\mathrm{f}\}\langle\Psi_1\rangle
\end{aligned}$$

Substituting the values of Ψ_m according to equation (2.52) and rewriting in a matrix form it has

$$\begin{bmatrix} \mathrm{D}_0 & \sigma A[\mathrm{D}_0] \\ \sigma A[\mathrm{D}_0] & \mathrm{D}_0 \end{bmatrix} \begin{Bmatrix} u_0 \\ u_1 \end{Bmatrix} = \begin{Bmatrix} \mathrm{f}_0 \\ \mathrm{f}_1 \end{Bmatrix} \tag{5.39}$$

Similar procedure is used to calculate the displacement with Hermite Polynomial with degree two, it has

$$\begin{aligned}
\{u_0\}[\mathrm{D}_0]\langle\Psi_0^2\rangle + \{u_0\}\langle\xi_1\Psi_0^2\rangle\sigma A[\mathrm{D}_0] + \{u_1\}\langle\xi_1\Psi_1\Psi_0\rangle\sigma A[\mathrm{D}_0] + \{u_2\}\langle\xi_1\Psi_2\Psi_0\rangle\sigma A[\mathrm{D}_0] = \{\mathrm{f}\}\langle\Psi_0\rangle\\
\{u_1\}[\mathrm{D}_0]\langle\Psi_1^2\rangle + \{u_0\}\langle\xi_1\Psi_0\Psi_1\rangle\sigma A[\mathrm{D}_0] + \{u_1\}\langle\xi_1\Psi_1^2\rangle\sigma A[\mathrm{D}_0] + \{u_2\}\langle\xi_1\Psi_2\Psi_0\rangle\sigma A[\mathrm{D}_0] = \{\mathrm{f}\}\langle\Psi_1\rangle\\
\{u_2\}[\mathrm{D}_0]\langle\Psi_2^2\rangle + \{u_0\}\langle\xi_1\Psi_0\Psi_2\rangle\sigma A[\mathrm{D}_0] + \{u_1\}\langle\xi_1\Psi_1\Psi_2\rangle\sigma A[\mathrm{D}_0] + \{u_2\}\langle\xi_1\Psi_2^2\rangle\sigma A[\mathrm{D}_0] = \{\mathrm{f}\}\langle\Psi_2\rangle
\end{aligned}$$

Substituting the values of Ψ_m according to equation (2.52) and rewriting in a matrix form,

$$\begin{bmatrix} \mathrm{D}_0 & \sigma A[\mathrm{D}_0] & 0 \\ \sigma A[\mathrm{D}_0] & \mathrm{D}_0 & 2\sigma A[\mathrm{D}_0] \\ 0 & 2\sigma A[\mathrm{D}_0] & 2\sigma A[\mathrm{D}_0] \end{bmatrix} \begin{Bmatrix} u_0 \\ u_1 \\ u_2 \end{Bmatrix} = \begin{Bmatrix} \mathrm{f}_0 \\ \mathrm{f}_1 \\ \mathrm{f}_2 \end{Bmatrix} \tag{5.40}$$

With all $\{u_n\}$ known, it is calculated the energy density and energy flow and them statistical moments presented in Section 5.3.2.

Figure 5.17 shows two results for the mean of energy density calculated by using Monte Carlo simulation and Polynomial Chaos expansion with Moment equation. The calculated results of undamaged and damaged rods used the SEM in a 1/3-octave frequency band with centre frequency f_c = 160kHz. The polynomial chaos model was calculated with a Hermite polynomial of order 1 (PC1) with correlation coefficients of γ =0.0 and $\gamma = 0.75$. The results obtained by MC simulation used 500 samples.

As it can be seen, the mean of energy density presents a good agreement between the MC and PC methods, which represents a typical behaviour observed for all others evaluations using different values of polynomial order and correlation coefficient. Figure 5.18 shows the

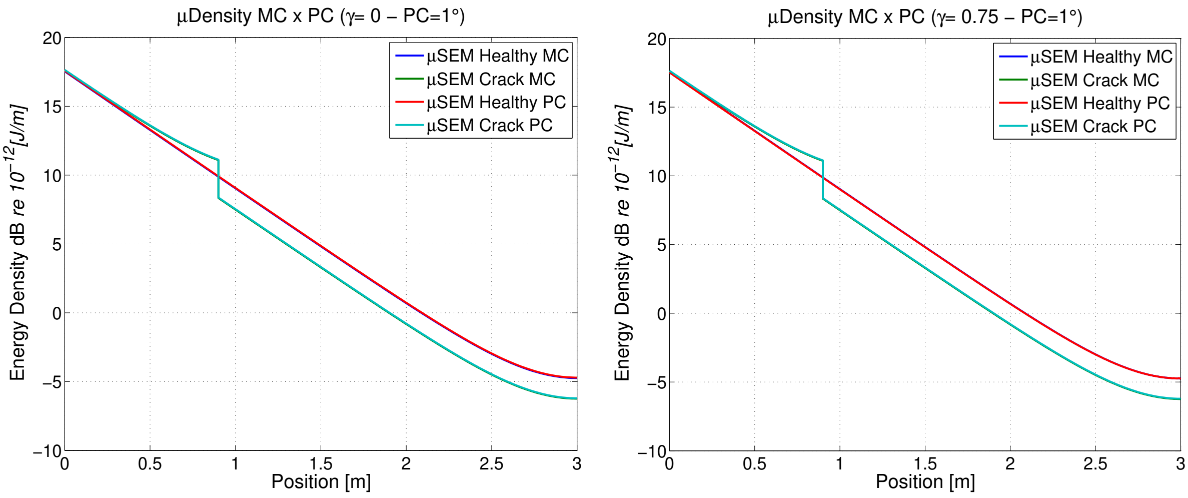

(a) (b)

Figure. 5.17: Mean of Energy Density for undamaged and damaged Rod using PC-order 1 with: a)γ = 0.0; b)γ = 0.75

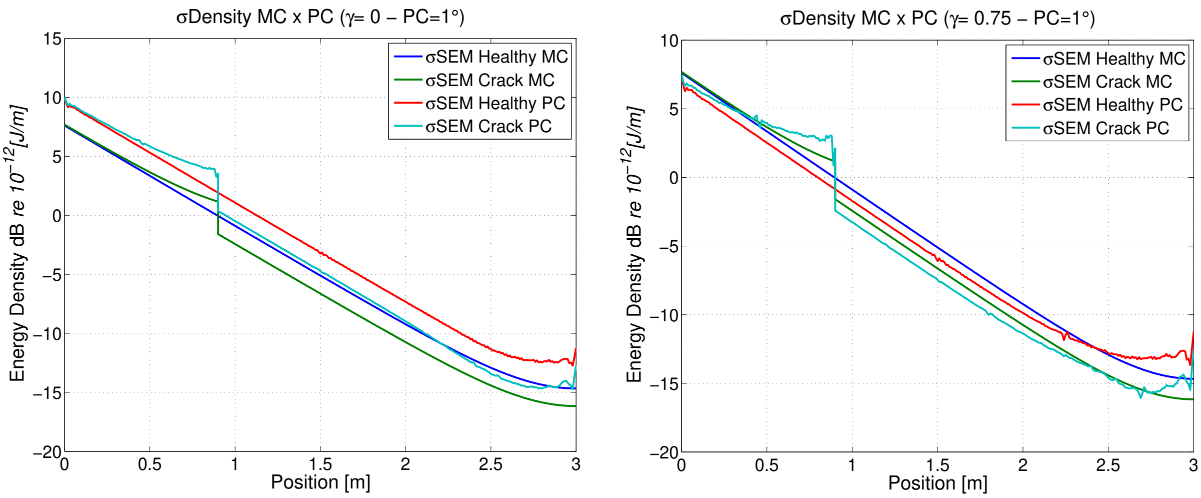

(a) (b)

Figure. 5.18: Standard Deviation of Energy Density for undamaged and damaged Rod using PC1 with: a)γ = 0.0; b)γ = 0.75

corresponding results for the standard deviation of energy density. In these cases, PC results present a small difference related to the signal amplitude compared with the MC results. However, there is a better approximation when $\gamma = 0.75$ as compared with $\gamma = 0.0$, which indicates that the correlation coefficient can improve the results if evaluated at the statistical basis. For the PC damage model, it was also observed an oscillatory behavior in the regions close to the crack position and at the rod right end. It seems to come from the approximations at the Moment Equations. Figures 5.19 and 5.20 show the results for the mean and standard deviation of energy flow calculated by MC and PC. The PC model was of order 1 (PC1) and the correlation coefficients values were $\gamma = 0.0$ and $\gamma = 0.75$. The MC simulation results were performed using 500 samples. Correspondingly, the energy flow results present a similar behaviour as

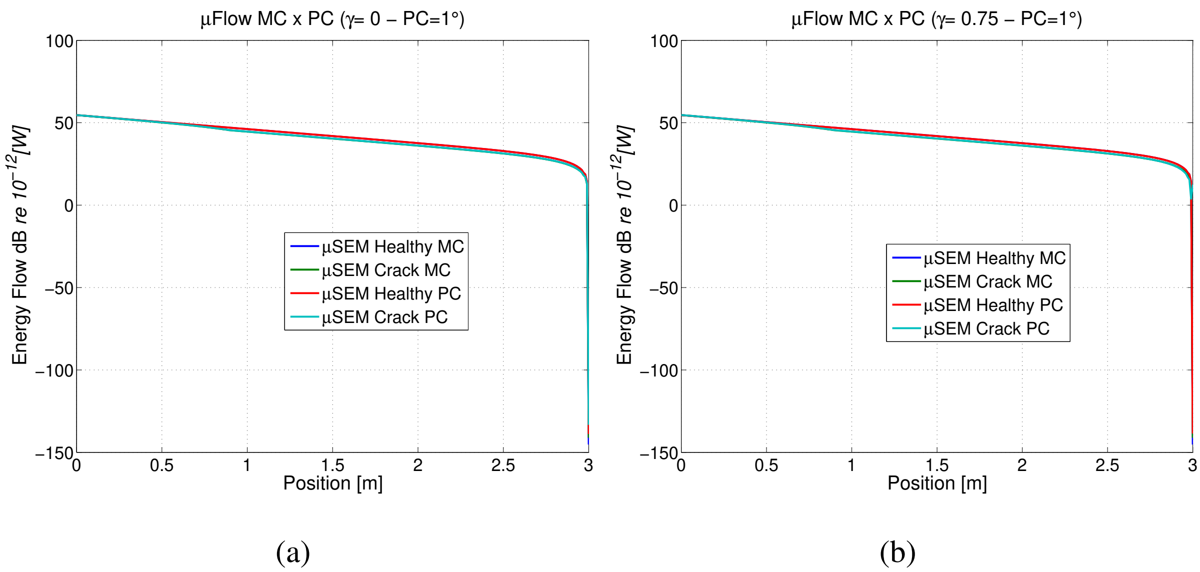

Figure. 5.19: Mean of Energy Flow for undamaged and damaged Rod using PC1 with: γ = 0.0; b)γ = 0.75

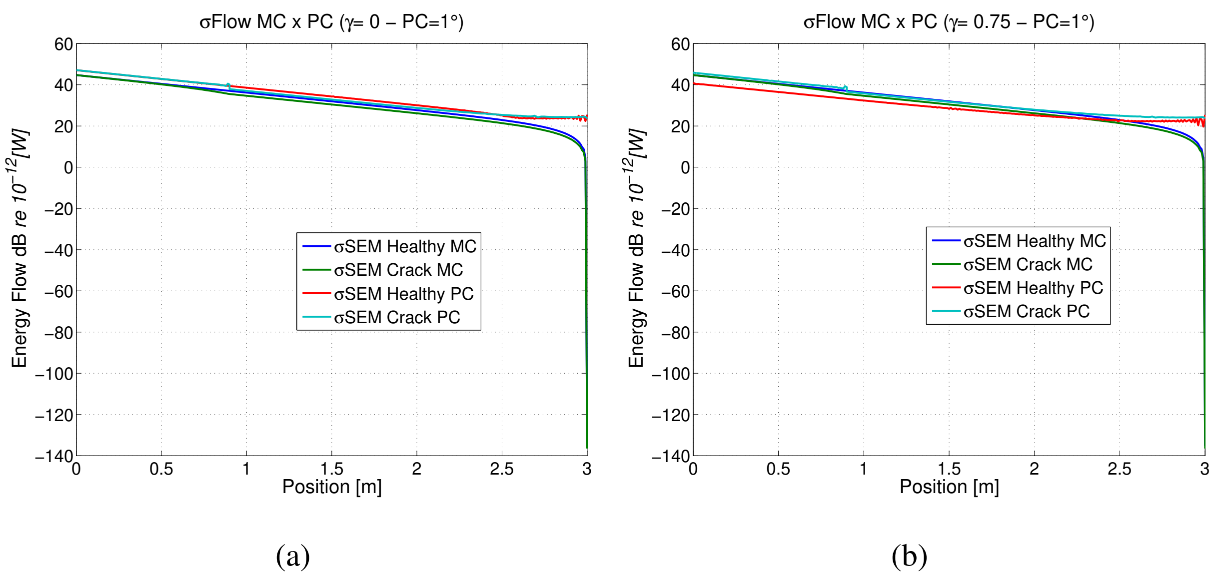

Figure. 5.20: Standard Deviation of Energy Flow for undamaged and damaged Rod using PC1 with: a)γ = 0.0; b)γ = 0.75

observed for the energy density, where there is a good agreement for the mean while for the standard deviation the approximation depends on the correlation coefficient. Also, for the PC damage model it was observed a divergent behaviour in the regions close to the crack position and at the rod right end. Figures 5.21, 5.23, 5.22 and 5.24 shows the results for the mean and standard deviation of energy density and energy flow calculated by MC and PC, with the same values of sample size, material properties, rod geometry and correlation coefficients, but with a Hermite polynomial of order 2 (PC2). These results confirm the observations extracted in the analysis of the case PC1.

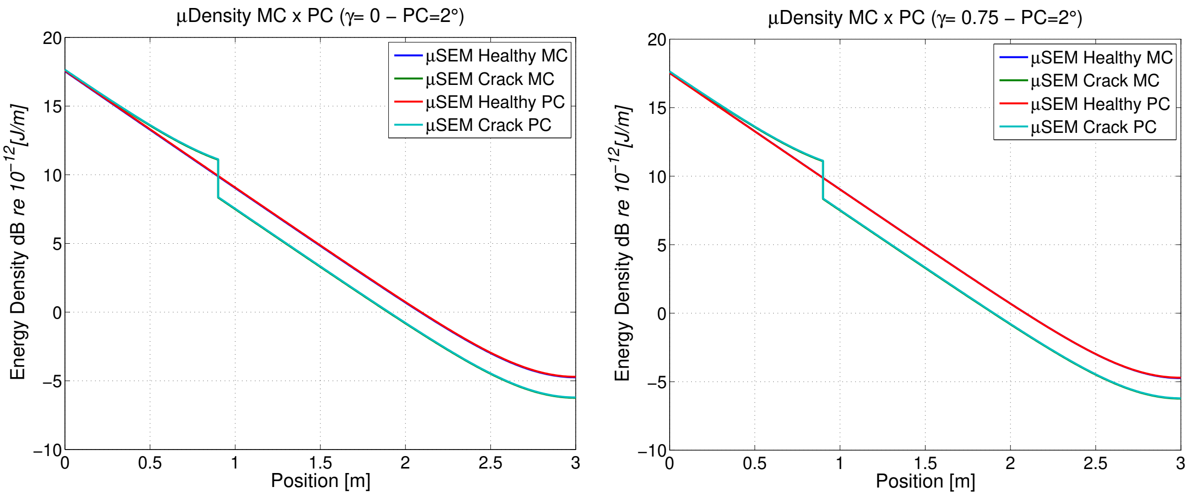

(a) (b)

Figure. 5.21: Mean of Energy Density for undamaged and damaged Rod using PC2 with: a)γ = 0.0; b)γ = 0.75

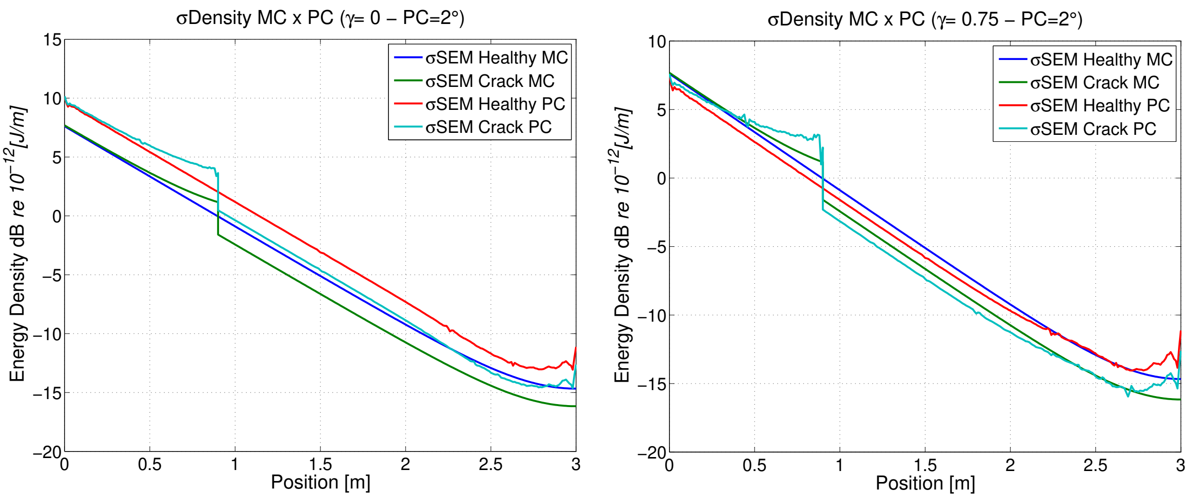

(a) (b)

Figure. 5.22: Standard Deviation of Energy Density for undamaged and damaged Rod using PC2 with: a)γ = 0.0; b)γ = 0.75

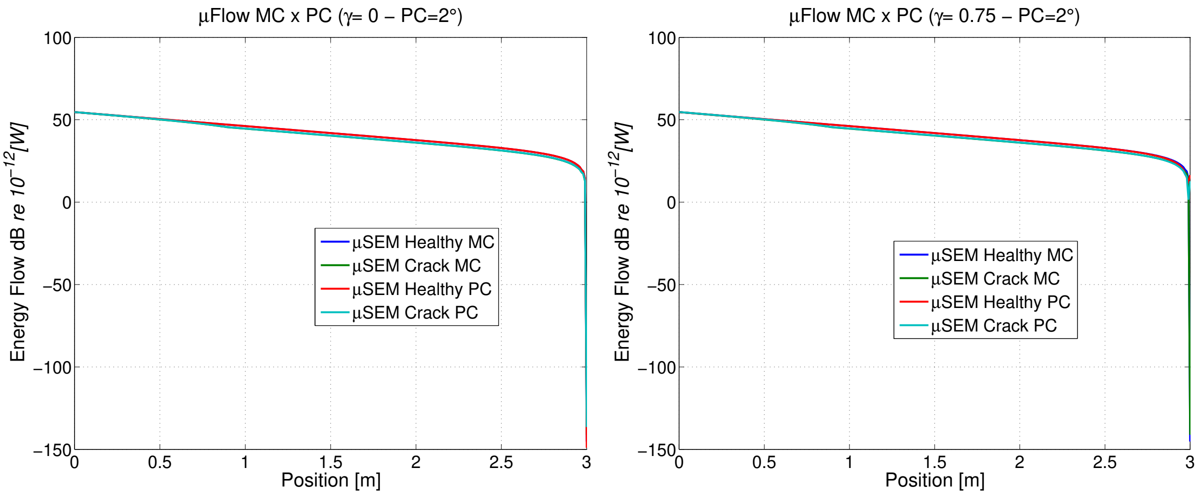

(a) (b)

Figure. 5.23: Mean of Energy Flow for undamaged and damaged Rod using PC-order 2 with: a)γ = 0.0; b)γ = 0.75

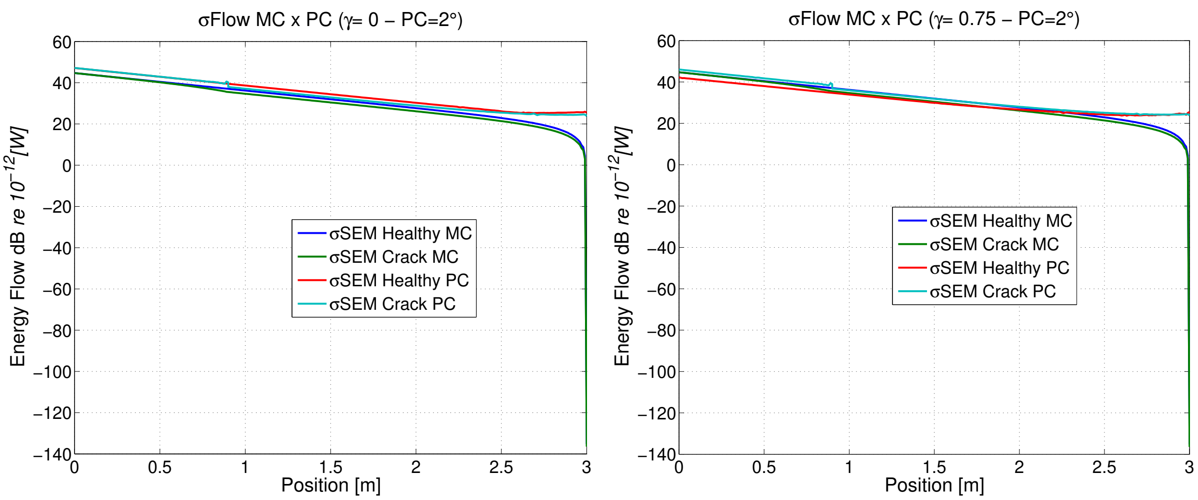

(a) (b)

Figure. 5.24: Standard Deviation of Energy Flow for undamaged and damaged Rod using PC2 with: a)γ = 0.0; b)γ = 0.75

As shown above, a study about the energy flow patterns used by localised damage in rod structures including uncertainties in a geometric parameter was presented. As shown above, a study about the energy flow patterns used by localised damage in structures rod-like, including uncertainties in a geometric parameter was presented. The developed formulation solves the problem in two steps: first, the structure is modelled by the SEM and the mean and variance of displacement responses obtained by using the Polynomial Chaos expansion; second, the mean and variance of energies are calculated applying the expectation into the equations of energy density and energy flow. The Monte Carlo Simulation solution is the reference being used to validate the results obtained by PC. For all simulated cases, the mean of energy density and energy flow presents a good agreement between the MC and PC methods independently of the values of polynomial order and correlation coefficients. The standard deviation does not converge very well, but its results indicate that it can be improved with a better estimation of the correlation coefficients. Of course, it is preliminaries results using a very simple examples in order do check the proposed method. Thus, more tests need to be conducted to verify the extension and robustness of this method.

5.4 Closure

To summarize, this chapter presented methods to detect damage in a structure. It started with a literature review of the methods. We focused on methods to detect damage based on Spectral Element Method including uncertain parameters. Two techniques were proposed, the first one developed an explicit formulation to calculate crack depth from measured system responses. Either, experimental and simulated test were used to verify the performance of the theory. The second estimation was made based on energy method and PC by including uncertainties parameters. Both techniques showed satisfying results in damage assessment for this kind of structure. On the other hand, more tests should be realised to verify the influence of different types of waves which is present in beam for example. It is an open topic and should be explored, by extending the theory for structures like beam and plate.

6 Conclusions

The studies proposed in this thesis were a method for identification of distributed properties of structural systems by using FRF, as well as techniques to detect damage by considering uncertainties in the structure. Summary and detailed discussions have been presented at the of relevant chapters. The purpose of this chapter is to recapitulate the main findings, unifying them and to suggest some further research directions.

6.1 Summary of the contributions made

A stochastic approach of the SEM for undamaged and damaged rod and beam structures were formulated. It was used uncertainty into structure properties model as longitudinal rigidity (EA), flexural rigidity (EI) and mass per unit length (ρA). Thus, a stochastic Spectral Element Method was developed to express these parameters as a spatially correlated random field. The random field is expanded in a spectral decomposition known as the Karhunen-Loève expansion. Since some parameters cannot be assumed with a Gaussian marginal, a non-Gaussian translation random field is used based on memoryless non-linear transformations. Once our interest was in detect structural damage, we developed a new formulation for damaged spectral element (rod and beam) with a stochastic basis.

For damage detection, two techniques were proposed. The first one, an explicit formulation to calculate crack depth from measured system responses was proposed and validated with numerical and experimental tests. The second, a detection is based on energy method and PC by including uncertainties parameters. The novel in this approach is to include uncertainties in "derived parameters"as energy(flow and density). Both techniques showed satisfying results in damage assessment for a structure like-rod. On the other hand, more tests should be realised to verify the influence of different types of waves (e.g. evanescent waves) can generate in the damage detection. It is an open topic and should be explored by extending the theory to structures like beam and plate.

A technique to estimate spatially distributed parameters of samples of a stochastic structure using a KL expansion and sensitivity-based FRF model updating was proposed. Randomness was included in the rigidity and mass per unit length of a structure. As a stochastic model is employed, the sensitivity-based method using FRF is also developed for a stochastic model based on spectral beam elements. This study tries to simulate a realistic situation where the true model parameters, EA, EI and ρA can deviate from the baseline homogeneous values. The objective was to reconstruct the distributed random field from the measured FRF obtained for a sample of a stochastic model of the beam. Two numerical tests and an experimental test were presented to verify the developed theory. In brief, the proposed methodology showed acceptable performance by comparing numerical and experimental results.

In summary, the work conducted in this thesis achieves the following:

- New formulation of the stochastic damaged spectral element for rod and beam (Chapter 3).
- Spatially distributed parameters estimation of a samples stochastic structure using a KL expansion and sensitivity-based FRF model updating (Chapter 4).
- An explicit formulation to calculate crack depth from measured system responses (Chapter 5).
- To include uncertainties in “derived parameters”as energy density and energy flow (Chapter 5).

6.2 Suggestions for further work

The study conducted in this thesis throws open questions. The following are some important areas of research which emerge immediately from this study:

- *Stochastic spectral element for a plate*, here we presented a theory for rod and beam and developed an approach for a damaged element, although we missed the subject for a structure plate-like.
- *Assessment of the damage in other kinds of structures*, it was presented an explicit formulation to calculate the depth crack in a structure like-rod, but it should be applied to a structure like beam, which will imply in new formulation for crack depth (α) and includes the effect of evanescent waves. Also refine the study to determine the damage position.
- To apply the damage detection technique *in a system with multi-cracks*.
- To include uncertainties in “derived parameters”as energy density and energy flow *applying for beam* and adopted the theory to *use the Generalized Polynomial Chaos Method*.

References

ADELMAN, H.M. and HAFTKA, R.T. Sensitivity analysis of discrete structural systems. **AIAA Journal**, v. 24, 823–832, 1986.

ADHIKARI, S. Doubly spectral stochastic finite-element method for linear structural dynamics. **American Society of Civil Engineers**, v. 1, 264–276, 2011.

ADHIKARI, S. **Structural Dynamic Analysis with Generalized Damping Models**. Wiley, 2013.

ADHIKARI, S. and FRISWELL, M. Distributed parameter model updating using the karhunen-loève expansion. **Mechanical Systems and Signal Processing**, v. 24, 326–339, 2010.

ADHIKARI, S. and MANOHAR, C.S. Transient dynamics of stochastically parametered beams. **ASCE Journal of Engineering Mechanics**, v. 126, n. 11, 1131–1140, November 2000.

AJITH, V. and GOPALAKRISHNAN, S. Spectral element approach to wave propagation in uncertain beam structures. **Journal of Mechanics of materials and strucutres**, v. 5(4), 637–659, 2010.

ALLEMANG, R. The modal assurance criterion (mac): Twenty years of use and abuse. In **IMAC-XX:Conference & Exposition on Structural Dynamics**. 2002.

ALLEMANG, R. and BROWN, D. A correlation coefficient for modal vector analysis. In **1st International Modal Analysis Conference, Orlando, USA.** 1982.

ARRUDA, J. Objective functions for the nonlinear curve-fit of frequency response functions. **AIAA Journal**, v. 30(3), 855–857, 1992.

ARRUDA, J. and SANTOS, J.D. Mechanical joint paramenter estimation using frequency response function and component mode synthesis. **Mechanical Systems and Signal Processing**, v. 7(6), 493–508, 1993.

ARRUDA, J.R.F. and DUARTE, M.A.V. Parameter estimation andmodel updating of rotor-bearing systems by the direct curve fit of frequency response functions. In **3rd International Conference on Rotordynamics, Lyon, France.** 1990.

ASTER, R.C. and THURBER, C.H. **Parameter estimation and inverse problems**. Academic Press Publications, 2012.

BALMES, E. A finite element updating procedure using frequency response functions applications to the mit/serc interferometer test bed. In **In 11th International Modal Analysis Conference, San Diego, USA**. 1993.

BANERJEE, J.R. Coupled bending torsional dynamic stiffness matrix for beam elements. **International Journal for Numerical Methods in Engineering**, v. 28, n. 6, 1283–1298, 1989.

BANERJEE, J.R. Dynamic stiffness formulation for structural elements a general approach. **Journal Computers& Structures**, v. 63(1), 101–103, 1997.

BANERJEE, J.R. Dynamic stiffness formulation for structural elements: A general approach. **Computer and Structures**, v. 63, n. 1, 101–103, 1997.

BANERJEE, J.R. and FISHER, S.A. Coupled bending torsional dynamic stiffness matrix for axially loaded beam elements. **International Journal for Numerical Methods in Engineering**, v. 33, n. 4, 739–751, 1992.

BANERJEE, J.R. and WILLIAMS, F.W. Exact bernoulli-euler dynamic stiffness matrix for a range of tapered beams. **International Journal for Numerical Methods in Engineering**, v. 21, n. 12, 2289–2302, 1985.

BANERJEE, J.R. and WILLIAMS, F.W. Coupled bending-torsional dynamic stiffness matrix for timoshenko beam elements. **Computer and Structures**, v. 42, n. 3, 301–310, 1992.

BANERJEE, J.R. and WILLIAMS, F.W. Free-vibration of composite beams - an exact method using symbolic computation. **Journal of Aircraft**, v. 32, n. 3, 636–642, 1995.

BARUCH, M. Optimization procedure to correct stiffness and flexibility matrices using vibration test data. **AIAA Journal**, v. 16(4), 346–351, 1978.

BARUCH, M. Optimal correction of mass and stiffness matrices using measured modes. **AIAA Journal**, v. 20(11), 1623–1626, 1982.

BARUCH, M. and ITZHAC, Y.B. Optimisation weighted orthogonalisation of measured modes. **AIAA Journal**, v. 16(1), 1208–1210, 1978.

BECK, J. and AU, S. Bayesian updating of structural models and reliability using markov chain monte carlo simulation. **Journal of Engineering Mechanics**, v. 128(4), 380–391, 2002.

BECK, J.L. and KATAFYGIOTIS, L.S. Updating models and their uncertainties. I: bayesian statistical framework. **Journal of Engineering Mechanics**, v. 124, n. 4, 455–461, 1998.

BERMAN, A. and NAGY, E.J. Improvement of a large analytical model using test data. **AAIA Journal**, v. 21(8), 1168–1173, 1983.

BESKOS, D. and NARAYANAN, G. Use of dynamic influence coefficients in forced vibration problems with the aid of fast fourier transform. **Journal Computers and Structures**, v. 9(2), 145–150, 1978.

BOHRNSTEDT, G.W. and GOLDBERGER, A.S. On the exact covariance of products of random variables. **Journal of the American Statistical Association**, v. (64) 328, 1439–1442, 1969.

CAESAR, B. Update and identification dynamic mathematical models. In **Proc. of the 4th IMAC, 394-401, Los Angeles, California**. 1986.

CAESAR, B. Updating system matrices using modal test data. In **Proc. of the 5th IMAC, 453-459, London, England**. 1987.

CALFISCH, R. Monte carlo and quasi mone carlo methods. **Acta Numerica**, v. 1, 2–49, 1998.

CARVALHO, J.; DATTA, B.N.; GUPTA, A. and LAGADAPATI, M. A direct method for model updating with incomplete measured data and without spurious modes. **Mechanical Systems and Signal Processing**, v. 21(7), 2715–2731, 2007.

CAWLEY, P. and ADAMS, R. The location of defects in structures from measurements of natural frequencies. **Journal Strain Analysis**, v. 14, 49–57, 1979.

CAWLEY, P.; ADAMS, R.; PYE, C.J. and STONE, B. A vibration technique for non- destructively assessing the integrity of structures. **Journal Mechanical Engineering Science**, v. 20, 93–100, 1978.

CHO, P. and BERNHARD, R. Energy flow analysis of coupled beams. **Journal of Sound and Vibration**, v. 211, 593–605, 1998.

COLLINS, J.D.; HART, G.C.; HASSELMAN, T.K. and KENNEDY, B. Statistical identification of structures. **AIAA Journal**, v. 12, n. 2, 185–190, 1974.

COTTIN, N.; FELGENHAUER, H. and NATKE, H.G. On the parameter identification of elastomechanical systems using inout and output residuals. **Ingenieure Archiv**, v. 54(5), 378–387., 1984.

CURSI, J.S.D. and SAMPAIO, R. **Modelagem Estocástica e Geração de Amostras de Variáveis e Vetores Aleatórios**. SBMAC (Notas em Matemática Aplicada; v. 66), 2012.

DESSOMBZ, O.; THOUVEREZ, F.; LAINE, J.P. and JEZEQUEL, L. Calcul des valeurs et vecteurs propres d une structure stochastique par projection sur un chaos polynomial. calculede fonctions de transfert stochastiques. Relatório técnico, École Centrale de Lyon - Laboratoire de Tribologie et Dynamique des Systemes, 2000.

DESSOMBZ, O.; THOUVEREZ, F.; LAINE, J.P. and JEZEQUEL, L. Expansion of stochastic frequency response function on polynomial chao. Relatório técnico, École Centrale de Lyon, 2001.

DIMAROGONAS, A.D. Vibration of cracked structures: a state of the art review. **Engineering Fracture Mechanics**, v. 55, 831–857, 1996.

DOEBLING, S.W.; FARRAR, C.R. and PRIME, M. A review of vibration-based damage identification methods. Relatório técnico, Engineering Analysis Group Los Alamos National Laboratory, 1998.

DOEBLING, S.W.; FARRAR, C.R.; PRIME, M. and SHEVITZ, D.W. Damage identification and health monitoring of structural and mechanical systems from changes in their vibration characteristics- a literature review. Relatório técnico, Los Alamos National Laboratory -University of California, 1996.

DOYLE, J.F. **Wave Propagation in Structures**. Springer Verlag, New York, 1989.

DOYLE, J.F. **Wave propagation in structures : spectral analysis using fast discrete Fourier transforms**. Mechanical engineering. Springer-Verlag New York, Inc., New York, second ed., 1997.

DURAND, J.F.; SOIZE, C. and GAGLIARDINI, L. Structural acoustic modeling of automotive vehicles in presence of uncertainties and experimental identification and validation. **Journal Acoustical Society of America**, v. 124, 1513 – 1525, 2008.

DUTANG, C. A note on random numbers. Relatório técnico, Cambrige, 2008.

EWINS, D.J. **Modal Testing: Theory and Practice**. Research Studies Press, 1984.

FABRO, A.T.; RITTO, T.G.; SAMPAIO, R. and ARRUDA, J.R.F. Stochastic analysis of a cracked rod modeled via the spectral element method. **Mechanics Research Communications**, v. 37, 326–331, 2010.

FANG, S.; REN, W.X. and PERERA, R. A stochastic model updating method for parameter variability quantification based on response surface models and monte-carlo simulation. **Mechanical Systems and Signal Processing**, v. 33, 83–96, 2012.

FARRAR, C. and WORDER, K. **Structural Health Monitoring: A Machine Learning Perspective**. Wiley, 2013.

FARRAR, C.R. and WORDEN, K. An introduction to structural health monitoring. **Philosophical Transactions of the royal society**, v. 365, 303 – 315, 2007.

FERGUSON, N.J. and PILKEY, W.D. Literature review of variants of dynamic stiffness method, Part 1: The dynamic element method. **The Shock and Vibration Digest**, v. 25, n. 2, 3–12, 1993a.

FERGUSON, N.J. and PILKEY, W.D. Literature review of variants of dynamic stiffness method, Part 2: Frequency-dependent matrix and other. **The Shock and Vibration Digest**, v. 25, n. 4, 3–10, 1993b.

FINNVEDEN, S. Spectral finite element analysis of the vibration of straight fluid-filled pipes with flanges. **Journal of Sound and Vibration**, 1997.

FLYNN, E.B.; TODD, M.; J. CROXFORD, B.D. and WILCOX, P. Enhanced detection through low-order stochastic modeling for guided-wave structural health monitoring. **Structural Health Monitoring**, 2012.

FONSECA, J.R.; FRISWELL, M.I.; MOTTERSHEAD, J.E. and LEES, A.W. Uncertainty identification by the maximum likelihood method. **Journal of Sound and Vibration**, v. 288, n. 3, 587–599, DEC 6 2005.

FRISWELL, M.I. The adjustment of structural parameters using a minimum variance estimator. **Mechanical Systems and Signal Processing**, v. 3, 143–155, 1989.

FRISWELL, M.I. Using vibration data and statistical measures to locate damage in structures. **Modal Anal. Int. J. Anal. Exp. Modal Anal.**, v. 9, 239–254, 1994.

FRISWELL, M.I. Damage identification using inverse methods. **Philosophical Transactions of the royal society**, v. 2007, 393 – 410, 2007.

FRISWELL, M.I.; MOTTERSHEAD, J. and AHMADIAN, H. Combining subset selection and parameter constraints in model updating. **ASME Journal of Vibration and Acoustics**, v. 120(4), 854–859, 1998.

FRISWELL, M.I. and MOTTERSHEAD, J.E. **Finite element model updating in structural dynamics**. Kluwer Academic Publishers, 1995.

FRITZEN, C. Identification of mass, damping and stiffness matrices of mechanical systems. **ASME Journal of Vibration, Acoustics, Stress and Reliability in Design**, v. 108(4), 9–16, 1986.

FRITZEN, C. and JENNEWEIN, D. Damage detection based on model updating methods.

Mechanical Systems and Signal Processing, v. 12(1), 163 – 186, 1998.

FRITZEN, C.P. Localization and correction of errors in finite elementmodels based on experimental data. In **In 17th International Seminar on Modal Analysis, Katholieke Universiteit Leuven, Belgium**. 1992.

GDOUTOS, E.E. **Fracture Mechanics: an Introduction**. Ed. Kluwer Academic Publishers, 1993.

GHANEM, R. and BRZAKALA, W. Stochastic finite-element analysis of soil lauers with random interface. **Journal of Engineering Mechanics**, v. 122, 361–369, 1996.

GHANEM, R. and KRUGER, R.M. Numerical solution of a spectral stochastic finite element systems. **Computers Methods Apply Mechanical Engineering**, v. 129, 289–303, 1996.

GHANEM, R. and SPANOS, P. **Stochastic Finite Elements - A Spectral Approach**. Sprin, 1991.

GLADWELL, G. and AHMADIAN, H. Generic element matrices suitable for finite element updating. **Mechanical Systems and Signal Processing**, v. 9(6), 601–614, 1996.

GOODMAN, L.A. On the exact variance of products. **Journal of the American Statistical Association**, v. (55) 292, 708–713, 1960.

GOPALAKRISHNAN, S.; CHAKRABORTY, A. and MAHAPATRA, D.R. **Spectral Finite Element Method**. Springer Verlag, New York, 2007.

GOVERS, Y. and LINK, M. Stochastic model updating covariance matrix adjustment from uncertain experimental modal data. **Mechanical Systems and Signal Processing**, v. 24(3), 696–706, 2010.

GRAFE, Henning. **Model Updating of Large Structural Dynamics Models Using Measured Response Functions**. 1998. Tese (Doutorado). Imperial College of Science, Technology and Medicine University of London Model.

GRIGORIU, M. **Applied Non-Gaussian Processes**. New York: Prentice Hall, 1995.

GRIGORIU, M. Simulation of stationary non-gaussian translation processes. **Journal of Engineering Mechanics**, v. 124, n. 2, 121–126, 1998.

HAAG, T.; HERRMANN, J. and HANSS, M. Identification procedure for epistemic uncertainties using inverse fuzzy arithmetic. **Mechanical Systems and Signal Processing**, v. 24(7), 2021–2034, 2010.

HASHEMI, S.M. and RICHARD, M.J. Free vibrational analysis of axially loaded bending-torsion coupled beams: a dynamic finite element. **Computer and Structures**, v. 77, n. 6, 711–724, 2000.

HASHEMI, S.M.; RICHARD, M.J. and DHATT, G. A new Dynamic Finite Element (DFE) formulation for lateral free vibrations of Euler-Bernoulli spinning beams using trigonometric shape functions. **Journal of Sound and Vibration**, v. 220, n. 4, 601–624, 1999.

HAZEWINKEL, M. **Encyclopaedia of Mathematics:Fibonacci Method-H**. Springer Science & Business Media., 1989.

HEYLEN, W. and LAMMENS, S. Frac : a consistent way of comparing frequency response functions. In **Proceedings of the Conference on Identification in Engineering Systems, Swansea, UK**. 1996.

HUA, X.; NI, Y.; CHEN, Z. and KO, J. An improved perturbation method for stochastic finite element model updating. **International Journal for Numerical Methods in Engineering**, v. 73(13), 1845–1864, 2008.

HUANG, S.P.; QUEK, S.T. and PHOON, K. Convergence study of the truncated karhunen-loève expansion for simulation of stochastic processes. **International Journal for Numerical Methods in Engineering**, v. 52, 1029–1043, 2001.

IBRAHIM, S.R.; DAMBROGIO, W.; SALVINI, P. and SESTIERI, S. Direct updating of non-conservative finite element models using measured input - output. In **In 10th International Modal Analysis Conference, San Diego, USA**. 1992.

IMREGUN, M.; SANLITURK, K.Y. and EWINS, D.J. Finite element model updating using frequency response function data-ii.case study on a medium size finite element model. **Mechanical Systems and Signal Processing**, v. 9(2), 203–213, 1995a.

IMREGUN, M.; VISSER, W.J. and EWINS, D.J. Finite element model updating using frequency response function data-i. theory and initial investigation. **The shock and Vibration**, v. 9(2), 187–202, 1995b.

J.C. WOHLEVER, R.B. Mechanical energy flow models of rods and beams. **Journal of Sound and Vibration**, v. 153, 1–19, 1992.

KATAFYGIOTIS, L.S. and BECK, J.L. Updating models and their uncertainties. II: model identifiability. **Journal of Engineering Mechanics**, v. 124, n. 4, 463–467, 1998.

KHODAPARAST, H. **Stochastic Finite Element Model Updating and its Application in Aeroelasticity**. 2010. Tese (Doutorado). University of Liverpool.

KHODAPARAST, H.H. and MOTTERSHEAD, J. Efficient methods in stochastic model updating. In **Proceedings of ISMA**. 2008.

KHODAPARAST, H.H.; MOTTERSHEAD, J.E. and FRISWELL, M.I. Perturbation methods for the estimation of parameter variability in stochastic model updating. **Mechanical System and Signal Processing**, v. 22, n. 8, 1751–1773, 2008.

KIN, J.T. and STUBBS, N. Crack detection in neam-type strucuture using frequency data. **Journal of Sound and Vibration**, v. 259(1), 145–160, 2003.

KLEIBER, M. and HIEN, T. **The Stochastic Finite Element Method**. John Wiley, 1992.

KRAWCZUK, M. Application of spectral beam finite element with a crack and iterative search technique for damage detection. **Finite Elements in Analysis and Design**, v. 80, 1809–1816, 2002.

KRAWCZUK, M.; GRABOWSKA, J. and PALACZ, M. Longitudinal wave propagation. part i- comparison of rod theories. **Journal of Sound and Vibration**, v. 295, 461–478, 2006a.

KRAWCZUK, M.; GRABOWSKA, J. and PALACZ, M. Longitudinal wave propagation. part ii- analysis of crack influence. **Journal of Sound and Vibration**, v. 295, 479–490, 2006b.

KRAWCZUK, M.; PALACZ, M. and OSTACHOWICS, W. The dynamic analysis of a cracked timoshenko beam by the spectral elemet method. **Journal of Sound and Vibration**, v. 264, 1139–1153, 2002.

LEE, U. **Spectral Element Method in Structural Dynamics**. BInha University Press, 2004.

LINK, M. Identification and correction of errors in analytical models using test data theoretical and practical bounds. In **In International Conference on Space- craft Structures and Mechanical Testing (ESA/ESTEC)**. 1990.

LINK, M. Updating analytical models by using local and global parameters and relaxed optimisation requirements. **Mechanical Systems and Signal Processing**, v. 12, 7–22, 1998.

LINK, M. and SANTIAGO, O. Updating and localizing structural errors based on minimization of equation errors. In **In International Conference on Space- craft Structures and Mechanical Testing (ESA/ESTEC)**. 1991.

LINK, M.; WEILAND, M. and BASSAGAN, J.M. Direct physical matrix identication as compared to phase resonance testing: An assessment based on practical application. 1987.

MACHADO, M.R. and SANTOS, J.M.C.D. Reliability analysis of damaged beam spectral element with parameter uncertainties. **Shock and Vibration**, v. 2015, 12 pages, 2015.

MAIA, N.; SILVA, J.; ALMAS, E. and SAMPAIO, R. Damage detection in strutures: from mode shape to frequency response function methods. **Mechanical Systems and Signal Processing**, v. 17, 489–498, 2003.

MAIA, N.M.M. and SILVA, J.M.M., editores. **Theoretical and Experimental Modal Analysis**. Engineering Dynamics Series. Research Studies Press, Taunton, England, 1997. Series Editor, J. B. Robetrs.

MAÎTRE, O.L. and KNIO, O. **Spectral methods for uncertainty quantification**. Springer, 2010.

MANOHAR, C.S. and ADHIKARI, S. Dynamic stiffness of randomly parametered beams. **Probabilistic Engineering Mechanics**, v. 13, n. 1, 39–51, January 1998.

MARES, C.; MOTTERSHEAD, J.E. and FRISWELL, M.I. Stochastic model updating: part 1 - theory and simulated example. **Mechanical System and Signal Processing**, v. 20, n. 7, 1674–1695, 2006.

MEIROVITCH, L. **Principles and techniques of vibrations**. Prentice-Hal, 1997.

MESSINA, A.; WILLIANS, E. and CONTURSI, T. Strucutral damage detection by a sensitivity and statistical-based method. **Journal of Sound and Vibration**, v. 216(5), 680–797, 1998.

MILLER, S. and CHILDERS, D. **Probability and Random Processes**. Academic Pres, 2012.

MONTALVAO, D.; MAIA, N. and RIBEIRO, A. A review of vibration-based structural health monitoring with special emphasis on composite materials. **The Shock and Vibration Digest**, v. 38, 10 – 22, 2006.

MORASSI, A. and VESTRONI, F. **Dynamic methods for damage detection in strucutres**. Springer New York, 2008.

MOTTERSHEAD, J.; FRISWELL, M.; NG, G. and BRANDON, J. Geometric parameters for finite element model updating of joints and constraints. **Mechanical Systems and Signal Processing**, v. 10(2), 171–182, 1996.

MOTTERSHEAD, J.; MARES, C.; JAMES, S. and FRISWELL, M. Stochastic model updating: Part 2: Application to a set of physical structures. **Mechanical Systems and Signal Processing**, v. 20(8), 2171–2185, 2006.

MOTTERSHEAD, J.E. and FOSTER, C.D. On the treatment of ill-conditioning in spatial parameter estimation from measured vibration data. **Mechanical Systems and Signal Processing**, v. 5(2), 139–154, 1991.

MOTTERSHEAD, J.E. and FRISWELL, M. Model updating in strucutral dynamics: A survey. **Journal of Sound and Vibration**, v. 167(2), 347– 375, 1993.

MOTTERSHEAD, J.E.; LINK, M. and FRISWELL, M.I. The sensitivity method in finite element model updating: A tutorial. **Mechanical Systems and Signal Processing**, v. 25, 2275–2296, 2011.

MOTTERSHEAD, J.E.; LINK, M.; SILVA, T.A.N.; GOVERS, Y. and KHODAPARAST, H. **Vibration Engineering and Technology of Machinery**. Springer International Publishing, 2015.

NARKIS, Y. Identification of crack location in vibrating simply supported beams. **Journal of Sound and Vibration**, v. 172(4), 549 – 558, 1994.

NATKE, H. Die korrektur des rechenmodells eines elastomechanischen systems mittels gemessener erzwungener schwingungen. **Ingenieur-Archiv**, v. 46, 169–184, 1977.

NATKE, H. Properties of various residuals within updating of mathematical models. **Inverse Problems in Engineering**, v. 1, 329–348, 1988a.

NATKE, H. Updating computational models in the frequency domain based on measured data: a survey. **Probabilistic Engineering Mechanics**, v. 3, 28–35, 1988b.

NATKE, H. **Einfuhrung in in Theorie und Praxis der Zeitreihen und Modalanalyse,**. Vieweg Verlag, 1992.

NG, C.; VEIDT, M. and LAM, H. Probabilistic damage characterisation in beams using guided waves. **Procedia Engineering**, v. 14, 490 – 497, 2011.

OSTACHOWICZ, W.M. Damage detection of structures using spectral finite element method. **Computers & Structures**, v. 86, 454–462, 2008.

OWOLABI, G.; SWAMIDAS, A. and SESHADRI, R. Crack detection in beams using changes in frequencies and amplitudes of frequency response functions. **Journal of Sound and Vibration**, v. 265, 1–22, 2003.

PALACZ, M. and KRAWCZUK, M. Vibration parameters for damage detection in structures. **Journal of Sound and Vibration**, v. 249(5), 999–1010, 2002.

PAPOULIS, A. and PILLAI, S.U. **Probability, random variables and stochastic processes.** McGraw-Hill, Boston, 2002.

PASCUAL, R.; GOLINVAL, J. and RAZETO, M. A frequency domain correlation technique for model correlation and updating. 1997.

PASCUAL, R.; GOLINVAL, J. and RAZETO, M. On-line damage assessment using operating deflection shapes. 1999.

PAVLOVIC, R.; KOZIC, P. and RAJKOVIC, P. Influence of randomly varying damping coefficient on the dynamic stability of continuous systems. **European Journal of Mechanics of Solids**, v. 24, 81–87, 2005.

PAZ, M. **Structural Dynamics: Theory and Computation**. Van Nostrand, Reinhold, second ed., 1980.

PHOON, K.K.; HUANG, H.W. and QUEK, S.T. Simulation of strongly non-gaussian processes using karhunen-loeve expansion. **Structural Safety**, v. 20(2), 1881198, 2005.

POIRION, F. and SOIZE, C. Monte carlo construction of karhunen-loeve expansion for non-gaussian random fields. In **Proceedings of the 13th ASCE Engineering Mechanics Division Conference**. 1999.

PUIG, B., P.F. and SOIZE, C. Non-gaussian simulation using hermite polynomial expansion: convergences and algorithms. **Probabilistic Engineering Mechanics**, v. 17(3), 253Dc264, 2002.

RUBINSTEIN, R.Y. **Simulation and the Monte Carlo Method, 2nd Edition**. Wiley, 2008.

RUI, Q.; OUYANG, H. and H.Y.WANG. An efficient statistically equivalent reduced method on stochastic model updating. **Appl Math Model**, v. 37, 6079–6096, 2013.

SAKAMOTO, S. and GHANEM, R. Simulation of multi-dimensional non-gaussian non-stationary random fields. **Probabilistic Engineering Mechanics**, v. 17(2), 2002.

SAMPAIO, R. and LIMA, R. **Modelagem Estocástica e Geração de Amostras de Variáveis e Vetores Aleatórios**. SBMAC (Notas em Matemática Aplicada; v. 70), 2012.

SANTOS, E.; ARRUDA, J. and SANTOS, J.D. Modeling of coupled structural systems by an energy spectral element method. **Journal of Sound and Vibration**, v. 36, 1 – 24, 2008.

SANTOS, J.M.C.D. and ZIMMERMAN, D.C. Structural damage detection using minimum rank update theory and parameter estimation. In **Proceedings of the AIAA/ASME/AHS Adaptive Structures Forum**. 1996.

SCHEVENELS, M.; LOMBAERT, G. and DEGRANDE, G. Application of the stochastic finite element method for gaussian and non-gaussian systems. In **Proceedings of International Conference on Noise and Vibration Engineering**. 2004.

SINOU, J.J. Numerical investigations of a robust identification of crack loca- tion and size in beams using only changes in ratio pulsations of the cracked beams. **Structural Engineering Mechanics**, v. 25(6), 691–716, 2007.

SINOU, J.J. A review of damage detection and health monitoring ofmechanical systems fromchanges in themeasurement of linear and non-linear vibrations. Relatório técnico, Laboratoire de Tribologie et Dynamique des Systemes UMR-CNRS 5513 Ecole Centrale de Lyon, 2013.

SOBOL', I.M. **A primer for the Monte Carlo method**. CRC Press, 1994.

SOHN, H.; FARRAR, C.; HEMEZ, F.; SHUNK, D.; STINEMATES, D. and NADLER, B. A review of structural health monitoring literature: 1996-2001. Relatório técnico, Los Alamos National Laboratory, USA, 2003.

SOHN, H.; FARRAR, C.R.; HUNTER, N.F. and WORDEN, K. Structural health monitoring using statistical pattern recognition techniques. **Journal Dynamic Systems Measurement and Control**, v. 123, 706–711, 2001.

SOHN, H.; WORDEN, K. and FARRAR, C.R. Statistical damage classification under changing environmental and operational conditions. **Journal of intelligent material systems and structures**, v. 13, 561–574, 2002.

SOIZE, C. Robust updating of uncertain computational models using experimental modal analysis. **AIAA Journal**, v. 46(11), 2955–2965, 2008.

STEFANOU, G. The stochastic finite element method: Past, present and future. **Computer Methods in Applied Mechanics and Engineering**, v. 198, 1031 – 1051, 2009.

SU, Z. and YE, L. **Identification of Damage Using Lamb Waves**. Springer, 2009.

SUTTER, T.R. Comparison of several methods for calculating vibration mode shape derivatives. **AIAA Journal**, v. 26, 1506–1511, 1988.

SUTTER, T.R. and BROOKS, P. Sensitivity of frequancy response function of linear dynamic systems to variations in desing parametr values. **Journal of Sound and Vibration**, v. 126, 1167–172, 1988.

TADA, H.; PARIS, P. and IRWIN, G.R. **Stress Analysis of Cracks Handbook**. Del Research Corporatoin, 1973.

TITURUS, B. and FRISWELL, M. Regularization in model updating. **International Journal for Numerical Methods in Engineering**, v. 75, 440–478, 2008.

VANHONACKER, P. Sensitivity analysis of mechanical structures based on experimentally determined modal parameters. In **Proceeding of the 7th IMAC, Las Vegas, NV**. 1989.

VANLI, O.A. and JUNG, S. Statistical updating of finite element model with lamb wave sensing data for damage detection problems. **Mechanical Systems and Signal Processing**, 2013.

VIO, R.; ANDREANI, P. and WAMSTEKER, W. Nmerical simularin of non-gaussian random fields with prescribed correlation structure. Relatório técnico, ESA IUE Obsevatory and Max-Planck Institut fur Extraterrestrische Physik, 2001.

WEINBERG, G. and L.GUNN. Simulation of statistical distributions using the memory-less nonlinear transformation. Relatório técnico, DSTO Defence Science and Technology Organisation-Australia Government, 2011.

WIENER, N. The homogeneous caos. **American Journal of Mathematics**, v. 60, 897–936, 1938.

WOLFE, M.A. **Numerical Methods for Unconstrained Optimazation**. Amsterdam:Van Nostrand Reinhold, 1978.

XIU, D. **Numerical Methods for Computations-A Spectral method approcah**. Princeton University Press, 2010.

XIU, D. and KARNIADAKIS, G.E. The wiener - askey polynomial chaos for stochastic differential equations. Relatório técnico, Brown University,Division of Applied Mathematics,182 George Street,Providence,RI, 2003.

XU, Y.; ZHANG, J.; LI, J. and WANG, X. Stochastic damage detection method for building structures with parametric uncertainties. **Journal of Sound and Vibration**, v. 330, 4725 – 4737, 2011.

YAMAZAKI, F.; SHINOZUKA, M. and DASGUPTA, G. Neumann expansion for stochastic finite element analysis. **Journal Engineering Mechanics-ASCE**, v. 114 (8), 1335–1354, 1988.

ZANG, C.; FRISWELL, M. and IMREGUN, M. Structural health monitoring and damage assessment using measured frfs from multiple sensors, part i: The indicator of correlation criteria. In **In Proceedings of the 5th International Conference on Damage Assessment of Structures, Southampton, UK**. 2003.

ZANG, C. and IMREGUN, M. Structural damage detection using artificial neural networks and measured frf data reduced via principal component projection. **Journal of Sound and Vibration**, v. 242(5), 813–827, 2001.

ZHU, W.; REN, Y. and WU, W. Stochastic fem based on local averages of random vector fields. **Journal Engineering Mechanics-ASCE**, v. 118 (3), 496–511, 1992.

Appendix A – Spectral element matrices

This appendix contains exact closed-form expression of the elements of deterministic and stochastic spectral stiffness and mass matrices presented in the body of this thesis.

A.1 Undamaged rod matrix elements

A.1.1 Stochastic

$$
\begin{aligned}
Ko_{11} &= -\frac{e^{2ikL}k^2\left(2e^{2ikL}ik\mathrm{wj}\cos(\mathrm{wjxe})-2ik\mathrm{wj}\cos(\mathrm{wj}(L+\mathrm{xe}))+\left(4k^2-\left(1+e^{2ikL}\right)\mathrm{wj}^2\right)\sin(\mathrm{wjxe})+2\left(\mathrm{wj}^2-2k^2\right)\sin(\mathrm{wj}(L+\mathrm{xe}))\right)}{\left(-1+e^{2ikL}\right)^2\left(\mathrm{wj}^3-4k^2\mathrm{wj}\right)}\\
Ko_{12} &= -\frac{k^2\left(e^{2ikL}\left(2ik\mathrm{wj}\cos(\mathrm{wj}(L+\mathrm{xe}))+\left(4k^2-\mathrm{wj}^2\right)\sin(\mathrm{wjxe})+2\left(\mathrm{wj}^2-2k^2\right)\sin(\mathrm{wj}(L+\mathrm{xe}))\right)-\mathrm{wj}(2ik\cos(\mathrm{wjxe})+\mathrm{wj}\sin(\mathrm{wjxe}))\right)}{\left(-1+e^{2ikL}\right)^2\left(\mathrm{wj}^3-4k^2\mathrm{wj}\right)}\\
Ko_{21} &= Ko_{12}\\
Ko_{22} &- \frac{e^{2ikL}k^2\left(-2ik\mathrm{wj}\cos(\mathrm{wjxe})+2e^{2ikL}ik\mathrm{wj}\cos(\mathrm{wj}(L+\mathrm{xe}))+2\left(2k^2-\mathrm{wj}^2\right)\sin(\mathrm{wjxe})-\left(4k^2-\left(1+e^{2ikL}\right)\mathrm{wj}^2\right)\sin(\mathrm{wj}(L+\mathrm{xe}))\right)}{\left(-1+e^{2ikL}\right)^2\left(\mathrm{wj}^3-4k^2\mathrm{wj}\right)}
\end{aligned}
\tag{A.1}
$$

$$
\begin{aligned}
Mo_{11} &= \frac{e^{2ikL}\left(4\sin(\mathrm{wj}(L+\mathrm{xe}))k^2+2e^{2ikL}i\mathrm{wj}\cos(\mathrm{wjxe})k-2i\mathrm{wj}\cos(\mathrm{wj}(L+\mathrm{xe}))k-\left(4k^2+\left(-1+e^{2ikL}\right)\mathrm{wj}^2\right)\sin(\mathrm{wjxe})\right)}{\left(-1+e^{2ikL}\right)^2\left(\mathrm{wj}^3-4k^2\mathrm{wj}\right)}\\
Mo_{12} &= \frac{e^{2ikL}\left(4\sin(\mathrm{wj}(L+\mathrm{xe}))k^2+2i\mathrm{wj}\cos(\mathrm{wj}(L+\mathrm{xe}))k+\left(\mathrm{wj}^2-4k^2\right)\sin(\mathrm{wjxe})\right)-\mathrm{wj}(2ik\cos(\mathrm{wjxe})+\mathrm{wj}\sin(\mathrm{wjxe}))}{\left(-1+e^{2ikL}\right)^2\left(\mathrm{wj}^3-4k^2\mathrm{wj}\right)}\\
Mo_{21} &= Mo_{12}\\
Mo_{22} &= \frac{e^{4ikL}\mathrm{wj}(2ik\cos(\mathrm{wj}(L+\mathrm{xe}))+\mathrm{wj}\sin(\mathrm{wj}(L+\mathrm{xe})))-e^{2ikL}\left(4\sin(\mathrm{wjxe})k^2+2i\mathrm{wj}\cos(\mathrm{wjxe})k+\left(\mathrm{wj}^2-4k^2\right)\sin(\mathrm{wj}(L+\mathrm{xe}))\right)}{\left(-1+e^{2ikL}\right)^2\left(\mathrm{wj}^3-4k^2\mathrm{wj}\right)}
\end{aligned}
\tag{A.2}
$$

$$
\begin{aligned}
Ke_{11} &= -\frac{e^{2ikL}k^2\left(\left(\left(1+e^{2ikL}\right)\mathrm{wj}^2-4k^2\right)\cos(\mathrm{wjxe})+\left(4k^2-2\mathrm{wj}^2\right)\cos(\mathrm{wj}(L+\mathrm{xe}))+2ik\mathrm{wj}\left(e^{2ikL}\sin(\mathrm{wjxe})-\sin(\mathrm{wj}(L+\mathrm{xe}))\right)\right)}{\left(-1+e^{2ikL}\right)^2\left(\mathrm{wj}^3-4k^2\mathrm{wj}\right)}\\
Ke_{12} &= -\frac{k^2\left(\mathrm{wj}(\mathrm{wj}\cos(\mathrm{wjxe})-2ik\sin(\mathrm{wjxe}))+e^{2ikL}\left(\left(\mathrm{wj}^2-4k^2\right)\cos(\mathrm{wjxe})+\left(4k^2-2\mathrm{wj}^2\right)\cos(\mathrm{wj}(L+\mathrm{xe}))+2ik\mathrm{wj}\sin(\mathrm{wj}(L+\mathrm{xe}))\right)\right)}{\left(-1+e^{2ikL}\right)^2\left(\mathrm{wj}^3-4k^2\mathrm{wj}\right)}\\
Ke_{21} &= Ke_{12}\\
Ke_{22} &= -\frac{e^{2ikL}k^2\left(2\left(\mathrm{wj}^2-2k^2\right)\cos(\mathrm{wjxe})+\left(4k^2-\left(1+e^{2ikL}\right)\mathrm{wj}^2\right)\cos(\mathrm{wj}(L+\mathrm{xe}))-2ik\mathrm{wj}\left(\sin(\mathrm{wjxe})-e^{2ikL}\sin(\mathrm{wj}(L+\mathrm{xe}))\right)\right)}{\left(-1+e^{2ikL}\right)^2\left(\mathrm{wj}^3-4k^2\mathrm{wj}\right)}
\end{aligned}
\tag{A.3}
$$

$$
\begin{aligned}
Me_{11} &= \frac{e^{2ikL}\left(\left(4k^2+\left(-1+e^{2ikL}\right)\mathrm{wj}^2\right)\cos(\mathrm{wjxe})+2ik\left(2ik\cos(\mathrm{wj}(L+\mathrm{xe}))+e^{2ikL}\mathrm{wj}\sin(\mathrm{wjxe})-\mathrm{wj}\sin(\mathrm{wj}(L+\mathrm{xe}))\right)\right)}{\left(-1+e^{2ikL}\right)^2\left(\mathrm{wj}^3-4k^2\mathrm{wj}\right)}\\
Me_{12} &= \frac{\mathrm{wj}(\mathrm{wj}\cos(\mathrm{wjxe})-2ik\sin(\mathrm{wjxe}))+e^{2ikL}\left(-4\cos(\mathrm{wj}(L+\mathrm{xe}))k^2+2i\mathrm{wj}\sin(\mathrm{wj}(L+\mathrm{xe}))k+\left(4k^2-\mathrm{wj}^2\right)\cos(\mathrm{wjxe})\right)}{\left(-1+e^{2ikL}\right)^2\left(\mathrm{wj}^3-4k^2\mathrm{wj}\right)}\\
Me_{21} &= Me_{12}\\
Me_{22} &= \frac{e^{2ikL}\left(4\cos(\mathrm{wjxe})k^2-2i\mathrm{wj}\left(\sin(\mathrm{wjxe})-e^{2ikL}\sin(\mathrm{wj}(L+\mathrm{xe}))\right)k+\left(-4k^2-e^{2ikL}\mathrm{wj}^2+\mathrm{wj}^2\right)\cos(\mathrm{wj}(L+\mathrm{xe}))\right)}{\left(-1+e^{2ikL}\right)^2\left(\mathrm{wj}^3-4k^2\mathrm{wj}\right)}
\end{aligned}
\tag{A.4}
$$

A.2 Damaged rod matrix elements

A.2.1 Deterministic

$$
\begin{aligned}
K_{0d_{11}} &= EAk\Big\{\Big[4\left(k\left(\Theta\left(k^2L_1\Theta-1\right)+2L\right)+\sin(2kL)\right)+k\Theta\Big(4\left(k^2L_1\Theta-1\right)\cos(2k(L-L_1))\\
&\quad + k(\Theta(\sin(2k(L-2L_1))-\sin(2kL)-2\sin(2kL_1))+8L_1\sin(2k(L-L_1)))+4\cos(2kL)\\
&\quad + 4\cos(2kL_1)\Big)\Big]\Big/\Big[4(k\Theta(\cos(k(L-2L_1))+\cos(kL))+2\sin(kL))^2\Big]\Big\}\\
K_{0d_{12}} &= EAk\left\{\frac{\left(k^2\Theta(L-2L_1)\sin(k(L-2L_1))+\left(k^2L\Theta-2\right)\sin(kL)-2kL\cos(kL)\right)}{(k\Theta(\cos(k(L-2L_1))+\cos(kL))+2\sin(kL))^2}\right\}\\
K_{0d_{21}} &= K_{0d_{12}}\\
K_{0d_{22}} &= EAk\Big\{\Big[4\left(k^3\Theta^2(L-L_1)+2kL+\sin(2kL)-k\Theta\right)+k\Theta Bigl(4\cos(2kL_1)\left(k^2\Theta(L-L_1)-1\right)\\
&\quad - k\Theta(\sin(2k(L-2L_1))+2\sin(2k(L-L_1))+\sin(2kL))+8k(L-L_1)\sin(2kL_1)+4\cos(2k(L-L_1))\\
&\quad + 4\cos(2kL)\Big)\Big]\Big/\Big[4(k\Theta(\cos(k(L-2L_1))+\cos(kL))+2\sin(kL))^2\Big]\Big\}
\end{aligned}
\tag{A.5}
$$

$$
\begin{aligned}
M_{0d_{11}} &= \rho A\Big\{\Big[4k\left(k^2L_1\Theta^2+\Theta+2L\right)-4\sin(2kL)+k\Theta\Big(-4\cos(2kL)+4\left(L_1\Theta k^2+1\right)\cos(2k(L-L_1))\\
&\quad - 4\cos(2kL_1)+8kL_1\sin(2k(L-L_1))+k\Theta(\sin(2kL)-\sin(2k(L-2L_1))+2\sin(2kL_1))\Big)\Big]\Big/\Big[4k\Big(k\Theta\Big(\cos(kL)\\
&\quad + \cos(k(L-2L_1))\Big)+2\sin(kL)\Big)^2\Big]\Big\}\\
M_{0d_{12}} &= \rho A\left\{\frac{(L-2L_1)\Theta\sin(k(L-2L_1))k^2-2L\cos(kL)k+\left(L\Theta k^2+2\right)\sin(kL)}{k(k\Theta(\cos(kL)+\cos(k(L-2L_1)))+2\sin(kL))^2}\right\}\\
M_{0d_{21}} &= M_{0d_{12}}\\
M_{0d_{22}} &= \rho A\Big\{\Big[4k\left(k^2(L-L_1)\Theta^2+\Theta+2L\right)-4\sin(2kL)+k\Theta\Big(-4\cos(2kL)-4\cos(2k(L-L_1))\\
&\quad + 4\left((L-L_1)\Theta k^2+1\right)\cos(2kL_1)+k\Theta(\sin(2kL)+\sin(2k(L-2L_1))+2\sin(2k(L-L_1)))\\
&\quad + 8k(L-L_1)\sin(2kL_1)\Big)\Big]\Big/\Big[4k(k\Theta(\cos(kL)+\cos(k(L-2L_1)))+2\sin(kL))^2\Big]\Big\}
\end{aligned}
\tag{A.6}
$$

A.2.2 Stochastic

$$SkLo_{11} = -\frac{k^2\left(-2ik\cos(\mathrm{wjxe})+2e^{-2ikL_1}ik\cos(\mathrm{wj}(L_1+\mathrm{xe}))+\mathrm{wj}\sin(\mathrm{wjxe})-e^{-2ikL_1}\mathrm{wj}\sin(\mathrm{wj}(L_1+\mathrm{xe}))\right)}{4k^2-\mathrm{wj}^2}$$

$$SkLo_{12} = \frac{e^{-ikL_1}k^2(\sin(\mathrm{wj}(L_1+\mathrm{xe}))-\sin(\mathrm{wjxe}))}{\mathrm{wj}}$$

$$SkLo_{21} = SkLo_{12}$$

$$SkLo_{22} = -\frac{k^2\left(2e^{-2ikL_1}ik\cos(\mathrm{wjxe})-2ik\cos(\mathrm{wj}(L_1+\mathrm{xe}))+e^{-2ikL_1}\mathrm{wj}\sin(\mathrm{wjxe})-\mathrm{wj}\sin(\mathrm{wj}(L_1+\mathrm{xe}))\right)}{4k^2-\mathrm{wj}^2}$$

$$SmLo_{11} = \frac{-2ik\cos(\mathrm{wjxe})+\mathrm{wj}\sin(\mathrm{wjxe})+e^{-2ikL_1}(2ik\cos(\mathrm{wj}(L_1+\mathrm{xe}))-\mathrm{wj}\sin(\mathrm{wj}(L_1+\mathrm{xe})))}{4k^2-\mathrm{wj}^2}$$

$$SmLo_{12} = \frac{e^{-ikL_1}(\sin(\mathrm{wj}(L_1+\mathrm{xe}))-\sin(\mathrm{wjxe}))}{\mathrm{wj}}$$

$$SmLo_{21} = SmLo_{12}$$

$$SmLo_{22} = \frac{-2ik\cos(\mathrm{wj}(L_1+\mathrm{xe}))+e^{-2ikL_1}(2ik\cos(\mathrm{wjxe})+\mathrm{wj}\sin(\mathrm{wjxe}))-\mathrm{wj}\sin(\mathrm{wj}(L_1+\mathrm{xe}))}{4k^2-\mathrm{wj}^2}$$

$$SkRo_{11} = -\frac{k^2\left(e^{-2ikL_1}(\mathrm{wj}\sin(\mathrm{wjxe})-2ik\cos(\mathrm{wjxe}))+e^{-2ikL}(2ik\cos(\mathrm{wj}(L-L_1+\mathrm{xe}))-\mathrm{wj}\sin(\mathrm{wj}(L-L_1+\mathrm{xe})))\right)}{4k^2-\mathrm{wj}^2}$$

$$SkRo_{12} = \frac{e^{-ikL}k^2(\sin(\mathrm{wj}(L-L_1+\mathrm{xe}))-\sin(\mathrm{wjxe}))}{\mathrm{wj}}$$

$$SkRo_{21} = SkRo_{12}$$

$$SkRo_{22} = \frac{k^2\left(2ik\cos(\mathrm{wj}(L-L_1+\mathrm{xe}))-ie^{2ik(L_1-L)}(2k\cos(\mathrm{wjxe})-i\mathrm{wj}\sin(\mathrm{wjxe}))+\mathrm{wj}\sin(\mathrm{wj}(L-L_1+\mathrm{xe}))\right)}{4k^2-\mathrm{wj}^2}$$

$$SmRo_{11} = \frac{e^{-2ikL_1}(\mathrm{wj}\sin(\mathrm{wjxe})-2ik\cos(\mathrm{wjxe}))+e^{-2ikL}(2ik\cos(\mathrm{wj}(L-L_1+\mathrm{xe}))-\mathrm{wj}\sin(\mathrm{wj}(L-L_1+\mathrm{xe})))}{4k^2-\mathrm{wj}^2}$$

$$SmRo_{12} = \frac{e^{-ikL}(\sin(\mathrm{wj}(L-L_1+\mathrm{xe}))-\sin(\mathrm{wjxe}))}{\mathrm{wj}}$$

$$SmRo_{21} = SmRo_{12}$$

$$SmRo_{22} = \frac{-2ik\cos(\mathrm{wj}(L-L_1+\mathrm{xe}))+e^{2ik(L_1-L)}(2ik\cos(\mathrm{wjxe})+\mathrm{wj}\sin(\mathrm{wjxe}))-\mathrm{wj}\sin(\mathrm{wj}(L-L_1+\mathrm{xe}))}{4k^2-\mathrm{wj}^2}$$

$$SkLe_{11} = -\frac{k^2\left(-\mathrm{wj}\cos(\mathrm{wjxe})+e^{-2ikL_1}\mathrm{wj}\cos(\mathrm{wj}(L_1+\mathrm{xe}))-2ik\sin(\mathrm{wjxe})+2e^{-2ikL_1}ik\sin(\mathrm{wj}(L_1+\mathrm{xe}))\right)}{4k^2-\mathrm{wj}^2}$$

$$SkLe_{12} = \frac{e^{-ikL_1}k^2(\cos(\mathrm{wjxe})-\cos(\mathrm{wj}(L_1+\mathrm{xe})))}{\mathrm{wj}}$$

$$SkLe_{21} = SkLe_{12}$$

$$SkLe_{22} = -\frac{k^2\left(-e^{-2ikL_1}\mathrm{wj}\cos(\mathrm{wjxe})+\mathrm{wj}\cos(\mathrm{wj}(L_1+\mathrm{xe}))+2ik\left(e^{-2ikL_1}\sin(\mathrm{wjxe})-\sin(\mathrm{wj}(L_1+\mathrm{xe}))\right)\right)}{4k^2-\mathrm{wj}^2}$$

$$SmLe_{11} = \frac{-\text{wj}\cos(\text{wjxe}) - 2ik\sin(\text{wjxe}) + e^{-2ikL_1}(\text{wj}\cos(\text{wj}(L_1+\text{xe})) + 2ik\sin(\text{wj}(L_1+\text{xe})))}{4k^2-\text{wj}^2}$$

$$SmLe_{12} = +\frac{e^{-ikL_1}(\cos(\text{wjxe}) - \cos(\text{wj}(L_1+\text{xe})))}{\text{wj}}$$

$$SMe^1_{21} = SMe^1_{12}$$

$$SmLe_{22} = \frac{\text{wj}\cos(\text{wj}(L_1+\text{xe})) + e^{-2ikL_1}(2ik\sin(\text{wjxe}) - \text{wj}\cos(\text{wjxe})) - 2ik\sin(\text{wj}(L_1+\text{xe}))}{4k^2-\text{wj}^2}$$

$$SkRe_{11} = -\frac{k^2\left(e^{-2ikL}(\text{wj}\cos(\text{wj}(L-L_1+\text{xe})) + 2ik\sin(\text{wj}(L-L_1+\text{xe}))) - e^{-2ikL_1}(\text{wj}\cos(\text{wjxe}) + 2ik\sin(\text{wjxe}))\right)}{4k^2-\text{wj}^2}$$

$$SkRe_{12} = \frac{e^{-ikL}k^2(\cos(\text{wjxe}) - \cos(\text{wj}(L-L_1+\text{xe})))}{\text{wj}}$$

$$SkRe_{21} = SkRe_{12}$$

$$SkRe_{22} = \frac{k^2\left(-\text{wj}\cos(\text{wj}(L-L_1+\text{xe})) + e^{2ik(L_1-L)}(\text{wj}\cos(\text{wjxe}) - 2ik\sin(\text{wjxe})) + 2ik\sin(\text{wj}(L-L_1+\text{xe}))\right)}{4k^2-\text{wj}^2}$$

$$SmRe_{11} = \frac{e^{-2ikL}(\text{wj}\cos(\text{wj}(L-L_1+\text{xe})) + 2ik\sin(\text{wj}(L-L_1+\text{xe}))) - e^{-2ikL_1}(\text{wj}\cos(\text{wjxe}) + 2ik\sin(\text{wjxe}))}{4k^2-\text{wj}^2}$$

$$SmRe_{12} = \frac{e^{-ikL}(\cos(\text{wjxe}) - \cos(\text{wj}(L-L_1+\text{xe})))}{\text{wj}}$$

$$SmRe_{21} = SmRe_{12}$$

$$SmRe_{22} = \frac{\text{wj}\cos(\text{wj}(L-L_1+\text{xe})) + e^{2ik(L_1-L)}(2ik\sin(\text{wjxe}) - \text{wj}\cos(\text{wjxe})) - 2ik\sin(\text{wj}(L-L_1+\text{xe}))}{4k^2-\text{wj}^2}$$

A.3 Undamaged beam matrix elements

A.3.1 Deterministic

$$K_{11} = -\frac{1}{2}i\left(1 - e^{-2ikL}\right)k^3;$$

$$K_{12} = \left(-\frac{1}{2} + \frac{i}{2}\right)e^{(-1-i)kL}\left(-1 + e^{(1+i)kL}\right)k^3;$$

$$K_{13} = e^{-ikL}k^4L;$$

$$K_{14} = \left(\frac{1}{2} + \frac{i}{2}\right)e^{(-1-i)kL}\left(e^{ikL} - e^{kL}\right)k^3;$$

$$K_{22} = \frac{1}{2}\left(1 - e^{-2kL}\right)k^3;$$

$$K_{23} = \left(\frac{1}{2} + \frac{i}{2}\right)e^{(-1-i)kL}\left(e^{ikL} - e^{kL}\right)k^3;$$

$$K_{24} = e^{-kL}k^4L;$$

$$K_{33} = -\frac{1}{2}i\left(1 - e^{-2ikL}\right)k^3; \qquad K_{34} = \left(-\frac{1}{2} + \frac{i}{2}\right)e^{(-1-i)kL}\left(-1 + e^{(1+i)kL}\right)k^3;$$

$$K_{44} = \frac{1}{2}\left(1 - e^{-2kL}\right)k^3$$

$$M_{11} = -\frac{i\left(1 - e^{-2ikL}\right)}{2k};$$

$$M_{12} = \frac{(1-i) - (1-i)e^{(-1-i)kL}}{2k};$$

$$M_{13} = e^{-ikL}L; \qquad M_{14} = -\frac{\left(\frac{1}{2} + \frac{i}{2}\right)\left(e^{-kL} - e^{-ikL}\right)}{k};$$

$$M_{22} = -\frac{-1 + e^{-2kL}}{2k};$$

$$M_{23} = -\frac{\left(\frac{1}{2} + \frac{i}{2}\right)\left(e^{-kL} - e^{-ikL}\right)}{k}; \qquad M_{24} = e^{-kL}L;$$

$$M_{33} = -\frac{i\left(1 - e^{-2ikL}\right)}{2k}; \qquad M_{34} = \frac{(1-i) - (1-i)e^{(-1-i)kL}}{2k};$$

$$M_{44} = -\frac{-1 + e^{-2kL}}{2k}$$

A.3.2 Stochastic

$$Ko_{11} = \frac{k^4\left(-2ik\cos(\mathrm{wjxe})+2e^{-2ikL}ik\cos(\mathrm{wj}(L+\mathrm{xe}))+\mathrm{wj}\sin(\mathrm{wjxe})-e^{-2ikL}\mathrm{wj}\sin(\mathrm{wj}(L+\mathrm{xe}))\right)}{4k^2-\mathrm{wj}^2}$$

$$Ko_{12} = -\frac{k^4\left((1+i)k\cos(\mathrm{wjxe})-\mathrm{wj}\sin(\mathrm{wjxe})+e^{(-1-i)kL}((-1-i)k\cos(\mathrm{wj}(L+\mathrm{xe}))+\mathrm{wj}\sin(\mathrm{wj}(L+\mathrm{xe})))\right)}{2ik^2+\mathrm{wj}^2}$$

$$Ko_{13} = \frac{e^{-ikL}k^4(\sin(\mathrm{wj}(L+\mathrm{xe}))-\sin(\mathrm{wjxe}))}{\mathrm{wj}}$$

$$Ko_{14} = -\frac{k^4\left(e^{-ikL}((1+i)k\cos(\mathrm{wj}(L+\mathrm{xe}))+i\mathrm{wj}\sin(\mathrm{wj}(L+\mathrm{xe})))-e^{-kL}((1+i)k\cos(\mathrm{wjxe})+i\mathrm{wj}\sin(\mathrm{wjxe}))\right)}{2k^2+i\mathrm{wj}^2}$$

$$Ko_{22} = \frac{k^4\left(2k\cos(\mathrm{wjxe})-2e^{-2kL}k\cos(\mathrm{wj}(L+\mathrm{xe}))-\mathrm{wj}\sin(\mathrm{wjxe})+e^{-2kL}\mathrm{wj}\sin(\mathrm{wj}(L+\mathrm{xe}))\right)}{4k^2+\mathrm{wj}^2}$$

$$Ko_{23} = -\frac{k^4\left(e^{-ikL}((-1+i)k\cos(\mathrm{wjxe})+\mathrm{wj}\sin(\mathrm{wjxe}))+e^{-kL}((1-i)k\cos(\mathrm{wj}(L+\mathrm{xe}))-\mathrm{wj}\sin(\mathrm{wj}(L+\mathrm{xe})))\right)}{2ik^2-\mathrm{wj}^2}$$

$$Ko_{24} = \frac{e^{-kL}k^4(\sin(\mathrm{wj}(L+\mathrm{xe}))-\sin(\mathrm{wjxe}))}{\mathrm{wj}}$$

$$Ko_{33} = \frac{k^4\left(-2ik\cos(\mathrm{wj}(L+\mathrm{xe}))+e^{-2ikL}(2ik\cos(\mathrm{wjxe})+\mathrm{wj}\sin(\mathrm{wjxe}))-\mathrm{wj}\sin(\mathrm{wj}(L+\mathrm{xe}))\right)}{4k^2-\mathrm{wj}^2}$$

$$Ko_{34} = -\frac{k^4\left((1+i)k\cos(\mathrm{wj}(L+\mathrm{xe}))-e^{(-1-i)kL}((1+i)k\cos(\mathrm{wjxe})+\mathrm{wj}\sin(\mathrm{wjxe}))+\mathrm{wj}\sin(\mathrm{wj}(L+\mathrm{xe}))\right)}{2ik^2+\mathrm{wj}^2}$$

$$Ko_{44} = \frac{k^4\left(2k\cos(\mathrm{wj}(L+\mathrm{xe}))-e^{-2kL}(2k\cos(\mathrm{wjxe})+\mathrm{wj}\sin(\mathrm{wjxe}))+\mathrm{wj}\sin(\mathrm{wj}(L+\mathrm{xe}))\right)}{4k^2+\mathrm{wj}^2}$$

$$Mo_{11} = \frac{-2ik\cos(\mathrm{wjxe})+2e^{-2ikL}ik\cos(\mathrm{wj}(L+\mathrm{xe}))+\mathrm{wj}\sin(\mathrm{wjxe})-e^{-2ikL}\mathrm{wj}\sin(\mathrm{wj}(L+\mathrm{xe}))}{4k^2-\mathrm{wj}^2}$$

$$Mo_{12} = \frac{(1+i)k\cos(\mathrm{wjxe})-\mathrm{wj}\sin(\mathrm{wjxe})+e^{(-1-i)kL}((-1-i)k\cos(\mathrm{wj}(L+\mathrm{xe}))+\mathrm{wj}\sin(\mathrm{wj}(L+\mathrm{xe})))}{2ik^2+\mathrm{wj}^2}$$

$$Mo_{13} = \frac{e^{-ikL}(\sin(\mathrm{wj}(L+\mathrm{xe}))-\sin(\mathrm{wjxe}))}{\mathrm{wj}}$$

$$Mo_{14} = \frac{e^{-ikL}((1+i)k\cos(\mathrm{wj}(L+\mathrm{xe}))+i\mathrm{wj}\sin(\mathrm{wj}(L+\mathrm{xe})))-e^{-kL}((1+i)k\cos(\mathrm{wjxe})+i\mathrm{wj}\sin(\mathrm{wjxe}))}{2k^2+i\mathrm{wj}^2}$$

$$Mo_{22} = \frac{2k\cos(\mathrm{wjxe})-2e^{-2kL}k\cos(\mathrm{wj}(L+\mathrm{xe}))-\mathrm{wj}\sin(\mathrm{wjxe})+e^{-2kL}\mathrm{wj}\sin(\mathrm{wj}(L+\mathrm{xe}))}{4k^2+\mathrm{wj}^2}$$

$$Mo_{23} = \frac{e^{-ikL}((-1+i)k\cos(\mathrm{wjxe})+\mathrm{wj}\sin(\mathrm{wjxe}))+e^{-kL}((1-i)k\cos(\mathrm{wj}(L+\mathrm{xe}))-\mathrm{wj}\sin(\mathrm{wj}(L+\mathrm{xe})))}{2ik^2-\mathrm{wj}^2}$$

$$Mo_{24} = \frac{e^{-kL}(\sin(\mathrm{wj}(L+\mathrm{xe}))-\sin(\mathrm{wjxe}))}{\mathrm{wj}}$$

$$Mo_{33} = \frac{-2ik\cos(\mathrm{wj}(L+\mathrm{xe}))+e^{-2ikL}(2ik\cos(\mathrm{wjxe})+\mathrm{wj}\sin(\mathrm{wjxe}))-\mathrm{wj}\sin(\mathrm{wj}(L+\mathrm{xe}))}{4k^2-\mathrm{wj}^2}$$

$$Mo_{34} = \frac{(1+i)k\cos(\mathrm{wj}(L+\mathrm{xe}))-e^{(-1-i)kL}((1+i)k\cos(\mathrm{wjxe})+\mathrm{wj}\sin(\mathrm{wjxe}))+\mathrm{wj}\sin(\mathrm{wj}(L+\mathrm{xe}))}{2ik^2+\mathrm{wj}^2}$$

$$Mo_{44} = \frac{-2e^{-2kL}k\cos(\mathrm{wjxe})+2k\cos(\mathrm{wj}(L+\mathrm{xe}))+\mathrm{wj}\left(\sin(\mathrm{wj}(L+\mathrm{xe}))-e^{-2kL}\sin(\mathrm{wjxe})\right)}{4k^2+\mathrm{wj}^2}$$

and for even j are

$$Ke_{11} = \frac{k^4\left(-\text{wj}\cos(\text{wjxe})+e^{-2ikL}\text{wj}\cos(\text{wj}(L+\text{xe}))-2ik\sin(\text{wjxe})+2e^{-2ikL}ik\sin(\text{wj}(L+\text{xe}))\right)}{4k^2-\text{wj}^2}$$

$$Ke_{12} = -\frac{k^4\left(\text{wj}\cos(\text{wjxe})+(1+i)k\sin(\text{wjxe})-e^{(-1-i)kL}(\text{wj}\cos(\text{wj}(L+\text{xe}))+(1+i)k\sin(\text{wj}(L+\text{xe})))\right)}{2ik^2+\text{wj}^2}$$

$$Ke_{13} = \frac{e^{-ikL}k^4(\cos(\text{wjxe})-\cos(\text{wj}(L+\text{xe})))}{\text{wj}}$$

$$Ke_{14} = -\frac{k^4\left(e^{-kL}((1-i)k\sin(\text{wjxe})-\text{wj}\cos(\text{wjxe}))+e^{-ikL}(\text{wj}\cos(\text{wj}(L+\text{xe}))-(1-i)k\sin(\text{wj}(L+\text{xe})))\right)}{2ik^2-\text{wj}^2}$$

$$Ke_{22} = \frac{k^4\left(\text{wj}\cos(\text{wjxe})-e^{-2kL}\text{wj}\cos(\text{wj}(L+\text{xe}))+2k\sin(\text{wjxe})-2e^{-2kL}k\sin(\text{wj}(L+\text{xe}))\right)}{4k^2+\text{wj}^2}$$

$$Ke_{23} = -\frac{k^4\left(e^{-ikL}(-\text{wj}\cos(\text{wjxe})-(1-i)k\sin(\text{wjxe}))+e^{-kL}(\text{wj}\cos(\text{wj}(L+\text{xe}))+(1-i)k\sin(\text{wj}(L+\text{xe})))\right)}{2ik^2-\text{wj}^2}$$

$$Ke_{24} = \frac{e^{-kL}k^4(\cos(\text{wjxe})-\cos(\text{wj}(L+\text{xe})))}{\text{wj}}$$

$$Ke_{33} = \frac{k^4\left(-e^{-2ikL}\text{wj}\cos(\text{wjxe})+\text{wj}\cos(\text{wj}(L+\text{xe}))+2ik\left(e^{-2ikL}\sin(\text{wjxe})-\sin(\text{wj}(L+\text{xe}))\right)\right)}{4k^2-\text{wj}^2}$$

$$Ke_{34} = -\frac{k^4\left(-\text{wj}\cos(\text{wj}(L+\text{xe}))+e^{(-1-i)kL}(\text{wj}\cos(\text{wjxe})-(1+i)k\sin(\text{wjxe}))+(1+i)k\sin(\text{wj}(L+\text{xe}))\right)}{2ik^2+\text{wj}^2}$$

$$Ke_{44} = \frac{k^4\left(e^{-2kL}\text{wj}\cos(\text{wjxe})-\text{wj}\cos(\text{wj}(L+\text{xe}))+2k\left(\sin(\text{wj}(L+\text{xe}))-e^{-2kL}\sin(\text{wjxe})\right)\right)}{4k^2+\text{wj}^2}$$

$$Me_{11} = \frac{-\text{wj}\cos(\text{wjxe})-2ik\sin(\text{wjxe})+e^{-2ikL}(\text{wj}\cos(\text{wj}(L+\text{xe}))+2ik\sin(\text{wj}(L+\text{xe})))}{4k^2-\text{wj}^2}$$

$$Me_{12} = \frac{\text{wj}\cos(\text{wjxe})+(1+i)k\sin(\text{wjxe})-e^{(-1-i)kL}(\text{wj}\cos(\text{wj}(L+\text{xe}))+(1+i)k\sin(\text{wj}(L+\text{xe})))}{2ik^2+\text{wj}^2}$$

$$Me_{13} = \frac{e^{-ikL}(\cos(\text{wjxe})-\cos(\text{wj}(L+\text{xe})))}{\text{wj}}$$

$$Me_{14} = \frac{e^{-kL}((1-i)k\sin(\text{wjxe})-\text{wj}\cos(\text{wjxe}))+e^{-ikL}(\text{wj}\cos(\text{wj}(L+\text{xe}))-(1-i)k\sin(\text{wj}(L+\text{xe})))}{2ik^2-\text{wj}^2}$$

$$Me_{22} = \frac{\text{wj}\cos(\text{wjxe})-e^{-2kL}\text{wj}\cos(\text{wj}(L+\text{xe}))+2k\sin(\text{wjxe})-2e^{-2kL}k\sin(\text{wj}(L+\text{xe}))}{4k^2+\text{wj}^2}$$

$$Me_{23} = \frac{e^{-ikL}(-\text{wj}\cos(\text{wjxe})-(1-i)k\sin(\text{wjxe}))+e^{-kL}(\text{wj}\cos(\text{wj}(L+\text{xe}))+(1-i)k\sin(\text{wj}(L+\text{xe})))}{2ik^2-\text{wj}^2}$$

$$Me_{24} = \frac{e^{-kL}(\cos(\text{wjxe})-\cos(\text{wj}(L+\text{xe})))}{\text{wj}}$$

$$Me_{33} = \frac{\text{wj}\cos(\text{wj}(L+\text{xe}))+e^{-2ikL}(2ik\sin(\text{wjxe})-\text{wj}\cos(\text{wjxe}))-2ik\sin(\text{wj}(L+\text{xe}))}{4k^2-\text{wj}^2}$$

$$Me_{34} = \frac{-\text{wj}\cos(\text{wj}(L+\text{xe}))+e^{(-1-i)kL}(\text{wj}\cos(\text{wjxe})-(1+i)k\sin(\text{wjxe}))+(1+i)k\sin(\text{wj}(L+\text{xe}))}{2ik^2+\text{wj}^2}$$

$$Me_{44} = \frac{e^{-2kL}\text{wj}\cos(\text{wjxe})-\text{wj}\cos(\text{wj}(L+\text{xe}))+2k\left(\sin(\text{wj}(L+\text{xe}))-e^{-2kL}\sin(\text{wjxe})\right)}{4k^2+\text{wj}^2}$$

A.4 Damaged beam matrix elements

A.4.1 Deterministic

$$\mathbf{Sk}_{0L} = \begin{bmatrix} Sk_{0L_{11}} & Sk_{0L_{12}} & Sk_{0L_{13}} & Sk_{0L_{14}} \\ 0 & Sk_{0L_{22}} & Sk_{0L_{23}} & Sk_{0L_{24}} \\ 0 & 0 & Sk_{0L_{33}} & Sk_{0L_{34}} \\ sym & 0 & 0 & Sk_{0L_{44}} \end{bmatrix}$$

$$Sk_{0L_{11}} = -\frac{1}{2}i\left(1 - e^{-2ikL_1}\right)k^3; \qquad Sk_{0L_{12}} = \left(-\frac{1}{2} + \frac{i}{2}\right)e^{(-1-i)kL_1}\left(-1 + e^{(1+i)kL_1}\right)k^3$$
$$Sk_{0L_{13}} = e^{-ikL_1}k^4L_1; \qquad Sk_{0L_{14}} = \left(\frac{1}{2} + \frac{i}{2}\right)e^{(-1-i)kL_1}\left(e^{ikL_1} - e^{kL_1}\right)k^3$$
$$Sk_{0L_{22}} = \left(-\frac{1}{2} + \frac{i}{2}\right)e^{(-1-i)kL_1}\left(-1 + e^{(1+i)kL_1}\right)k^3; \qquad Sk_{0L_{23}} = e^{-ikL_1}k^4L_1$$
$$Sk_{0L_{24}} = \left(\frac{1}{2} + \frac{i}{2}\right)e^{(-1-i)kL_1}\left(e^{ikL_1} - e^{kL_1}\right)k^3; \qquad Sk_{0L_{33}} = -\frac{1}{2}i\left(1 - e^{-2ikL_1}\right)k^3$$
$$Sk_{0L_{34}} = \left(-\frac{1}{2} + \frac{i}{2}\right)e^{(-1-i)kL_1}\left(-1 + e^{(1+i)kL_1}\right)k^3; \qquad Sk_{0L_{44}} = \frac{1}{2}\left(1 - e^{-2kL_1}\right)k^3$$

$$\mathbf{Sk}_{0R} = \begin{bmatrix} Sk_{0R_{11}} & Sk_{0R_{12}} & Sk_{0R_{13}} & Sk_{0R_{14}} \\ 0 & Sk_{0R_{22}} & Sk_{0R_{23}} & Sk_{0R_{24}} \\ 0 & 0 & Sk_{0R_{33}} & Sk_{0R_{34}} \\ sym & 0 & 0 & Sk_{0R_{44}} \end{bmatrix}$$

$$Sk_{0R_{11}} = \frac{1}{2}i\left(e^{-2ikL} - e^{-2ikL_1}\right)k^3; \qquad Sk_{0R_{12}} = \left(-\frac{1}{2} + \frac{i}{2}\right)e^{(-1-i)k(L+L_1)}\left(e^{(1+i)kL} - e^{(1+i)kL_1}\right)k^3$$
$$Sk_{0R_{13}} = e^{-ikL}k^4(L - L_1); \qquad Sk_{0R_{14}} = \left(-\frac{1}{2} - \frac{i}{2}\right)\left(e^{-ikL} - e^{-k(L-(1-i)L_1)}\right)k^3$$
$$Sk_{0R_{22}} = \frac{1}{2}\left(-e^{-2kL} + e^{-2kL_1}\right)k^3; \qquad Sk_{0R_{23}} = \left(\frac{1}{2} + \frac{i}{2}\right)\left(e^{-kL} - e^{-ikL-(1-i)kL_1}\right)k^3$$
$$Sk_{0L_{24}} = e^{-kL}k^4(L - L_1); \qquad Sk_{0R_{33}} = \frac{1}{2}i\left(-1 + e^{2ik(L_1-L)}\right)k^3$$
$$Sk_{0R_{34}} = \left(\frac{1}{2} - \frac{i}{2}\right)\left(-1 + e^{(1+i)k(L_1-L)}\right)k^3; \qquad Sk_{0R_{44}} = -\frac{1}{2}\left(-1 + e^{2k(L_1-L)}\right)k^3$$

$$\mathbf{Sm}_{0L} = \begin{bmatrix} Sm_{0L_{11}} & Sm_{0L_{12}} & Sm_{0L_{13}} & Sm_{0L_{14}} \\ 0 & Sm_{0L_{22}} & Sm_{0L_{23}} & Sm_{0L_{24}} \\ 0 & 0 & Sm_{0L_{33}} & Sm_{0L_{34}} \\ sym & 0 & 0 & Sm_{0L_{44}} \end{bmatrix}$$

$$Sm_{0L_{11}} = -\frac{i\left(1-e^{-2ikL_1}\right)}{2k}; \qquad Sm_{0L_{12}} = \frac{(1-i)-(1-i)e^{(-1-i)kL_1}}{2k}$$
$$Sm_{0L_{13}} = e^{-ikL_1}L_1; \qquad Sm_{0L_{14}} = -\frac{\left(\frac{1}{2}+\frac{i}{2}\right)\left(e^{-kL_1}-e^{-ikL_1}\right)}{k}$$
$$Sm_{0L_{22}} = -\frac{-1+e^{-2kL_1}}{2k}; \qquad Sm_{0L_{23}} = -\frac{\left(\frac{1}{2}+\frac{i}{2}\right)\left(e^{-kL_1}-e^{-ikL_1}\right)}{k}$$
$$Sm_{0L_{24}} = e^{-kL_1}L_1; \qquad Sm_{0L_{33}} = -\frac{i\left(1-e^{-2ikL_1}\right)}{2k}$$
$$Sm_{0L_{34}} = \frac{(1-i)-(1-i)e^{(-1-i)kL_1}}{2k}; \qquad Sm_{0L_{44}} = -\frac{-1+e^{-2kL_1}}{2k}$$

$$\mathbf{Sm}_{0R} = \begin{bmatrix} Sm_{0R_{11}} & Sm_{0R_{12}} & Sm_{0R_{13}} & Sm_{0R_{14}} \\ 0 & Sm_{0R_{22}} & Sm_{0R_{23}} & Sm_{0R_{24}} \\ 0 & 0 & Sm_{0R_{33}} & Sm_{0R_{34}} \\ sym & 0 & 0 & Sm_{0R_{44}} \end{bmatrix}$$

$$Sm_{0R_{11}} = \frac{i\left(e^{-2ikL}-e^{-2ikL_1}\right)}{2k}; \qquad Sm_{0R_{12}} = -\frac{\left(\frac{1}{2}-\frac{i}{2}\right)\left(e^{(-1-i)kL}-e^{(-1-i)kL_1}\right)}{k}$$
$$Sm_{0R_{13}} = e^{-ikL}(L-L_1); \qquad Sm_{0R_{14}} = \frac{\left(\frac{1}{2}+\frac{i}{2}\right)\left(e^{-ikL}-e^{-k(L-(1-i)L_1)}\right)}{k}$$
$$Sm_{0R_{22}} = \frac{-e^{-2kL}+e^{-2kL_1}}{2k}; \qquad Sm_{0R_{23}} = -\frac{\left(\frac{1}{2}+\frac{i}{2}\right)\left(e^{-kL}-e^{-ikL-(1-i)kL_1}\right)}{k}$$
$$Sm_{0L_{24}} = e^{-kL}(L-L_1); \qquad Sm_{0R_{33}} = \frac{i\left(-1+e^{2ik(L_1-L)}\right)}{2k}$$
$$Sm_{0R_{34}} = -\frac{\left(\frac{1}{2}-\frac{i}{2}\right)\left(-1+e^{(1+i)k(L_1-L)}\right)}{k}; \qquad Sm_{0R_{44}} = -\frac{-1+e^{2k(L_1-L)}}{2k}$$

A.4.2 Stochastic

$$SkLo_{11} = \frac{k^4\left(-2ik\cos(\mathrm{wjxe})+\mathrm{wj}\sin(\mathrm{wjxe})+e^{-2ikL_1}(2ik\cos(\mathrm{wj}(L_1+\mathrm{xe}))-\mathrm{wj}\sin(\mathrm{wj}(L_1+\mathrm{xe})))\right)}{4k^2-\mathrm{wj}^2}$$

$$SkLo_{12} = -\frac{k^4\left((1+i)k\cos(\mathrm{wjxe})-\mathrm{wj}\sin(\mathrm{wjxe})+e^{(-1-i)kL_1}((-1-i)k\cos(\mathrm{wj}(L_1+\mathrm{xe}))+\mathrm{wj}\sin(\mathrm{wj}(L_1+\mathrm{xe})))\right)}{2ik^2+\mathrm{wj}^2}$$

$$SkLo_{13} = \frac{e^{-ikL_1}k^4(\sin(\mathrm{wj}(L_1+\mathrm{xe}))-\sin(\mathrm{wjxe}))}{\mathrm{wj}}$$

$$SkLo_{14} - \frac{k^4\left(e^{-ikL_1}((1+i)k\cos(\mathrm{wj}(L_1+\mathrm{xe}))+i\mathrm{wj}\sin(\mathrm{wj}(L_1+\mathrm{xe})))-e^{-kL_1}((1+i)k\cos(\mathrm{wjxe})+i\mathrm{wj}\sin(\mathrm{wjxe}))\right)}{2k^2+i\mathrm{wj}^2}$$

$$SkLo_{22} = \frac{k^4\left(2k\cos(\mathrm{wjxe})-2e^{-2kL_1}k\cos(\mathrm{wj}(L_1+\mathrm{xe}))-\mathrm{wj}\sin(\mathrm{wjxe})+e^{-2kL_1}\mathrm{wj}\sin(\mathrm{wj}(L_1+\mathrm{xe}))\right)}{4k^2+\mathrm{wj}^2}$$

$$SkLo_{23} = -\frac{k^4\left(e^{-ikL_1}((-1+i)k\cos(\mathrm{wjxe})+\mathrm{wj}\sin(\mathrm{wjxe}))+e^{-kL_1}((1-i)k\cos(\mathrm{wj}(L_1+\mathrm{xe}))-\mathrm{wj}\sin(\mathrm{wj}(L_1+\mathrm{xe})))\right)}{2ik^2-\mathrm{wj}^2}$$

$$SkLo_{24} = \frac{e^{-kL_1}k^4(\sin(\mathrm{wj}(L_1+\mathrm{xe}))-\sin(\mathrm{wjxe}))}{\mathrm{wj}}$$

$$SkLo_{33} = \frac{k^4\left(-2ik\cos(\mathrm{wj}(L_1+\mathrm{xe}))+e^{-2ikL_1}(2ik\cos(\mathrm{wjxe})+\mathrm{wj}\sin(\mathrm{wjxe}))-\mathrm{wj}\sin(\mathrm{wj}(L_1+\mathrm{xe}))\right)}{4k^2-\mathrm{wj}^2}$$

$$SkLo_{34} = -\frac{k^4\left((1+i)k\cos(\mathrm{wj}(L_1+\mathrm{xe}))-e^{(-1-i)kL_1}((1+i)k\cos(\mathrm{wjxe})+\mathrm{wj}\sin(\mathrm{wjxe}))+\mathrm{wj}\sin(\mathrm{wj}(L_1+\mathrm{xe}))\right)}{2ik^2+\mathrm{wj}^2}$$

$$SkLo_{44} = \frac{k^4\left(-2e^{-2kL_1}k\cos(\mathrm{wjxe})+2k\cos(\mathrm{wj}(L_1+\mathrm{xe}))+\mathrm{wj}\left(\sin(\mathrm{wj}(L_1+\mathrm{xe}))-e^{-2kL_1}\sin(\mathrm{wjxe})\right)\right)}{4k^2+\mathrm{wj}^2}$$

$$SkRo_{11} = \frac{k^4\left(e^{-2ikL_1}(\mathrm{wj}\sin(\mathrm{wjxe})-2ik\cos(\mathrm{wjxe}))+e^{-2ikL}(2ik\cos(\mathrm{wj}(L-L_1+\mathrm{xe}))-\mathrm{wj}\sin(\mathrm{wj}(L-L_1+\mathrm{xe})))\right)}{4k^2-\mathrm{wj}^2}$$

$$SkRo_{12} = -\frac{k^4\left(e^{(-1-i)kL_1}((1+i)k\cos(\mathrm{wjxe})-\mathrm{wj}\sin(\mathrm{wjxe}))+e^{(-1-i)kL}((-1-i)k\cos(\mathrm{wj}(L-L_1+\mathrm{xe}))+\mathrm{wj}\sin(\mathrm{wj}(L-L_1+\mathrm{xe})))\right)}{2ik^2+\mathrm{wj}^2}$$

$$SkRo_{13} = \frac{e^{-ikL}k^4(\sin(\mathrm{wj}(L-L_1+\mathrm{xe}))-\sin(\mathrm{wjxe}))}{\mathrm{wj}}$$

$$SkRo_{14} = -\frac{k^4\left(e^{-ikL}((1+i)k\cos(\mathrm{wj}(L-L_1+\mathrm{xe}))+i\mathrm{wj}\sin(\mathrm{wj}(L-L_1+\mathrm{xe})))-e^{-k(L-(1-i)L_1)}((1+i)k\cos(\mathrm{wjxe})+i\mathrm{wj}\sin(\mathrm{wjxe}))\right)}{2k^2+i\mathrm{wj}^2}$$

$$SkRo_{22} = \frac{k^4\left(e^{-2kL_1}(2k\cos(\mathrm{wjxe})-\mathrm{wj}\sin(\mathrm{wjxe}))+e^{-2kL}(\mathrm{wj}\sin(\mathrm{wj}(L-L_1+\mathrm{xe}))-2k\cos(\mathrm{wj}(L-L_1+\mathrm{xe})))\right)}{4k^2+\mathrm{wj}^2}$$

$$SkRo_{23} = -\frac{k^4\left(e^{-ikL-(1-i)kL_1}((-1+i)k\cos(\mathrm{wjxe})+\mathrm{wj}\sin(\mathrm{wjxe}))+e^{-kL}((1-i)k\cos(\mathrm{wj}(L-L_1+\mathrm{xe}))-\mathrm{wj}\sin(\mathrm{wj}(L-L_1+\mathrm{xe})))\right)}{2ik^2-\mathrm{wj}^2}$$

$$SkRo_{24} = \frac{e^{-kL}k^4(\sin(\mathrm{wj}(L-L_1+\mathrm{xe}))-\sin(\mathrm{wjxe}))}{\mathrm{wj}}$$

$$SkRo_{33} = \frac{k^4\left(-2ik\cos(\mathrm{wj}(L-L_1+\mathrm{xe}))+e^{2ik(L_1-L)}(2ik\cos(\mathrm{wjxe})+\mathrm{wj}\sin(\mathrm{wjxe}))-\mathrm{wj}\sin(\mathrm{wj}(L-L_1+\mathrm{xe}))\right)}{4k^2-\mathrm{wj}^2}$$

$$SkRo_{34} = -\frac{k^4\left((1+i)k\cos(\mathrm{wj}(L-L_1+\mathrm{xe}))-e^{(1+i)k(L_1-L)}((1+i)k\cos(\mathrm{wjxe})+\mathrm{wj}\sin(\mathrm{wjxe}))+\mathrm{wj}\sin(\mathrm{wj}(L-L_1+\mathrm{xe}))\right)}{2ik^2+\mathrm{wj}^2}$$

$$SkRo_{44} = \frac{k^4\left(2k\cos(\mathrm{wj}(L-L_1+\mathrm{xe}))-e^{2k(L_1-L)}(2k\cos(\mathrm{wjxe})+\mathrm{wj}\sin(\mathrm{wjxe}))+\mathrm{wj}\sin(\mathrm{wj}(L-L_1+\mathrm{xe}))\right)}{4k^2+\mathrm{wj}^2}$$

$$SmLo_{11} = \frac{-2ik\cos(\mathrm{wjxe})+\mathrm{wj}\sin(\mathrm{wjxe})+e^{-2ikL_1}(2ik\cos(\mathrm{wj}(L_1+\mathrm{xe}))-\mathrm{wj}\sin(\mathrm{wj}(L_1+\mathrm{xe})))}{4k^2-\mathrm{wj}^2}$$

$$SmLo_{12} = \frac{(1+i)k\cos(\mathrm{wjxe})-\mathrm{wj}\sin(\mathrm{wjxe})+e^{(-1-i)kL_1}((-1-i)k\cos(\mathrm{wj}(L_1+\mathrm{xe}))+\mathrm{wj}\sin(\mathrm{wj}(L_1+\mathrm{xe})))}{2ik^2+\mathrm{wj}^2}$$

$$SmLo_{13} = \frac{e^{-ikL_1}(\sin(\mathrm{wj}(L_1+\mathrm{xe}))-\sin(\mathrm{wjxe}))}{\mathrm{wj}}$$

$$SmLo_{14} = \frac{e^{-ikL_1}((1+i)k\cos(\mathrm{wj}(L_1+\mathrm{xe}))+i\mathrm{wj}\sin(\mathrm{wj}(L_1+\mathrm{xe})))-e^{-kL_1}((1+i)k\cos(\mathrm{wjxe})+i\mathrm{wj}\sin(\mathrm{wjxe}))}{2k^2+i\mathrm{wj}^2}$$

$$SmLo_{22} = \frac{2k\cos(\mathrm{wjxe})-2e^{-2kL_1}k\cos(\mathrm{wj}(L_1+\mathrm{xe}))-\mathrm{wj}\sin(\mathrm{wjxe})+e^{-2kL_1}\mathrm{wj}\sin(\mathrm{wj}(L_1+\mathrm{xe}))}{4k^2+\mathrm{wj}^2}$$

$$SmLo_{23} = \frac{e^{-ikL_1}((-1+i)k\cos(\mathrm{wjxe})+\mathrm{wj}\sin(\mathrm{wjxe}))+e^{-kL_1}((1-i)k\cos(\mathrm{wj}(L_1+\mathrm{xe}))-\mathrm{wj}\sin(\mathrm{wj}(L_1+\mathrm{xe})))}{2ik^2-\mathrm{wj}^2}$$

$$SmLo_{24} = \frac{e^{-kL_1}(\sin(\mathrm{wj}(L_1+\mathrm{xe}))-\sin(\mathrm{wjxe}))}{\mathrm{wj}}$$

$$SmLo_{33} = \frac{-2ik\cos(\mathrm{wj}(L_1+\mathrm{xe}))+e^{-2ikL_1}(2ik\cos(\mathrm{wjxe})+\mathrm{wj}\sin(\mathrm{wjxe}))-\mathrm{wj}\sin(\mathrm{wj}(L_1+\mathrm{xe}))}{4k^2-\mathrm{wj}^2}$$

$$SmLo_{34} = \frac{(1+i)k\cos(\mathrm{wj}(L_1+\mathrm{xe}))-e^{(-1-i)kL_1}((1+i)k\cos(\mathrm{wjxe})+\mathrm{wj}\sin(\mathrm{wjxe}))+\mathrm{wj}\sin(\mathrm{wj}(L_1+\mathrm{xe}))}{2ik^2+\mathrm{wj}^2}$$

$$SmLo_{44} = \frac{2k\cos(\mathrm{wj}(L_1+\mathrm{xe}))-e^{-2kL_1}(2k\cos(\mathrm{wjxe})+\mathrm{wj}\sin(\mathrm{wjxe}))+\mathrm{wj}\sin(\mathrm{wj}(L_1+\mathrm{xe}))}{4k^2+\mathrm{wj}^2}$$

$$SmRo_{11} = \frac{e^{-2ikL_1}(\mathrm{wj}\sin(\mathrm{wjxe})-2ik\cos(\mathrm{wjxe}))+e^{-2ikL}(2ik\cos(\mathrm{wj}(L-L_1+\mathrm{xe}))-\mathrm{wj}\sin(\mathrm{wj}(L-L_1+\mathrm{xe})))}{4k^2-\mathrm{wj}^2}$$

$$SmRo_{12} = \frac{e^{(-1-i)kL_1}((1+i)k\cos(\mathrm{wjxe})-\mathrm{wj}\sin(\mathrm{wjxe}))+e^{(-1-i)kL}((-1-i)k\cos(\mathrm{wj}(L-L_1+\mathrm{xe}))+\mathrm{wj}\sin(\mathrm{wj}(L-L_1+\mathrm{xe})))}{2ik^2+\mathrm{wj}^2}$$

$$SmRo_{13} = \frac{e^{-ikL}(\sin(\mathrm{wj}(L-L_1+\mathrm{xe}))-\sin(\mathrm{wjxe}))}{\mathrm{wj}}$$

$$SmRo_{14} = \frac{e^{-ikL}((1+i)k\cos(\mathrm{wj}(L-L_1+\mathrm{xe}))+i\mathrm{wj}\sin(\mathrm{wj}(L-L_1+\mathrm{xe})))-e^{-k(L-(1-i)L_1)}((1+i)k\cos(\mathrm{wjxe})+i\mathrm{wj}\sin(\mathrm{wjxe}))}{2k^2+i\mathrm{wj}^2}$$

$$SmRo_{22} = \frac{e^{-2kL_1}(2k\cos(\mathrm{wjxe})-\mathrm{wj}\sin(\mathrm{wjxe}))+e^{-2kL}(\mathrm{wj}\sin(\mathrm{wj}(L-L_1+\mathrm{xe}))-2k\cos(\mathrm{wj}(L-L_1+\mathrm{xe})))}{4k^2+\mathrm{wj}^2}$$

$$SmRo_{23} = \frac{e^{-ikL-(1-i)kL_1}((-1+i)k\cos(\mathrm{wjxe})+\mathrm{wj}\sin(\mathrm{wjxe}))+e^{-kL}((1-i)k\cos(\mathrm{wj}(L-L_1+\mathrm{xe}))-\mathrm{wj}\sin(\mathrm{wj}(L-L_1+\mathrm{xe})))}{2ik^2-\mathrm{wj}^2}$$

$$SmRo_{24} = \frac{e^{-kL}(\sin(\mathrm{wj}(L-L_1+\mathrm{xe}))-\sin(\mathrm{wjxe}))}{\mathrm{wj}}$$

$$SmRo_{33} = \frac{-2ik\cos(\mathrm{wj}(L-L_1+\mathrm{xe}))+e^{2ik(L_1-L)}(2ik\cos(\mathrm{wjxe})+\mathrm{wj}\sin(\mathrm{wjxe}))-\mathrm{wj}\sin(\mathrm{wj}(L-L_1+\mathrm{xe}))}{4k^2-\mathrm{wj}^2}$$

$$SmRo_{34} = \frac{(1+i)k\cos(\mathrm{wj}(L-L_1+\mathrm{xe}))-e^{(1+i)k(L_1-L)}((1+i)k\cos(\mathrm{wjxe})+\mathrm{wj}\sin(\mathrm{wjxe}))+\mathrm{wj}\sin(\mathrm{wj}(L-L_1+\mathrm{xe}))}{2ik^2+\mathrm{wj}^2}$$

$$SmRo_{44} = \frac{2k\cos(\mathrm{wj}(L-L_1+\mathrm{xe}))-e^{2k(L_1-L)}(2k\cos(\mathrm{wjxe})+\mathrm{wj}\sin(\mathrm{wjxe}))+\mathrm{wj}\sin(\mathrm{wj}(L-L_1+\mathrm{xe}))}{4k^2+\mathrm{wj}^2}$$

and for even j are

$$SkLe_{11} = \frac{k^4\left(-\mathrm{wj}\cos(\mathrm{wjxe})-2ik\sin(\mathrm{wjxe})+e^{-2ikL_1}(\mathrm{wj}\cos(\mathrm{wj}(L_1+\mathrm{xe}))+2ik\sin(\mathrm{wj}(L_1+\mathrm{xe})))\right)}{4k^2-\mathrm{wj}^2}$$

$$SkLe_{12} = -\frac{k^4\left(\mathrm{wj}\cos(\mathrm{wjxe})+(1+i)k\sin(\mathrm{wjxe})-e^{(-1-i)kL_1}(\mathrm{wj}\cos(\mathrm{wj}(L_1+\mathrm{xe}))+(1+i)k\sin(\mathrm{wj}(L_1+\mathrm{xe})))\right)}{2ik^2+\mathrm{wj}^2}$$

$$SkLe_{13} = \frac{e^{-ikL_1}k^4(\cos(\mathrm{wjxe})-\cos(\mathrm{wj}(L_1+\mathrm{xe})))}{\mathrm{wj}}$$

$$SkLe_{14} = -\frac{k^4\left(e^{-kL_1}((1-i)k\sin(\mathrm{wjxe})-\mathrm{wj}\cos(\mathrm{wjxe}))+e^{-ikL_1}(\mathrm{wj}\cos(\mathrm{wj}(L_1+\mathrm{xe}))-(1-i)k\sin(\mathrm{wj}(L_1+\mathrm{xe})))\right)}{2ik^2-\mathrm{wj}^2}$$

$$SkLe_{22} = \frac{k^4\left(\mathrm{wj}\cos(\mathrm{wjxe})+2k\sin(\mathrm{wjxe})-e^{-2kL_1}(\mathrm{wj}\cos(\mathrm{wj}(L_1+\mathrm{xe}))+2k\sin(\mathrm{wj}(L_1+\mathrm{xe})))\right)}{4k^2+\mathrm{wj}^2}$$

$$SkLe_{23} = -\frac{k^4\left(e^{-ikL_1}(-\mathrm{wj}\cos(\mathrm{wjxe})-(1-i)k\sin(\mathrm{wjxe}))+e^{-kL_1}(\mathrm{wj}\cos(\mathrm{wj}(L_1+\mathrm{xe}))+(1-i)k\sin(\mathrm{wj}(L_1+\mathrm{xe})))\right)}{2ik^2-\mathrm{wj}^2}$$

$$SkLe_{24} = \frac{e^{-kL_1}k^4(\cos(\mathrm{wjxe})-\cos(\mathrm{wj}(L_1+\mathrm{xe})))}{\mathrm{wj}}$$

$$SkLe_{33} = \frac{k^4\left(\mathrm{wj}\cos(\mathrm{wj}(L_1+\mathrm{xe}))+e^{-2ikL_1}(2ik\sin(\mathrm{wjxe})-\mathrm{wj}\cos(\mathrm{wjxe}))-2ik\sin(\mathrm{wj}(L_1+\mathrm{xe}))\right)}{4k^2-\mathrm{wj}^2}$$

$$SkLe_{34} = -\frac{k^4\left(-\mathrm{wj}\cos(\mathrm{wj}(L_1+\mathrm{xe}))+e^{(-1-i)kL_1}(\mathrm{wj}\cos(\mathrm{wjxe})-(1+i)k\sin(\mathrm{wjxe}))+(1+i)k\sin(\mathrm{wj}(L_1+\mathrm{xe}))\right)}{2ik^2+\mathrm{wj}^2}$$

$$SkLe_{44} = \frac{k^4\left(e^{-2kL_1}\mathrm{wj}\cos(\mathrm{wjxe})-\mathrm{wj}\cos(\mathrm{wj}(L_1+\mathrm{xe}))+2k\left(\sin(\mathrm{wj}(L_1+\mathrm{xe}))-e^{-2kL_1}\sin(\mathrm{wjxe})\right)\right)}{4k^2+\mathrm{wj}^2}$$

$$SkRe_{11} = \frac{k^4\left(e^{-2ikL}(\mathrm{wj}\cos(\mathrm{wj}(L-L_1+\mathrm{xe}))+2ik\sin(\mathrm{wj}(L-L_1+\mathrm{xe})))-e^{-2ikL_1}(\mathrm{wj}\cos(\mathrm{wjxe})+2ik\sin(\mathrm{wjxe}))\right)}{4k^2-\mathrm{wj}^2}$$

$$SkRe_{12} = -\frac{k^4\left(e^{(-1-i)kL_1}(\mathrm{wj}\cos(\mathrm{wjxe})+(1+i)k\sin(\mathrm{wjxe}))-e^{(-1-i)kL}(\mathrm{wj}\cos(\mathrm{wj}(L-L_1+\mathrm{xe}))+(1+i)k\sin(\mathrm{wj}(L-L_1+\mathrm{xe})))\right)}{2ik^2+\mathrm{wj}^2}$$

$$SkRe_{13} = \frac{e^{-ikL}k^4(\cos(\mathrm{wjxe})-\cos(\mathrm{wj}(L-L_1+\mathrm{xe})))}{\mathrm{wj}}$$

$$SkRe_{14} = -\frac{k^4\left(e^{-k(L-(1-i)L_1)}((1-i)k\sin(\mathrm{wjxe})-\mathrm{wj}\cos(\mathrm{wjxe}))+e^{-ikL}(\mathrm{wj}\cos(\mathrm{wj}(L-L_1+\mathrm{xe}))-(1-i)k\sin(\mathrm{wj}(L-L_1+\mathrm{xe})))\right)}{2ik^2-\mathrm{wj}^2}$$

$$SkRe_{22} = \frac{k^4\left(e^{-2kL_1}(\mathrm{wj}\cos(\mathrm{wjxe})+2k\sin(\mathrm{wjxe}))-e^{-2kL}(\mathrm{wj}\cos(\mathrm{wj}(L-L_1+\mathrm{xe}))+2k\sin(\mathrm{wj}(L-L_1+\mathrm{xe})))\right)}{4k^2+\mathrm{wj}^2}$$

$$SkRe_{23} = -k^4\left(\frac{e^{-kL}(\mathrm{wj}\cos(\mathrm{wj}(L-L_1+\mathrm{xe}))+(1-i)k\sin(\mathrm{wj}(L-L_1+\mathrm{xe})))}{2ik^2-\mathrm{wj}^2}-\frac{e^{-k(iL+(1-i)L_1)}(\mathrm{wj}\cos(\mathrm{wjxe})+(1-i)k\sin(\mathrm{wjxe}))}{2ik^2-\mathrm{wj}^2}\right)$$

$$SkRe_{24} = \frac{e^{-kL}k^4(\cos(\mathrm{wjxe})-\cos(\mathrm{wj}(L-L_1+\mathrm{xe})))}{\mathrm{wj}}$$

$$SkRe_{33} = \frac{k^4\left(\mathrm{wj}\cos(\mathrm{wj}(L-L_1+\mathrm{xe}))+e^{2ik(L_1-L)}(2ik\sin(\mathrm{wjxe})-\mathrm{wj}\cos(\mathrm{wjxe}))-2ik\sin(\mathrm{wj}(L-L_1+\mathrm{xe}))\right)}{4k^2-\mathrm{wj}^2}$$

$$SkRe_{34} = \frac{k^4\left(-e^{(1+i)k(L_1-L)}\mathrm{wj}\cos(\mathrm{wjxe})+\mathrm{wj}\cos(\mathrm{wj}(L-L_1+\mathrm{xe}))+(1+i)k\left(e^{(1+i)k(L_1-L)}\sin(\mathrm{wjxe})-\sin(\mathrm{wj}(L-L_1+\mathrm{xe}))\right)\right)}{2ik^2+\mathrm{wj}^2}$$

$$SkRe_{44} = \frac{k^4\left(e^{2k(L_1-L)}\mathrm{wj}\cos(\mathrm{wjxe})-\mathrm{wj}\cos(\mathrm{wj}(L-L_1+\mathrm{xe}))+2k\left(\sin(\mathrm{wj}(L-L_1+\mathrm{xe}))-e^{2k(L_1-L)}\sin(\mathrm{wjxe})\right)\right)}{4k^2+\mathrm{wj}^2}$$

$$SmLe_{11}=\frac{-\mathrm{wj}\cos(\mathrm{wjxe})-2ik\sin(\mathrm{wjxe})+e^{-2ikL_1}(\mathrm{wj}\cos(\mathrm{wj}(L_1+\mathrm{xe}))+2ik\sin(\mathrm{wj}(L_1+\mathrm{xe})))}{4k^2-\mathrm{wj}^2}$$

$$SmLe_{12}=\frac{\mathrm{wj}\cos(\mathrm{wjxe})+(1+i)k\sin(\mathrm{wjxe})-e^{(-1-i)kL_1}(\mathrm{wj}\cos(\mathrm{wj}(L_1+\mathrm{xe}))+(1+i)k\sin(\mathrm{wj}(L_1+\mathrm{xe})))}{2ik^2+\mathrm{wj}^2}$$

$$SmLe_{13}=\frac{e^{-ikL_1}(\cos(\mathrm{wjxe})-\cos(\mathrm{wj}(L_1+\mathrm{xe})))}{\mathrm{wj}}$$

$$SmLe_{14}=\frac{e^{-kL_1}((1-i)k\sin(\mathrm{wjxe})-\mathrm{wj}\cos(\mathrm{wjxe}))+e^{-ikL_1}(\mathrm{wj}\cos(\mathrm{wj}(L_1+\mathrm{xe}))-(1-i)k\sin(\mathrm{wj}(L_1+\mathrm{xe})))}{2ik^2-\mathrm{wj}^2}$$

$$SmLe_{22}=\frac{\mathrm{wj}\cos(\mathrm{wjxe})+2k\sin(\mathrm{wjxe})-e^{-2kL_1}(\mathrm{wj}\cos(\mathrm{wj}(L_1+\mathrm{xe}))+2k\sin(\mathrm{wj}(L_1+\mathrm{xe})))}{4k^2+\mathrm{wj}^2}$$

$$SmLe_{23}=\frac{e^{-ikL_1}(-\mathrm{wj}\cos(\mathrm{wjxe})-(1-i)k\sin(\mathrm{wjxe}))+e^{-kL_1}(\mathrm{wj}\cos(\mathrm{wj}(L_1+\mathrm{xe}))+(1-i)k\sin(\mathrm{wj}(L_1+\mathrm{xe})))}{2ik^2-\mathrm{wj}^2}$$

$$SmLe_{24}=\frac{e^{-kL_1}(\cos(\mathrm{wjxe})-\cos(\mathrm{wj}(L_1+\mathrm{xe})))}{\mathrm{wj}}$$

$$SmLe_{33}=\frac{\mathrm{wj}\cos(\mathrm{wj}(L_1+\mathrm{xe}))+e^{-2ikL_1}(2ik\sin(\mathrm{wjxe})-\mathrm{wj}\cos(\mathrm{wjxe}))-2ik\sin(\mathrm{wj}(L_1+\mathrm{xe}))}{4k^2-\mathrm{wj}^2}$$

$$SmLe_{34}=\frac{-\mathrm{wj}\cos(\mathrm{wj}(L_1+\mathrm{xe}))+e^{(-1-i)kL_1}(\mathrm{wj}\cos(\mathrm{wjxe})-(1+i)k\sin(\mathrm{wjxe}))+(1+i)k\sin(\mathrm{wj}(L_1+\mathrm{xe}))}{2ik^2+\mathrm{wj}^2}$$

$$SmLe_{44}=\frac{e^{-2kL_1}\mathrm{wj}\cos(\mathrm{wjxe})-\mathrm{wj}\cos(\mathrm{wj}(L_1+\mathrm{xe}))+2k\left(\sin(\mathrm{wj}(L_1+\mathrm{xe}))-e^{-2kL_1}\sin(\mathrm{wjxe})\right)}{4k^2+\mathrm{wj}^2}$$

$$SmRe_{11}=\frac{e^{-2ikL}(\mathrm{wj}\cos(\mathrm{wj}(L-L_1+\mathrm{xe}))+2ik\sin(\mathrm{wj}(L-L_1+\mathrm{xe})))-e^{-2ikL_1}(\mathrm{wj}\cos(\mathrm{wjxe})+2ik\sin(\mathrm{wjxe}))}{4k^2-\mathrm{wj}^2}$$

$$SmRe_{12}=\frac{e^{(-1-i)kL_1}(\mathrm{wj}\cos(\mathrm{wjxe})+(1+i)k\sin(\mathrm{wjxe}))-e^{(-1-i)kL}(\mathrm{wj}\cos(\mathrm{wj}(L-L_1+\mathrm{xe}))+(1+i)k\sin(\mathrm{wj}(L-L_1+\mathrm{xe})))}{2ik^2+\mathrm{wj}^2}$$

$$SmRe_{13}=\frac{e^{-ikL}(\cos(\mathrm{wjxe})-\cos(\mathrm{wj}(L-L_1+\mathrm{xe})))}{\mathrm{wj}}$$

$$SmRe_{14}=\frac{e^{-k(L-(1-i)L_1)}((1-i)k\sin(\mathrm{wjxe})-\mathrm{wj}\cos(\mathrm{wjxe}))+e^{-ikL}(\mathrm{wj}\cos(\mathrm{wj}(L-L_1+\mathrm{xe}))-(1-i)k\sin(\mathrm{wj}(L-L_1+\mathrm{xe})))}{2ik^2-\mathrm{wj}^2}$$

$$SmRe_{22}=\frac{e^{-2kL_1}(\mathrm{wj}\cos(\mathrm{wjxe})+2k\sin(\mathrm{wjxe}))-e^{-2kL}(\mathrm{wj}\cos(\mathrm{wj}(L-L_1+\mathrm{xe}))+2k\sin(\mathrm{wj}(L-L_1+\mathrm{xe})))}{4k^2+\mathrm{wj}^2}$$

$$SmRe_{23}=\frac{e^{-kL}(\mathrm{wj}\cos(\mathrm{wj}(L-L_1+\mathrm{xe}))+(1-i)k\sin(\mathrm{wj}(L-L_1+\mathrm{xe})))}{2ik^2-\mathrm{wj}^2}-\frac{e^{-k(iL+(1-i)L_1)}(\mathrm{wj}\cos(\mathrm{wjxe})+(1-i)k\sin(\mathrm{wjxe}))}{2ik^2-\mathrm{wj}^2}$$

$$SmRe_{24}=\frac{e^{-kL}(\cos(\mathrm{wjxe})-\cos(\mathrm{wj}(L-L_1+\mathrm{xe})))}{\mathrm{wj}}$$

$$SmRe_{33}=\frac{\mathrm{wj}\cos(\mathrm{wj}(L-L_1+\mathrm{xe}))+e^{2ik(L_1-L)}(2ik\sin(\mathrm{wjxe})-\mathrm{wj}\cos(\mathrm{wjxe}))-2ik\sin(\mathrm{wj}(L-L_1+\mathrm{xe}))}{4k^2-\mathrm{wj}^2}$$

$$SmRe_{34}=-\frac{-e^{(1+i)k(L_1-L)}\mathrm{wj}\cos(\mathrm{wjxe})+\mathrm{wj}\cos(\mathrm{wj}(L-L_1+\mathrm{xe}))+(1+i)k\left(e^{(1+i)k(L_1-L)}\sin(\mathrm{wjxe})-\sin(\mathrm{wj}(L-L_1+\mathrm{xe}))\right)}{2ik^2+\mathrm{wj}^2}$$

$$SmRe_{44}=\frac{-\mathrm{wj}\cos(\mathrm{wj}(L-L_1+\mathrm{xe}))+e^{2k(L_1-L)}(\mathrm{wj}\cos(\mathrm{wjxe})-2k\sin(\mathrm{wjxe}))+2k\sin(\mathrm{wj}(L-L_1+\mathrm{xe}))}{4k^2+\mathrm{wj}^2}$$